

University of Southampton Research Repository ePrints Soton

Copyright © and Moral Rights for this thesis are retained by the author and/or other copyright owners. A copy can be downloaded for personal non-commercial research or study, without prior permission or charge. This thesis cannot be reproduced or quoted extensively from without first obtaining permission in writing from the copyright holder/s. The content must not be changed in any way or sold commercially in any format or medium without the formal permission of the copyright holders.

When referring to this work, full bibliographic details including the author, title, awarding institution and date of the thesis must be given e.g.

AUTHOR (year of submission) "Full thesis title", University of Southampton, name of the University School or Department, PhD Thesis, pagination

UNIVERSITY OF SOUTHAMPTON

FACULTY OF SOCIAL AND HUMAN SCIENCE

Geography and Environment

**Simulating complex hydro-geomorphic changes
in lake-catchment systems**

by

Ying Wang

Thesis for the degree of Doctor of Philosophy (PhD)

August 2013

UNIVERSITY OF SOUTHAMPTON

ABSTRACT

FACULTY OF SOCIAL AND HUMAN SCIENCE

Geography and Environment

Thesis for the degree of Doctor of Philosophy (PhD)

SIMULATING COMPLEX HYDRO-GEOMORPHIC CHANGES IN LAKE-CATCHMENT SYSTEMS

Ying Wang

Management of lake-catchment systems is a long-term challenge for prevention of hazard risk and further sustainable development. Climate change and human activities are two important factors that concurrently affect the hydrology and sediment regimes within systems. Many soil conservation and sediment control techniques are known and widely studied based on experimental field plots. Catchments are complex dynamic systems. Spatially-distributed and process-based models provide powerful tools to simulate the complex behaviour of hydro-geomorphological processes in response to climate change and human impact on fluvial systems. Accordingly, this study addresses the principles, testing and application of an established cellular automata landscape evolution model (CAESAR) to study the dynamic non-linear behaviour of complex systems, past and present interactions among landscape elements and environmental controls, and potential future impacts. The results from a series of simulations of different systems (simple catchment, Old Alresford Pond, UK and Holzmaar, Germany) over different timescales (50 years to 5000 years), demonstrate a rapid catchment response to climatic drivers. This is characterised by variations, particularly peaks of modelled sediment discharge controlled by the magnitude and frequency of floods and droughts happened in a single year or a period of time. The effect of vegetation cover also plays an important role in accelerating the delivery of sediment or protecting the catchment from soil erosion. This erosional response is validated by comparing modelled sediment discharge and system evolution to magnetic susceptibility and accumulation rates of lake sediments, as well as documented data. The non-linear properties of complex systems, such as thresholds, feedback mechanisms and self-organised capability, are shown to exist in these simulations. This study also provides the probabilistic results of potential erosion risks in terms of future natural and human pressures. The modelling application permits a better understanding of the relationship between environmental forcings and complex dynamic system evolution processes. In addition, it allows investigations of the extent to which past and present human-environmental interactions generate subsequent impacts for the purpose of effective landscape management.

Contents

ABSTRACT	iii
Contents	v
List of tables	xiii
List of figures	xv
DECLARATION OF AUTHORSHIP	xxiii
Acknowledgements	xxv
Chapter 1: Introduction	1
1.1 Background	1
1.2 Aims of research	3
1.3 Objectives of PhD research	5
1.4 Structure of the thesis	6
Chapter 2: The Complexity of River Systems – from Past to Future	9
2.1 Landscape behaviour to environmental changes	9
2.1.1 Hydrological process of flooding	9
2.1.2 Geomorphic process of soil erosion	11
2.2 Understanding the past from lake sediment records	13
2.2.1 Dating methods	13
2.2.2 Sediment fingerprinting methods	17
2.3 The dynamics of river systems	20

2.3.1 System complexity	20
2.3.2 Modelling complex systems	23
2.4 Summary	26
Chapter 3 Numerical models and CAESAR	27
3.1 Introduction	27
3.2 Numerical modelling	27
3.3 Cellular automata models	32
3.4 CAESAR model	36
3.4.1 Model structure	36
3.4.2 Hydrological process	36
3.4.3 Flowing routing	37
3.4.4 Erosion and deposition process	38
3.4.5 Slope process	40
3.4 Summary	41
Chapter 4: Methodology	43
4.1 Introduction	43
4.2 Lake sediment records	44
4.2.1 Site 1 Alresford Pond, Hampshire, UK	44
4.2.1.1 Data collection and sampling	44
4.2.1.2 Chronology	45

4.2.1.3 Magnetic properties of sediments and soils	47
4.2.2 Site 2 Holzmaar, Eifel region, Germany	51
4.3 CAESAR parameters setup	52
4.3.1 Model input and output files	52
4.3.2 Digital elevation model	52
4.3.3 Particle size distribution	53
4.3.3.1 Alresford Catchment	54
4.3.3.2 Holzmaar Catchment	55
4.4 Creation of precipitation data	55
4.4.1 Precipitation series for Alresford Catchment between AD1889 and 2009	55
4.4.2 Precipitation series for Holzmaar Catchment between 3500 BC and AD 2007	57
4.4.3 Precipitation series for future projection of Alresford catchment between AD 2010 and 2099	59
4.5 Land use	62
4.5.1 Alresford Catchment	62
4.5.1.1 Preliminary creation of land use index, M value	62
4.5.1.2 Calibration of rainfall and land use parameters	64
4.5.2 Holzmaar catchment	72
4.6 Spin up period testing	74
4.6 Summary	76

Chapter 5: Modelling sediment and water discharge in a chalk catchment since 1889	79
5.1 Introduction	79
5.2 Site description	80
5.2.1 Introduction	80
5.2.2 Geology and Geomorphology features	82
5.2.3 Hydrology and precipitation features	84
5.2.4 Land use and vegetation features	86
5.3 Model setup	89
5.4 Analysis of lake sediment achieves	89
5.4.1 Dating recent lake sediments by spheroidal carbonaceous particles (SCP)	89
5.4.2 Magnetic susceptibility analysis	96
5.5 Results	101
5.5.1 Modelling Results	101
5.5.2 Model validation	107
5.6 Discussion	108
5.6.1 Catchment response to environmental changes	108
5.6.2 Model validation	112
5.7 Summary	117
 Chapter 6: Simulating catchment response to environmental changes over 5000 years	 119

6.1 Introduction	119
6.2 Site description	120
6.2.1 West Eifel Volcanic Field	120
6.2.2 Why choose Holzmaar?	123
6.2.3 Holzmaar catchment	124
6.3 Model setup	127
6.4 Results	128
6.4.1 Catchment sensitivity to land use and climate changes	128
6.4.2 Catchment behaviour to environmental changes	132
6.5 Discussion	134
6.5.1 Overall patterns of model validation.....	134
6.5.2 Model validation for the time period of 5000 - 3750 calendar year BP	137
6.5.3 Model validation for the time period of 2750-1750 calendar year BP	139
6.5.4 Model validation for the time period of 1750-1000 calendar year BP	140
6.5.5 Model validation for the time period of 1000-0 calendar year BP	140
6.6 Summary	142
 Chapter 7: The role of non-linearity and self-organisation in complex river systems	 145
7.1 Introduction	145
7.2 Methods	147
7.3 Results	150

7.3.1 Simple catchment	150
7.3.2 Holzmaar catchment	154
7.3.3 Alresford catchment	157
7.4 Discussion	159
7.4.1 Non-linear behaviour	159
7.4.1.1 Critical state / threshold	159
7.4.1.2 Feedback	161
7.4.2 Self-organisation behaviour	163
7.5 Summary	168
Chapter 8: Testing a modelling approach to simulate the behaviour of hydro- geomorphological processes based on future climate scenarios	171
8.1 Introduction	171
8.2 Model setup	175
8.3 Results and interpretations	176
8.3.1 Catchment response to future climate change	176
8.3.1.1 Annual changes in water and sediment discharge	176
8.3.1.2 Seasonal changes in water and sediment discharge	179
8.3.1.3 Changes based on different sized events	184
8.3.2 Catchment response to future land use change	190
8.3.3 The impact of future climate and deforestation	194
8.4 Summary	196

Chapter 9: Synthesis and future research	199
9.1 System complexity	200
9.1.1 The complexity of system responses to environmental controls	202
9.1.2 The application of complexity theory	203
9.2 The complexity of modelling	206
9.2.1 Model performance	206
9.2.1.1 The complexity of system prediction.....	206
9.2.1.2 Modelling calibration.....	207
9.2.1.3 Modelling validation	208
9.2.2 Modelling constraints.....	210
9.3 Future perspectives and further work.....	211
Bibliography	213

List of tables

Table 3.1	Comparison of Models.	30-31
Table 3.2	Comparison of modelling and natural erosion processes.	39
Table 4.1	Location and sample site description with pictures.	49-50
Table 4.2	Data structure of projected precipitation.	61
Table 4.3	NDVI values and correlated M values.	64
Table 4.4	Selected tests of precipitation and land use series.	68
Table 4.5	Correlation for simulations with initial condition and varying M values, Alresford Pond catchment.	72
Table 4.6	Correlation analysis of water discharge.	75
Table 5.1	Land use (%) of the Alresford catchment in 2000 calculated from the Land Cover Map 2000 (Data source: Southampton GeoData Institute).	87
Table 5.2	Dates for each 10% of the SCP cumulative percentage profile combined with the depth of AP 09-03.	92
Table 5.3	Calibration between SCP chronology and artificial radioisotopes records.	95
Table 5.4	Magnetic properties of soil samples.	100
Table 5.5	Number of flooding days with a magnitude greater than 2, 5, 8 and 10 for original and effective rainfall inputs, maximum and minimum water discharge.	114
Table 5.6	Total, maximum and minimum sediment discharges and their differences.	115

	Geographical, morphometric and chemical characteristics of Lake Holzmaar, Germany (after Scharf, 1987; Scharf and Menn, 1992; Scharf and Oehms, 1992; Lottermoser <i>et al.</i> , 1997; Zolitschka, 1998; Lücke <i>et al.</i> , 2003; Baier <i>et al.</i> , 2004a; Kienel <i>et al.</i> , 2005).	126
Table 6.1	Combination of different runs in first simulation.	148
Table 7.1	Total every 30-year sediment discharge (m ³) for all climate change scenarios at three probability levels.	188
Table 8.1	Comparisons of annual maximum of (a) rainfall, (b) water discharge and (c) sediment discharge between baseline and projected data for climate change scenarios.	189-190
Table 8.2	Total amount of projected sediment discharge for every land use and climate change scenarios in the future.	191
Table 8.3		

List of figures

Figure 1.1	Research programme structure	6
Figure 2.1	A schematic description of the characteristics of complex system (from NECSI research project, 2013).	22
Figure 2.2	The mechanism and framework of top-down and bottom-up approaches (from Grimm, 1999; Perry and Bond, 2012).	25
Figure 3.1	Schematic diagram of CAESAR scanning algorithm: (1) Water flow from grid cells to the three downstream neighbours on the right. (2) All the cells are upslope, no water is pushed. (3) The same process is repeated from right to left until all the water is left in the base of the valley. (4) Water is pushed out of the catchment from top to bottom. (from Coulthard <i>et al.</i> , 2002)	35
Figure 4.1	Location of sediment cores (Data source: Google Earth, 2009).	45
Figure 4.2	Images of a typical spheroidal carbonaceous particle by light microscope (left, from Martins <i>et al.</i> , 2010) and scanning electron microscopy (right, from Rose, 1990).	46
Figure 4.3	Map showing location of soil sampling points.	48
Figure 4.4	DEM of (a) Alresford catchment and (b) Holzmaar catchment.	53
Figure 4.5	Average grain size distributions for Alresford catchment.	54
Figure 4.6	Average grain size distributions for Holzmaar catchment.	55
Figure 4.7	Location of weather stations (from Google Earth, 2011).	56
Figure 4.8	The location of Lake Holzmaar and weather stations Gillenfeld and Trier.	57
Figure 4.9	The combination of annual rainfall data for Holzmaar catchment, (a) original high and medium resolution rainfall data (1500-1950AD); (b) rainfall reconstructed from pollen (-3050 BC-1950AD); (c) adjusted all rainfall data (-3050 BC-1950AD).	58

Figure 4.10	An example of rainfall prediction under the low emission scenario in the period of 2010-2039 (2020s).	59
Figure 4.11	Modelled hourly water discharge under different M values.	62
Figure 4.12	M values for Alresford Catchment (AD. 1880-2009).	64
Figure 4.13	Location of gauging station and Alresford pond.	65
Figure 4.14	Comparison of simulated water discharge with documentary records (1982-2009).	66
Figure 4.15	Comparison of precipitation (a) and documented flow (b) data for Alresford for 2005.	67
Figure 4.16	Comparison of modelled water discharge (blue) and recorded flow (red) for (a),(e) Test 1, (b),(f) Test 4, (c),(g) Test 5, (d),(g) Test 8 with different M values (0.012 and 0.015) for Alresford catchment in 2005.	70
Figure 4.17	Comparison between (a) original and groundwater-adjusted precipitation; (b) simulated water discharge with effective rainfall and documentary flow records (1982-2009).	72
Figure 4.18	The relationship between M values and the percentage of arboreal pollen.	73
Figure 4.19	M value vegetation cover record converted from arboreal pollen for Holzmaar catchment between 2000 AD and 3000 BC.	73
Figure 4.20	Graph of sediment discharges for every 11 years.	74
Figure 5.1	Location of Alresford Pond in Hampshire, Southern England (from Edina Digimap 1:5000 and the Centre for Ecology & Hydrology).	81
Figure 5.2	Changes of shape and size of Alresford Pond from 1870s to 1990s (from Edina Historic Digimap 1:10560).	81
Figure 5.3	East-west transect of Alresford District (after Farrant, 2002).	83

Figure 5.4	Geology of Alresford Catchment. Where superficial deposits are present, the bedrock geology will be concealed (from British Geological Survey and Southampton GeoData Institute).	83
Figure 5.5	Annual precipitation at Alresford (1882-2009) (Data source: Met Office).	84
Figure 5.6	Average monthly precipitation in Alresford between 1961 and 1990 (Data source: Met Office).	85
Figure 5.7	Alresford Catchment and its streams (Data source: Ordnance Survey). Black arrows indicate flow directions.	85
Figure 5.8	Average monthly flows in the Alresford catchment from 1959 to 1999 (from National River Flow Archive, the Centre for Ecology & Hydrology).	86
Figure 5.9	Land use of the Alresford catchment in 2000 (Data source: Southampton GeoData Institute).	88
Figure 5.10	SCP concentration profile for core AP 09-03.	91
Figure 5.11	Cumulative SCP percentage profiles of south and central England showing confidence limits for each 10% (from Rose and Appleby, 2005).	92
Figure 5.12	Combined cumulative percentage of SCP profile for Alresford Pond.	93
Figure 5.13	Linear regression of SCP cumulative percentage profile. The black plots represent date markers with error margins, the black dashed line is their linear regression line (equation: $y = -1.2083x + 2416.2$, $R^2 = 0.9795$). The solid purple and blue lines are the linear regressions of low ($-1.4782x + 2959$, $R^2 = 0.9847$) and upper ($y = -1.0128x + 2023.7$, $R^2 = 0.9674$) error margins.	93
Figure 5.14	Comparison of SCP concentration between core AP 09-01 and ALR1 (after Susanna Black, 2007).	96

	(a)Magnetic susceptibility profiles for core AP 09-01, AP 09-02 and AP 09-03;(b) Enlarged views of magnetic susceptibility profiles for core AP 09-01, AP 09-02 and AP 09-03 at the depth of 10-100 cm. Red lines showing correlation points of peak and trough values between cores.	98
Figure 5.15		
	Bivariate plot of (a) χ_{LF} against $\chi_{FD}\%$ for samples of lake sediment AP09-03 (1976-2009) and soils; (b) χ_{FD} against $\chi_{FD}\%$ values for topsoil samples.	100
Figure 5.16		
	(a) Total annual adjusted effective precipitation used to drive catchment simulation; (b) land cover index (M value); (c) total annual sediment discharge; (d) total cumulative sediment discharge.	102
Figure 5.17		
	Erosion and deposition in Alresford catchment at different time phases (a) 1896-1910, (b) 1911-1925, (c) 1946-1960 and (d) 1995-2009 compared with (e) DEM before simulation.	105
Figure 5.18		
	Patterns of erosion and deposition at different time phases (a) 1896-1910, (b) 1911-1925 and (c) 1995-2000.	106
Figure 5.19		
	Comparison of modelled annual sediment discharge and lake sediment accumulation rate from 1889 to 2009.	108
Figure 5.20		
	Record of modelled monthly water discharge.	109
Figure 5.21		
	(a) Annual precipitation (b) forest cover represented in M values (c) logged low frequency susceptibility (d) total annual sediment discharge.	110
Figure 5.22		
	Flood frequency distribution of 'original rainfall' and 'effective rainfall' water discharge.	114
Figure 5.23		
	Geomorphic patterns after simulation of (a) effective rainfall, (b) original rainfall over 151 years.	116
Figure 5.24		
	(a) Distribution of maar lakes in the west Eifel region (from Scharf and Menn, 1992; Negendank et al., 1990); (b) Location of	121
Figure 6.1		

	Eifel volcanic field (from Sirocko <i>et al.</i> , 2013).	
Figure 6.2	Aerial photograph of Lake Holzmaar (from http://www.gesundland-vulkaneifel.de/gesundland/vulkanismus/maare-kraterseen/holzmaar.html).	123
Figure 6.3	Location of Lake Holzmaar and its catchment (from Zolitschka, 1998; Lücke <i>et al.</i> , 2003).	125
Figure 6.4	Average monthly distribution of precipitation from 1961 to 1990 in the Holzmaar catchment, Germany.	127
Figure 6.5	(a) Decadal precipitation; (b) annual forest-cover in M values; (c) total sediment discharge every 50 years; light grey shadows highlight forest cover reduction and pink shadows highlight precipitation peaks.	129
Figure 6.6	Erosion and deposition during (a) 5000-3000 calendar year BP (3050-1000 BC) and (b) 2999-0 calendar year BP (999 BC-1950 AD) in Holzmaar catchment. Positive values indicate erosion and negative values indicate deposition. Blue circles with numbers indicate focus areas that are discussed.	133
Figure 6.7	Comparison of (a) non-arboreal pollen percentages (NAP %), (b) Magnetic susceptibility, (c) sediment accumulation rate of mineral material from lake sediment records and (d) modelled total sediment discharge from CAESAR in the Holzmaar catchment.	136
Figure 6.8	Simplified pollen data from Lake Holzmaar for 11, 000 varve years (from Litt <i>et al.</i> , 2009).	138
Figure 6.9	Chronological table for land use and pollen record (after Löhre and Nortmann, 2008; Herbig and Sirocko, 2012).	139
Figure 7.1	DEM of the designed simple catchment.	148
Figure 7.2	Sediment grain size distributions for run 1 to 4 (coarse sediment) and run 5 (fine sediment).	149

Figure 7.3	Simulated daily sediment discharge for 300 days.	150
Figure 7.4	Simulated daily sediment discharge for 25,000 days. Inserted graph shows the simulation for 300 days under same initial conditions, the vertical scale is recalculated for comparison. Red solid line is the smoothed trend of temporal sediment discharge.	151
Figure 7.5	Regular hourly rainfall distribution and simulated water discharge.	152
Figure 7.6	Spatial pattern of simulation after 25,000 days. Left: catchment elevation model; right: net erosion (positive value) and deposition (negative value) of catchment.	152
Figure 7.7	Simulated daily sediment discharge (Qs) from different M values over 25,000 days.	153
Figure 7.8	Simulated sediment discharges with alternative grain size distribution (finer) over 25,000 days. Inserted graph shows the simulation for original grain size distribution (coarser) under same initial conditions. Red solid lines are the smoothed trend of temporal sediment discharge.	153
Figure 7.9	Comparison of simulated sediment discharge and rainfall and non-arboreal pollen (NAP %). The entire timescale is divided into four phases representing specific time periods in terms of variability in sediment yield.	155
Figure 7.10	Bivariate plots for 4 phases (cal. yr BP). Phase I: ca.5000-2800; Phase II: ca.2800-1700; Phase III: ca.1700-1100 and Phase IV: ca.1100-0. Left: non-forest cover (NAP %) versus sediment discharge (QS); Right: Rainfall versus sediment discharge (QS).Red dotted lines are smoothed trend of sediment discharge for Phase II and IV.	155
Figure 7.11	Relationship between vegetation cover (M value) and sediment discharge, showing in two phases (1889-1960 and 1960-2009). Red dotted lines are regression lines.	157

Figure 7.12	Relationship between precipitation and sediment discharge, showing in two phases (1889-1960 and 1960-2009). Red dotted lines are regression lines.	158
Figure 7.13	Relationship between water and sediment discharge for simple catchment over 25,000 days.	161
Figure 7.14	Comparison between simulated sediment discharge and rainfall in Alresford catchment.	163
Figure 7.15	Magnitude-frequency distribution of modelled sediment discharge for the simple catchment (upper) and the simulation from Coulthard and Van De Wiel (lower, 2007).	164
Figure 7.16	Magnitude-frequency distribution of sediment discharge for Alresford catchment in two time phases: 1889-1960 and 1961-2009.	165
Figure 7.17	Magnitude-frequency distribution of modelled sediment discharge for Holzmaar catchment in four time phases: Phase I: ca.5000-2800 cal. yr BP; Phase II: ca.2800-1700 cal. yr BP; Phase III: ca.1700-1100 and Phase IV: ca.1100-0 cal. yr BP.	167
Figure 8.1	Flow chart of modelling results analysis.	176
Figure 8.2	The distribution of mean annual water discharge lumped every 30 years for the Low, Medium and High emission scenarios. The lower and upper limits of each box are baseline and 50% probability level, respectively. The down whiskers are 10% probability level and the up whiskers are 90% probability level.	177
Figure 8.3	Cumulative daily sediment discharges for all probability levels (blue, red and green lines) and baseline (black lines) in the periods of 2020s, 2050s and 2080s (vertically) under the Low, Medium and High emission scenarios (horizontally).	179
Figure 8.4	Comparison of mean monthly water discharge and baseline results (1961-1990) for all probability projections from 2010-	181

	2099 under three different emission scenarios.	
Figure 8.5	Comparison of mean monthly sediment discharge and baseline results (1961-1990) for all probability projections from 2010-2099 under three different emission scenarios.	182
Figure 8.6	Relative changes (%), to the 1961-1990 baseline, in mean monthly (a) precipitation, (b) water and (c) sediment discharge for the future periods at 10%, 50% and 90% probability levels under medium scenario in 2050s.	184
Figure 8.7	Frequency distribution plots of daily flow for all future climate change scenarios (straight lines) compared with 1961-1990 baseline results (black dashed line).	185
Figure 8.8	Frequency distribution plots of daily Sediment discharge for all future climate change scenarios (column charts) compared with 1961-1990 baseline results (black line).	186
Figure 8.9	Total sediment yields for different land use scenarios within three climate change bounds in the future 100 years (from 2010 to 2090).	191
Figure 8.10	Cumulative sediment discharge for each scenario (blue =clear, red=original, green=forest; dotted line = 10% probability level, straight line =50% probability level, dashed line=90% probability level).	192
Figure 8.11	Sediment response to land use changes under different emission scenarios; upper: distribution of mean 30 year total sediment discharge; Lower: calculated total sediment discharge (m3).	195
Figure 9.1	Complexity of the erosion process in fluvial system (modified from Knighton, 1998; Michaelides and Wainwright, 2004; Quinton, 2004; Brazier, 2012).	201

DECLARATION OF AUTHORSHIP

I,

Ying Wang

declare that the thesis entitled

Simulating Complex Hydro-geomorphic Changes in Lake-Catchment Systems

and the work presented in the thesis are both my own, and have been generated by me as the result of my own original research. I confirm that:

- this work was done wholly or mainly while in candidature for a research degree at this University;
- where any part of this thesis has previously been submitted for a degree or any other qualification at this University or any other institution, this has been clearly stated;
- where I have consulted the published work of others, this is always clearly attributed;
- where I have quoted from the work of others, the source is always given. With the exception of such quotations, this thesis is entirely my own work;
- I have acknowledged all main sources of help;
- where the thesis is based on work done by myself jointly with others, I have made clear exactly what was done by others and what I have contributed myself;
- none of this work has been published before submission

Signed:

Date:.....

Acknowledgements

I would like to extend my heartfelt thanks to the following people who have provided constant encouragement and support, invaluable help and advice during my 4-year PhD research.

My supervisors, Professor John Dearing, Professor David Sear and Dr Peter Langdon, for giving me the opportunity to discover the interests of palaeoenvironment and modelling research, and keeping me on the straight; your support and guidance help improve my ability of independent thinking of science and English skills, and broaden my views on scientific disciplines, which will benefit me for life; your time, patience and advice is truly appreciated. Thanks also go to Professor Tom Coulthard from the University of Hull for important guidance on CAESAR modelling, which is the most important section of this research. My thanks are also given to Professor Bernd Zolitschka from Universität Bremen for his support to my various questions and data requirement.

All of the staff and fellow postgrad students of the Environment and Geography at the University of Southampton for their help to my requests of information and data, technical supports of GIS and lab experiments, proof-reading supports and your efforts to create a friendly environmental to work in; in practically Dr Julian Leyland, Ms Hayley Essex, Mr Simon Dixon, Ms Sarah Pogus, Ms Katherine Hesketh and members of Palaeoenvironmental Laboratory (PLUS).

I wish to thank my family, my dear parents Mr Huning Wang, Mrs Lanping Tang, Mr Changyang Fang, Mrs Guoli Li and my husband Mr Yichun Fang. Without your love, encouragement, understanding, your concern to my life and your confidence in me, I cannot reach the end of journey. I am so lucky to be loved by all of you and I cannot thank you all enough.

Finally, I acknowledge the graduate school of University of Southampton for tuition funding of this PhD research for the last three years.

Thank you very much all.

Chapter 1

Introduction

1.1 Background

The river basin is an environmental unit, structured by gravitational processes (Newson, 1994). The influence of environmental change on catchment behaviour, and the complex and hierarchical structure of a river catchment system (Leopold *et al.*, 1964) have both been recognised with growing interest since the 1950s (Schumm, 1965; Gregory and Walling, 1973; Costa *et al.*, 1995; Knox, 2000; Lewin *et al.*, 2005). Climate change as an environmental driver is represented principally by precipitation and runoff; for example, the occurrence of extreme floods and droughts, influences soil moisture and erosion. Other factors include catchment management and human activities, tectonic activities and base-level effects (Macklin *et al.*, 2012). Therein human activities affecting land-use and cover have an impact on flow regime, sediment supply over time and geomorphology, which result in the diversity and complexity of fluvial systems (Macklin *et al.*, 2006). In practice, deforestation and cultivation may leave the catchment bare and, under the same rainfall amount and intensity, soil loss from the surface can be several orders of magnitude higher than where there is full plant cover, with excess sediment in channels (Williams, 2012). Fluvial systems respond to these factors by depositing and transporting transient sediment through catchment erosion and by adjusting landforms resulting from changing of sediment supply and size, including channel dimensions and patterns. Moreover, the nature of a river catchment is recorded by sedimentary signals and sequences over thousands of years to decadal timescales.

Both internal (autogenic adjustment within the system) and external (climate and land cover changes) environmental controls (Hancock, 2012) are discernible in changing the behaviour of river hydrology, sedimentation and morphology and

display features of non-linearity with feedback mechanisms. For instance, large flooding events may produce rapid sediment delivery but sediment may also be accumulated in periods of infrequent or smaller floods. Furthermore, different thresholds and relatively small changes in environmental factors may trigger significant changes in erosion rates and patterns. Self-organised capability (Phillips, 1995; 2009) alters the quasi-equilibrium states in lake-catchment systems over long time series (Macklin *et al.*, 2012). Taking account of river dynamics and complexity, models can either isolate an individual forcing by controlling for other parameters or combine possible variables to investigate system response to different forcings (Dearing, 2006). Comparison between modelling results and empirical data can help to test models' ability to quantify soil erosion and has been an important tool in further understanding of landscape evolution in time and space (e.g. Coulthard *et al.*, 2012).

According to the annual report of European Environment Agency (2012), the average temperature over land in Europe in the last decade was 1.3 °C warmer than the pre-industrial level (end of the 19th century). Over the same period, precipitation has increased in northern and north-western Europe but it has decreased in southern Europe. Storm frequency was increasing from the 1960s to 1990s but was followed by a decrease to the present. The IPCC Fourth Assessment Report (AR4) suggests that continued greenhouse gas emissions at or above current rates would cause further warming and the likely range of temperature change will reach 1.1 to 6.4 °C at 2099 compared to the level of 1980 -1999. It is very likely that hot extremes, heat waves and heavy precipitation events will become more frequent with increases in the amount of precipitation in high-latitudes, while decreases are likely in most subtropical land regions. The UKCP09 report (UK Climate Projection, 2009) predicted that southern England will experience increasing precipitation in the range of +10% to +30% in winter and decreasing precipitation of almost 40% in summer at 2080. In terms of land use, it is reported that erosion rates in England and Wales have been increasing due to the intensification of agriculture, especially the adoption of

winter cereals (Boardman *et al.*, 1990) in the lowlands and overgrazing in the uplands (Evans, 1977) since the 1970s. Recent research suggests that agriculture demand could increase by 25-180% by the 2050s (Johnson *et al.*, 2009; Weatherhead and Knox 2000; Henrique *et al.*, 2008). All of these documents indicate extensive stress on soil erosion either occurred or possibly will occur under future climate and land use conditions. Therefore, scientific assessment of catchment erosion by using suitable projected scenarios in the coming 100 years is necessary for further research on sustainable catchment environmental management.

Management of the catchment environment is a long-term challenge for the prevention of hazard and further sustainable development. The aims of sustainable catchment management include flood forecasts/warnings, water resource protection and development, irrigation management, pollution control, fisheries protection, land-use management and soil erosion control (Newson, 1994). There is growing institutional and governmental concern about how rivers have responded or are expected to respond to deforestation, agriculture, urbanization or climate change in order to stabilize and maintain present river environments, or to develop appropriate policies in response to those changes (James and Marcus, 2006). Therefore, knowing the fundamental behaviour of hydro-geomorphological processes in fluvial systems over a range of timescales can provide important information about internal properties, likely trajectories, predictability and interactions with other systems, all of which are essential for creating the tools and strategies needed for sustainable catchment development and management (Dearing and Zolitschka, 1999; Dai *et al.*, 2009).

1.2 Aims of research

In this study, I hope to explore to what extent past and present interactions between climate and human activities will generate future impacts for the purpose of reducing catchment risk through effective landscape management. Many soil conservation and

sediment control techniques are known and widely studied, including for instance reduced tillage or zero tillage, cover crops, grass buffer strips between fields or along rivers and sediment retention ponds (Verstraeten *et al.*, 2002). The effects of most of these techniques have been analysed using experimental field plots. However, their impact at a catchment scale is not obvious. A conservation strategy should therefore integrate a variety of suitable control techniques into a catchment management plan. To evaluate the impact of a series of possible management scenarios, a stronger spatially distributed model is needed.

Conventional flood risk studies have therefore focused on statistically based methodologies for the determination of extreme water levels in drainage basins at a specific point of interest. Statistics is a science of description, based on mathematical principles which identify the variation in a set of observations of a process (White, 2007). However, catchments are complex dynamic systems, where responses in the sediment delivery to human actions or meteorological events may reverberate over large distances with significant time lags (Dearing and Jones, 2003). Thus, it is desirable to explore the use of spatially distributed and process-based models to simulate the behaviour of hydro-geomorphological processes in a fluvial system over long timescales. Cellular models can incorporate many processes within a simple framework that allows continuous feedback effects to generate emergent properties. However, there are some limitations such as grid scales, vegetation changes and soil particle size distributions. Therefore, an improved cellular automaton model which is capable of modelling amalgamative slope, fluvial and hydrological processes over different time scales is needed. The overall goal of this study is to test and apply an established cellular automata landscape evolution model (CAESAR) to study the dynamic non-linear behaviour of complex systems, past and present interactions among landscape elements and environmental controls, and potential future impacts. It is addressed by a specific set of objectives listed below.

1.3 Objectives of the research

- 1) To investigate the effects of climate change and human activities (e.g. land use changes, watercress cultivation etc.) on river-catchment evolution.
- 2) To develop and applying a dynamic model to simulate the landscape evolution of catchments over different timescales (approximately 150 years and 5000 years).
- 3) To compare short term (151 years) modelled water and sediment discharge with instrumental data, empirical data (e.g. sediment flux data and magnetic data obtained from sediment records).
- 4) To compare modelled temporal and spatial pattern of erosion and deposition to real field observations of catchment geomorphology (e.g. the elevation difference can be calculated and displayed by ArcMap over different periods to show the erosion and deposition conditions spatially).
- 5) To compare the behaviour of long term (5000 years) modelled sediment discharge with laminated lake sediment record (e.g. Zolitschka, 1998).
- 6) To interpret the contribution of climate and land use to sediment movement through the results from both long-term and short-term simulations.
- 7) To explore the role of non-linearity and self-organised criticality and their behaviour in complex river catchment system (from designed simple catchment to real dynamic systems)
- 8) To apply the model to simulate the nature of hydro-geomorphological processes based on a series of possible scenarios built for land use and climate changes in the coming 50-100 years.

The processes required to achieve these objectives according to the time line: from the past to the future, are configured in Figure 1.1.

1.4 Structure of the thesis

Following this introduction, the heart of this thesis concentrates on testing model simulations by comparing model outputs of water and sediment discharges to environmental behaviour from observed and lake sediment records. Once the model is calibrated and validated to be robust enough to capture the dynamics of the river system, it is driven forward to explore regional hydro-geomorphic response to likely future projections of environmental changes and hence appropriate landscape management.

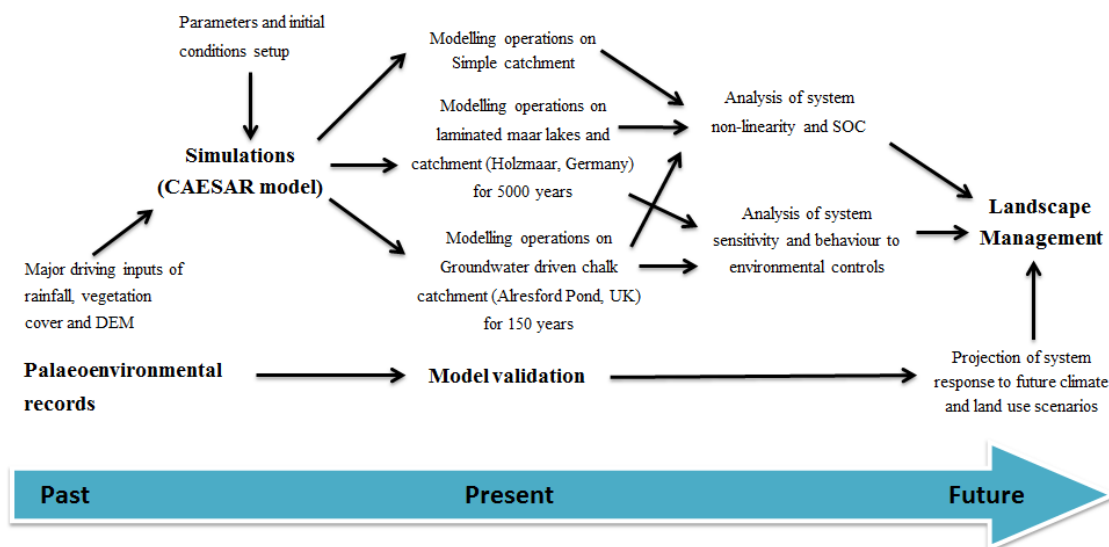


Figure 1.1 Research programme structure

Chapter 2 reviews landscape behaviour to environmental changes, previous approaches used to investigate environmental changes in complex fluvial systems and the urgent requirement for models.

Chapter 3 provides a background of numerical model development and application with specification to cellular automata models and detailed introduction to the CAESAR model, which will be used in this thesis.

Chapter 4 outlines methods used in this research, including preparation of

palaeoenvironmental data for the two catchments, creations of input files for all the simulations and initial conditions setup.

Chapter 5 illustrates modelling results from Alresford catchment for a 151 year period and the construction of chronology and magnetism properties from lake sediment. Spatial and temporal comparison between simulation outputs and environmental information is applied for model validation and to provide some insights to the hydro-geomorphic response of a chalk catchment to environmental drivers.

Chapter 6 tests the feasibility of CAESAR model for long term simulations by comparing modelled sediment with lake sediment archives over 5000 years. It also highlights the human influence on the natural environment.

Chapter 7 is the key discussion chapter that demonstrates the role of non-linearity and self-organisation in complex fluvial systems. It provides evidence for the non-linear behaviour in different fluvial systems and possible factors that control them.

Chapter 8 describes the application of the CAESAR model to Alresford catchment under future climate and land use change scenarios in the next 100 years.

Chapter 9 offers a synthesis of all key findings in the research and considers future study directions.

Chapter 2

The Complexity of River Systems – from Past to Future

2.1 Landscape behaviour to environmental changes

More and more research is drawing our attention to the perspective that a river catchment is a complex cascading system (Dearing and Jones, 2003) affected by the destructive power of human impact and nature on both local and global scales. One of the direct effects of human actions and climatic events on fluvial systems is landscape evolution, with materials such as sediment shifting from one place to another (Church, 2010) through erosional processes and subsequent mobilisation and deposition by running water, wind, glacial ice etc. (de Moor and Verstraeten, 2008). The nature of this forcing-response system may influence landscape development, ecosystem sustainability in both temporal and spatial scales and, in turn, influence the global climate through atmospheric oceanic cycles (Dearing and Jones, 2003). The annual report of the European Environment Agency (EEA, 2012) has highlighted a decrease in river flows in southern and eastern Europe, increases in the frequency and magnitude of both flood and drought events, earlier flowering and harvest dates for cereal crops, increased water demand for irrigation, and reduction in forest growth in central and western Europe. It is important to recognise that geomorphological processes in response to environmental changes are based on the hydrological cycle (e.g. the impact of precipitation on runoff) and land surface cover effects. Therefore, there is a need for adequate knowledge of system sensitivity to climate and human forcings in hydrological and geomorphic processes, for the sake of the sustainable management of drainage basins.

2.1.1 Hydrological process of flooding

Widespread flooding is a natural disaster and has long been recognized as one of the most damaging, dangerous and costly hazards in the United Kingdom. For example, the historic town of Lewes on the River Ouse in East Sussex was hit by serious

floods that devastated the town centre and caused millions of pounds worth of damage in 2000 (White, 2007). It is estimated that localised flooding in England and Wales may increase by up to four-fold by 2080 (Burningham *et al.*, 2008), primarily as a result of global warming. As a consequence, roughly five million people and two million properties will be at a risk of flooding. In this sense, flood risk is an issue of considerable concern and rational risk assessment has become one of the most important challenges that currently face river basin managers in the UK (Macklin and Rumsby, 2007).

A flood begins when main channel water levels are sufficient to exceed local bank height (Lane *et al.*, 2007). Thus, flood risk is driven by changes of rainfall in the river channel, which may impact on both flow magnitude and river channel conveyance. In Bronstert's (2003) view, floods can be divided into two categories according to the size of the affected area and the duration of precipitation. Extensive or plain floods are caused by rainfall lasting several days or even weeks in connection with high antecedent soil saturation. Flooding results from extensive and long-lasting rainfall, partly related to the melting of snow and ice, occurs mostly on plains and in large areas when the dikes along the main rivers can no longer contain the flood discharge. Local or flash floods are a kind of flooding mainly caused by short, high intensity precipitation (e.g. thunderstorms) in small catchments. Flash floods occur primarily in hilly or mountainous areas due to prevailing convective rainfall mechanisms, thin soils, and high runoff velocities. The duration of this type of flood event is short, but it frequently causes severe damage as a result of the intensive rainfall and short warning time for these events. Although the risk of flooding is mainly concentrated in lowland regions, catchment headwaters, with their generally higher precipitation rates and quicker responses, are also important source areas for runoff generation (Marshall *et al.*, 2009).

It is generally accepted that increased precipitation resulting from climate change (White, 2007) and sea level rise, coupled with pressure from increased urbanization and land use changes (Brown and Damery, 2002) as a consequence of human activities, are critical factors for flooding, which is therefore likely to become more frequent and severe in the future. Yin and Li (2001) attributed the magnitude of flooding and its long duration to the detrimental human intervention within the river

basin, which included vegetation destruction and soil erosion in the upper reaches; decrease of the flood storage capacity due to land reclamation and siltation; and the construction of levees that caused flood levels to rise due to restricted flood discharge capacity. Marshall *et al.* (2009) focused their work on the impact of modern agricultural practices, especially grassland management, on the increasing risk of flooding based on changes in soil structure and runoff processes (O'Connell *et al.* 2007). There is also evidence that climate change could be responsible for increases in the magnitude of peak flows (Middelkoop *et al.*, 2001; Milley *et al.*, 2002) and flood frequency (Hunt 2002). On the basis of a wide array of proxy sources, such as ice cores, tree rings, corals, and lake sediments, it has been concluded that the 20th century is at least as warm as any other century of the last millennium, and may be even warmer (Bronstert, 2003). Along with global warming, increasingly heavy precipitation at continental and global scales supports the view that the global hydrological cycle is intensifying (Huntington 2006), forcing Europe into a relatively flood-rich period.

When attempting to justify flood defence works or improvements in monitoring and prediction, traditional flood management strategies have either overlooked the important social dimensions of public hazard understanding and vulnerability, or they have incorporated these factors through inappropriate quantitative measures, such as cost-benefit analysis. Instead, there is a need to adopt long-term risk management strategies grounded in an understanding of exposure to the flood hazard, characteristics and patterns of vulnerability, and the relationships between different stakeholders in the perception of flood risk (Brown and Damery, 2002).

2.1.2 Geomorphic process of soil erosion

Soil is essential for human subsistence. The erosion of soil can occur at widely varying rates over fields, floodplains, water bodies, and even along a typical landscape profile within a field (Foster, 1988). Driven by water, soil erosion can be categorised as sheet, rill, concentrated flow, gully and stream channel erosion (Foster, 1988), and occurs in three forms or stages (Zhang *et al.*, 1996). The first stage is sheet erosion, which is principally caused by raindrop impact, and removes soil in a thin, almost imperceptible layer. Rill erosion is the development of numerous small,

eroded channels across a landscape due to surface runoff. These small channels are formed because of natural areal variations in the erosion resistance of the soil and small variations in elevation and slope. Flows from a large number of rills concentrate in gullies during the final stage of soil erosion, and gullies are fairly permanent topographic features (Bennett, 1974; Zhang *et al.*, 1996). Accordingly, understanding the controls on recent changes in soil erosion, sediment delivery, and sediment yield is of benefit to policy makers tasked with the management of rivers with high sediment loads (Walling, 1997).

Although soil erosion is a natural process, increasing population and economic development, associated with anthropogenic activity (such as intensified land use and forestry, overgrazing, deforestation, vegetation clearance and global climate change due to emission of greenhouse gases; Bronstert, 2003; Walling, 1997) may accelerate erosion and add sediment loads. Soil erosion and the delivery of eroded sediments to river channels can reduce soil productivity, generate downstream damage (Ritchie and McHenry, 1990) and pose substantial financial burdens on society. Problems related to soil erosion on arable land have numerous detrimental impacts, including the loss of topsoil and fertilisers, decreased crop yield (when plants are eroded or covered with sediment deposits) and accessibility (due to gullies) in the short-term, and decreased soil productivity in the long-term (Verstraeten *et al.*, 2002, Ward *et al.*, 2009). Sediment delivery also affects channel and floodplain morphology (e.g. Asselman and Middelkoop, 1995; De Moor *et al.*, 2008), the ecological functioning of floodplains (Richards *et al.*, 2002), and sediment deposition rates in reservoirs and ponds (Verstraeten and Poesen 1999). Other problems associated with soil erosion include pollution of surface water with suspended sediment and other pollutants adsorbed to sediment particles (e.g. phosphates or heavy metals); silting of riverbeds, reservoirs and ponds requiring costly dredging operations; muddy flooding in local villages and substantial financial and psychological damage resulting from public infrastructure and private property (e.g. Boardman, 2010; Verstraeten and Poesen, 1999; Verstraeten *et al.*, 2002).

2.2 Understanding the past from lake sediment records

An understanding of past environmental changes that have occurred over previous decades and centuries is undoubtedly crucial to enable greater understanding of present and future landscape evolution and system assessment under the influence of human and natural drivers such as climatic fluctuations and shifts in land use. Learning from the past through comprehensive palaeo-environmental archives could contribute to establishing the trajectories of forcing and response that led to current conditions (Dearing and Jones, 2003) and the possible thresholds for sensitivity or resilience to particular climate and human impacts in the future (Dearing, 2006). It is well known that rivers are efficient conveyors of water and sediment to lakes (Williams, 2012). Information on erosion and deposition availability, transporting energy in catchment, hydrological and geomorphological processes and landscape evolution can be discerned by exploring sediments (Dearing, 1991). Foulds *et al.* (2013) investigated the change in sedimentation style of an agro-industrial alluvium (Swale catchment) in northern England by using a combination of methods, including geomorphological mapping, sedimentological and geochemical analysis, dating controls, land use history with palynological evidence and climate proxies. They suggested the transformation of the Swale floodplain is a reflection of regional land use and climate signals of the Anthropocene. Therefore, efforts to understand the nature of river systems often start with efficient studies of sediments using a series of approaches and technologies.

2.2.1 Dating methods

After 1950, with the development of technology (e.g. modern topographical mapping and high resolution aerial photography), earth science entered an era of unprecedented prosperity, leading to a rapid expansion of exploration and monitoring practices for earth surface environments (Church, 2010). One significant achievement was the development of dating methods due to an urgent requirement for precise and reliable chronology. In addition, statistics were introduced into empirical science to quantify landscape variability. Radioisotope measurement pioneered in the early 1970s provided methods for establishing high resolution sediment chronology to recover data on environmental changes stored in lake

sediments (van de Post *et al.*, 1997; Oldfield & Appleby 1984). In addition, accurate dating is of importance in interpreting changing rates and sources of allochthonous sediments related to soil erosion (Xue & Yao, 2011; Dearing, 1991).

For dating long sedimentary sequences, radiocarbon (^{14}C), which is produced in the atmosphere by the interaction of cosmic rays (Olsson, 1986), is appropriate for dating organic remains within the time range of about 500 to 40,000 years old (Smol, 2002). The decreasing of ^{14}C content at the decay rate, when carbon replenishment stops because of an organism such as plant or animal dies, provides an age measurement. Owing to the limitations of radiocarbon dating for modern sediment (younger than 300 years), the short-lived radioactive isotopes of, for instance lead (^{210}Pb) and caesium (^{137}Cs), are employed and developed. Lead-210, with a half-life of 22.26 years, is constantly decaying in the uranium decay series. It falls onto the soil surface or directly into lakes by precipitation or dry deposition from the atmosphere and is removed by water and deposited as sediment (Appleby, 2001). Two simple models, referred to as constant initial concentration (CIC) and constant rate of ^{210}Pb supply (CRS) models are widely applied to calculate sediment age (Robbins, 1978; Appleby and Oldfield, 1978; Appleby, 2001). The CIC model is useful for homogeneous sediment that has a constant rate of accumulation. The CRS model is more suitable for lakes where the sediment accumulation rate varies inversely with the concentration of ^{210}Pb , or where the pattern of sediment focussing has been changed. Battarbee *et al.* (1985) reported accelerated soil erosion following forest clearance by correlating changes in sediment accumulation with afforestation history in seven lake catchments in the UK that have similar geological and climatic conditions, based on ^{210}Pb dates. Under some circumstances of physical or biological disturbance of surficial sediment, neither of the two models is valid, and so independent dating evidence for certain time periods is essential to validate the ^{210}Pb results. Radioactive fallout caesium-137, one of the artificial radionuclides released after the onset of atmospheric nuclear weapons tests in 1954, can be used as a tracer to independently date sediment records. As a consequence of such nuclear fission, ^{137}Cs was globally distributed in the stratosphere and redeposited to the Earth's surface as precipitation-facilitated fallout, with a peak in fallout in 1963 (Jerry *et al.*, 1990; Davis, 1963; Longmore, 1982). The nuclear power plant accident at Chernobyl in 1986 was another source of ^{137}Cs fallout, but the distribution of

fallout was uneven and had a limited impact on global fallout patterns (Appleby, 2001; Volchok and Chieco, 1986; Jerry *et al.*, 1990). The spatial distribution of ^{137}Cs has been studied by McHenry and Bubenzer (1985) to explore the movement and deposition pattern of eroded materials within watersheds. Quine and Walling (1993) have demonstrated the potential of determining the topographical controls on the variations in ^{137}Cs derived soil erosion rates for arable fields with different soil types in lowland UK. Recent studies combining ^{137}Cs and ^{210}Pb dating methods have provided more reliable relationships between the age and depth of lake sediment cores for estimating soil erosion rates. Appleby (2008) reviewed studies of the widespread applicability of the fallout radionuclide method and its success in dating sediment records from lakes varying in size, sedimentation rate and environmental conditions.

In addition to these commonly used radioisotopes, spheroidal carbonaceous particles preserved in sediments, which are related to fossil fuel burning, can also be used as time markers. Fossil fuels such as coal and oil droplets are burned at temperatures approaching 1750°C to produce heat and power for energy industries (Rose, 2001). The products of incomplete combustion of fossil fuels are porous spheroids composed mainly of elemental carbon called spheroidal carbonaceous particles (SCPs) (Goldberg 1985). SCPs are diffused into the atmosphere with flue gases and are stored in sediments either by precipitation or dry deposition. SCPs are not produced from wood or charcoal combustion, and hence have no natural sources (Rose 2001). Changes in the distribution and concentration of SCPs are closely related to atmospheric deposition from industrial emissions that consequently make SCPs as indicators of atmospheric contaminants. Vukic and Appleby (2003) investigated SCPs in sediment collected from a reservoir in the Czech Republic and found the distribution of SCPs was mainly influenced by wind and inlet-induced currents, correlated well with local industry pollution. Rose *et al.* (2002) collected and analysed data on atmospheric flux, catchment soil and lake sediment SCP profiles from five mountain areas cross Europe with various pollutant features. These data all indicated that catchment soils are a primary sink for deposited SCPs derived from atmospheric pollutants, which could lead to greater input of contaminants to lake systems through increasing soil erosion (Bragg and Tallis, 2001; Rose *et al.* 2002)

As SCPs are stable in lake sediments, they have been developed for sediment dating by Renberg and Wik (1984, 1985) in Sweden over the last 20-25 years. Rose (1990, 1994) improved the Renberg and Wik methods of SCPs dating in terms of extraction, sensitivity and precision. This was later widely applied as age equivalent markers for dating throughout the United Kingdom and Ireland to explore the regionality of time trends (Rose, 1995; 1999b; 2005). Similar temporal patterns were found in the SCP records across the UK and Ireland: the start of the SCP records at the time of the Industrial Revolution, sharp increases in SCP concentration following the boom in electricity generation after the Second World War, and a subsurface concentration peak. Since SCPs have steady movement and accumulation, Yang *et al.* (2001) proved the applicability of using SCP profile in peat cores to provide a recent chronology by comparing SCP records in lake sediments with the catchment peats from Lochnagar, Scotland. The record of peat SCPs matched the three features of SCP dating, implying that the SCP dating method is suitable for use in peats, where ^{210}Pb dating is not appropriate due to the remobilisation of trace metals. A combined methodology consisting of radioisotope or radiocarbon ages and SCPs was used for chronology in further research (e.g. Charman *et al.*, 2004, 2012 and Rose *et al.*, 1999a). These studies concluded that converting SCP concentrations to cumulative percentages can diminish localised differences in SCP profiles and allows for better cross correlation and date allocation. This method was effectively applied across the whole of the UK to determine the regional temporal trends (Rose and Appleby, 2005).

Annual laminations or varves have in recent years been applied and developed in palaeo-environmental investigations with growing interest because they provide reliable and high resolution chronology and environmental records (Lamoureux, 2001). Starting from the pioneering work that defined the term ‘varve’ as the annual cycle of deposition, De Geer (1912) used the chronological information stored in varves to estimate the age of ice sheet retreat (Zolitschka, 2007). Chronology construction from laminated sediment was developed and extended from proglacial environments to absolutely date the Late-glacial period (Lotter, 1991; Landmann *et al.*, 1996; Brauer *et al.*, 1999) and measure the duration of the Younger Dryas (Goslar *et al.*, 1993; Litt *et al.*, 2001). Varves were also widely used to test the reliability of other dating methods, for example radiocarbon dating (Björck *et al.*,

1987; Wohlfarth *et al.*, 1995; Goslar *et al.*, 1995; Oldfield *et al.*, 1997; Hajdas *et al.*, 2000), radioisotope dating (Appleby *et al.*, 1979; Anderson *et al.*, 1994; Reinikainen *et al.*, 1997), tephrochronology (Zolitschka *et al.*, 1995; Zillén *et al.*, 2002), palaeomagnetism secular variation (Saarinen, 1998; Snowball and Sandgren, 2002; Ojala and Tiljander, 2003) and historic events (Lüder *et al.*, 2006), and to calculate the curves of shoreline displacement rate (Renberg and Segerström, 1980). A prerequisite for the chronology is to determine the annual structure of varve based sediment through counting varves and thickness measurements (Ojala and Tiljander, 2003; Zolitschka, 2007). This includes varve micro-facies analysis conducted on large-scale thin sections (Neugebauer *et al.*, 2012) via scanning electron microscopes (Dean *et al.*, 1999), optical microscopes (Lang and Zolitschka, 2001) and digital image analysis (Saarinen and Petterson, 2001); photographs of the levelled sediment surface (Renberg, 1981; Petterson *et al.*, 1999) and X-ray radiographs from embedded sediment blocks (Saarnisto, 1986; Ojala and Francus, 2002; Ojala, 2005). It was suggested by Ojala *et al.* (2012) that a typical chronology provides an accuracy of $\pm 1-4\%$. However, they also emphasised the importance of varve chronology verification with other independent dating methods due to the unavoidable systematic errors associated with some poorly preserved or indistinct varves. Tylmann *et al.* (2013) applied a multiple dating method using varve counting, ^{210}Pb , ^{137}Cs and optically stimulated luminescence (OSL) for sediments from a lake in northern Poland, which demonstrated the need for cross-checking varve ages.

2.2.2 Sediment fingerprinting methods

Changes in sediment sources and sediment yield to lakes can be used as a means of monitoring catchment hydro-geomorphic processes or identifying landscape sensitivity to various disturbances. Many qualitative and quantitative techniques, such as use of sediment geochemical characteristics, sediment accumulation rate (Ritchie and McHenry, 1990) and mineral magnetism (Walling and Woodward, 1992; Foster and Walling, 1994), have been developed to investigate erosion patterns in fluvial systems. Foster *et al.* (2011) reconstructed sediment yields by using sediment accumulation rates to estimate erosion pressure across England and Wales. They addressed the correlation between the sediment yield and the sediment accumulation

rate and warned that shallow lowland lakes are under the greatest threat from sediment accumulation. Dearing *et al.* (2008) demonstrated the trajectories of human-environment interactions in the Lake Erhai catchment (SW China) from sediment properties including pollen, particle size, geochemistry, stable carbon isotopes and mineral magnetism, providing insight into the sustainability of the modern agricultural system.

Environmental changes related to various physical weathering and erosional processes, in addition to anthropogenic processes, result in different production, transport and deposition conditions for magnetic minerals (Nowaczyk, 2001). All materials display some magnetic properties (Smith, 1999) regardless of strength. These properties can be measured and materials classified according to their behaviour during exposure to an external magnetic field (Sandgren and Snowball, 2001). Magnetic susceptibility is probably the most common magnetic parameter (Sandgren and Snowball, 2001) and the measurement is simple and fast to perform, non-destructive, and yields characteristic patterns with values that span several orders of magnitude (Nowaczyk, 2001). It is proven to be useful for dating and correlation between sediment cores when applying the correspondence of peaks in susceptibility to horizons with high heavy-mineral concentrations (Thompson, 1986). Appley (1985) applied magnetic susceptibility in combination with ^{210}Pb , ^{137}Cs and ^{14}C dating methods to build the chronology of sedimentation in a Scottish lake catchment, and found that these tracers can be mutually rectified for a better dating framework. The variation in susceptibility also provided evidence of links between erosional activities and climate or land use changes. A clear and detailed chronology of sediments from Blelham Tarn in Cumbria, England, was established by van de Post *et al.* (1997) using radioisotopes together with magnetic measurement. They identified surface soils as the main source of rapid acceleration in sedimentation in recent decades and suggested that erosion is closely related to increased pressure from sheep farming.

There are numerous types and a range of concentrations of magnetic minerals preserved in lake sediments that are indicative of soil and slope processes and land use changes. Therefore, measuring the magnetic susceptibility of sediments is the basis for classifying catchment sediment sources and tracing sediment movements

through time (Foster *et al.*, 2003). The majority of magnetic minerals settling in lake sediments are derived from the atmosphere, surrounding catchment erosion, and bedload that is transported in rivers and streams then deposited as sediment in the lake's drainage basin (Sandgren and Snowball, 2001). Atmospheric sources of magnetic minerals within catchments include volcanic ash and dust transported by storms, and anthropogenic pollution. In some lake sediments, detrital minerals, in-situ pedogenic processes, authigenic or diagenetic production and magnetic bacteria are also important sources of magnetic minerals (Dearing, 1999a). Dearing and Flower (1982) showed that the peak of magnetic susceptibility of material in Lough Neagh, in Northern Ireland, corresponded to maximum monthly rainfall. They concluded that high susceptibility was linked to the high proportion of coarser particles delivered to the lake in flood events, thereby providing a process linkage between erosion of substrate or possibly soils and susceptibility records of detrital allochthonous influx (Thompson *et al.*, 1975). By measuring the magnetic susceptibility of lake sediment in Petit Lac d'Annecy (France), Foster *et al.* (2003) demonstrated that magnetic susceptibility records track seasonal discharge. They also argued that cycles of agricultural expansion and deforestation may be the major causes of shifts in the sediment system over the late Holocene.

Furthermore, annually laminated lake sediments can be used in studies of palaeo-environmental evolution by calculating influx and accumulation rate of allochthonous and autochthonous materials based on variations in varve thickness and composition (Snowball *et al.*, 1999). The formation of varved sediment is a complex process related to different environmental factors such as variability of temperature and precipitation, vegetation cover and human activities. It is a consequence of extreme climatic events, snow melt, hydrological cycles, sediment supply, physical and chemical processes in the lakes and their control on biological productivity, which may result in erosion, transportation and deposition of minerogenic and organic materials (O'Sullivan, 1983; Hicks *et al.*, 1994; Hughen *et al.*, 1996; Petterson, 1996; Lotter and Birks, 1997; Cooper *et al.*, 2000). Veski *et al.* (2004) developed a better understanding of the connection between the extreme cold event at 8200 yr B.P. and the weakening of the Atlantic thermohaline circulation through temperature reconstruction from varved sediments in Eastern Europe after verification with records from Greenland ice-core. Ojala *et al.* (2008) established the

seasonal nature of Holocene climatic change from the laminations in Lake Nautajärvi in southern Finland and suggested a good correlation between organic varve thickness and seasonal warmth in the early Holocene. Diatom records, preserved in the formation of laminations in Loe Pool, UK which are attributed to the seasonal algal production and sedimentation, were linked to the local mining history by Simola *et al.* (1981). High resolution pollen analysis of laminated lake sediments provides a useful approach to the study of alternating episodes of vegetation change and stability (O'Sullivan, 1983; Saarnisto, 1986). Laminations identified in several lakes in eastern Finland provided precise pollen diagrams and chemical analyses resulting in accurate reconstructions of cultivation history in association with changing human environmental preferences (Grönlund, 1991; Taavitsainen *et al.*, 1998), and the impact of local slash-and-burn cultivation on changes in forest structure (Pitkänen and Huttunen, 1999).

2.3 The dynamics of river systems

Since the 1980s, our understanding of the relationship between environmental changes and catchment behaviour has developed dramatically, with growing recognition that fluvial systems are complex and dynamic. It is generally accepted that erosion or deposition is usually linked to increased volume or intensity of precipitation. A conventional framework that regards the conversion of rainfall to discharge and transport materials in river basins as a simple, linear diffusive process (Paola, 2000) has gradually been replaced by complexity theory that considers fluvial material movement as non-linear in terms of natural and human forcing (Hancock, 2012). The processes driving these non-linear changes in palaeo-environmental time series are difficult to separate (Anderson *et al.* 2006). This complexity of catchment, as a cascading system, exists across a wide range of spatial and temporal scales (Dearing *et al.* 2006a) which may obstruct both generalisation of observations between different systems and assumptions of homogeneity within one system (Coulthard and Van De Wiel, 2012).

2.3.1 System complexity

There is no explicit definition of complexity theory since complexity research covers multi-disciplinary boundaries. Manson (2001) has classified complexity theory into

three sections based on a discipline by discipline method: mathematical and information complexity theory, chaos and catastrophe theory and aggregate complexity. The process by which something becomes complex is described as a punctuated equilibrium dynamic by Paczuski and Bak (1999). They explained that systems behave complexly in response to accumulated perturbations; stasis periods allow the system to remember the past, and minor disturbances can force stable systems to undergo dramatic changes. Malanson (1999) identified the science of complexity as a combination of simple processes derived from reductionism to generate holistic systems that evolve through a feedback mechanism, leading to non-linearity and exhibiting criticality (Bak, 1997). Furthermore, complexity theory encompasses a number of related theories concerned with dynamic systems over a wide range of scales that originated in non-linear relationships between changing entities (Manson, 2001; Murray *et al.*, 2009). Complexity in natural landform patterns forms from non-linear processes and in open systems by the exchange of energy, material or information (Werner, 1999). The most complex systems are random (Casti, 1994) and intrinsically complicated, staying at the boundary between order and disorder (e.g. self-organised criticality, Carson and Doyle, 1999). Complex systems will display potentially emergent behaviour (Bar-Yam, 1997) that is developed from non-linear evolution and the interactions of many dynamic components. The behaviour of the system cannot be simply inferred from the original components or the processes operating on them (Werner, 1999).

Complexity exists in earth surface processes and landform formations (Malanson, 1999) due to the multiple components required to frame an environmental system, and its multi-scale, long term, multi-discipline and multivariate characteristics (Mulligan and Wainwright, 2012a). For example, the large scale geomorphology can determine the topological structure of the drainage network in a catchment and a change in any part of these highly connected flows will significantly control the whole stream flow hydrograph (Mulligan and Wainwright, 2012b). Furthermore, the spatial and temporal variability of climate, vegetation cover and land-use determines the potential seasonal and long term regime of rivers, devastating flood or drought events, and the downstream impact of channel engineering. In this complex river system, sediment transport to lakes is highly intermittent due to sediment release and storage, even with constant drivers (Jerolmack and Paola, 2007). Relatively simple

and locally non-linear interactions give rise to the complicated, irregular behaviours and spatially distributed patterns observed in fluvial systems (Murray *et al.*, 2009; Church, 2010). This is described as deterministic complexity or chaos, which is characterised by its sensitivity to initial conditions and by the increasing divergence of results over time (Phillips, 1992c). The extent to which fluvial systems are affected by environmental changes or disturbances and system interconnectivity may impact the complex behaviour by multiple degrees of freedom or adjustment (Phillips, 2007). Therefore, a complex system is constantly changing (Manson, 2001) through balanced feedback. Once a critical point (Scheffer *et al.*, 2009; Scheffer *et al.*, 2012) is passed, the system is propelled toward an alternative state. Where a system evolves to the point of maximum connectivity it may display the property of self-organized criticality (Bak, 1997). At this time, the variability in key conditions or processes may reflect internal adjustments rather than responses to external forcings. This leads to changes that are essentially unpredictable and non-linear with respect to potential external forces. A schematic description of the characteristics of the complex system is represented in Figure 2.1. It is clear that the key to the study of complex river systems is to develop a quantitative understanding of complexity. To achieve this, computer-simulation modelling (Malanson, 1999) is required to gain insights into the relationship between environmental controls and responding dynamic river systems.

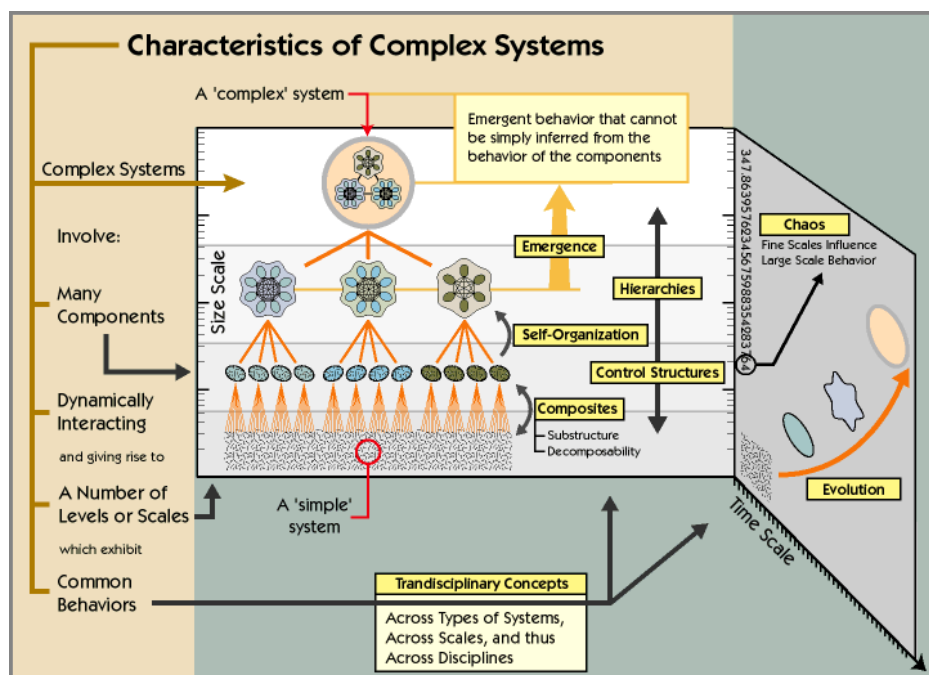


Figure 2.1 A schematic description of the characteristics of complex system (from NECSI research project, 2013).

2.3.2 Modelling complex systems

A model is regarded as a simplified abstraction of the real world with experience, intuition and mathematical skills (Pagels, 1988), creating a scientific method for system investigation in addition to theory and experimentation (Cross and Moscardini, 1985). Compared to limited observations, models allow simulations of past events at various scales. Numerical models act as virtual laboratories to improve our knowledge of environmental changes and processes of sediment transport in fluvial systems (Welsh, 2009). Through various hypotheses with controllable parameters, repeatable tests can be conducted to extend our understanding of the sensitivity of the landscape to numerous factors and processes (Coulthard and Van De Wiel, 2012). Models can also be used as tools for scenario development, enabling the assessment of potential and unexpected behaviours and offering the opportunities for simulation of future changes (Willgoose, 2004). Furthermore, models can reconcile differences between theory and field studies (Schlüter *et al.*, 2012) by controlling parameters to support our investigation of non-linear and complex system processes and their interactions.

For a long time, modelling science has been focused on a top-down approach, where conceptualisation of the whole system dynamics begins at the highest level and then requires definition of individual contributions and phenomena within the system (Wainwright, 2009; Mulligan and Wainwright, 2012a). For instance, a STELLA dynamic systems model describes the system components and their interactions through the graphical programming language (Costanza, 1988; Costanza *et al.*, 1998; Isee Systems, 2006). It considers system components as state variables or stocks (e.g. the amount of sediment accumulated in a catchment) controlled by flows (e.g. seasonal sediment flux) that are affected by auxiliary variables (e.g. environmental changes) via connectors (Costanza and Ruth, 1998). Birky (2001) built a STELLA based simulation of seasonal deciduous forest growth from six Maryland sites by comparing estimates of leaf biomass and productivity with remote sensing data. Their work proposed the availability of temporal variations in NDVI as an indicator of ecosystem stress, but concluded further validation with field measurements was

necessary. In a case study of Brazilian Amazonia, Portela and Rademacher (2001) demonstrated the impact of deforestation associated with different land use types on the quality and economic value of ecosystem services by using the STELLA dynamic model.

There is also growing appreciation that the environmental system is an agent-based complex system consisting of myriad autonomous entities or adaptive agents (Grimm *et al.*, 2005; Grimm *et al.*, 2006), and simulation models based on the bottom-up approach (Figure 2.2) have become widely used tools for effectively understanding the environment as a whole. This kind of modelling allows us to put individual agents together at a lower level of the system, formulate theoretical insights about their behaviours in a computer simulation and observe their interactions and emergent properties at a whole system level (Epstein *et al.*, 1996; Auyang, 1998; Grimm *et al.*, 2005). The Cellular automata (CA) model is a type of bottom-up model known for treating the complex system as a discrete space-time grid that is represented by a lattice of adjoining cells (Wolfram, 1984). The dynamics are operated by changes in the state of cells from one time step to the next by transition rules (Wolfram, 1994) and their relationships may be viewed as positive and negative feedbacks (Li, 1992) relying on the initial conditions of the grid and neighbouring cells' state (Fonstad, 2006). Smith (1991) used both a CA model and a non-linear wave theory to model surface erosion in order to illustrate landform development and related geomorphological features. The RillGrow model constructed by Favis-Mortlock (1996) and Favis-Mortlock *et al.* (2000) was efficiently used to simulate the development of rill networks. This model regards rill networks to be emergent and whole system responses to feedbacks between soil loss, changes in flow path and slope gradients. A novel model incorporating USLE (Universal Soil Loss Equation) factors and a CA modelling approach was developed for sheet erosion simulation (Heung *et al.*, 2013). Time and space components, which are absent from USLE, were taken into account in this model for better understanding of soil redistribution process controlled by environmental variables. Cellular automata are simple in construction, but regarded as an expression of potential phase changes and self-organised criticality in complex systems due to their complicated behaviour (Wolfram, 1984; Favis-Mortlock, 2012). Wootton (2001) linked the CA model to

empirical information on the species transition rate of mussel beds and suggested self-organized patterning in intertidal ecosystems.

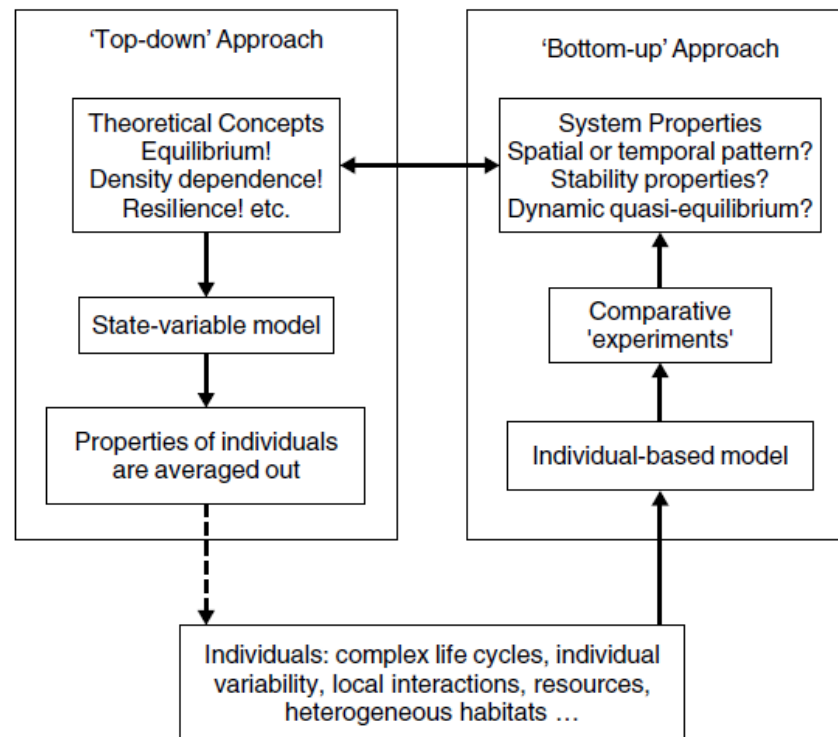


Figure 2.2 The mechanism and framework of top-down and bottom-up approaches (from Grimm, 1999; Perry and Bond, 2012).

Landscape evolution modelling based on CA is regarded as a simplified description of fluvial systems that tries to simulate changes in river dynamics, of which the CAESAR model is a good example. It has a strong focus on the processes of sediment erosion, movement and deposition, with empirical relationships that can help explore the effect of long-term landscape evolution on small catchments (Coulthard, 1998; 1999). CAESAR has been used in a number of studies, for example catchment geomorphic responses to climate and land use changes (Coulthard and Macklin, 2001; Coulthard *et al.*, 2005; Welsh *et al.*, 2009); modelling Holocene alluvial fan evolution via temporal changes in sediment discharge and morphological features (Coulthard *et al.*, 2002); the simulation of reach-scale alluvial dynamics such as channel incision, bed armouring and meander migration (Van De Wiel *et al.*, 2007); non-linear dynamics in complex fluvial systems and their self-organized critical phenomenon (Coulthard *et al.*, 2007; Van De Wiel and Coulthard, 2010); model validation by comparison with a process-based model (SIBERIA) for

testing ability to predict grassland catchment form and erosion (Hancock *et al.*, 2011); and prediction of the impact of future climate change on catchment sediment yield (Coulthard *et al.*, 2012). However, CAESAR and other landscape evolution models have limitations, for example, the parameters used to drive the model are mostly site specific and environmental controls are represented as spatially uniform (Hancock, 2006; Hancock *et al.*, 2012). Therefore, model calibration and validation with field data (e.g. lake sediment records) are necessary. A combined data and model approach is likely to be a good way to explore sediment transport laws and their processes in a complex river system from past to the future.

2.4 Summary

The focus of this thesis is the dynamic river-catchment system and its sensitivity to environmental changes, such as climate and human forcings acting on hydrological and geomorphic processes. Soil erosion and its impact (e.g. soil loss and increased flood risk) on ecosystem development receive increasing attention from scientists and policy makers. To assess the environmental implications of soil erosion and to develop sustainable management, quantitative data on soil erosion rates and effective simulations of landscape evolution at regional and global scales are needed. With the development of reliable chronology (e.g. radioactive isotopes, spheroidal carbonaceous particles and annual laminations), and sediment fingerprinting technologies (e.g. sediment chemical characteristics, sediment accumulation rate and mineral magnetism), lake sediment records can provide quantitative and qualitative data for monitoring catchment hydro-geomorphic processes and establishing the trajectories of forcing response from past to current conditions. Furthermore, complexity exists in dynamic earth surface processes: geomorphic changes may be manifested through non-linear dynamics of fluvial materials in response to external forcings and internal adjustments of the system. Computer-simulation modelling based on the bottom-up approach of cellular automata has been widely and successfully used to study the complex relationship between environmental controls and responding dynamic systems. Therefore, combining modelling data and lake sediment records through calibration and validation is likely to be a good way to explore sediment transport laws and their processes in a complex river system from past to the future.

Chapter 3

Numerical models and CAESAR

3.1 Introduction

A variety of management practices are used to alleviate the impact of significant environmental changes, for example, climate change, soil erosion and flooding, which can be driven by both natural and human activities. Where changes have occurred over recent decades, it is often difficult to assess the effectiveness of different procedures (Tucker and Hancock, 2010; Trimble, 2012). Field studies can provide detailed information of hydro-geomorphological processes. However, they have limitations in terms of cost and time needed to collect data because of the complexity of interactions and the difficulty of generalising from the results (Zhang *et al.* 1996). Such limitations highlight the need for cost-efficient models to estimate erosion after disturbance over a whole catchment and to address the complexities and consequences of catchment change on lakes (Anderson *et al.* 2006).

3.2 Numerical modelling

Over the past decades, a variety of computer-based numerical models have been developed for the purpose of determining soil erosion and the evolution of landscapes and river systems at different temporal scales. These models can be broadly categorised into conceptual models, system models (black-box models) and physical-based models according to the physical laws of hydrological cycle process (Darby and Van de Wiel, 2003).

Conceptual models are also named empirical models as they use simple mathematical-physical concepts and empirical relationships to describe hydrological or erosional process. The Universal Soil Loss Equation (USLE), the Revised Universal Soil Loss Equation (RUSLE), and variations on these, are frequently used to model overland flow or sheet-rill erosion (Wischmeier and Smith, 1978). The equation is in the form of: $A = RKLSCP$, where A is the average soil loss over the slope length; R is the erosion factor of rainfall and runoff; K is the factor of soil

erodibility; L is the slope length; S is the gradient; C is the cropping management factor and P is the erosion control practice factor. The USLE was developed as a tool for soil conservationists (Zhang *et al.* 1996) and is conceptually easy to understand. USLE and RUSLE have been accepted as useful models and have been applied and validated in a number of studies (Renard *et al.*, 1991; Busacca *et al.*, 1993; Angima *et al.*, 2003; Terranova *et al.*, 2009; Boyle *et al.*, 2011). However, the empirical nature of such conceptual models requires correct parameterisation of factors such as soil types, slope properties etc. De Roo *et al.* (1989) found that the equation is based upon statistical analysis of soil erosion data collected from small erosion plots, thus the process of sedimentation, soil losses and gains over neighbouring areas are not taken into account. The study by Svorin (2003) in a Mediterranean catchment of 4200 km² with a complicated geomorphology of hills, mountains and river plains showed that the erosion rates are generally overestimated in USLE. The greatest criticism of the USLE has been its ineffectiveness in applications outside the range of conditions for which it was developed (Nearing *et al.*, 1994).

System models regard catchments as a dynamic system to build a mathematic relationship between inputs (e.g. rainfall, snowmelt, catchment evapotranspiration capacity and sediment process) and outputs (e.g. water flow in cross-section). These simple, static relationships represent a ‘black box’ view of relationships between system variables (Birks, 1998; Anderson *et al.*, 2006). Examples of black box models include multiple regression models, neural network model, simple linear model (SLM) and linear perturbation Model (LPM) and have been widely used in flooding and rainfall-runoff forecasting (Shamseldin, 1997). They provide predictive tools which can advance our understanding of physical relations. However, there are several limitations to the applicability of traditional linear models to geographical systems. One of the most important limitations is that linear models which are based on ordinary least squares (OLS) regression are applicable to continuous response variables only. Certain geomorphologic variables, such as type of lithology and type of morphology, cannot be quantified on a continuous scale. Instead, these variables are usually defined as categories, with either nominal or ordinal scales (Macklin and Lewin, 2008). Furthermore, black box models do not show the operation of processes during simulations.

The physically-based distributed models are defined as models relying on a physically based momentum equation of runoff generation (Mulligan and Wainwright, 2012b). The effects of different land covers are also frequently considered to ascertain how land-use changes affect hydrological processes, erosion and waterborne transport of eroded materials in catchments (Ghaffari *et al.*, 2009). Hydrological models such as soil and water assessment tool (SWAT) (Ghaffari *et al.*, 2009), areal non-point source watershed environment response simulation (ANSWERS) (De Roo *et al.*, 1989), topography based hydrological model (TOPMODEL) (Beven, 1997), water erosion prediction project (WEPP) (Pandey *et al.*, 2009), CAESAR (Cellular Automata Evolution Slope and River model) (Coulthard *et al.*, 2007), etc. are being extensively applied across different landscape types with varying degrees of success (Hancock, 2012). Each of these physically-based models has their own individual advantages and disadvantages for prediction of sediment transport and hydrology. A comparison of these models is displayed in Table 3.1. Distributed parameter models have the potential for providing a more accurate simulation of a natural catchment by preserving and utilizing information concerning the areal distribution of all spatial variables and non-uniform processes incorporated into the model (De Roo *et al.*, 1989). They have the capability of forecasting the spatial pattern of hydrological conditions within a catchment as well as simple outflows and bulk storage volumes (Beven, 1985). Physical-based models let us gain insights into the behaviour and interactions of hydrology, erosion and slope processes in a dynamic river system, but their complexity may hamper the validation and thus can play a qualitative role rather than a quantitative role (Coulthard and Van De Wiel, 2012).

Table 3.1 Comparison of Models

Model Name	Objectives	Spatial Scales	Methods of Model	Parameters	Principle	Disadvantages
SWAT (Ghaffari <i>et al.</i> , 2009)	Predict the impact of land management practices on water, sediment and agricultural chemical yields	Large, complex watersheds	SCS curve number equation for runoff; Divide the watershed into hydrologic response units (HRUs); Penman-Monteith method of evapotranspiration;	DEM, soil properties, vegetation and land-cover data, climate data and land management practices	Physical-based distributed model	Not suitable for a single flooding process Uncertainty Too many parameters
TOPMODEL (Beven, 1997)	Simulate rainfall–runoff process in humid catchment	Basins smaller than about 500 km ²	Hydrological similarity of points in a catchment Topographic index $\ln(a/\tan b)$ (a is the area draining through a point from upslope and $\tan b$ is the slope angle)	DEM, climate data, soil moistures, landform features, soil properties, vegetation and hydrological characteristics	Semi-distributed model	Hillslope simulation Spatial variability Conflict of steady state
WEPP (Pandey <i>et al.</i> , 2009)	Predict and estimate soil loss and selected catchment management practices for soil conservation	Basins smaller than about 260 km ²	Infiltration theory Based on the mass balance formulation that uses the rill and inter-rill concept of soil erosion, which is a steady-state sediment continuity equation	Climate, Topography, vegetation and field management practices and soil types	Physical-based model	Difficult to obtaining a 'best fit' parameter set Not suitable for gully erosion
ANSWERS (De Roo <i>et al.</i> , 1989)	Estimate erosion, sediment yield and pollutants loss	Small catchments at about 200 km ²	Integrated with GIS tools Continuity equation Huggins methods of Surface storage potential , etc.	DEM, soil data (porosity, infiltration capacity etc.), crop data, surface data and channel data	Mathematical-based distributed model	Theoretical weaknesses High quality input data and model sensitivity
CAESAR (Coulthard <i>et al.</i> , 2007)	Simulate and investigate alluvial dynamics	4 to 40 km ²	'Flow-sweeping' algorithm Bedload transport formulae Multiple active layer Lateral erosion algorithm	DEM, hourly rainfall record, land cover record and grain size distribution	Cellular Automata	Small spatial and temporal scale Not for erosion of cohesive aggregates

STELLA (Costanza <i>et al.</i> , 1998)	Built an ecological and economic dynamic system	No limit	A modification of Van der Pols equation Ordinary differential equation Other mathematical functions and values set by users	Stocks (state variable), flows, auxiliary variables (algebraic or graphical relationship or fixed parameters) and information flow	Icon-based software package	Expert knowledge needed All the parameters and relationships are set by users
CHILD (Tucker and Bras, 1998)	Simulate the evolution of fluvial and hillslope landscapes under driving erosion and sedimentation processes and with a prescribed set of initial and boundary conditions	Small watersheds less than about 100 km ²	Irregular finite-difference gridding Climate forcing via discrete storm events with durations, etc Generation of runoff by infiltration-excess/saturation-excess mechanisms Coupled processes of stream erosion and channel migration, etc.	DEM or dynamic mesh points input, storm events and soil properties	TIN-based dynamic model	No treatment of suspended/wash load No expressions for landsliding / eolian transport Inapplicable in solution-dominated environments
PESERA (Licciardello <i>et al.</i> , 2009)	Predict potential soil loss and sheet and rill erosion rates under various land use types, soil and landscape characteristics.	Large areas, e.g. at 1-km resolution across most of Europe	Bucket model for runoff TopModel for subsurface flow Linear degree-day model for snow Physical conductivity model for depth of soil freezing Vegetation growth models Other equations for sediment yield	DEM, soil properties, land cover data, monthly climate data, land use, crops and planting dates, soil storage, erodibility and relief	Physical based, spatially distributed model	Tillage erosion and rain-splash are not considered No evaluation for changes in land management, land use or climate
PSYCHIC (Davison <i>et al.</i> , 2008)	phosphorus (P) and suspended sediment (SS) mobilisation in land runoff and subsequent delivery to watercourses	Catchment scale Field scale	Mean climate drainage model (MCDM) for water balance by land-use types Morgan–Morgan–Finney (MMF) model for sediment loss Other models for P loss, etc	Area of major crops, livestock numbers, monthly P applications as manures and excretal returns to land, soil properties, monthly climatic data, mean slope and population	Process-based model	No treatment of bank erosion or river routing and in-stream processing of P No transport of P to groundwater

However, this generalization is not absolute. Many physically-based models (e.g. computational fluid dynamics models, CFD), may contain empirical approaches. Furthermore, the availability of geographic information system (GIS) tools and remote sensing (RS) techniques makes it possible for models to use a mesh of grid cells to represent the landscape and channel network (Anhert, 1976) by integrating digital elevation models (DEM) with a traditional database (Pandey *et al.*, 2009). Compared to traditional modelling approaches, these newly developed landscape evolution and soil erosion models that use DEMs can simulate both erosion and deposition (Hancock *et al.*, 2011) and route water across a mesh of cells for a better representation of water and sediment movement (Coulthard, 2001). These models allow dynamic adjustment of landscape surface elevation (Tucker and Hancock, 2010) in response to runoff, erosion and deposition processes, thus spatially displaying terrain evolution through time. Among these models, model CAESAR, which applies the concept of cellular automata, can simulate interactions between processes represented by low level rules (relating to fundamental processes of energy and matter expressed as mathematical equations) to provide a spatially unambiguous landscape in the form of a series of cells (Dearing, 2007). This bottom-up approach that evolves changes and emergent phenomena through continuous interactions and feedbacks at local scales can model the complexity of ecosystems over relatively long time series (Dearing *et al.*, 2010). Details of cellular automata models and their water routing algorithm are discussed below.

3.3 Cellular automata models

The Cellular automata (CA) model consists of four basic components: cell, lattice, neighbour and law. It is a discrete dynamic model with time and space varying that provides simple interactions between cells for complex and stochastic behaviour (Nicholas, 2005). A typical CA model can be expressed as: $A = (G, E, U, T)$ (Ma *et al.*, 2009). Here G is a lattice of a series of spatial cells with geographic features, E is the finite state of cells, U is a definition of local neighbour cells and T is the transition rule that determines the changes in cell properties. Each and every cell has a specific state at

any given time step. However, the state of each cell at the next time step is decided by its relationships with neighbours and all the cells will change synchronously at the next time step. Therefore, cellular automata have five key features identified by Wolfram (1984):

- 1) All the cells are distributed in regular discrete lattices, which are generally created from different spatial resolution DEMs (e.g. 1m - 50m) and each cell is in the shape of a square.
- 2) Cells evolve in evenly spaced time steps with equal step-length time invariance.
- 3) Each cell has an explicit state and each state can only take on a finite set of discrete values.
- 4) The evolution state of each cell is decided by the same deterministic laws.
- 5) The transformational laws for cells depend on the interactions with immediate neighbouring cells.

Many geomorphic processes like soil erosion can be regarded as nonlinear and highly dynamic behaviours (Phillips, 1995). With nonlinear outputs and self-organisational tendency (Coulthard, 1999), a CA model is useful for simulating intricate landscape evolution through simple neighbouring interaction rules (Murray and Paola, 1994; Favis-Mortlock, 2000; Ma *et al.*, 2009). The CA model developed by Murray and Paola (1994, 1997) is generally considered as a pioneer in the history of 'reduced complexity' cellular models by using a simple water and sediment transport routing between cells. This model was initially developed to represent the multi-channel form of a braided stream by a grid of cells. Given an initial condition of uniform slope with white-noise roughness and high side walls to contain the flow, this model introduced water into some or all the cells at upstream and flowed row by row toward downstream, carrying sediment, until the end of the lattice (Murray and Paola, 1997). The elevation of each cell is altered according to the discharge dependent sediment transport rule and a lateral

erosion term (Coulthard *et al.*, 2007; Coulthard and Van De Wiel, 2012). They used the weighting algorithm to each cell that distributed water to one or all of the three immediate neighbour cells in the next row downstream (Equation 3).

$$Q_i = \left(\frac{s_i^n}{\sum s_i^n} \right) Q_0 \quad (3)$$

Where Q_i is the water discharge, S_i is the slope from cell 0 into downstream neighbour i (from left to right) and Q_0 is the total carried discharge. Eroded materials are moved to their adjacent cells also in terms of bed slope with the use of several sediment transport relations and an additional term representing surface-slope and flow-momentum effects to produce a realistic braided pattern (Murray, 2007).

By using a steady-state flow routing procedure and stream power-related sediment transport law (Brasington and Richards, 2007), this model allowed divergent and convergent flow and displayed the migrating channel patterns. Thus, it raised the possibility of modelling dynamic behaviour of fluvial system through a simplified physical approach. Thomas and Nicholas (2002, 2007) extended this original CA model by using a new cellular routing scheme (CRS) based upon the method of Murray and Paola (1994), but modified the discharge routing from each cell into the five immediate downstream neighbours. This allowed water to transfer at angles of up to approximately 60 degrees to the upstream direction rather than 45 degrees as used by Murray and Paola. The predictions of a braided river flow pattern were compared with field data, as well as the results from a more sophisticated 2-D hydraulic model (hydro2de) of the same reach. The CRS model has shown the capability of producing realistic predictions of channel morphology and indicated the potential of using CA approaches to provide a useful understanding of complex and dynamic fluvial systems. Coulthard *et al.* (2000, 2002, 2005 and 2007) introduced a CA model (CAESAR) for catchment landscape evolution. They developed a more sophisticated scanning algorithm that sweeps the water in four directions (Figure 3.1), recording the maximum flow depth from the cells over all scans. This enables many smaller cells to be used and also allows water flow

over obstacles, thus achieving a more complicated simulation of channel bed topography (Coulthard *et al.*, 2002). Sediment erosion and deposition can be calculated by using multiple grain sizes (from 1 to 256 mm) with either the Einstein Brown (1950) or the Wilcock and Crowe (2003) bedload transport equation, and they are integrated within a series of active layers allowing bed armouring, selective transport, suspended sediment and stratigraphy development. CAESAR can produce realistic sediment transport dynamics, providing large-scale, long-term watershed evolution and can be used to predict future behaviour (Coulthard, 1999; Coulthard *et al.*, 2005; Hancock *et al.*, 2012; Welsh *et al.*, 2009).

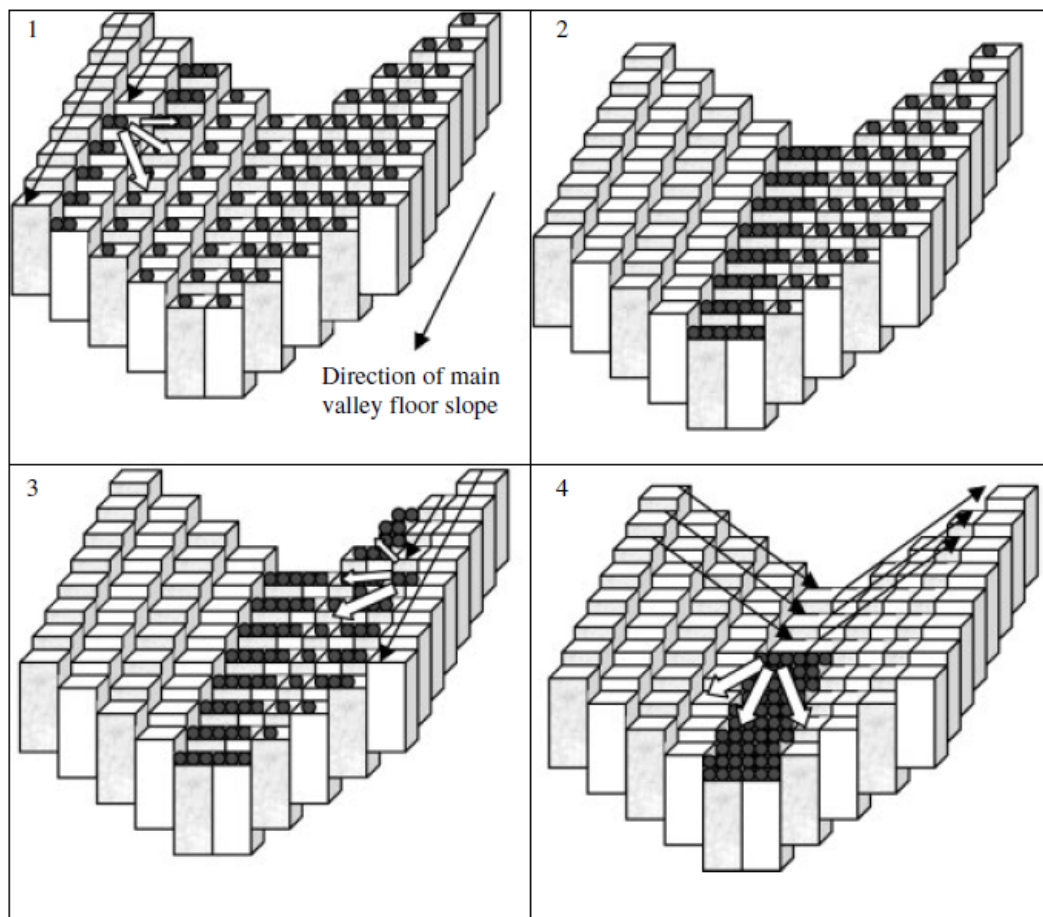


Figure 3.1 Schematic diagram of CAESAR scanning algorithm: (1) Water flow from grid cells to the three downstream neighbours on the right. (2) All the cells are upslope, no water is pushed. (3) The same process is repeated from right to left until all the water is left in the base of the valley. (4) Water is pushed out of the catchment from top to bottom. (from Coulthard *et al.*, 2002).

3.4 CAESAR model

3.4.1 Model structure

In theory, CAESAR is considered as a reduced-complexity model with simple operation where topography drives fluvial and slope processes that determine the spatial behaviour of the entire system over periods up to thousands of years (Coulthard *et al.*, 2012). CAESAR represents river catchments with a regular mesh of grid cells of uniform sizes based upon the cellular automata concept (Van de Wiel *et al.*, 2007). Each cell contains initial spatially distributed properties of elevation (m), water depth (m), vegetation cover (M values) and grain size distribution (μm); these properties are recorded in txt file format. For each iteration of landscape simulation, these properties are modified according to the interaction between an individual cell and its immediate neighbours based on rules that represent hydrological processes, multidirectional flow routing, fluvial erosion and deposition and slope processes. This consecutive iteration of a sequence of rules on each cell can alter the topography of the catchment which becomes the starting point for the next iteration. CAESAR can simulate landscape development in either catchment mode or reach mode. No external in-fluxes are required to drive the catchment mode except hourly rainfall data. For reach mode, extra data on points where sediment and water enter the system are necessary. Primary processes in CAESAR are described below and a full discussion of modelling rules can be found in Coulthard (1999).

3.4.2 Hydrological process

The hydrological model produces a combined surface and subsurface discharge (Q_{tot}) by using an hourly rainfall record as the input for the model. It is calculated from a modification of TOPMODEL (Beven and Kirkby, 1979) as following equations (Coulthard, 1999).

$$Q_{tot} = \frac{m}{T} \log \left(\frac{(r - j_t) + j_t \exp \left(\frac{rT}{m} \right)}{r} \right)$$

$$j_t = \frac{r}{\left(\frac{r - j_{t-1}}{j_{t-1}} \exp \left(\left(\frac{(0 - r)T}{m} \right) + 1 \right) \right)}$$
(4)

Where T is the time step (in seconds), r is the rainfall rate (m/h) and m is a scaling parameter that controls the changes of the soil moisture deficit (j_t). The runoff is multiplied by the cell size to obtain water which is added across the whole catchment.

If rainfall rate is equal to zero, calculation of discharges is modified to Equation 5:

$$Q_{tot} = \frac{m}{T} \log \left(1 + \left(\frac{j_t T}{m} \right) \right)$$

$$j_t = \frac{j_{t-1}}{1 + \left(\frac{j_{t-1} T}{m} \right)}$$
(5)

3.4.3 Flowing routing

The subsurface flow generated by hydrological model is routed according to the previously described ‘flow-sweeping’ algorithm (Coulthard *et al.*, 2012) and the amount is calculated with Equation 6.

$$Q_i = Q_0 \frac{s_i^x}{\sum s_i^x}$$
(6)

Here Q_i is the proportion of discharge flowing to the neighbouring cell i from the total flow (Q_0) in m^3/s , relative to the slope S between the cell and its relative neighbours i , ranging from 3 to 8.

If the total flow is greater than the subsurface flow, the excess is treated as surface runoff. Flow depth is determined from discharges using an adaption of Manning’s equation (Equation 7), where d is flow depth, Q is discharge, n is Manning’s roughness coefficient and S is slope.

$$d = \left(\frac{Qn}{S^{0.5}} \right)^{3/5} \quad (7)$$

Considering the depth of water d and elevation e (all in metres) for each neighbouring cell i , surface water discharge (Q_i) abstracted from total surface water (Q_0) can be re-written to Equation 8.

$$Q_i = Q_0 \frac{[(e+d)-e_i]^x}{\sum [(e+d)-e_i]^x} \quad (8)$$

The calculation of depth for the cells based upon the four-direction scanning algorithm is an important approximation to allow water to route over and around channel obstacles. Any water not removed out of the basin remains as storage within the grid, filling up topographic hollows in order not to interfere with the next iteration. Any flow trapped in corners and bends within the channel network remains as well, allowing the simulation of complex channel patterns as meanders.

3.4.4 Erosion and deposition process

Transport of sediment as either bedload or suspended load with different user defined grain size will result in spatially variable (both horizontally and vertically) sediment size distribution (Coulthard *et al.*, 2012). Therefore, CAESAR model uses the concept of an active layer system (Parker, 1990; Hoey and Fergusson, 1994; Toro-Escobar *et al.*, 1996) to store subsurface sediment data. This system includes: one surface active layer represents the exposed part of the regolith with a variable thickness (between 5cm and 30cm); several subsurface layers (strata) have fixed thickness (default $L_h=20\text{cm}$) and position that cover the upper part of buried regolith; a base layer builds up the lower part of buried regolith with different thickness depending on the number of strata overlaying it; and a fixed bedrock layer that cannot be eroded (Van de Wiel *et al.*, 2007). Erosion removes sediment and conversely deposition aggregates sediment, thus causing the active layer's thickness (L) to change. If there is insufficient sediment in the active layer (e.g. $L < 0.25 L_h$), a section of sub-surface stratum is incorporated into the active layer to make a new active layer. If deposition into the active layer causes it to increase

over $1.5L_h$, it will split to create a new sub-surface layer and a thinner active layer (Coulthard *et al.*, 2012; Hancock, 2012). Furthermore, erosion and deposition cause the transport of materials of multiple grain size between neighbouring cells. Over a long simulation (e.g. 1000 years) this allows previously deposited finer sediment to re-enter the system and to become available for future erosion.

Table 3.2 Comparison of modelling and natural erosion processes.

Erosion process	Chalk systems (e.g. Alresford Pond catchment)	Holzmaar	CAESAR model
Sheet erosion	Yes	Maybe	No
Rill erosion	Hillslope rilling	Maybe	Yes
Subsurface flow erosion	Yes	No	No
Gully erosion	Ephemeral gullies	Yes	Yes
Mass movement	Yes	Yes	Yes
Wind erosion	No	No	No
Bank erosion (meandering channels)	No	No	Yes

1. Boardman, 2003; 2. Dreibrodt *et al.*, 2010; 3. Coulthard *et al.*, 2000.

There is an extra turf fraction added to the surface active layer with the effect of protecting the surface from flood erosion. It is treated as a gravel layer with diameter larger than 0.26 m. The resistivity of this “vegetation”-covered surface was calculated using a field shear stress measurement developed by Prosser (1996). A linear vegetation re-growth model is also contained in monthly time steps to vegetate the surface fully in 10 years if there is no interference. If this turf mat is eroded, the model will treat the grass layer as washed out of the catchment.

The amount of sediment transported and deposited cell by cell that results in the morphological changes of the catchment is calculated with either a sand-based Einstein–Brown formulation (Einstein, 1950) or a mixed-size Wilcock and Crowe surface-based sediment transport formula (Wilcock and Crowe, 2003). Details of these two

approaches are described with examples by Coulthard *et al.* (2002) and Van De Wiel *et al.* (2007).

Here I describe some erosion processes that the CAESAR model can simulate and display as outputs, in comparison with those in observed natural systems (Table 3.2). Detailed contents of model availability, validation and limitations are discussed in the following chapters.

3.4.5 Slope process

Mass movement and soil creep are two important transient removal processes. When erosion happens, soil movement is not only driven by water flow but also depends on the gradient of slope between adjacent cells. When this threshold (normally 0.5 or 45 degrees) is exceeded, materials begin to move from an uphill cell to the lower neighbouring cells until the slope angle is under the threshold. Soil creep is determined by equation 9 at monthly time steps.

$$\text{Creep}(\text{year}^{-1}) = \frac{S0.01}{D_x} \quad (9)$$

When cells are close to the channel, sediments are transferred from the active layer to the active layer of the channel and the elevations and grain size properties of these cells are updated simultaneously. Time steps are varied between 10^{-6} and 10^4 seconds that restrict erosion to 10% of the average slope, preventing inaccuracies and computational instability (Coulthard *et al.*, 2000).

3.5 Summary

The development of computer technologies has promoted a boom in numerical models from simple conceptual models to system models based on statistic relationships between inputs and outputs or on more complicated physically-based distribution

models. A detailed comparison of nine widely used physical models, including their principles, parameters, methods, spatial scales and disadvantages is reported in this chapter. Among these models, cellular automata models, which allow dynamic adjustment of landscape surface elevation (Tucker and Hancock, 2010) in response to runoff, erosion and deposition processes, thus spatially displaying terrain evolution through time, are the focus of this study. Details of cellular automata models and their water routing algorithm are also discussed. This study applies the CAESAR landscape evolution model to explore system sensitivity to environmental controls and to interpret complexity in the behaviour of the study systems. The CAESAR model simulates landscape development by moving water across a regular grid of cells and changing cell elevations according to erosion and deposition from fluvial and slope processes. The four main parts to CAESAR, a hydrological model, the flow model, fluvial erosion and deposition and slope processes, are discussed in this chapter to provide a general insight into the capacity of CAESAR to be usefully applied in this research project.

Chapter 4

Methodology

4.1 Introduction

That landscapes are sensitive to human and climatic forces highlights the need to comprehend the interactions between environmental change and system response. To achieve a realistic depiction of long term landscape evolution, various methods are necessary. This chapter describes the methodology used in the study which can be divided into two parts. Firstly, lake sediment records were used to assess the impact of natural patterns of environmental change and climate variability on sediment transport (Brüchmann *et al.*, 2004), as well as to validate modelling outputs of sediment delivery within basins. Lake sediments were analysed for chronology, and soils were characterised by their magnetic properties to produce an historical reconstruction of sediment sources to the lakes. Secondly, the CAESAR model (for a detailed description of this model see chapter 3) was used to simulate slope and river processes both in the past and in the future. For catchment simulation, CAESAR requires simple input files, including landscape data, hourly precipitation and human actions, which are represented by alterations to the degree of vegetation cover and particle-size distribution data. It can generate spatial patterns of sediment movement and catchment outputs in the form of water and sediment discharge, and grain size distributions through space and time. A detailed methodology for the creation of these input files, data adjustment and calibration with documentary records, and the testing of model spin up period is described in this chapter. Further specific methodological detail about model parameter setup for each simulation is described in the following related chapters.

4.2 Lake sediment records

4.2.1 Site 1 Alresford Pond, Hampshire, UK

4.2.1.1 Data collection and sampling

The accumulation of material in lake sediment is often the result of hydrological processes, including the transport of suspended sediment into the limnetic system. Collection of sediment cores is, to some extent, the most important step in palaeolimnological study, as core analysis can provide an integrated history of environmental change related to climatic or human-induced changes (Dearing and Foster, 1986). In this study, sample sites were chosen close to the inflow to explore different sediment accumulation patterns. Therefore, three continuous, representative and undisturbed sediment cores were taken from two sites within the old Alresford pond basin in 2009. Two cores were close to the Nythe Stream in the northeast of the pond, and the other core was near another inflow, the Bishops Sutton Stream in the southeast. The location of these coring sites is shown in Figure 4.1. In the context of this research focussing on human impact, the more recent uppermost sediments were of most interest. A Uwitec gravity corer fitted with a 59.5 mm diameter PVC tube was used effectively to sample these unconsolidated, high water-content sediments. Three sediment profiles were collected, of lengths 68.5 cm (AP 09-01), 78 cm (AP 09-02) and 64 cm (AP 09-03). All three cores were sectioned into contiguous 0.5 cm thick samples by a vertical type extruder. To establish a chronological sediment sequence, a Russian corer was used to collect additional longer cores at site AP 09-03. With this device, sediments were extracted and enclosed in a series of rotating chambers of semi cylindrical form, in 50 cm sections with a 10 cm overlap, continuously to the depth of 400 cm. Samples collected by the Russian corer from 50 cm to 400 cm in depth were subsampled at 1 cm intervals. Every sample was stored in a plastic bag and weighed wet, dried by lyophilisation, and then reweighed. Dry mass density (g cm^{-3}) was calculated as the ratio of dry sample weight to sample volume.



Figure 4.1 Location of sediment cores (Data source: Google Earth, 2009).

4.2.1.2 Chronology

Carbonaceous particles are mainly composed of elemental carbon and although physically vulnerable are chemically robust. They are resistant to continuous chemical attack by strong acids that remove unwanted fractions of the sediment during preparation and leave SCP (spheroidal carbonaceous particles) materials without damage. Sectioned samples from site AP 09-03 were chosen for SCP analysis at 1 cm intervals for the uppermost levels (0-60cm) and at coarser 5 cm intervals lower down the cores (60-210cm). For core AP 09-01, samples were analysed every 0.5 cm by the SCP method. Chemical preparation and analysis for SCPs followed the method described in Rose (1990; 1994) with some modification owing to the high organic content and low levels of siliceous matter in samples from Alresford Pond.

Procedures are described below:

First, 0.1-0.12 g of accurately weighed dried sediment was placed into a 12 ml centrifuge tube and 3 ml conc. Nitric acid (HNO_3) were added. Tubes were left overnight in a fume cupboard. Next, a further 3 ml conc. HNO_3 were added, and contents were boiled in a water bath for 2 hours at 80-90°C. Tubes were filled with

distilled water and centrifuged at 1500 rpm for 5 minutes then decanted. The step using HNO_3 in a water bath was repeated as necessary until all organic materials were removed. Rinsing, centrifuging and decanting were repeated at least twice and then the residue transferred to a weighed and labelled 10 ml glass vial. This was centrifuged and the supernatant pipetted off before slide-making. A known subsample of the remaining suspension was pipetted onto a coverslip and mounted it on a microscope slide with a little aquamount.

The number of SCPs was counted at x400 magnification under a light microscope. SCP concentrations are presented as ‘number of particles per gram dry mass of sediment’ (g DM^{-1}). Standardised criteria for counting SCPs have been proposed by Rose (2008) on the basis of their particle morphology (Figure 4. 2). SCPs have a spheroidal three-dimensional morphology rather than a spherical morphology, a distinctive black colour and may exhibit porosity (Swindles, 2010).

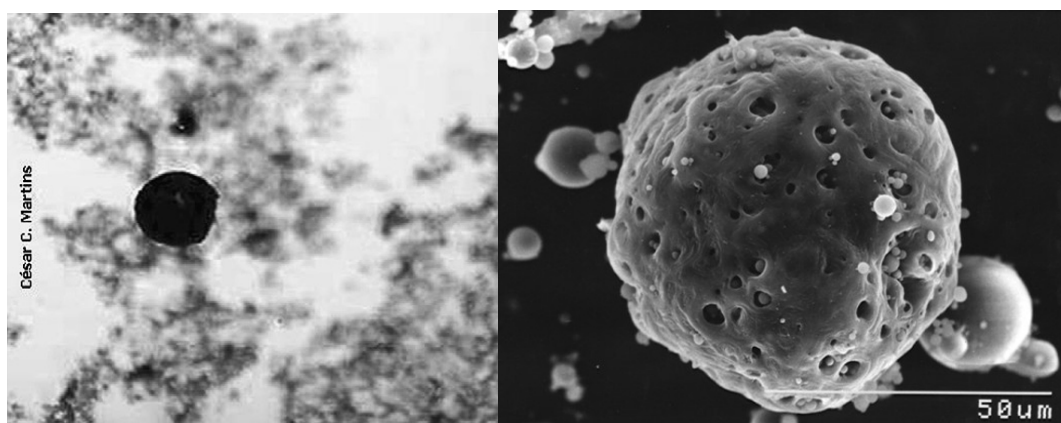


Figure 4.2 Images of a typical spheroidal carbonaceous particle by light microscope (left, from Martins *et al.*, 2010) and scanning electron microscopy (right, from Rose, 1990).

In order to calibrate the SCP chronology, 6 samples from core AP 09-03 at depths of 8cm, 8.5cm, 30.5cm, 40cm, 42cm and 50cm have been used for conventional ^{210}Pb and ^{137}Cs measurement by gamma spectrometry. This work was carried out by GAU-Radioanalytical Laboratories (NOC, Southampton).

This provided a chronology for the core, from which lake sediment accumulation rate was also calculated on the basis of dry mass loading to the lake according to the formula:

$$\begin{aligned} & \text{Accumulation rates (g cm}^{-2} \text{ year}^{-1}) \\ & = \text{Sediment chronology (cm year}^{-1}) \times \text{Dry bulk density (g cm}^{-3}) \end{aligned}$$

4.2.1.3 Magnetic properties of sediments and soils

Magnetic behaviour includes ferromagnetism (e.g. pure iron), ferrimagnetism (e.g. magnetite), canted antiferromagnetism (e.g. haematite), paramagnetism (e.g. biotite and pyrite) and diamagnetism (e.g. quartz and calcium carbonate; Dearing, 1999b). These behaviours arise from different minerals or crystals which vary in the strength of their attraction to magnetic fields, thereby influencing the ratio of the amount of magnetization generated (M) to the applied magnetic field (H). The relationship is defined as magnetic volume susceptibility κ , and is expressed by Dearing (1999b) as:

$$\kappa = M/H \quad (1)$$

Mass specific magnetic susceptibility (χ) is obtained by dividing the magnetic volume susceptibility κ by the dry sample density ρ and is expressed as

$$\chi = \kappa/\rho \quad (2)$$

Magnetic records in lake sediments reveal the characteristics and ratios of sediment sources. Occasionally, within a particular lake, variation in susceptibility and related magnetic properties seen as between-core correlations can represent synchronous events in sedimentation patterns (Thompson and Morton, 1979).

Lake sediment cores taken from the lake basin in 2009 by gravity corer were used for magnetic analysis. They were sampled at 0.5 cm intervals and all the samples were freeze-dried prior to magnetic analyses in case alteration of magnetic materials occurred. Dry and wet bulk densities were calculated in terms of mass per unit volume for each sample for magnetic concentration calculation. The sectioned and dried sediments were packed firmly into small clean plastic pots (volume ~ 10 ml).

Magnetic susceptibility in both low (470 Hz) and high (4700 Hz) frequency was estimated at room temperature by using Bartington susceptibility system dual frequency sensor (MS2B).

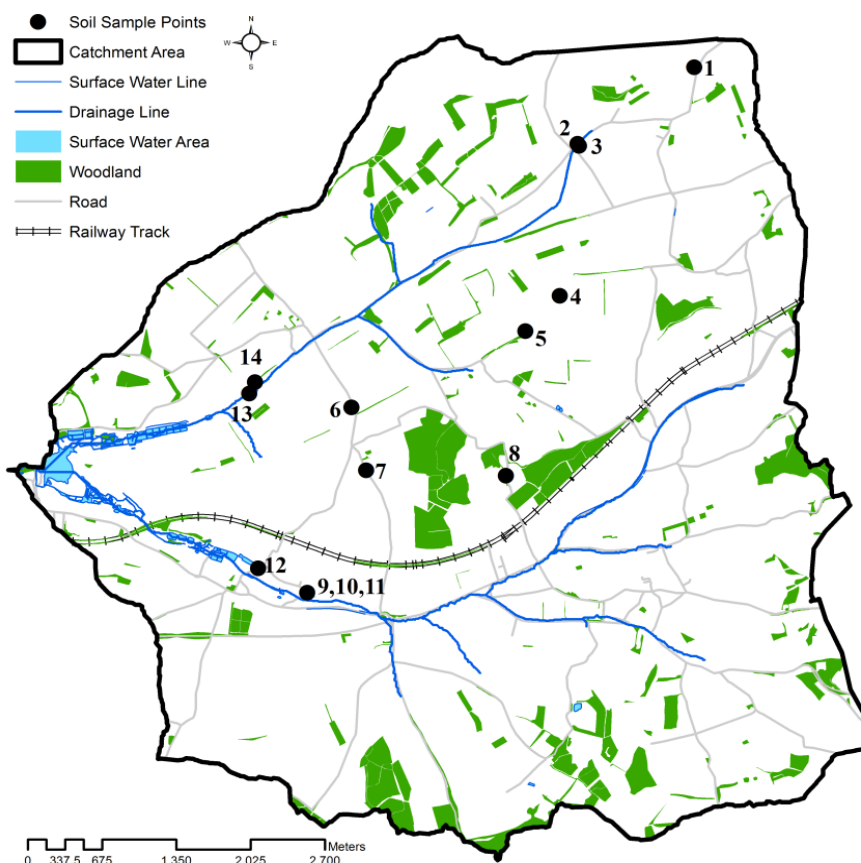
















Figure 4.3 Map showing location of soil sampling points.

Magnetic property is indicative of soil forming processes (Blundell *et al.*, 2009). Its variation in topsoils can reflect changes in authogenic inputs, allogeneic inputs and weathering inputs of iron, interacting with soil transport, diagenesis and dissolution (Maher, 1998). Surface soils were sampled from different land use types along the channels and streams over the chalk catchment (Figure 4. 3). All the samples were dried and prepared for further measurement. The concentration of ferrimagnetic minerals was determined by measuring mass magnetic susceptibility ($\chi_{LF} 10^{-6} \text{ m}^3 \text{ kg}^{-1}$) and frequency dependent susceptibility ($\chi_{FD} 10^{-8} \text{ m}^3 \text{ kg}^{-1}$). Calculations of percentage frequency dependent susceptibility ($\chi_{FD} \%$) give a fingerprint for magnetically enhanced topsoil (Dearing *et al.*, 1996). Information about topsoil samples is summarised in Table 4.1.

Table 4.1 Location and sample site description with pictures.

Sample No	Long.(N)	Lat.(W)	Elev. (m)	Description	Pictures
1	51°07.599	1°04.439	186	Lower Chalk, lots of flints, thin soil, arable land	
2	51°07.221	1°05.368	130	Head-clay silt sand gravel, arable land more organic soil groundwater pump station nearby	
3	51°07.209	1°05.354	131	Head-clay silt sand gravel grassland	
4	51°06.453	1°05.519	126	Brown clay, fine soil with a large amount of flint, bare arable land	
5	51°06.276	1°05.790	108	Bare arable land Head-clay silt sand gravel Coagulate, poor structure	
6	51°05.904	1°07.154	91	Head-clay silt sand gravel Arable land with some wheat	
7	51°05.586	1°07.044	113	Brown clay containing flint, mostly grassland	

8	51°05.550	1°05.958	148	Mostly grassland with small woodland, brown clay with flints	
9	Close to Bishop Sutton stream watercress line			Dried stream River terrace deposit	
10	Close to Bishop Sutton stream watercress line			Sand and gravel	
11	Close to Bishop Sutton stream watercress line			Grassland	
12	51°05.817	1°08.831	68	Watercress bed, head1-clay silt sand gravel, partly arable, partly grassland	
13	51°05.989	1°07.968	74	Alluvial-clay/silt/sand/ gravel, bare arable land (maize), trace of soil erosion	
14	51°06.036	1°07.903	77	Alluvia-clay/silt/sand/ gravel, wet and muddy	

4.2.2 Site 2 Holzmaar, Eifel region, Germany

For investigation of climatic and anthropogenic influences on a river system, a highly accurate chronology (with seasonal resolution) is a prerequisite (Anderson and Dean, 1988; Merkt and Müller, 1999; Smith *et al.*, 2004). Therefore, the laminated varve-dated sediment sequence of Lake Holzmaar, with statistical uncertainties under 10 years per 1000 years for the Holocene, is a favoured proxy data archive for palaeoclimate and environmental reconstruction (Zolitschka *et al.*, 2000). Sediment cores were collected and recovered from Lake Holzmaar in 1984, 1990 and 1992 by Zolitschka (1998). High resolution calendar year ages were established by counting the sediment varve layers and calibrated by AMS ^{14}C dates. Sediment in Lake Holzmaar contains up to 25% total organic carbon and up to 28% biogenic silica which may raise the sedimentary accumulation by this amount. The CAESAR model regards sediment as a detrital signal, and minerogenic particles are theoretically related to mean erosion rates (Dearing, 1986). Therefore, values of organic matter, biogenic opal and calcite have been removed from total sediment accumulation rates (SAR). The minerogenic sediment accumulation rate (SAR-min) in the unit of $\text{mg cm}^{-2} \text{ yr}^{-1}$ is used to provide an approximation (with mean temporal resolution of 28 years) of mineral sediment transfer into the lake for comparison to the simulated results. In addition, magnetic susceptibility and non-arboreal pollen percentages (NAP %) have also been analysed from the same sedimentary sequence but sampled at different time-increments to measure, respectively, the amount of ferromagnetic minerals in the lake sediments and the relative amount of woodland cover in the catchment. Magnetic susceptibility data, together with SAR-min data were mainly used to calibrate modelling results of sediment discharge. NAP% data were used to create a vegetation cover index of M values in the CAESAR modelling and subsequent paleoenvironmental history analysis. In this study, we focus on the sediment record from present to the past 5000 years. No new data were collected from the sediment or catchment except for the DEM and precipitation data used in the modelling.

4.3 CAESAR parameters setup

4.3.1 Model input and output files

In this research, CAESAR was running in catchment mode. The rainfall input file required to generate runoff over the catchment was in the format of a single column of precipitation values with units of millimetre per hour for the whole duration of simulation. This file was created by either Microsoft Excel or Notepad and saved as a .txt file. The data in the land use input file were represented as M values that were converted from vegetation cover data, and saved in .txt format as well. Other parameters (e.g. particle size distribution, min/max time step, run duration and water depth threshold etc.) were set according to each simulation. Input file creation and parameter setup are described in more detail later.

During the run, the model calculates the drainage area and scanning region when all the initial variables have been loaded. In the main loop, water is flowing according to the multi-direction law and the amount eroded and deposited between cells is recorded simultaneously. CAESAR produces two kinds of outputs. After the simulation, changes of surface elevation, calculated water depth in cells, difference in elevation showing deposition and erosion and grain size redistribution are stored in form of ASCII text data that can be imported into ArcGIS to display the spatial and temporal patterns of erosion and deposition. Another kind of output file contains data on water discharge (m^3/s) and sediment discharge (m^3) both in total and for nine user-defined grain size classifications at a specified interval (hourly or daily) for further statistical and hydrographical analysis.

4.3.2 Digital elevation model

In CAESAR, catchment geomorphology is represented as a digital elevation model (DEM) to define watersheds and to calculate slope and flow direction. Although DEMs with 10 m or better resolution can improve the accuracy of landscape evolution modelling over the given terrain, increasing the resolution results in an exponential increase in the number of grid cells. The DEM should cover the whole catchment, and cutting down the number of cells can help eliminate unnecessary calculations and reduce computational time (Parsons and Fonstad, 2007). CAESAR

has been applied with cell sizes from 1m to 100m, which is suited to applications with 250,000 to 500,000 cells, though it can run with up to 2 million cells (Coulthard, 1999). Considering the area of Alresford Pond catchment, a 10 m by 10 m LIDAR (Light Detection And Ranging) based DEM (Southampton GeoData Institute, UK) was used for simulations. Similarly, A LIDAR-based digital ground model (DGM) with a cell dimension of 10 m by 10 m was obtained for the Holzmaar catchment. It was then converted to a DEM using GIS tools as the initial basin morphology for modelling.

To eliminate errors within raw DEMs, it is vital to remove data artefacts such as sinks and pinnacles in the DEM. Hydrological correction is also important to ensure that the drainage network is consecutive and straightforward to the exit point. This process was implemented using hydrological modelling tools (ArcGIS Hydro extension toolset) developed by ESRI for surface water modelling. After filling sinks, creating a flow direction, calculating flow accumulation, creating the drainage network and dividing the sub catchment, DEMs were corrected and converted for CAESAR modelling in the form of raster ASCII files (Figure 4. 4).

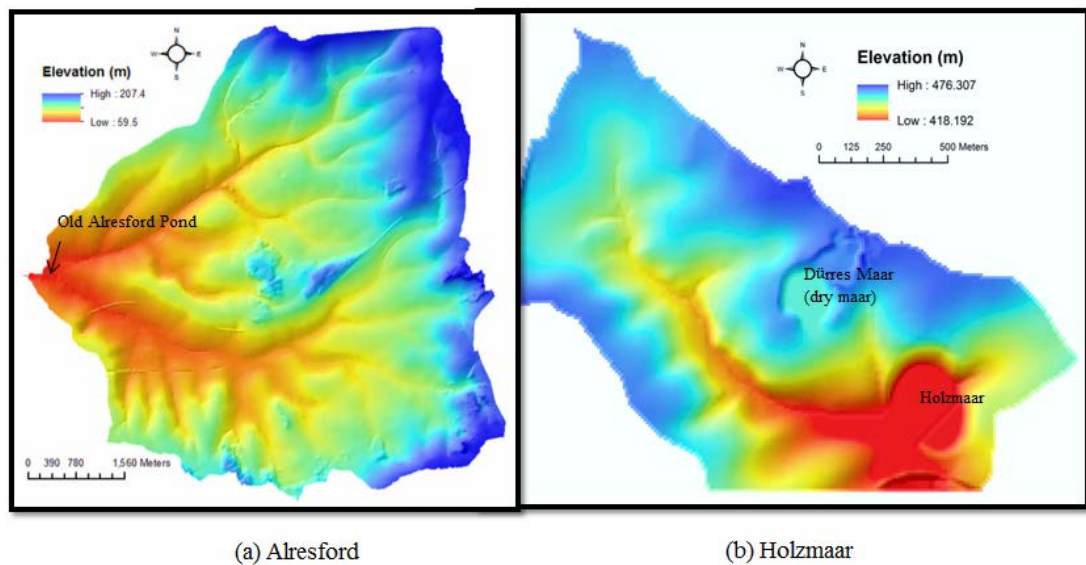


Figure 4.4 DEM of (a) Alresford catchment and (b) Holzmaar catchment.

4.3.3 Particle size distribution

Additional information on soil particle size distribution is required to drive the model.

4.3.3.1 Alresford Catchment

Soil particle size for the initial condition was subdivided into 9 fractions: <4 μm , 4-62.5 μm , 62.5-500 μm , 500-1000 μm , 1000-2000 μm , 2000-4000 μm , 4000-16000 μm , 16000-64000 μm and 64000-128000 μm . The finest two fractions of clays and silts were treated as suspended sediment, and the proportion of each particle size fraction is shown in Figure 4.5. Defining the initial conditions of particle sizes throughout the whole catchment is quite hard, so the distribution of particle size was spatially unvaried at the start of the simulation and changed and dimensionally re-arranged during iteration to reach equilibrium (Coulthard *et al.*, 2002; Welsh *et al.*, 2009). The distribution of particle size data was obtained from Sear *et al.* (1999) who illustrated the sediment classes associated with groundwater- dominated chalk river catchments in UK. This field survey for chalk catchments is a part of the River Habitat Survey (RHS, Raven *et al.*, 1998) of the physical features for UK rivers. Areas, exclusively in England, of Cretaceous chalk that are unaffected by the hydrological influences of overlying clays and other impervious drift deposits were defined as chalk rivers and estimated for total count of sediment size classes (%). Although particle size data are not directly related to the study site, the information from RHS is a good representation of the morphological diversity in the chalk stream type and, by further assessment of the hydrogeomorphological diversity, Sear *et al.* (1999) argued that chalk rivers do share some features in common.

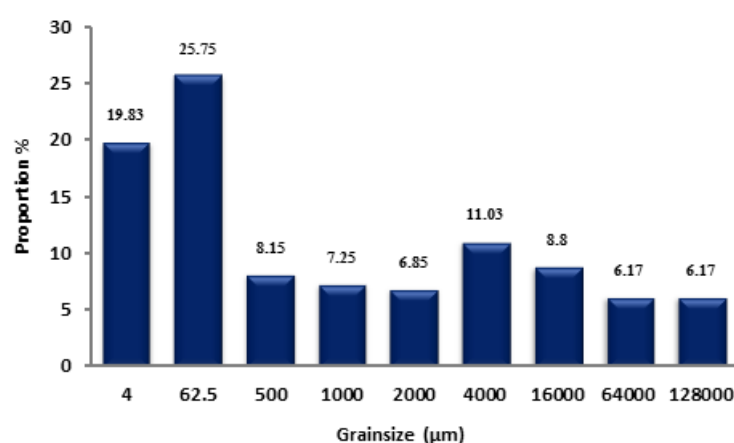


Figure 4.5 Average grain size distributions for Alresford catchment (from Sear *et al.*, 1999).

4.3.3.2 Holzmaar Catchment

In terms of the limited studies on sediment particle size in the Holzmaar catchment, it was suggested by Professor Bernd Zolitschka (personal communication, 2011) that catchment rocks are of Lower Devonian age (Ems, Siegen) and that soils consist of clay, silt and sand, delineated as silty-sandy loam. Therefore, grain size fraction was subdivided into: $<2\ \mu\text{m}$, $2\text{--}6.3\ \mu\text{m}$, $6.3\text{--}20\ \mu\text{m}$, $20\text{--}63\ \mu\text{m}$, $63\text{--}200\ \mu\text{m}$, $200\text{--}600\ \mu\text{m}$, $600\text{--}2000\ \mu\text{m}$, $2000\text{--}4000\ \mu\text{m}$ and $4000\text{--}6000\ \mu\text{m}$ (Andreas Lücke and Bernd Zolitschka, personal communication in 2011). Similar to Alresford catchment, the finest fractions of clay and fine silt were treated as suspended sediment, and the proportion of each fraction is shown in Figure 4.6.

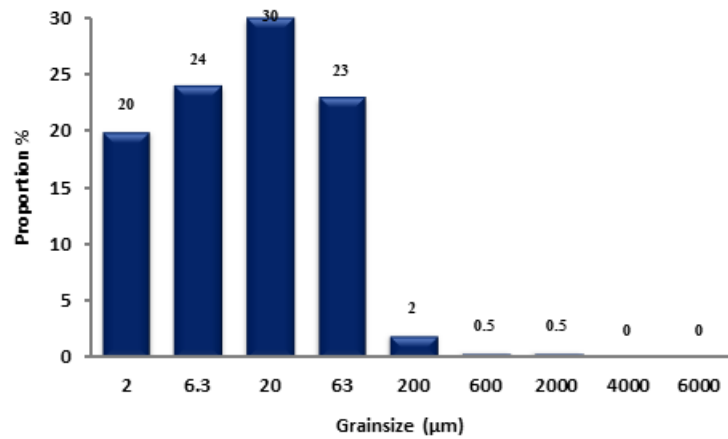


Figure 4.6 Average grain size distributions for Holzmaar catchment.

4.4 Creation of precipitation data sets

4.4.1 Precipitation series for Alresford Catchment between AD1889 and 2009

Hourly precipitation data for Alresford catchment during the period from 1889 to 2009 are derived from two kinds of data source. One is the direct hourly rainfall data obtained from nearby weather stations, and the other is created from the daily rainfall records from the closest weather stations. All these data were obtained from UK Met Office and British Atmospheric Data Centre. In terms of distance and altitude, hourly rainfall data from weather station ODIHAM was used as main data source. However, because of missing data, data from station MIDDLE WALLOP (Figure 4.7) was

used to supply the missing and incorrect information. These cover the period from 1980 to 2009 and were divided every 4 years (2006-2009, 2002-2005, 1998-2001, 1994-1997, 1990-1993, 1986-1989 and 1982-1985) for using as templates to adjust daily precipitation records into hourly records. Correlation analysis was carried out to compare the recalculated daily records of these 4-year templates (1980-2009) with the daily rainfall data (1889-1979) collected from BISHOPS SUTTON, CHILLAND and OTTERBOURNE (about 2-15 km away) stations which was also split into 4 year subsets. All of the 4-year templates covering the time period 1980-2009 were duplicated and multiplied by the factors derived from the daily records. Their best correlative templates, generating an hourly precipitation sequence back to 1889. Their relationship can be expressed simply as the function below:

$$\text{Precipitation (1889-1979)}_{\text{hourly}} = \text{Precipitation (1980-2009)}_{\text{hourly}} \times [\text{Precipitation (1889-1979)}_{\text{daily}} / \text{Precipitation (1980-2009)}_{\text{daily}}]$$

Limitations may exist where this approach reflects only rainfall magnitude changes. However, Coulthard *et al.* (2000, 2002) have argued that changes in magnitude are much more important in determining erosion patterns than changes in frequency.



Figure 4.7 Location of weather stations (form Google Earth, 2011).

4.4.2 Precipitation series for Holzmaar Catchment between 3500 BC and AD 2007

To establish an hourly precipitation record back into the Holocene (approximately 5000 years), precipitation reconstruction based on documented evidence and natural proxy records (i.e. tree-ring, pollen etc.) is needed. A sequence of proxy records of palaeoprecipitation at various time scales for the Holzmaar region have been applied and adapted for the modelling requirements. These data sets include the following:

- a) High resolution meteorological data: hourly precipitation data between 2004 and 2007 from Gillenfeld station (online source) and daily precipitation data between 1908 and 2007 from Trier station (European Climate Assessment & Dataset project, Figure 4.8).
- b) Medium resolution reconstructed palaeoprecipitation for the European area on a 0.5° grid: monthly independently reconstructed precipitation covering the last 235 years (Casty *et al.*, 2007) and seasonal reconstructed precipitation covering the period 1500-1900 AD (Pauling *et al.*, 2006).
- c) Low resolution precipitation reconstructed from pollen data at annual to decadal scale (Litt *et al.*, 2009).

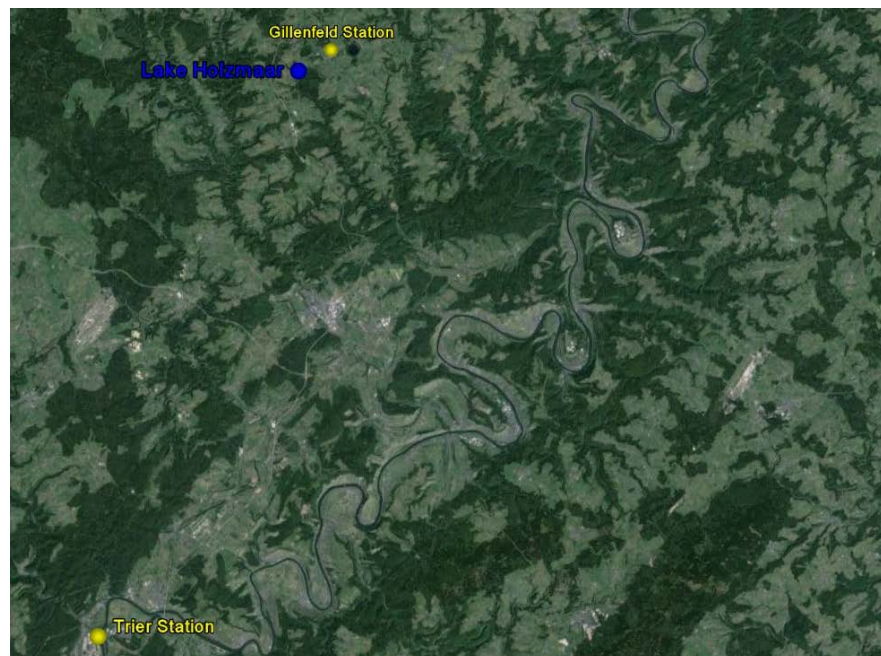


Figure 4.8 The location of Lake Holzmaar and weather stations Gillenfeld and Trier.

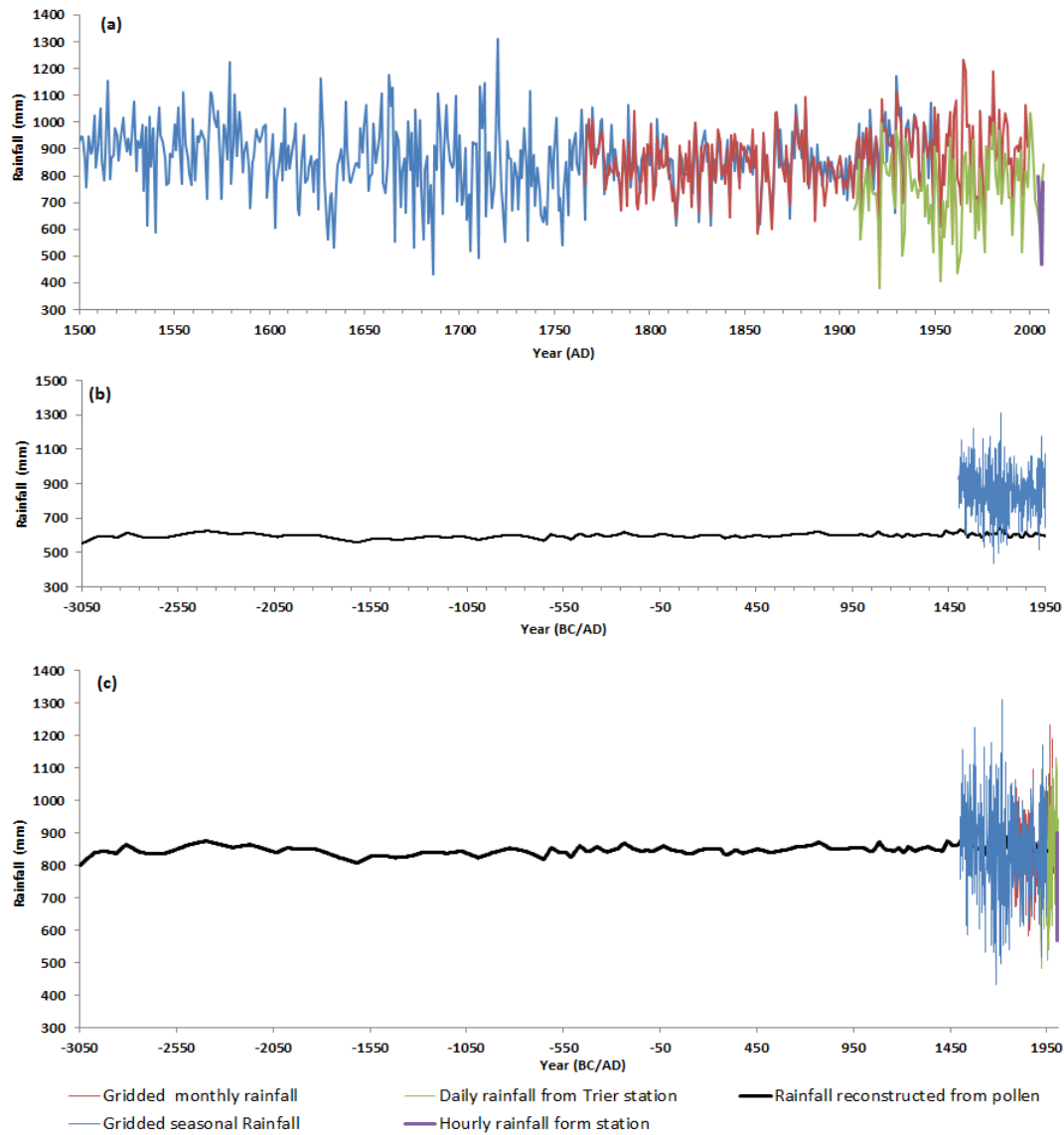


Figure 4.9 The combination of annual rainfall data for Holzmaar catchment, (a) original high and medium resolution rainfall data (1500-1950 AD); (b) rainfall reconstructed from pollen (-3050 BC-1950 AD); (c) adjusted all rainfall data (-3050 BC-1950 AD).

Medium and high resolution data sets were compared firstly with each other for calibration (Figure 4. 9a). Both monthly and seasonal precipitation data for the period of 1750 -1950 were found to be coherent. However, compared with the meteorological data from the Gillenfeld and Trier gauging stations, reconstructed precipitation values (1750-1950) are overestimated, despite having similar patterns and a correlation coefficient of 0.7. Therefore, seasonal reconstructed precipitation available from Pauling *et al.* (2006) was adjusted in terms of the daily precipitation

data from Trier station (Figure 4.9c). Comparison between precipitation data reconstructed from pollen (Litt *et al.*, 2009) and tree-ring based gridded palaeoprecipitation (Pauling *et al.*, 2006) for the same period (1500-1700 AD) suggested an underestimation of values in the former (Figure 4.9b), so adjustment was also applied to give confidence that the long term precipitation record is suitable for modelling in CAESAR. An hourly precipitation record for 5000 years was then created by using similar methodology as that applied to Alresford catchment. Again, the 4-year hourly precipitation (2004-2007) was repeated for 5000 years and scaled against reconstructed palaeoprecipitation and daily precipitation for each year.

4.4.3 Precipitation series for future projection of Alresford catchment between AD 2010 and 2099

For better understanding of the nature and magnitude of future environmental change impacts, this research attempts to predict flow and sediment discharge in the Alresford catchment. It is therefore important to gain an insight into future precipitation change, as precipitation drives these variables and is the main input to the modelling. Precipitation series for given time horizons (e.g. 2020s, 2050s and 2070s), were constructed from the baseline time series and future scenarios were represented as monthly mean values. For this purpose, a reference period 1961-1990 was selected as the baseline. This is the standard World Meteorological Organisation period (Prudhomme *et al.*, 2003) because it includes several examples of natural climatic variation, for example dry (1970s) and wet (1980s) periods (Wigley and Jones, 1987). The data used for this baseline period were based on observed data from the nearby gauging station in the Alresford area, which is strongly moderated by groundwater (see chapter 4.5). The data for the future scenarios were generated by perturbing the reference data with climate change factors derived from the UKCP09 (UK climate projections, 2009).

The UKCP09 projects the response of the climate system to a given emissions or atmospheric CO₂ concentration scenario, providing probabilistic projections by using a set of perturbed physics ensemble (PPE) simulations of the Met Office HadCM3 climate model (Murphy *et al.*, 2009; Christerson *et al.*, 2012). This approach expresses probability as the relative degree to which each possible climate result is

supported by the evidence available. The UKCP09 provides outputs of climate change factors from downscaled projections at a resolution of 25 km grid squares across the UK, based on 10,000 equally probable samples of climate change factors (see details in Murphy *et al.*, 2009 and the UKCP09 website, <http://ukclimateprojections.defra.gov.uk/>). However, running the large ensemble of 10,000 samples for each time slice is too computationally intensive. For the purpose of this study, we utilised data of cumulative distribution functions (CDFs) that consist of 107 values of daily precipitation according to 107 probability levels, ranging from 1% to 99%. Given the evidence that probability levels between 10% and 90% are robust, we selected samples at 10%, 50% and 90% probability level from CDFs data, which can be interpreted as *very likely to be less than* for a cumulative possibility of 90%, *very likely to be greater than* for a cumulative possibility of 10% and *median/central estimates* for 50% cumulative possibility (Murphy *et al.*, 2009). All the data are available for downloading from the UKCP09 User Interface (see website <http://ukclimateprojections-ui.defra.gov.uk/ui/admin/login.php>) at different time scales with three emission scenarios. Future greenhouse gas emission scenarios applied in UKCP09 are selected from the IPCC Special Report on Emission Scenarios (SRES) and relabelled as High, Medium and Low in correspondence to the A1F1, A1B and B1 emission scenarios (see details of SRES in Nakićenović *et al.*, 2000). The structure of data is summarised in Table 4.2 and an example of the monthly rainfall data for the low emission scenario in the 2020s is shown in Figure 4.10.

The hourly increments of precipitation for the three time windows 2010-2039, 2040-2069 and 2070-2099 were multiplied by the difference between future and baseline averaged monthly values as follows:

$$\text{Rainfall}_{\text{future, hour}} = \text{Rainfall}_{\text{baseline, hour}} \times (\text{Rainfall}_{\text{future, month}} / \text{Rainfall}_{\text{baseline, month}})$$

This function was applied to each time series and all three emission scenarios under three probability levels. This method allows a good representation of not only changes in mean precipitation (Madsen *et al.*, 2012), but also changes in precipitation variability with well-preserved probabilistic information. Because the rainfall scenarios are monthly based and must be converted to an hourly resolution for

modelling requirement, it may be that rainfall frequency changes are more poorly represented than magnitude changes.

Table 4.2 Data structure of projected precipitation.

Emission scenarios	High emissions			Medium emissions			Low emission		
	10%	50%	90%	10%	50%	90%	10%	50%	90%
Probability level									
2020s (2010-2039)	Hourly Rainfall	Hourly Rainfall	Hourly Rainfall	Hourly Rainfall	Hourly Rainfall	Hourly Rainfall	Hourly Rainfall	Hourly Rainfall	Hourly Rainfall
2050s (2040-2069)	Hourly Rainfall	Hourly Rainfall	Hourly Rainfall	Hourly Rainfall	Hourly Rainfall	Hourly Rainfall	Hourly Rainfall	Hourly Rainfall	Hourly Rainfall
2080s (2070-2099)	Hourly Rainfall	Hourly Rainfall	Hourly Rainfall	Hourly Rainfall	Hourly Rainfall	Hourly Rainfall	Hourly Rainfall	Hourly Rainfall	Hourly Rainfall

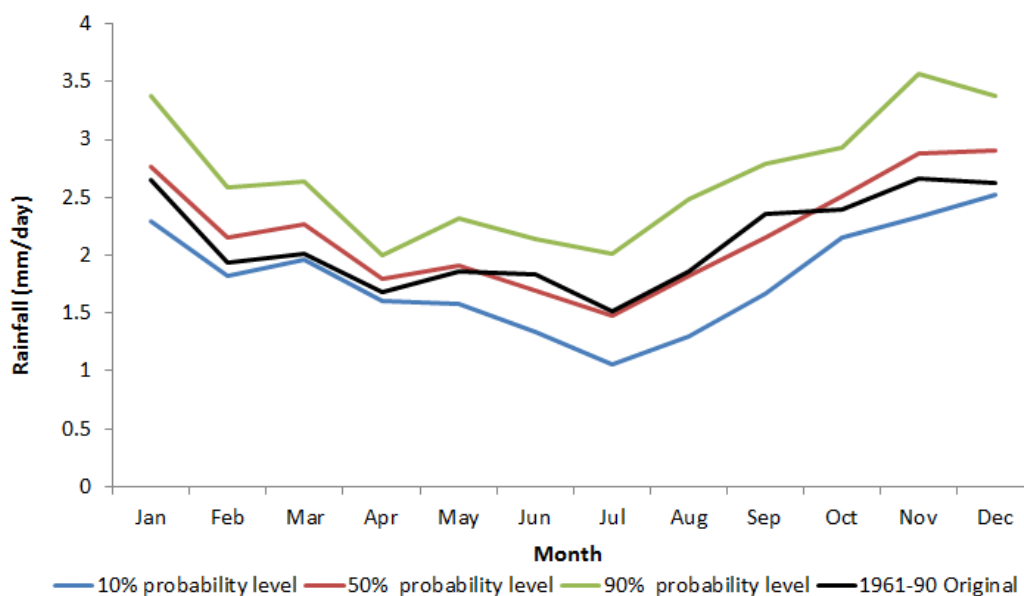


Figure 4.10 An example of rainfall prediction under the low emission scenario in the period of 2010-2039 (2020s).

4.5 Land use

In CAESAR, to simulate changes of vegetation cover, a variable M from TOPMODEL (Beven and Kirkby, 1979) is important for its effect on hydrograph recession curves. This parameter M , which represents the effect of vegetation cover on catchment, affects the hydrograph peak for a given storm and the rate of rise and fall in the water table, effectively controlling soil moisture deficit. At low M values, the water table is closer to the surface and the water is lost more rapidly from the soil. In contrast, high M values reduce the transmissivity within the soil. The value of M normally ranges from 0.005 (grassland) to 0.02 (forest), with the same temporal resolution as the precipitation input file (Coulthard *et al.*, 2002; 2005). For instance, a completely-forest vegetated landscape represented by a high M value such as 0.02 generates a stable flood hydrograph (Figure 4.11). Likewise, landscape with no forest cover represented by a lower M value such as 0.005, displays a rapid increase in water discharge and rapid peak discharges.

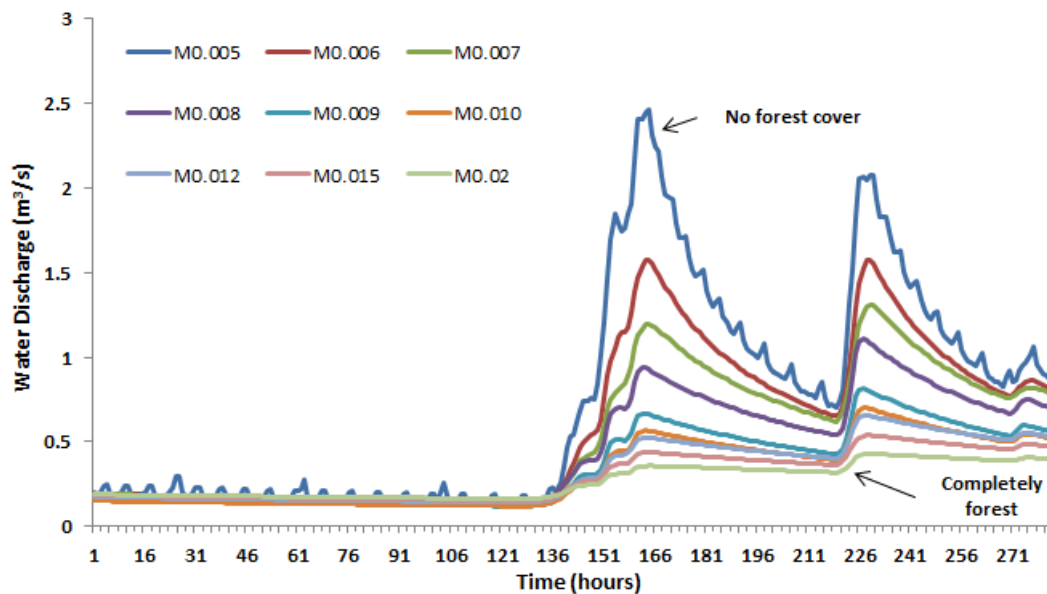


Figure 4.11 Modelled hourly water discharge under different M values.

4.5.1 Alresford Catchment

4.5.1.1 Preliminary creation of land use index, M value

In order to create M value series to track the land use history in the past, it is necessary to scale the M values to forest cover. Since, there is no direct historical documentation on forest cover record for Alresford Pond catchment, three kinds of data set were investigated:

- NDVI (Normalised Difference Vegetation Index) from remote sensing data (USGS, U.S Geological Survey) and Land Cover Map 2000 (Southampton GeoData Institute, UK)
- The 1930s land use map (Ordnance Survey, UK)
- Pollen data from published articles and theses (Waton, 1983)

Remote sensing images from the Landsat 1, 3, 5 and 7 satellites have been used to inspect land use changes since 1976. From these images, NDVI was calculated. The NDVI is known to be correlated with the green leaf area (Carlson *et al.*, 1990) and its relationship with changes in vegetation cover has been extensively studied, theoretically and empirically (e.g. Rouse *et al.*, 1973; Tucker, 1979; Purevdorj *et al.*, 1998; Plessis, 1999; Pettorelli *et al.*, 2005). The NDVI is derived from the ratio of visible red (RED, 0.58 to 0.68 μm) to near infrared (NIR, 0.7 to 1.1 μm) reflectance [$\text{NDVI} = (\text{NIR} - \text{RED}) / (\text{NIR} + \text{RED})$], based on the principle that chlorophyll absorbs visible red light whereas the leaf structure scatters near infrared radiation (Pettorelli *et al.*, 2005). NDVI values are in a range of -1 to 1, where positive values indicate vegetation cover and they increase with vegetation cover increase. To ensure comparability, the same wavelength bands were used (Landsat-1 and 3, MSS bands 5 and 6 and Landsat-5 and 7, TM/ETM+ bands 3 and 4) to calculate NDVI. Calculation of NDVI was carried out using ERDAS IMAGINE 9.0 software, and positive values of NDVI were scaled and normalised to M values ranging from 0.005 to 0.02 (Table 4.3). The Land cover Map of 2000 suggests a contemporary forest cover for the Alresford area of approximately 10%, which is less than the value of NDVI. Discrepancies may occur owing to the fact that NDVI is an indicator of vegetation 'greenness'. Over 50% arable land in the catchment may contribute to the green leaf areas. Therefore, vegetation cover, including both forest and arable was included in the creation of M values for Alresford catchment. The M value is calculated as: $\text{M value} = \text{forest cover \%} \times 0.02 + \text{arable cover \%} \times 0.012 + \text{grassland and others \%} \times 0.005$.

Table 4.3 NDVI values and correlated M values.

Year	1976	1982	1985	1987	1995	2000	2003	2006
Mean NDVI	0.2359	0.0074	0.1870	0.2368	0.5506	0.3696	0.4568	0.2884
M value	0.0085	0.0051	0.0078	0.0086	0.0133	0.0105	0.0119	0.0093

Before 1976, there are few land use maps and no aerial photographs available, so other data sources are required to extend the history of land use changes. The 1930s historical land use map shows a value of 15% forest cover and 25 % arable cover for the catchment, which gives an M value of 0.0086 according to the equation. A palynological study of the landscape around Winchester suggests an arboreal pollen percentage of approximately 25% for the period of 1880 to 1910 and 20% from 1910 to 1940. The M value was calculated more directly via $M \text{ value} = \text{arboreal pollen \%} \times 0.02 + \text{non arboreal pollen \%} \times 0.005$. Consequently, records of historical land use were normalised and converted into a series of M values between 0.005 and 0.013 as shown in Figure 4.12. Since this is the preliminary creation of M values, their availability for simulation needs to be calibrated with observed data (see the following section).

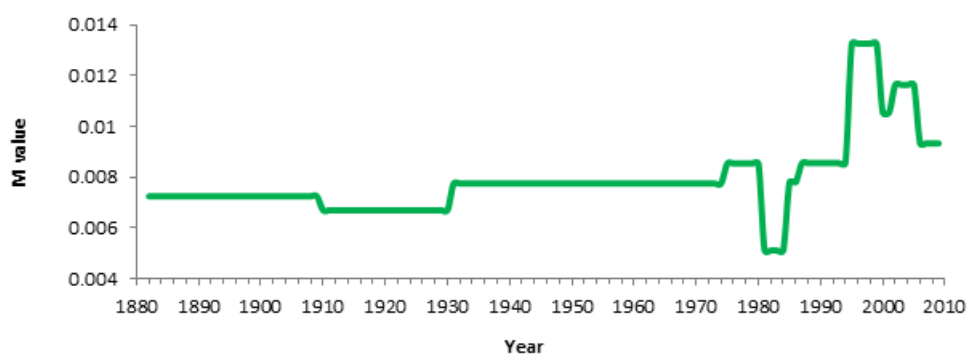


Figure 4.12 M values for Alresford Catchment (AD. 1880-2009).

4.5.1.2 Calibration of rainfall and land use parameters

Using the created input files of hourly rainfall and land use, simulations of water discharge (QW) were carried out from 1982 to 2009. The time series analysis of magnitude and shape of flood hydrographs was then compared to instrumental flow data from national river flow archives (NRFA) over the same period. The flow data

are from a combined gauging station of Alre, downstream of Alresford pond, with total catchment area of 57 km² (Figure 4.13).

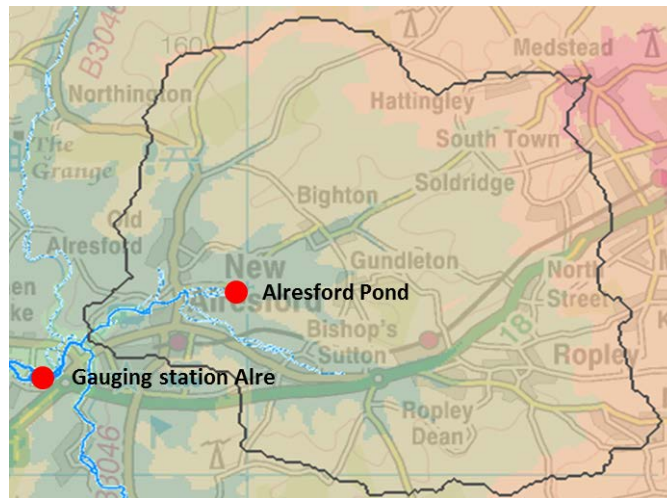


Figure 4.13 Location of gauging station and Alresford pond.

Water discharges were divided by their catchment areas for the comparability of simulated water discharge and measured flow data and the result is shown in Figure 4.14. Apparently, recorded flow and modelled water discharge show no correlation. Although the pattern of water discharge changes is similar to the observed data, the amount of flow is far from comparable (Figure 4.14a). It is obvious that modelled water discharge is underestimated for low flows and overestimated for flood discharge (Figure 4.14b). Furthermore, the modelled average water discharge is only 60% of the observed flow. This is due to the highly porous nature of chalk that gives it a great capacity to store water, which is typical of groundwater-dominated systems. The influence of groundwater on river flow is characterised as the base flow index (BFI). If a river has a BFI of 75% or greater, it is regarded as fed by groundwater. The water supply of chalk is almost entirely from groundwater and there is little surface runoff. If the flow is derived from a chalk aquifer, a river is a chalk river regardless of the surface geology (Smith *et al.*, 2003). Average BFI from 1958 to 2009 is 0.96 in Alresford catchment (from the Centre for Ecology & Hydrology), which means over 90% of stream flows is fed by groundwater flow. During the summer, little precipitation falling on chalk catchment is able to infiltrate downwards the aquifer because of the soil moisture deficit. The heavier rainfall and limited vegetation cover in winter produces most outflows from the aquifer. The aquifer rises

in winter (noticeably around December until March or April) and then declines steadily until the next winter, leading to a stable hydrograph with annual fluctuations (Berrie, 1992).

The CAESAR model is not designed for chalk catchments. Therefore, the effect of rainfall was not buffered by groundwater, which has the result that runoff is exaggerated to large crests when extreme storms take place and is reduced to excessively low values in drought periods. Clearly, given the significance of groundwater in the annual hydrological cycle of Alresford catchment, it is critical to consider the relationship of rainfall, groundwater and runoff in simulations.

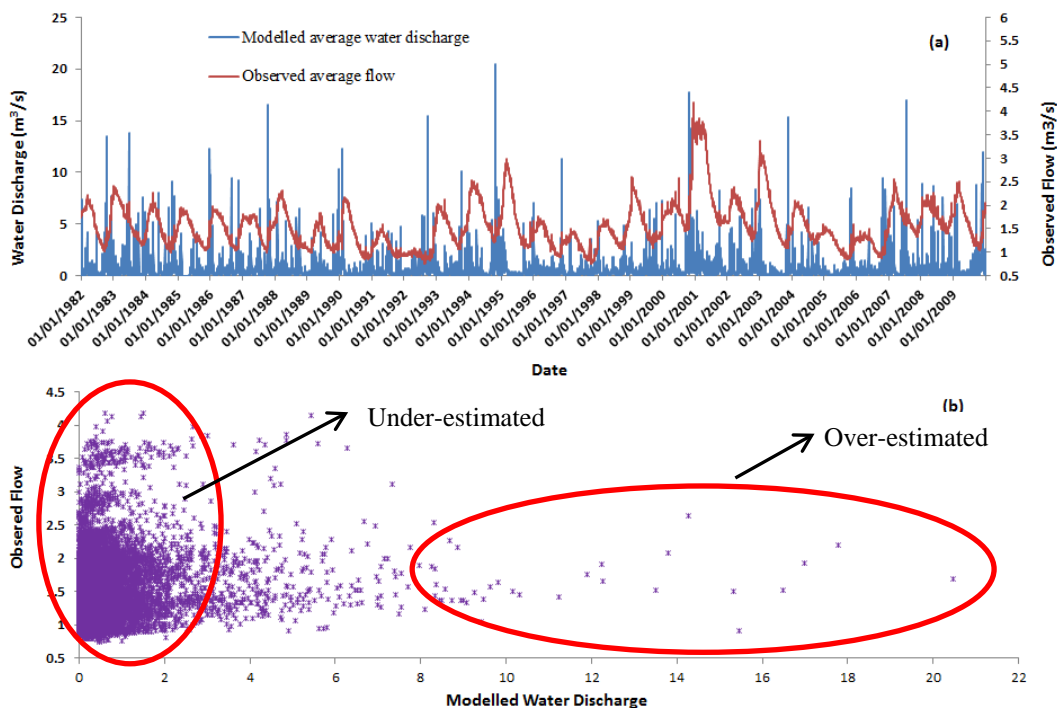


Figure 4.14 Comparison of simulated water discharge with documentary records (1982-2009).

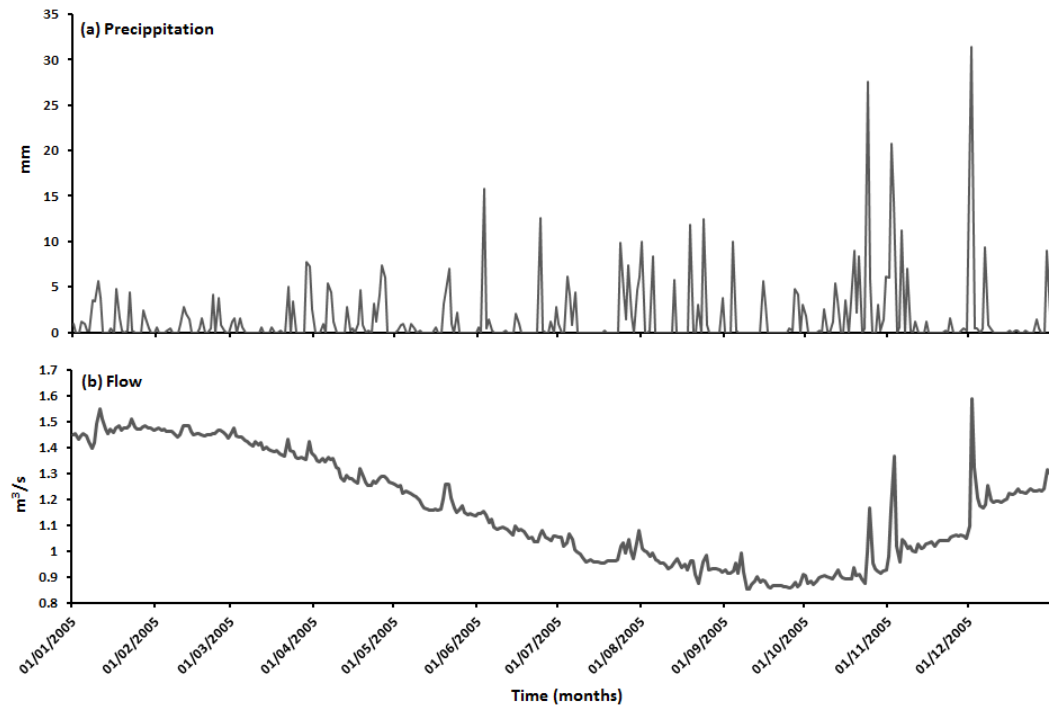


Figure 4.15 Comparison of precipitation (a) and documented flow (b) data for Alresford for 2005.

In terms of the groundwater effect (Figure 4.15), the stream flow for 2005 is, for example, in the range of 0.8-1.7 m³/s for Alresford catchment, while the precipitation magnitude ranges from 0-35 mm per day. Even when there was no rainfall event, the stream flow was mainly supplied by aquifer outflows, which helped to sustain flows through dry periods hence protecting the catchment from drought. When there was a strong storm event, most of the rainfall infiltrated into the chalk aquifer, so the flow increased only by a small amount. The shape and magnitude of the hydrograph also displays a clear seasonal trend. Therefore, in order to simulate realistic hydro-geomorphic changes in chalk catchments, groundwater, as a major component in the discharge, has been incorporated by moderating the precipitation series into a groundwater-adjusted effective precipitation series. A modified rainfall file is used to drive simulations instead of the original rainfall series.

The groundwater-adjusted precipitation was created by a trial and error adjustment approach to achieve the best comparison between modelled water discharge and recorded flow data. Several key features were essential to take into account in the trial:

- The storage of groundwater during periods of heavy rainfall that offsets sustained peaks of increased water discharge during flood periods.
- The supplement of groundwater in dry seasons that replenishes decreased stream flow.
- The effect of changing vegetation cover on catchment hydrology with an M parameter that impacts the magnitude and response time of the hydrograph.
- A convincing correlation between modelled and observed water discharge.

To assess the performance of the groundwater effect on water discharge, hourly precipitation data were altered using a series of factors according to rainfall intensity and seasonal characteristics. A succession of scenarios of adjusted precipitation sequence and land use were tested and a selection of these simulation results were presented and compared with observed flow data for 2005 (Table 4.4). The aim was to determine factors that are representative and adjustable for the daily water discharge trend for 2005 before applying them at longer time scales.

Table 4.4 *Selected tests of precipitation and land use series.*

Test No.	Rainfall Intensity P (mm/h)					M parameter
	P=0	0<P<1	1≤P<5	5≤P<15	P>15	
1	P+0.12	P-0.01	P*0.5	P*0.2		0.012 0.015
4	P+0.15(W) P+0.1(S)	P-0.01(W) P*0.65(S)	P*0.8(W) P*0.52(S)	P*0.6(W) P*0.4(S)	P*0.4 (W) P*0.26 (S)	0.012 0.015
5	P+0.15(W) P+0.1(S)	P*0.9(W) P*0.6(S)	P*0.7(W) P*0.4(S)	P*0.5(W) P*0.33(S)	P*0.3 (W) P*0.2 (S)	0.012 0.015
8	P+0.14(W) P+0.1(S)	P*0.85(W) P*0.6(S)	P*0.65(W) P*0.4(S)	P*0.45(W) P*0.33(S)	P*0.3 (W) P*0.2 (S)	0.012 0.015
❖ W represents winter season (October to March); S represents summer season (April to September).						

The precipitation series were adjusted by groundwater storage factors. Modelled water discharge is underestimated in the early months of the year in Test 1 (Figure 4.16a, e) due to the low magnitude of rainfall and insufficient groundwater replenishment. However, it produced a more suitable water discharge in summer. By considering the seasonal difference of groundwater storage and the distinctive effect of rainfall intensity on surface runoff, Test 4 and 5 (Figure 4.16b, c, f and g) display a similar trend to observed flow except the abrupt discharge peaks from heavy rainfall. Nevertheless, instead of reducing the discharge peaks after day 290 from extreme storms, much lower rainfall intensity in Test 5 diminished the runoff in summer dry periods. Furthermore, Test 8 (Figure 4.16d, e) shows an underestimated stream flow by reducing both the groundwater storage factor and rainfall magnitude, as well as showing little effect on peak deceleration. In order to smooth the flood hydrograph, land use changes represented by the M parameter, which plays a vital role in controlling the shape and magnitude of floods, were considered in these tests. Although a higher M value of 0.015 in Test 1, 4, 5 and 8 (Figure 4.16 e-h) suggests some effects of vegetation cover on diminishing modelled water discharge and peak flows in wet seasons (Figure 4.16 a-d), discrepancies between the two discharge data sets, especially at peak flows, still exist. Although, the correlation coefficient (r^2) implies stronger correlations between modelled and recorded water discharge for all simulations with the adjusted precipitation sequence, the highest value of r^2 for Test 5 (M=0.015) is 0.23, which demonstrates a poor match. The hydrological cycle in fluvial systems is complicated and the relationships of rainfall, groundwater and runoff cannot be simulated by simple linear approaches. Successful research approaches to modelling groundwater resources considered more factors such as soil water balance, evapotranspiration, temperature, infiltration and soil moisture deficits (Limbrick, 2002; Senarath, 1990). However, these factors are beyond the scope of this thesis.

M=0.012

M=0.015

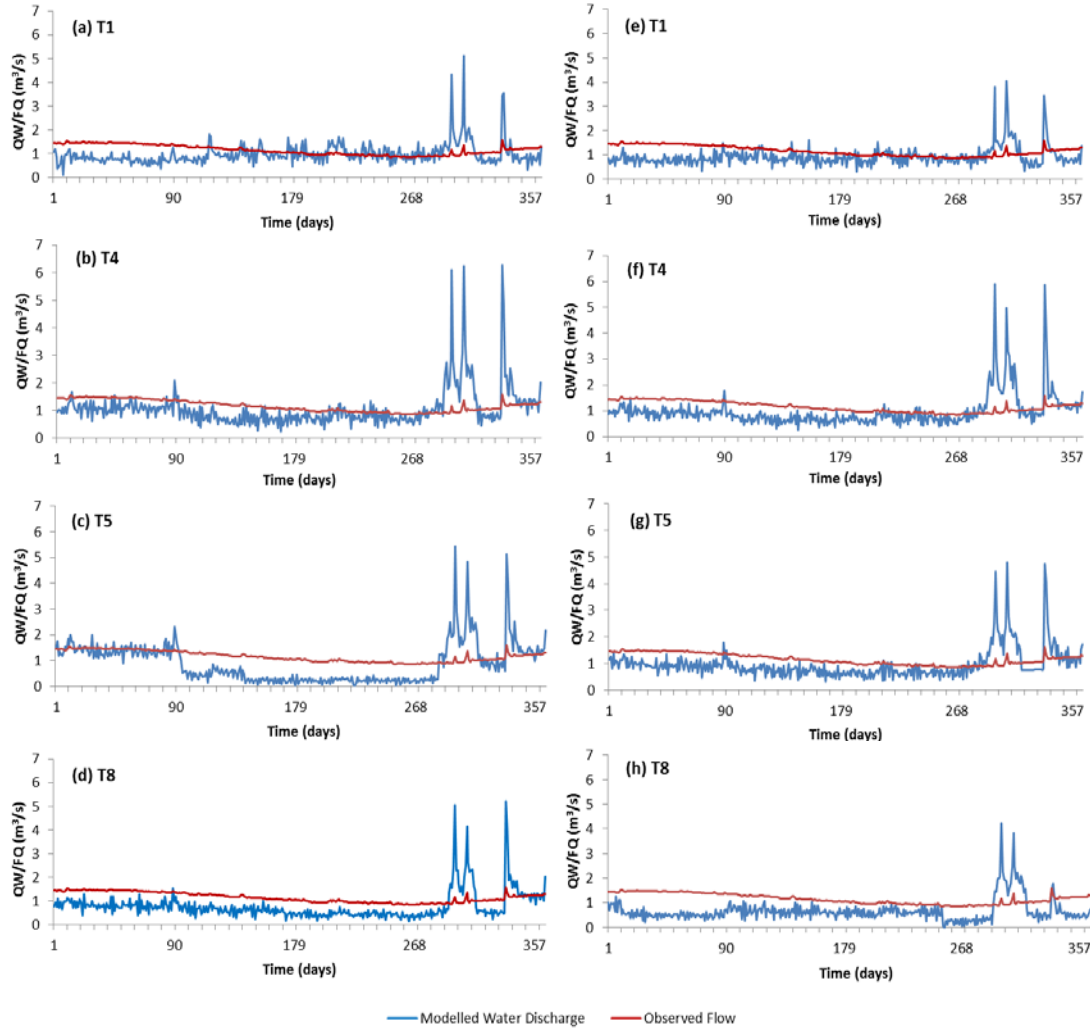


Figure 4.16 Comparison of modelled water discharge (blue) and recorded flow (red) for (a),(e) Test 1, (b),(f) Test 4, (c),(g) Test 5, (d),(g) Test 8 with different M values (0.012 and 0.015) for Alresford catchment in 2005.

For improved modelling of sediment transfer within a groundwater-fed chalk catchment, another factor, effective rainfall, was developed by reconstructing rainfall series from instrumental flow data. Based on the water discharge results and rainfall series from Test 5, the relationship between rainfall and stream flow was established with equation (1):

$$\text{Effective Rainfall (EF)} = 2.9445 * \text{Water discharge (QW)}^{0.7726} \quad (1)$$

Hourly effective rainfall series were created from documented flow data within the catchment from 1982 to 2009, and then they were applied to simulate water discharge (Test 10). As shown in Figure 4.17b, Test 10 produced a good match between recorded and modelled discharge data, replicating the reduced discharge through summer season and producing a sustained increasing discharge from the start of autumn to over the winter. The cumulative distribution of daily flows indicated that the model performs well for low flows, but consistently overestimated flows ranging from 1 to 2.25 m³/s and slightly underestimated peak flows. Discrepancies between the two flow data sets were unavoidable because the documented flow data were derived from a gauging station located downstream of Alresford Pond with a larger catchment area and may include water from other small streams that are not involved in the Alresford catchment. Theoretical flow data for a longer time scale were achieved by the association between modelled and observed discharge expressed in equation (2):

$$\text{Flow (FQ)} = -0.12892 \times QW^2 + 1.6454 \times QW - 0.5438 \quad (2)$$

Effective rainfall values take into account the annual pattern of groundwater storage; these were applied to simulate sediment discharge starting from 1889.

Further calibrations for the influence of vegetation cover parameter M on the flood hydrograph were carried out with a range of M values tested using effective rainfall for 2005. The M value that returned the best correlation (r^2) for modelled stream flows was 0.013 (Table 4.5). Therefore, the previously created M value of 0.012 for the catchment in 2005 was replaced by the new M value of 0.013. Accordingly, the M parameter series ranging from 1889 to 2009 was adjusted on this basis using the approach described in the section 4.5.1.1.

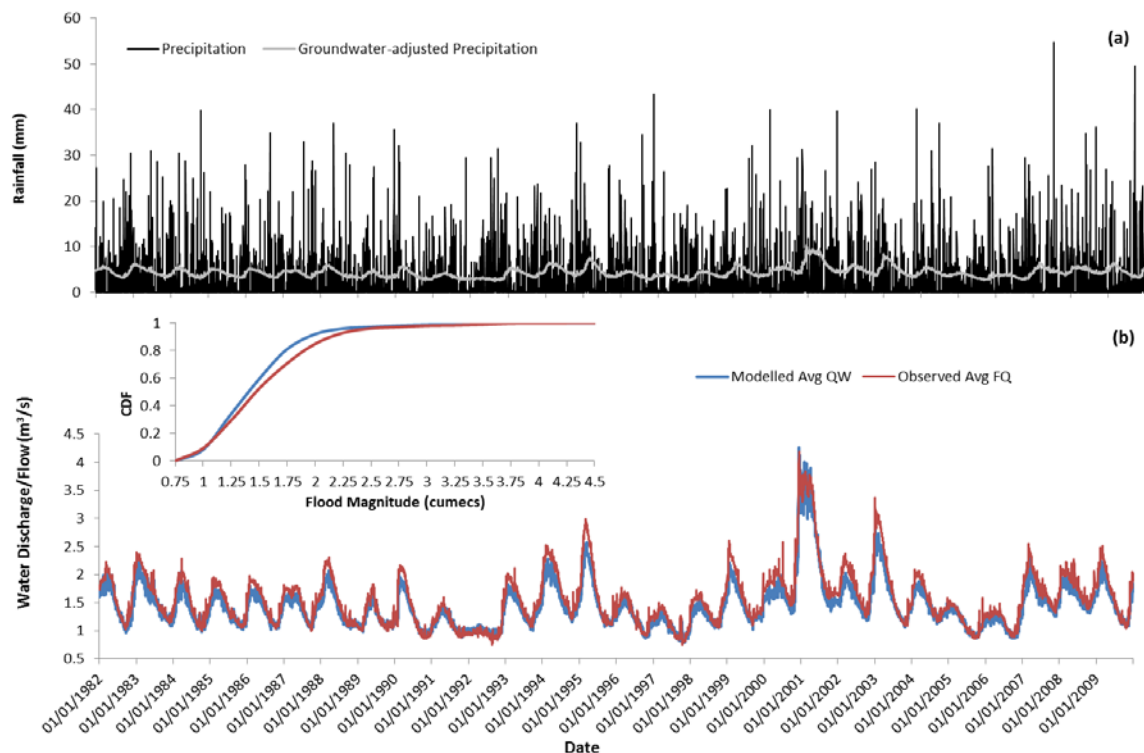


Figure 4.17 Comparison between (a) original and groundwater-adjusted precipitation; (b) simulated water discharge with effective rainfall and documentary flow records (1982-2009).

Table 4.5 Correlation for simulations with initial condition and varying M values, Alresford Pond catchment.

M Parameter	r^2 value	M Parameter	r^2 value
0.009	0.753	0.014	0.794
0.010	0.849	0.015	0.937
0.011	0.840	0.016	0.945
0.012	0.847	0.017	0.845
0.013	0.962	0.018	0.857

4.5.2 Holzmaar catchment

Since there is no direct record of forest cover inventories available for the Holzmaar catchment, the pollen record, in particular the ratio of arboreal and non-arboreal pollen, was analysed by Zolitschka (1998) and has been used to assign an M value for 5000 year simulation. It is difficult to calibrate M values in the absence of

available hydrological data in Holzmaar catchment. Therefore, we used the method of Welsh (2009) to link the percentages of arboreal pollen to M values. This method has been successfully applied for CAESAR modelling in Petit lac d'Annecy catchment, France, where the average arboreal pollen percentage was calibrated against historical forest cover records and aerial photographs. It suggested that an M value of 0.011 relates to an arboreal pollen percentage of about 70%, and the relationship between M values and pollen records is shown in Figure 4.18. As a consequence, a succession of M values was created from the pollen data in time series of 5000 years (Figure 4.19) to drive further long term simulations for Holzmaar catchment.

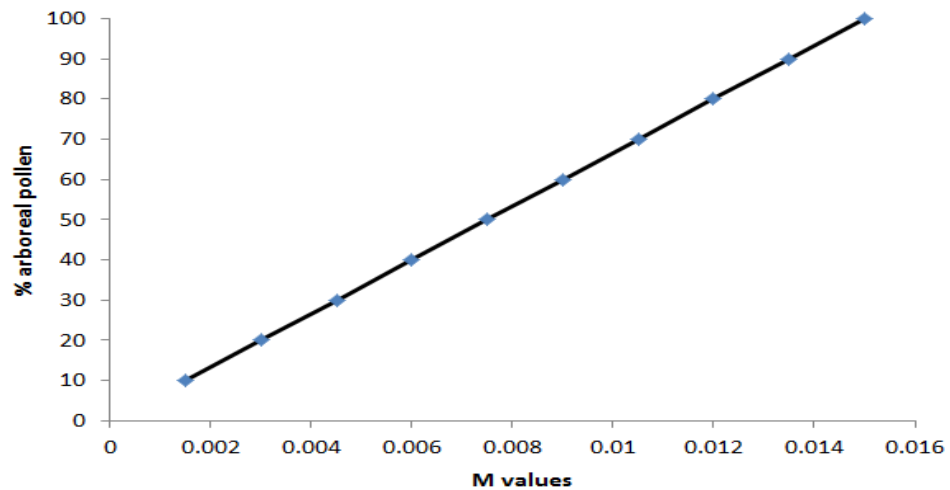


Figure 4.18 The relationship between M values and the percentage of arboreal pollen.

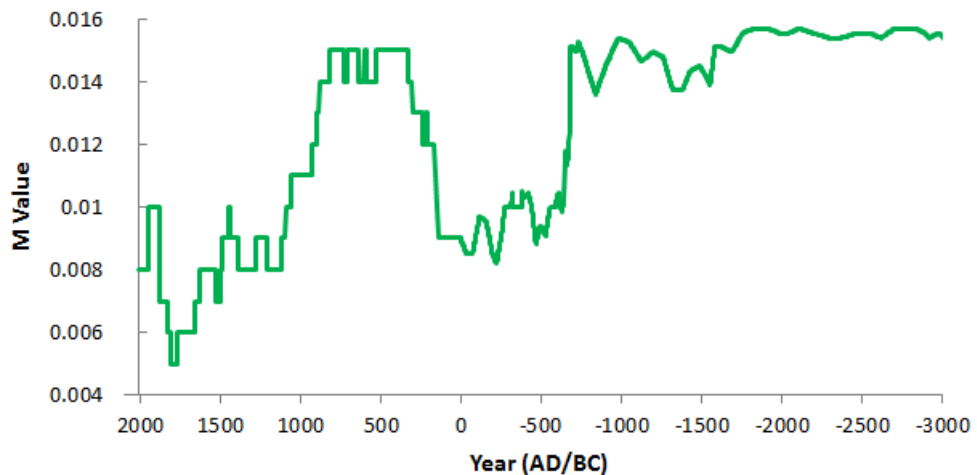


Figure 4.19 M value (vegetation cover) record converted from arboreal pollen for Holzmaar catchment between 2000 AD and 3000 BC.

4.6 Spin-up period testing

The simulation of both the Alresford Pond catchment for the short period of 1858 to 2009 and the Holzmaar catchment for a longer period of 5000 years were undertaken, driven by hourly precipitation and land-use history files, a bedrock file and a DEM. However, before real simulation, model spin up time must be tested to allow the model to become stable. The CAESAR model normally produced high sediment discharges in the first 10-30 years. Spin-up testing on the one hand allows the noise of surface roughness in the DEM to be removed and smoothed. On the other hand, this can sort the particle size distribution across the catchment in accordance with the sediment transport and water routing (Hancock, 2012). After repeating the 11-year hourly rainfall 10 times with a constant M value, the outputs were repeated every 11 years to determine the model spin-up period after which no appreciable change was observed.

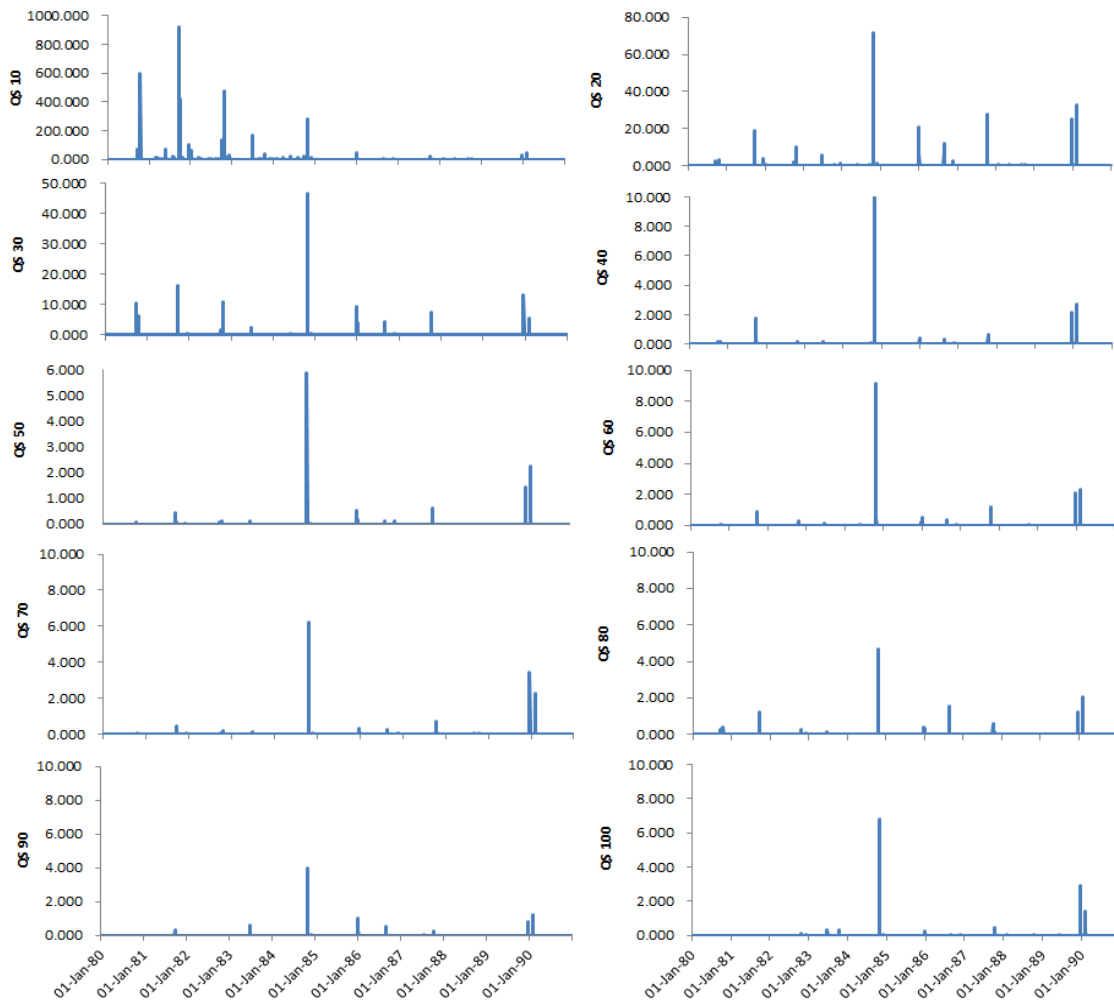


Figure 4.20 Graph of sediment discharges for every 11 years.

The initial high values of sediment output as a result of DEM smoothing process declined with time after the first 30 years of simulation. In this operation, fine materials, predominantly within channel cells, are eroded and sharp steps between cells rounded off to develop an armoured bed surface (Hancock *et al.*, 2011). The result of sediment discharges was calculated every 11 years and displayed in Figure 4.20. A sediment output of almost 3000 m³ was generated until the DEM smoothed down. From the 4th 11-year segment, the model displays regular patterns of sediment discharge with similar peaks and troughs. The correlation analysis of water discharge also proves that from the 4th 11-year water discharge is better correlated with each other (Table 4.6 yellow square). Therefore, it is necessary for the model to run for 30 or more years in order to stabilise. The outputs from simulations of landscape evolution in Alresford catchment were adjusted to remove this initial spin-up period.

A similar approach was applied in Holzmaar catchment, and a 50 year spin-up period was identified and subsequently removed from the original outputs of landscape evolution modelling.

Table 4.6 Correlation analysis of water discharge

Correlations											
		QW10	QW20	QW30	QW40	QW50	QW60	QW70	QW80	QW90	QW100
QW10	Pearson Correlation	1	.988**	.990**	.989**	.984**	.985**	.986**	.985**	.983**	.983**
	Sig. (2-tailed)	.	.000	.000	.000	.000	.000	.000	.000	.000	.000
	N	4018	4018	4018	4018	4018	4018	4018	4018	4018	4018
QW20	Pearson Correlation	.988**	1	.996**	.996**	.996**	.993**	.996**	.995**	.995**	.993**
	Sig. (2-tailed)	.000	.	.000	.000	.000	.000	.000	.000	.000	.000
	N	4018	4018	4018	4018	4018	4018	4018	4018	4018	4018
QW30	Pearson Correlation	.990**	.996**	1	.994**	.993**	.992**	.994**	.993**	.992**	.992**
	Sig. (2-tailed)	.000	.000	.	.000	.000	.000	.000	.000	.000	.000
	N	4018	4018	4018	4018	4018	4018	4018	4018	4018	4018
QW40	Pearson Correlation	.988**	.996**	.994**	1	.995**	.995**	.997**	.996**	.994**	.995**
	Sig. (2-tailed)	.000	.000	.000	.	.000	.000	.000	.000	.000	.000
	N	4018	4018	4018	4018	4018	4018	4018	4018	4018	4018
QW50	Pearson Correlation	.984**	.996**	.993**	.995**	1	.994**	.996**	.995**	.995**	.995**
	Sig. (2-tailed)	.000	.000	.000	.000	.	.000	.000	.000	.000	.000
	N	4018	4018	4018	4018	4018	4018	4018	4018	4018	4018
QW60	Pearson Correlation	.985**	.993**	.992**	.995**	.994**	1	.995**	.996**	.994**	.995**
	Sig. (2-tailed)	.000	.000	.000	.000	.000	.	.000	.000	.000	.000
	N	4018	4018	4018	4018	4018	4018	4018	4018	4018	4018
QW70	Pearson Correlation	.986**	.996**	.994**	.997**	.996**	.995**	1	.995**	.996**	.996**
	Sig. (2-tailed)	.000	.000	.000	.000	.000	.000	.	.000	.000	.000
	N	4018	4018	4018	4018	4018	4018	4018	4018	4018	4018
QW80	Pearson Correlation	.985**	.995**	.993**	.996**	.995**	.996**	.995**	1	.997**	.995**
	Sig. (2-tailed)	.000	.000	.000	.000	.000	.000	.000	.	.000	.000
	N	4018	4018	4018	4018	4018	4018	4018	4018	4018	4018
QW90	Pearson Correlation	.983**	.995**	.992**	.994**	.995**	.994**	.996**	.997**	1	.995**
	Sig. (2-tailed)	.000	.000	.000	.000	.000	.000	.000	.000	.	.000
	N	4018	4018	4018	4018	4018	4018	4018	4018	4018	4018
QW100	Pearson Correlation	.983**	.993**	.992**	.995**	.995**	.995**	.996**	.995**	.995**	1
	Sig. (2-tailed)	.000	.000	.000	.000	.000	.000	.000	.000	.000	.
	N	4018	4018	4018	4018	4018	4018	4018	4018	4018	4018

**, Correlation is significant at the 0.01 level (2-tailed).

4.7 Summary

Both lake sediment records and modelling approaches were discussed in detail in this methodology chapter.

For Alresford Pond, three sediment cores were taken in 2009 and sampled carefully for calculation and analysis of dry mass density, SCP chronology, sediment accumulation rates and magnetic susceptibility. Furthermore, surface soils were sampled in this chalk catchment as the measurement of magnetic properties of soils can support interpretations of sediment sources in cores. For the Holzmaar catchment, sedimentary information from a high-resolution varve chronology, the minerogenic sediment accumulation rate, magnetic susceptibility and non-arboreal pollen data were used, derived from published records. Lake sediment records were used to validate modelling outputs and to track the history of sediment transport within a basin for assessing landscape evolution under environmental changes.

The other important method is the setup of CAESAR parameters (e.g. DEMs, particle size distribution, rainfall and land use), particularly the creation of hourly rainfall and land cover data for all the simulations. For the Alresford catchment, an hourly rainfall series was produced using the hourly records (1982-2009) obtained directly from weather stations ODIHAM and MIDDLE WALLOP as a 4 year template. This short time series was repeated and adjusted to daily rainfall totals from BISHOPS SUTTON, CHILLAND and OTTERBOURNE stations to provide an hourly time series back to 1858. Hourly M values for Alresford catchment were created from a combination of NDVI, historical land use maps and pollen data. However, comparison between simulations and flow records from 1980 to 2009 showed a lack of correlation between instrumental and modelled water discharge due to groundwater influence on the chalk catchment. Groundwater-adjusted precipitation was created from a series of trial and error testing simulations by adjusting precipitation and m values to achieve the best correlation between modelled water discharge and recorded flow data. For the Holzmaar catchment, an hourly precipitation record was established back into the Holocene (~5000 years) based on the meteorological data and reconstructed palaeoprecipitation (i.e. tree-ring, pollen etc.) by using a method similar to that used for Alresford. We used the method of Welsh (2009), which has been successfully applied for CAESAR

modelling in Petit lac d'Annecy catchment, France, to link the percentages of arboreal pollen to M values for the Holzmaar. Finally, future precipitation probabilistic projections between 2010 and 2099 were created based on the UKCP09 data base at monthly scales, using the similar method for Alresford catchment. The limitation is that this rainfall creation approach only reflects rainfall magnitude changes. However, previous research from Coulthard *et al.* (2000, 2002) argued that changes in magnitude have much more important effect on erosion pattern than frequency. In essence, the approach is the only available method for creation of high-resolution and long-term rainfall series. Future landscape simulations based on projected rainfall scenarios were carried out for the Alresford only.

A serious limitation to running CAESAR is time. A simulation of about 150 years for Alresford catchment took approximately 12 days for the model to run and the trial and error testing simulations for 20 years need 30 hours. Further development of CAESAR as regards computing time is necessary.

It is important to note that the adjustment of M values for Alresford catchment via calibration of the NDVI with other data made the model work better. M values affect the hydrograph peak for a given storm and the rate of rise and fall in the water table, thereby controlling soil moisture deficit and representing the effect of vegetation cover on a catchment. However, in this case the increase of M values should not be taken indicate that the catchment has been really afforested. At the same time point as the M values were adjusted upward, new drainage systems (no represented in the model) came into effect in the catchment. The balance between high and low values in M values represented by the history or the changing pattern of vegetation cover is more important than actual values.

Chapter 5

Modelling sediment and water discharge in a chalk catchment since 1889

5.1 Introduction

Over the past 30 years, water erosion in English chalks landscapes has attracted much attention (Boardman and Robinson, 1985; Mutter and Burnham, 1990). It is suggested that calcium carbonate may increase the dispersibility of soils. Mutter and Burnham (1999) used plots to collect runoff and eroded soil of chalk land and concluded that chalky soils, as result of their alkaline reaction which makes calcium inactive in flocculation, are easily eroded. Chalk rivers derive their flows predominantly from groundwater discharge from chalk aquifers, and generally have a stable flow and temperature regime with a biodiversity habitat of high conservation importance. Evans (1990) reviewed the historical impact of woodland clearance on soil erosion in Neolithic chalk catchments, from the onset of accelerated erosion resulting from increasingly frequent floods, to the present day. Evidence of past human influence includes the physical modification of channel structures leading to frequent inundation of floodplains; increases of abstractions leading to siltation and vegetation changes; and the cultivation of crops and fisheries resulting in pollution, gravel cleaning etc. (Smith *et al.*, 2003). Studies on large erosion events have also emphasized that heavy rainfall, particularly intense storms that occur in autumn and winter, is an important trigger for erosion in areas with cultivation, especially on soils compacted by agricultural machinery (Boardman and Robinson, 1985; Fullen, 1985; Robinson, 1999). More sophisticated modelling technologies have been applied to determine the effect of environmental changes on chalk land development. For example, Favis-Mortlock *et al.* (1997) used the EPIC (Erosion-Productivity Impact Calculator) model to estimate erosion rate and change in soil profiles on the South Downs, UK, based on climate and land use stages and original loessial profiles. Their simulation indicates the effect of gradually intensifying agricultural activities on soil loss.

In this study, I aim to investigate soil erosion in association with its controlling factors in a chalk catchment (Alresford catchment, south England) at both temporal and spatial scales by applying a modelling approach, combined with lake sediment evidence. We use a landscape evolution model (CAESAR) to calculate sediment discharge over a period of 151 years. To elucidate a better understanding of sediment dynamics in chalk catchments as an indicator of environmental change, simulated results are compared with high resolution sedimentological archives and field data.

5.2 Site description

5.2.1 Introduction

There are considerable expanses of chalk outcrop in England. Chalk aquifers provide an important water resource, comprising approximately 53-60% of the groundwater abstraction (Bradford, 2002; Downing, 1998) in the UK. Rivers draining the chalk outcrop exhibit a relatively stable flow regime as reflected by their low relief in catchments and low sediment concentrations. However, low flows may also incur high levels of sediment deposition (Bradford, 2002; Sear *et al.*, 1999). The selected study site is a typical groundwater-fed chalk catchment.

Old Alresford Pond is located in the Hampshire basin, approximately 6 miles to the east of Winchester on gently rising slopes, east of the River Arle and its confluence with the River Itchen (Figure 5.1). It was formed following the suggestion of Bishop Godfrey de Lucy to construct the Great Weir between Old and New Alresford, for the purpose of diverting springs from nearby districts to supply downstream mills (Alresford Chamber of Commerce, 2011). The construction was completed by about 1189 (Environment Agency, 2007) as a balancing lake for River Itchen navigation and derives its name from ‘the ford over the river where the alder trees grow’. The pond area is approximately 0.3 square kilometres and the whole catchment area is about 42 square kilometres (Wilson, 2000). The pond is reported to have covered about 100 hectares when it was built (Environment Agency, 2007). The changes in the shape and size of the pond from the 1870s to the 1990s are shown in Figure 5.2. Old Alresford pond is very shallow with an average water depth of 0.35m in 2006

and the average residence time of water has been approximated to be less than one day (Environment Agency, 2006; 2007)

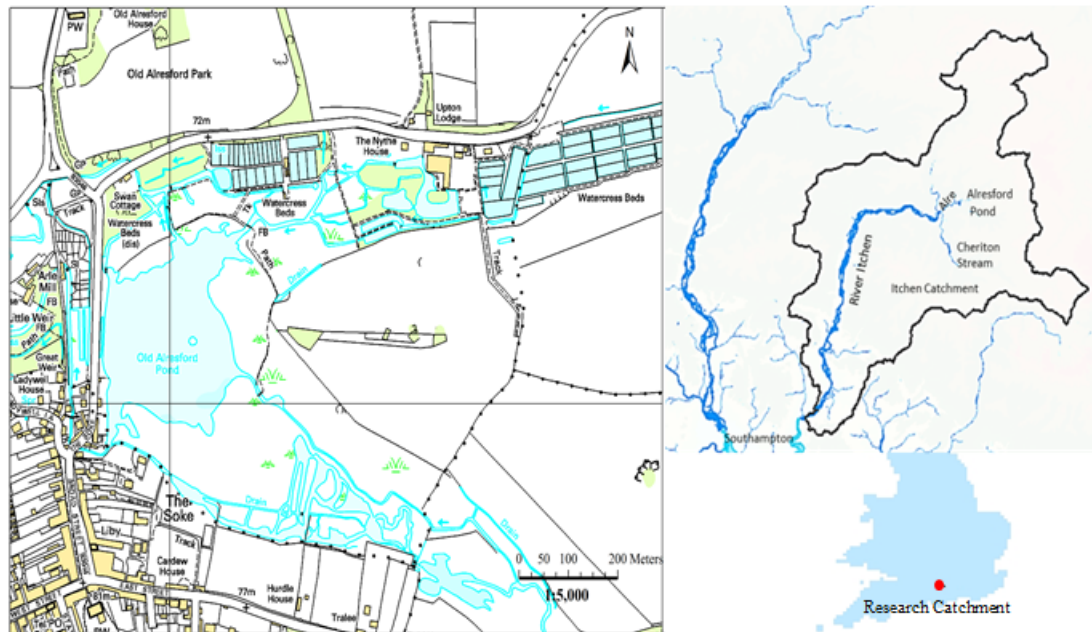


Figure 5.1 Location of Alresford Pond in Hampshire, Southern England (From Edina Digimap 1:5000 and the Centre for Ecology & Hydrology).

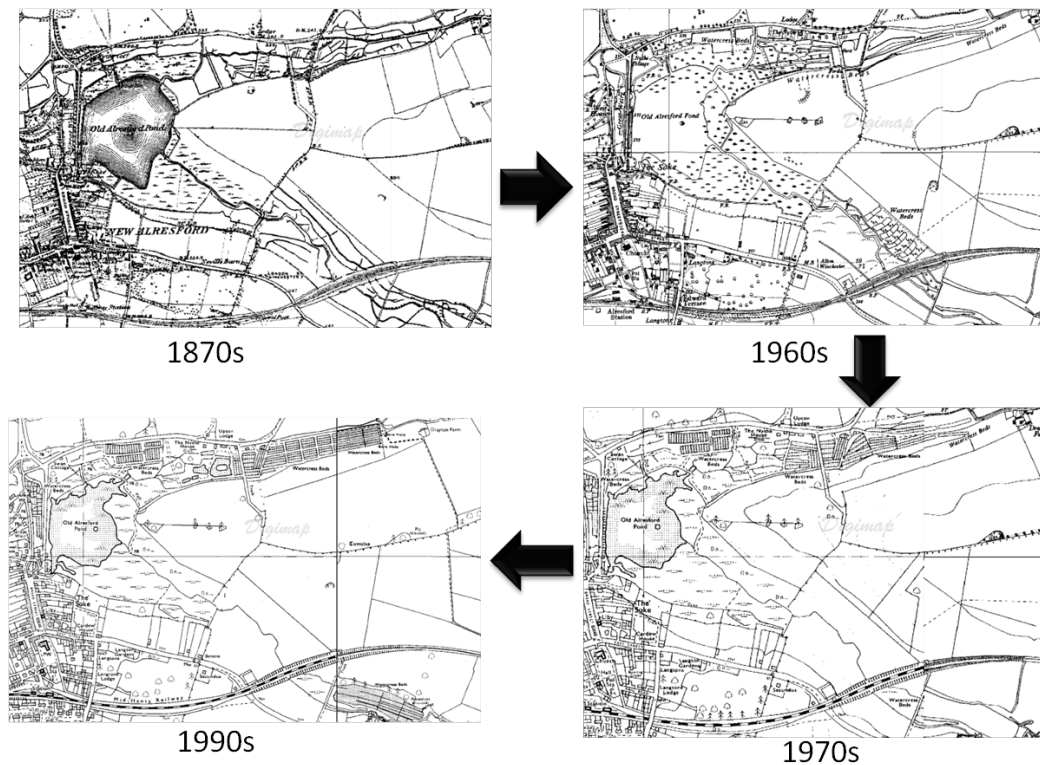


Figure 5.2 Changes of shape and size of Alresford Pond from 1870s to 1990s (Edina Historic Digimap 1:10560).

5.2.2 Geology and Geomorphology

Research based on boreholes revealed the stratigraphy (Figure 5.3) of the rocks beneath the Alresford catchment (Farrant, 2002). A thin Permo-Triassic sequence of limestone, siltstone, sandstone and breccia lies over the pre-Variscan Devonian-Carboniferous basement that predominantly consists of cleaved, reddish brown siltstone, mudstone, sandstone and hard recrystallized Carboniferous dolomites. Lower Cretaceous rocks (informally called 'Wealden Group') lay concealed at depth beneath the deposition of Lower Greensand (LGS) and Gault and overstep all the Jurassic formation until they rest on the Triassic (Melville and Freshney, 1982). The Upper Greensand (UGS) and basal beds of the chalk roughly follow the Gault outcrop across the majority of the catchment. The Upper Cretaceous chalk stratum in Alresford catchment belongs to the upper white chalk subgroup according to the lithological mapping from British Geological Survey (Bristow *et al.*, 1997). The upper chalk formation can be divided into several members, and from the geology map of this area (Figure 5.4), members of Newhaven chalk and Seaford chalk provide homogeneous bedrock over considerable areas of the catchment. Seaford chalk is a soft, fine-grained and smooth white chalk characterised by its conspicuous and semi-continuous large nodular flints with a thickness of 40-80 m. The Newhaven chalk unit is made up of firm, white, soft to medium hard chalks with extensive marl seams and flints varying between 50 and 75 m thick.

Soil develops as a result of physical, chemical and biological processes acting upon underlying rocks. Soils in Alresford catchment are composed of mainly silt loams or silty clay loams, rarely thicker than 23 cm over chalk bedrock (Favis-Mortlock *et al.*, 1997). Scattered over the chalk outcrop are accumulations of reddish brown and orange-brown clay containing clayey silt, sandy clay with rounded flint pebbles, and a variable proportion of fine- to medium- grained sands. This clay-with-flints has a thickness up to about 10 m and is found on the surface of the chalk and filling hollows (Monkhouse, 1964). Sand and gravel are come from river terrace depositions and gravelly heads in the major valleys.

A survey undertaken by the Environment Agency (2007) concluded that pond beds comprise gravels and clay alluvia on chalk bedrocks. Sediment depth survey carried

out by ADAS (Old Alresford Pond Analysis of Silt) in 1994 recorded that the average silt depth in the pond ranges between 2.5m to 3m.

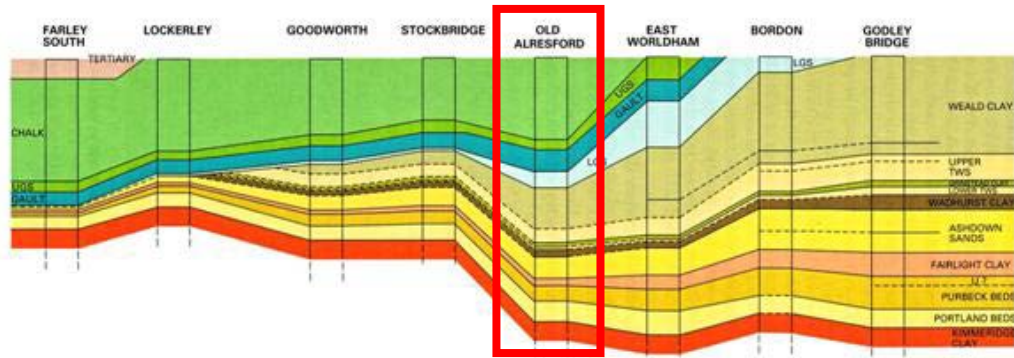


Figure 5.3 East-west transect of Alresford District (after Farrant, 2002).

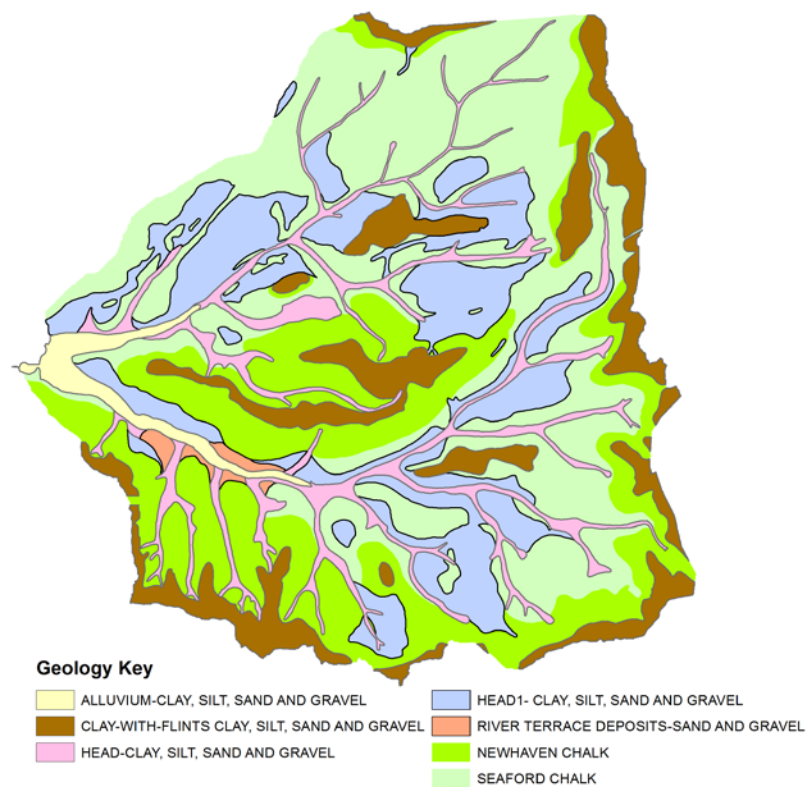


Figure 5.4 Geology of Alresford Catchment. Where superficial deposits are present, the bedrock geology will be concealed (from British Geological Survey and Southampton GeoData Institute).

5.2.3 Hydrology and precipitation features

Rainfall data obtained from Met Office reveals that yearly precipitation (1882-2009) ranges from approximately 400 mm at the lowest point (in 1921) to over 1160 mm at the highest (in 1927; Figure 5.5) with a mean of 780 mm. There are around 150 to 200 rainy days (i.e. greater than 0.2 mm precipitation) per year, of which nearly 74% are wet days (greater than 1.0 mm). The months of October to January receive the most rain, with over 80 mm in each month, and December is the wettest month throughout the basin (Figure 5.6). The lowest monthly average is in July, although April to August are all relatively dry months. Therefore, droughts are most common in spring and summer. This is a common characteristic in southern England, which may in part be attributed to a low frequency of Westerly flow. Consequently, irrigation may be necessary in this area to obtain a full yield of crops during April to August, although soil differences may modify or exacerbate the importance of the purely climatological factors (Monkhouse, 1964).

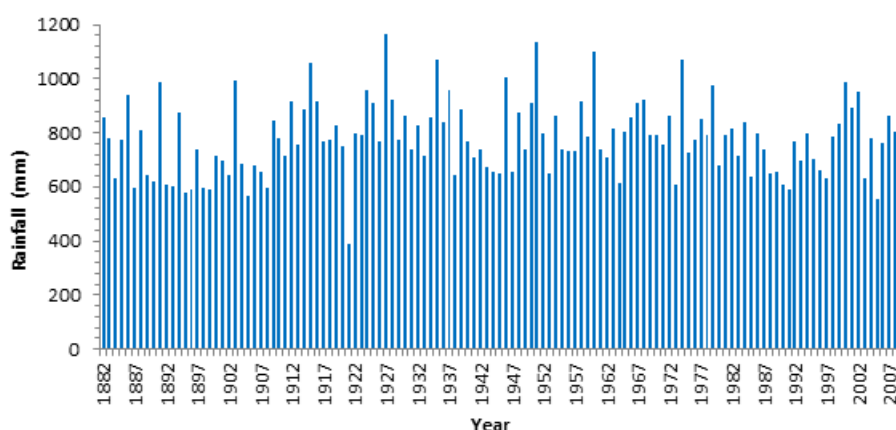


Figure 5.5 Annual precipitation at Alresford (1882-2009) (Data source: Met Office).

There are two streams flowing into Alresford Pond: one is the Bishops Sutton Stream from the south-east, and the other is the Nythe Stream from north-east (Figure 5.7). When the Nythe Stream reaches the pond, it splits into several small braided branches, receiving waters from nearby watercress beds and merging at a footbridge before entering the pond (Environment Agency, 2007). The flow route of Bishops Sutton Stream is complicated, with a fraction of flow draining into the by-pass channel and the remainder entering the pond. Outflows of the pond pass through a

series of watercress beds and a dam before joining the River Arle, which is the tributary of the River Itchen in the Solent River system. The water depth of Alresford Pond as estimated by an Environment Agency sediment survey (2006) was recorded with an average value of 0.35m and a range of 0.06 m to 2.2 m.

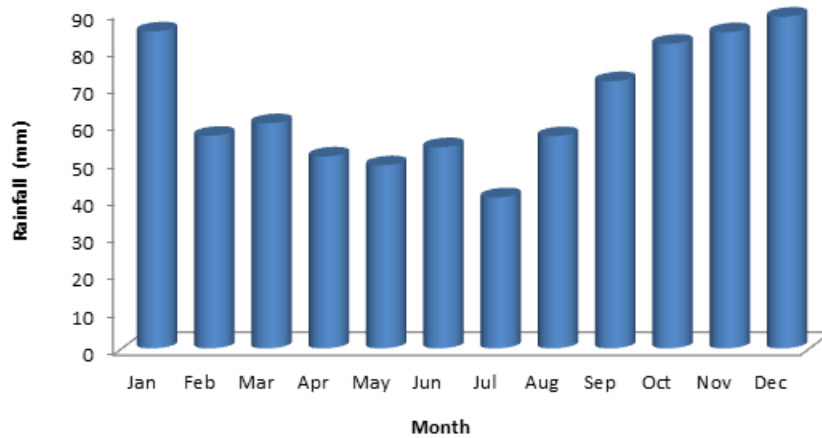


Figure 5.6 Average monthly precipitation in Alresford between 1961 and 1990 (Data source: Met Office).

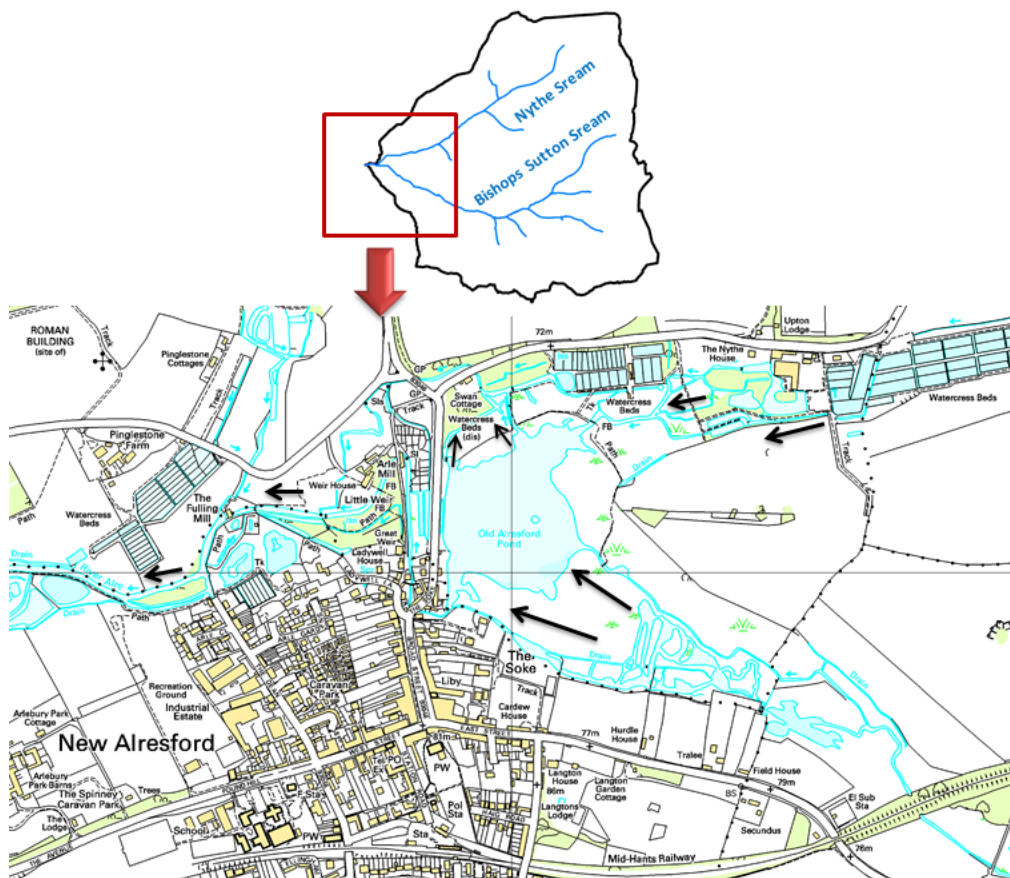


Figure 5.7 Alresford Catchment and its streams (Data source: Ordnance Survey). Black arrows indicate flow directions.

Chalk is microporous with low intrinsic permeability and water seeps through the material at a very slow rate. However, fissures of flints are normally well distributed throughout the chalk layer and thus play an important role as collectors and conduits forcing the movement of groundwater (Monkhouse, 1964). As the main aquifer in Alresford catchment, chalk strata store a large amount of groundwater and act as an important water resource to southern England. Average Base Flow Index (BFI), an index of proportion of water discharge fed by stored groundwater sources, can be 0.95 or more (from the Centre for Ecology & Hydrology), which explains the dominance of ground water in river flows and a low daily variability. Data obtained from gauging stations indicate that in a relatively dry summer (Figure 5.8), there is little infiltration downwards in the water table. Rainfall moistens only the surface soil and is subsequently lost through evapotranspiration. Therefore the complementarity of groundwater capacity mainly depends on the winter rainfall and regular flows from watercress farms. In a typical year, river flows are highest in the late winter and early spring, then decline gradually through the summer to a minimum in the autumn.

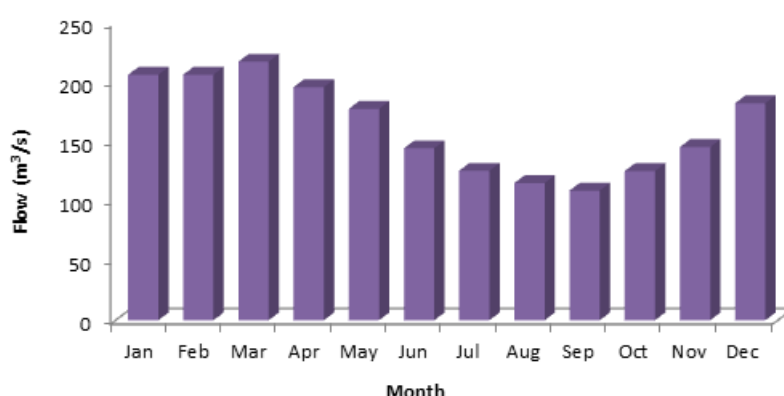


Figure 5.8 Average monthly flows in the Alresford catchment from 1959 to 1999 (from National River Flow Archive, the Centre for Ecology & Hydrology).

5.2.4 Land use and vegetation features

The landscape of Alresford catchment comprises rich farmland and extensive grassland surrounded by a wooded river valley and scattered modern housing estates (Figure 5.9). Waller and Hamilton (2000) investigated the vegetation history of the chalk land by a pollen sequence from the Caburn, East Sussex and suggested that soils were thicker and less calcareous during the mid-Holocene, and thus had large

areas of woodland dominated by oak at this time. However, as a result of population pressure, improved farm technologies and freer use of hired labour since approximately the eighteenth century, gradual processes of woodland clearance began. Most of the cultivable lands in the catchment were brought into use for agriculture and grazing pasture as a result of direct enclosure (Monkhouse, 1964). The remaining unexploited woodland consists of oak and beech, with more occasional areas of pinewood, birchwood and ashwood.

Chalk groundwater has an even temperature of about 10 °C throughout the year and has a mineralogically and biologically high quality (Casey and Smith, 1994). The watercress beds, distributed extensively around Alresford pond, are fed by the water from natural springs and overflowing boreholes that provide an ideal environment for watercress cultivation to receive a constant flow of cool water in summer and warm water in winter (Headworth, 1978). Since much of the water passes through the watercress beds before accessing the pond, outflow discharge may be influenced by disturbances from fertilization and harvesting in the watercress beds (Crisp, 1970). Meanwhile, sluices are used to regulate the flow of water to keep an appropriate water depth in the beds (Alresford Chamber of Commerce, 2011).

Table 5.1 Land use (%) of the Alresford catchment in 2000 calculated from the Land Cover Map 2000 (Data source: Southampton GeoData Institute).

Land Use Map 2000 target classes	Percentages of each class (%)
Woodland	9.4
Arable and Horticulture	56.6
Grassland	29.3
Open shrub heath, fen, marsh and swamp	0.1
Others (inland water, inland bare ground, built-up areas and gardens)	4.6

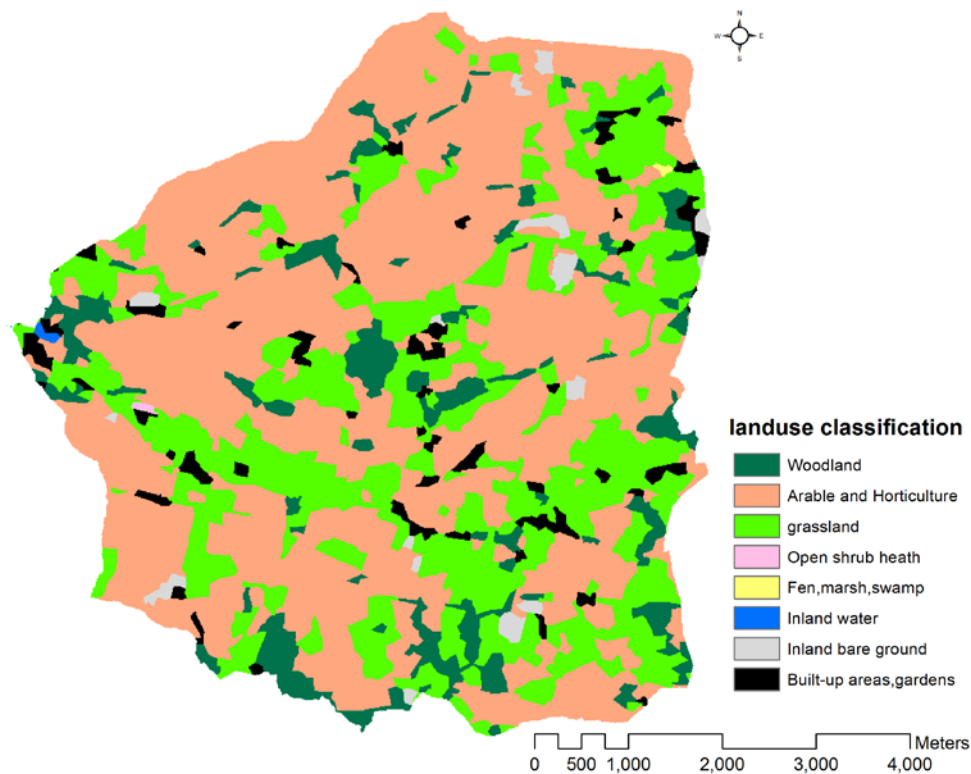


Figure 5.9 Land use of the Alresford catchment in 2000 (Data source: Southampton GeoData Institute).

The pond as a whole supports a rich aquatic swamp plant community (e.g. reed). The chalk stream has a diversity of fish species, notably brown trout (*Salmo trutta*) (Acornlry and Sear, 1999). Similar eutrophic lakes are rare in chalk stream valleys and Alresford Pond has been designated as a Site of Special Scientific Interest (SSSI) for the highest level of nature conservation. Recent research by Nature England (2009) reported that the pond remains heavily silted up and there is only a relatively small area of open water remaining which may produce unfavourable impacts on the catchment ecosystem. An algae bloom was reported in the summer of 2006 resulting from the shallow water depth and hot weather (Environment Agency, 2007). However, Casey (1981) found that outflow from watercress beds would be beneficial for chalk water to maintain water levels during periods of low flow. No macrophyte vegetation has been found in the pond after macrofossil data analysis as reported by the Environment Agency (2007).

5.3 Model setup

The following is a concise description of model setup, with more details given in chapter 4.

The simulation of Alresford catchment was carried out from 1858 to 2009 and the result of the first 30 years (1858-1888) was removed as a ‘spin-up’ period. The model was set up using a 10 m by 10 m DEM (section 4.3.2) and an hourly groundwater-adjusted effective rainfall series created by modulating meteorological records with observed flow data (section 4.4.1 and 4.5.1). The model was also driven by hourly M values which represent the land use history and vegetation cover of the catchment (section 4.5.1). Initial sediment distribution was divided into nine fractions and the finest of these fractions ($< 62.5 \mu\text{m}$, clays and silts) were treated as suspended sediment (section 4.3.3.1) in accordance with Sear *et al.* (1999). The outputs from CAESAR modelling include water (m^3/s) and sediment discharge (m^3) in different resolutions (hourly to annually). The results of hourly and daily water discharge are used for calibration of rainfall and M values. Meanwhile, the result of annually sediment discharge was compared with the dated lake sediment records for model validation and further analysis. Changes in surface elevation that reflect net erosion and deposition patterns of the system were saved as a series of DEMs at decadal intervals and displayed in visual images.

5.4 Analysis of lake sediment archives

5.4.1 Dating recent lake sediments by spheroidal carbonaceous particles (SCP)

The SCP concentration profile of the sediment core taken from Alresford Pond (labelled AP 09-03) is displayed in Figure 5.10. It has a similar temporal pattern according to the three major features described by Rose (1995, 2001). From the appearance of carbonaceous particles in the 195 cm sample, SCP concentrations are low ($< 500 \text{ gDM}^{-1}$) but increase slowly and steady over a period of decades from 155 cm to 50.5 cm. Followed by a rapid increase, the SCP concentration reaches to a peak of over 3500 gDM^{-1} at the 38.5 cm mark on the core. SCP concentrations decrease rapidly between 36.5 to 30.5 cm and although they fluctuate, continue to

decline with depth before rising slightly to a small peak at approximately 11.5 cm then followed by a slightly descent again towards the sediment surface.

Referring to the established SCP chronology for south and central England (Figure 5.11) from Rose and Appleby (2005), the cumulative percentage of SCP concentration profile of core AP 09-03 was calculated and each 10% marker was ascribed to the depth (Table 5.1). Years were associated with cumulative percentage and depth (Figure 5.12). Particularly important was the identification of the year 1850 as it defines conditions prior to the land use intensification and eutrophication in most European lakes in the 20th century (Rose *et al.*, 2011).

The linear regression of the SCP cumulative percentage profile with error margins was calculated to apply a timeline to all of the proxy records (Figure 5.13). With this, the sediment accumulation rate can be extrapolated linearly over the selected dates according to different sediment accumulation rate and density. However, the chronology of sediment exhibits an error range from ± 5 years to ± 25 years which may result in uncertainties in referred measurement of erosion and deposition. The majority of the dates fall within the regressed error bounds with the exception of those at the top of the core. Varied sedimentation rates and the lack of additional chronology information between 1970 and 2009 may result in the exception of the top core out of the line of linear regression.

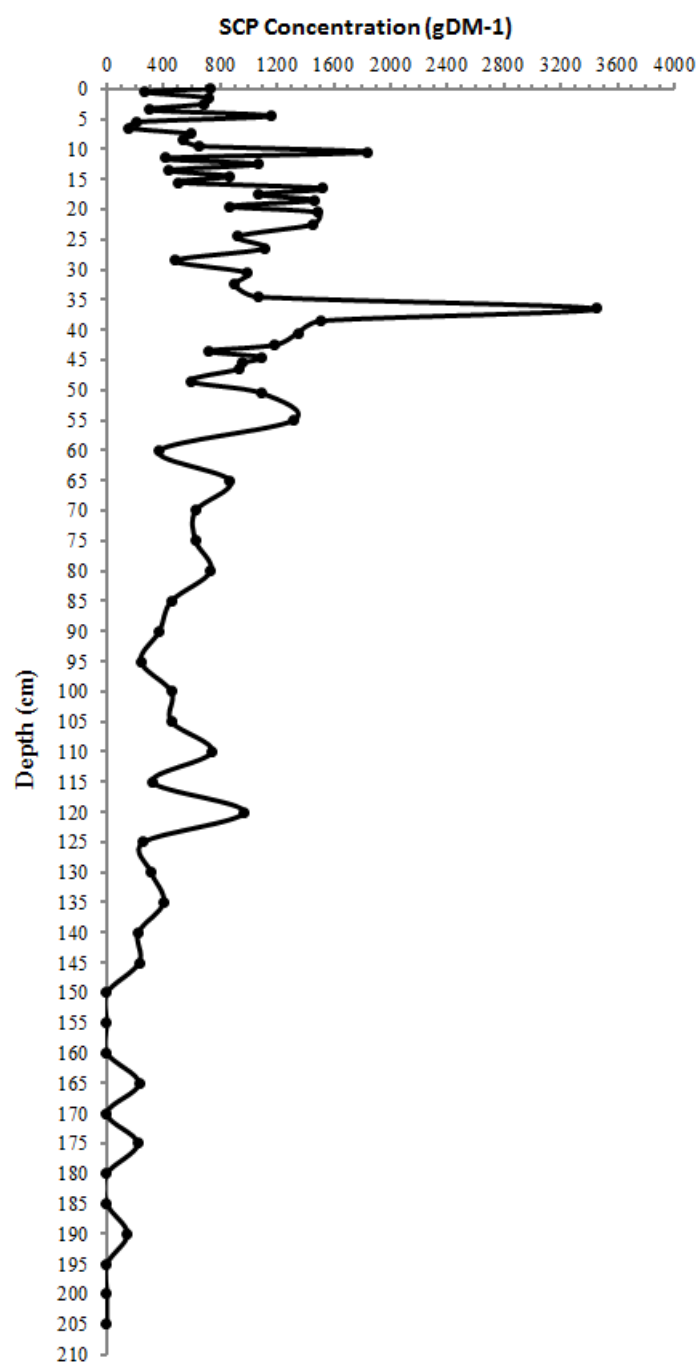


Figure 5.10 SCP concentration profile for core AP 09-03.

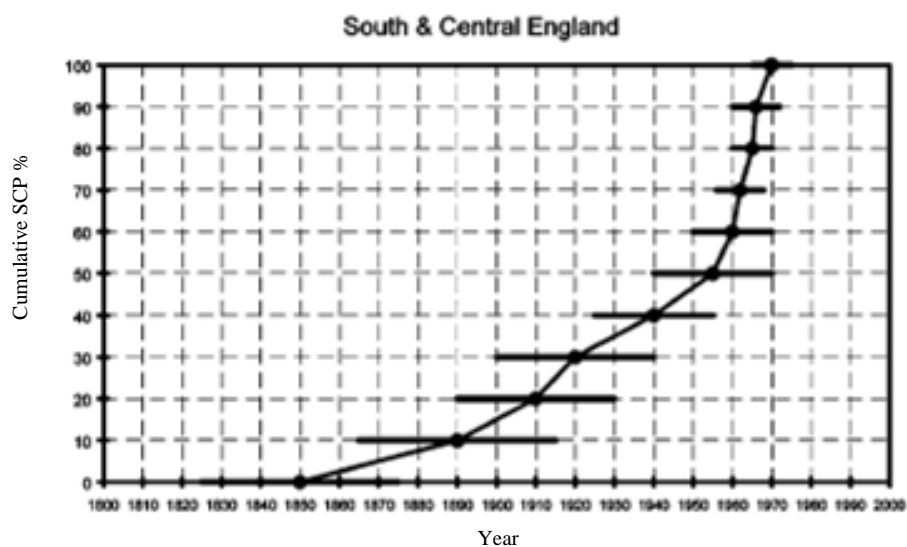


Figure 5.11 Cumulative SCP percentage profiles of south and central England showing confidence limits for each 10% (from Rose and Appleby, 2005).

Table 5.2 Dates for each 10% of the SCP cumulative percentage profile combined with the depth of core AP 09-03.

Cumulative Percentage of SCP (%)	Depth(cm)	Date with error margins
0	195	1850±25
10	129	1890±25
20	107.5	1910±20
30	82.5	1920±20
40	64	1940±15
50	55	1955±15
60	46.5	1960±10
70	44	1962±6
80	42	1965±5
90	40	1966±6
100 (SCP peak)	38.5	1970±5
Surface of the core	0	2009

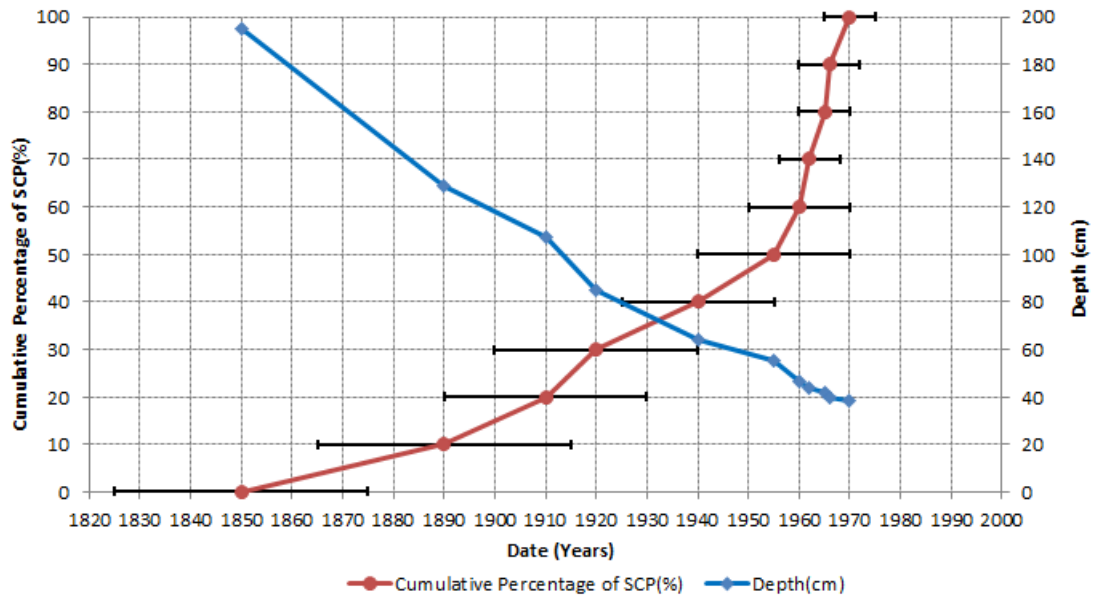


Figure 5.12 Combined cumulative percentage of SCP profile for Alresford Pond, with error margins according to Table 5.1.

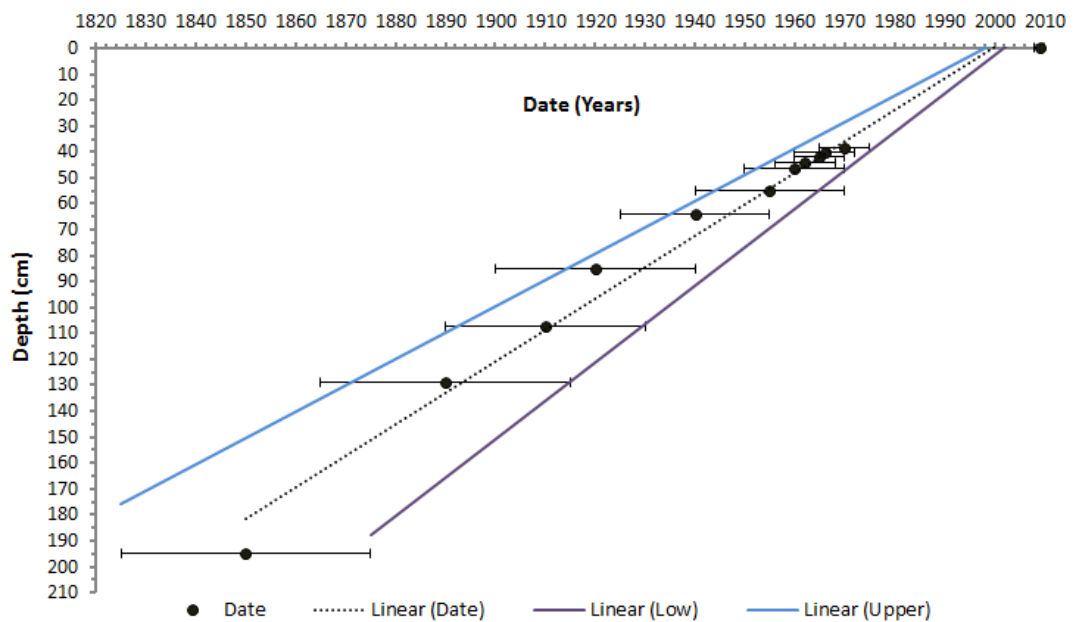


Figure 5.13 Linear regression of SCP cumulative percentage profile. The black plots represent date markers with error margins, the black dashed line is their linear regression line (equation: $y = -1.2083x + 2416.2$, $R^2 = 0.9795$). The solid purple and blue lines are the linear regressions of low ($-1.4782x + 2959$, $R^2 = 0.9847$) and upper ($-1.0128x + 2023.7$, $R^2 = 0.9674$) error margins. Error margins were shown according to the Table 5.2 of SCP chronology which is established in reference of published data from Rose and Appleby (2005).

According to these dates and error margins, the mean sedimentation rate for the period between 1970 and 2009 is around 1.1 to 1.28 cm per year, which is close to the rate of 1.14 to 1.39 cm per year for the post-1970 period reported by Rose and Tuner (2007). However, they did not obtain the start of the SCP record due to the short length of their core, although they estimated that the full industrial record should be enclosed within the upper 200 cm of sediment with an assumption of a virtually unchanged sediment accumulation rate. The commencement of the SCP record at 195 cm is in agreement with this estimation.

Selected samples from core AP 09-03 were measured for artificial radionuclide to calibrate the SCP chronology (Table 5.2). Unfortunately, inventories of ^{137}Cs and ^{241}Am in most samples are below the limit of detection, with an exception of weak detectable concentrations of ^{137}Cs and ^{241}Am at a depth of 30.5 cm and 50 cm respectively. However, these two values are not sufficient to calibrate the SCP chronology by linking the ^{137}Cs activity peaks to either the significant levels of weapon test fallout in 1963 or the 1986 Chernobyl accident (He *et al.*, 1996). Sediment mixing or accelerating sedimentation may result in the dilution of ^{137}Cs and ^{241}Am records at this site (Odgaard, 1993). Assuming that these two detectable values are concentration peaks of ^{137}Cs and ^{241}Am within the sediment profile, the estimated SCP dates are 1978 ± 5 for the depth of 30.5 cm and 1958 ± 10 for the depth of 50 cm. The ^{137}Cs peak in 1978 ± 5 is on the verge of 1986 Chernobyl fallout; however no marker of ^{137}Cs corresponding to the maximum of nuclear weapon testing was recorded. The more recent and relatively high fallout of the Chernobyl ^{137}Cs profile may obscure the weapons-attributed ^{137}Cs peaks by downward diffusion (Appleby, 2001). In this cases, the peak of ^{241}Am , another product of fallout from atmospheric weapon testing, which is proven to be less mobile than ^{137}Cs , may indicate the sediment dates of 1963 (Appleby *et al.*, 1991; Appleby, 2001). Both of the two SCP dates have a time lag from the dates identified by significant levels of atmospheric fallout. However, SCP dates of 1958 may broadly match the 1963 peak within error margins. These features are likely due to post depositional remobilisation of the sediment, downward diffusion of ^{137}Cs , or the compacting effect of lake sediment diagenesis that may pre-date the fallout events (Klaminder *et al.*, 2012). According to the SCP dates, the detectable values of ^{137}Cs and ^{241}Am concentration are both post-1954, the mark of the beginning of ^{137}Cs

and ^{241}Am records. This is a more straightforward evidence of correlation between SCP chronology and artificial radionuclide dating.

Table 5.3 Calibration between SCP chronology and artificial radioisotopes records.

Sample ID	Depth (cm)	^{241}Am (Bq/g)	^{137}Cs (Bq/g)	SCP Date
AP 09-03 16	8	<0.004	<0.006	2001 \pm 2
AP 09-03 17	8.5	<0.005	<0.004	2000 \pm 2
AP 09-03 61	30.5	<0.004	0.016 \pm 0.003	1978 \pm 5
AP 09-03 80	40	<0.002	<0.003	1966 \pm 5
AP 09-03 84	42	<0.002	<0.002	1965 \pm 5
AP 09-03 100	50	0.0047 \pm 0.0009	<0.002	1958 \pm 10

Since core AP 09-01 and AP 09-02 are not long enough to reach the start of SCP records, it is impossible to build the chronology for site AP 09-01 and AP 09-02 from these insufficient SCP records. However, these two cores were taken at the northern end of the pond, which is close to core ALR1 collected by Susanna Black (2007) at 2007, near the inflow of Nythe stream with consecutive SCP chronology. The comparison of SCP concentrations in equivalent depth, between core AP 09-01 and core ALR1 displays a similar pattern (Figure 5.14). Thus, the established SCP chronology was used to build the time scale for core AP 09-01, which was in turn used to date the following magnetic susceptibility sequence for both core AP 09-01 and AP 09-02 for the purpose of improving interpretation of environmental changes and their possible links.

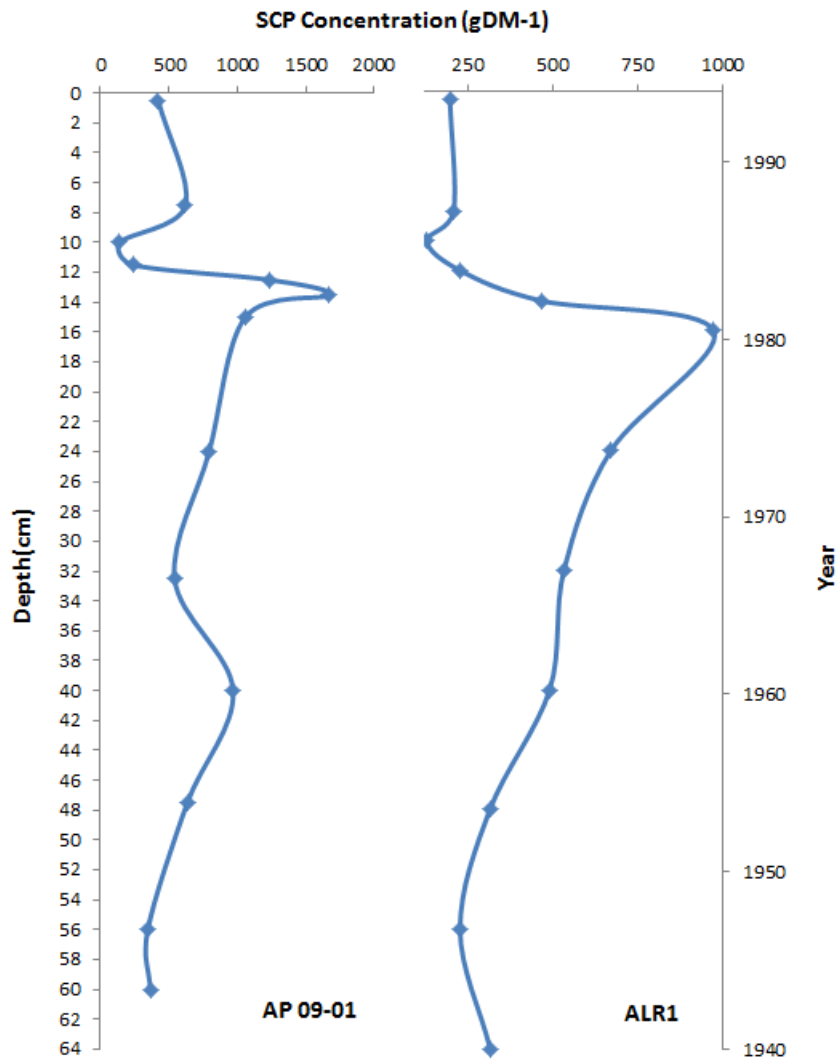


Figure 5.14 Comparison of SCP concentration between core AP 09-01 and ALR1 (after Susanna Black, 2007).

5.4.2 Magnetic susceptibility analysis

All the three cores were sliced at half centimetre intervals, producing a total of approximately 500 samples. Magnetic susceptibility, which relies on the changing volume of ferromagnetic minerals in lake sediments, was analysed for all samples. The susceptibility profiles shown in Figure 5.15a demonstrate considerable synchronous fluctuations with peaks and troughs in distinguishable values in cores with different length. The parallelism of susceptibility patterns between cores is more obvious in the upper parts of the sediment profiles, with a rapid increase from 22-18 cm or 45 cm to peaks at 13.5-10 cm or 36-22 cm for core AP 09-01/02 and AP 09-03 respectively, and then decline towards the top of the core. Each trace displays a

descent of susceptibility values in the lower sections with extremely low values of susceptibility that indicate a diamagnetism behaviour. Furthermore, the comparison of magnetic susceptibility between cores at the depth of 10-100 cm shows a clearer view of core correlations (Figure 5.15b). Magnetic records in lake sediments reveal the features and ratios of sediment sources, especially concerning the transport of iron-containing detrital soil to the lake. All the cores exhibit a high degree of correlation in susceptibility patterns suggesting a common source. Particularly, a noticeable small peak at the depth of 85cm in core AP09-03 is tracked in the other two cores at the depth of approximately 48cm and 45 cm, respectively. Before 1980, susceptibility values of all the cores are within a range of -0.02 - $0.12 \times 10^{-6} \text{m}^3 \text{kg}^{-1}$. However, core AP 09-03 displays extremely low values of susceptibility, which are almost an order of magnitude lower than the other two cores after 1980. Core AP 09-01 and 02 are taken close to the inflow of the Nythe stream, which has a low energy potential in channels as it splits into a series of meandering, braided channels before entering the pond. These braided channels received water from the Nythe and Drayton watercress beds and are densely vegetated (Environment Agency, 2007). Sediments from cores AP09-01 and 02 may be affected by the sediments from watercress beds and the intensive cultivation of watercress after 1980 may strongly enhance the magnetic properties in the sediments. As water flow approaches the pond from the Bishops Sutton stream, a proportion of this flow enters a channel with by-pass the pond entirely and the rest of the flow proceeds directly toward the pond without passing through watercress beds (Environment Agency, 2007). Therefore, the magnetic curve of core AP09-03 demonstrates a fast sediment accumulation and low magnetic concentration which is likely to be controlled by the dilution of autochthonous sediments and water dissolution (Dearing, 1999a). Sayer *et al.* (2007) demonstrated a low organic content (<10%) in the sediment close to the inflow of the the Bishops Sutton stream by measuring the LOI (loss on ignition). Their result suggested that the sediment influx from watercress beds in the catchment does not make up a large proportion of total sediment influx; hence the magnetic concentration was not enhanced by the sediment from theses watercress beds.

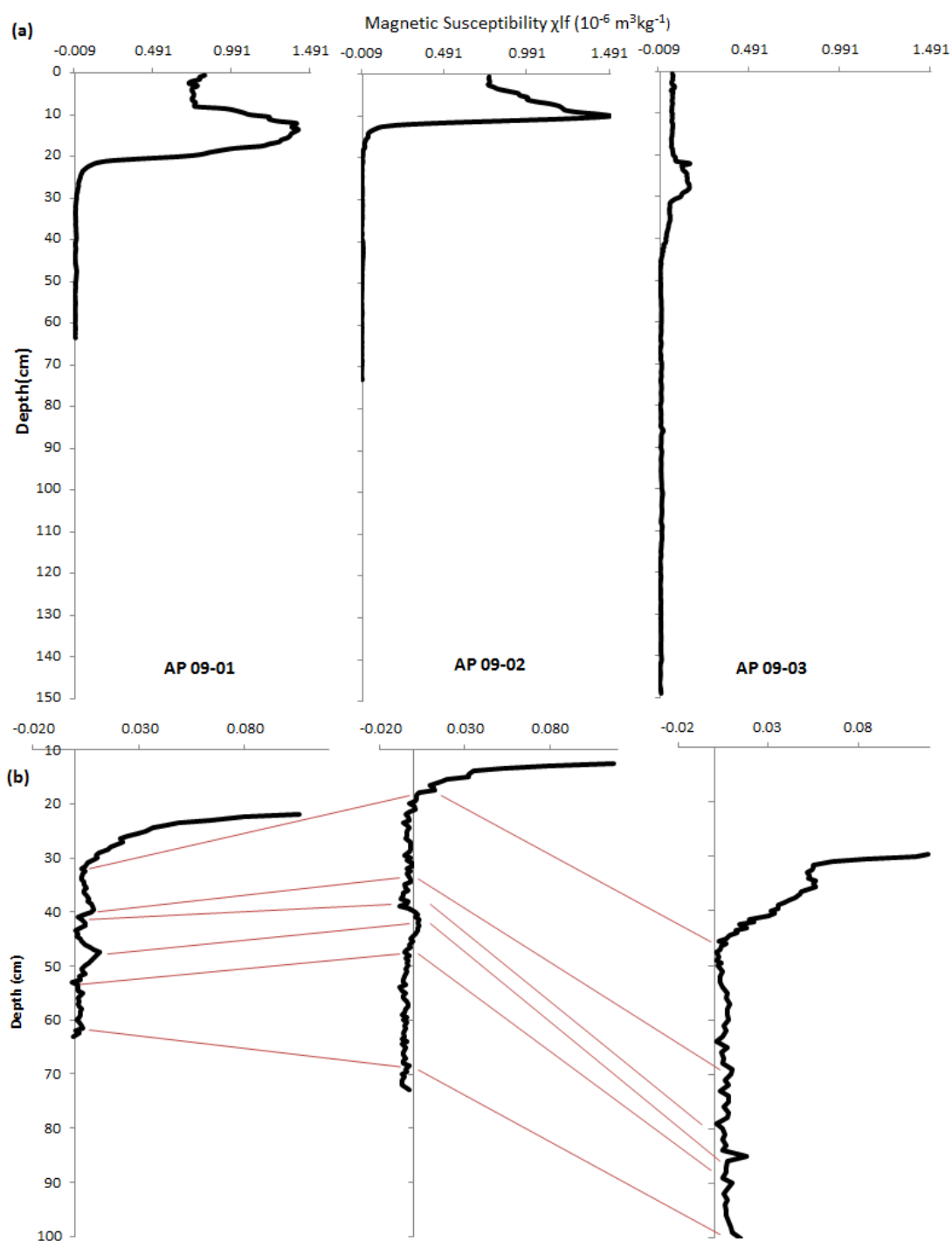


Figure 5.15 (a) Magnetic susceptibility profiles for core AP 09-01, AP 09-02 and AP 09-03; (b) Enlarged views of magnetic susceptibility profiles for core AP 09-01, AP 09-02 and AP 09-03 at the depth of 10-100 cm. Red lines showing correlation points of peak and trough values between cores.

Magnetic properties of topsoil samples are summarised in Table 5.3 and their scattered pattern is shown in figure 5.16. Sediment chemistry analyses taken by ADAS (1994) and Sayer *et al.* (2007) show a low level of organic matter (<10%) in

sediments which may indicate that magnetic properties of soils samples have not been affected by organic matter. All the samples show $\chi_{LF} > 0.1$ indicating that the presence of ferrimagnetic minerals (e.g. magnetite and maghemite) dominates the magnetic susceptibility of topsoils which may be derived from different sources (Blundell *et al.*, 2009b). Of these ferrimagnetic soils, 10 out of 14 (~71%) samples have χ_{FD} per cent values greater than 4 to a maximum value of approximately 11%, suggesting that grains with viscous superparamagnetic (VSPM) properties are present in >70% of samples (Mullins, 1977; Dearing *et al.*, 1996b). The plot of $\chi_{FD}\%$ versus χ_{FD} demonstrates a reasonably strong relationship ($r^2 = 0.6$) between the distribution of ferrimagnetic grains and the concentration of VSPM grains influenced by pedogenic enhancement (Blundell *et al.*, 2009a, b). Four samples have low χ_{FD} per cent values of < 2% and high χ_{LF} values, ranging from 0.4 to 0.7 ($10^{-6} \text{m}^3 \text{kg}^{-1}$), containing coarser multidomain (MD) or stable single domain (SSD) grains of magnetic iron oxide particles (Dearing *et al.*, 1996a). Soils with anthropogenic input of ferrimagnetic particles (different from pedogenic particles) in the upper soil horizons show high susceptibility values in combination with low frequency dependent magnetic susceptibility (Kapička *et al.*, 2000; Lu *et al.*, 2007). These four samples were taken from arable land and grassland close to Bishop Sutton stream, B3047 Alresford Road and Watercress Railway Line (location of samples are shown in Table 4.1 and Figure 4.3). Soil samples derived from the upper reaches of the channel and areas with high proportion of woodland show low values of χ_{LF} , ranging from 0.12-0.24 ($10^{-6} \text{m}^3 \text{kg}^{-1}$). Soil samples tend to show stronger magnetic properties than sediment, indicating they are sources of minerogenic materials for sediment supply (Figure 5.16a). Furthermore, some post depositional loss of magnetic minerals (e.g. dissolution) in sediments should also be considered.

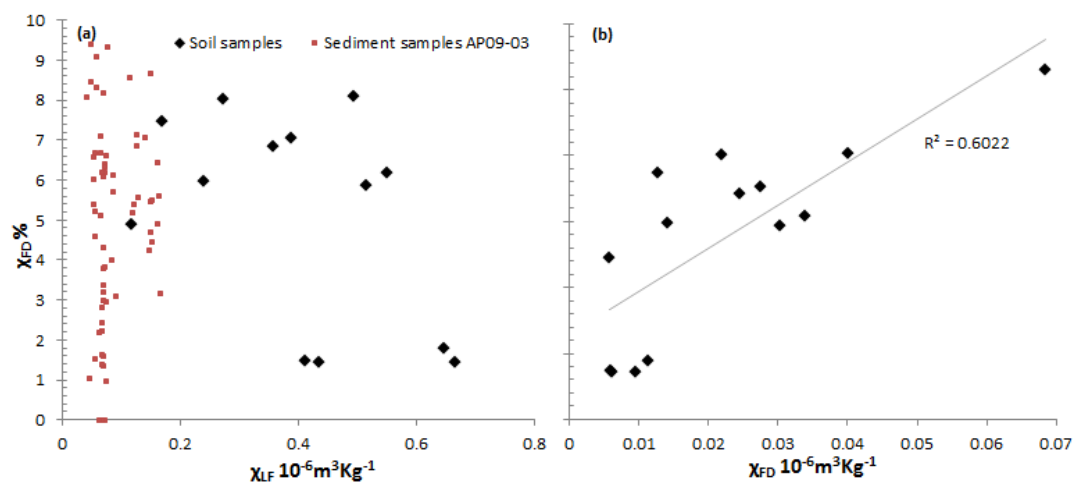


Figure 5.16 Bivariate plot of (a) χ_{LF} against $\chi_{FD}\%$ for samples of lake sediment AP09-03 (1976-2009) and soils; (b) χ_{FD} against $\chi_{FD}\%$ values for topsoil samples.

Table 5.4 Magnetic properties of soil samples.

Sample No.	χ_{LF} ($10^{-6} \text{m}^3 \text{Kg}^{-1}$)	$\chi_{FD}\%$	χ_{FD} ($10^{-6} \text{m}^3 \text{Kg}^{-1}$)
1	0.358596	6.830	0.024
2	0.17093	7.456	0.013
3	0.11832	4.901	0.006
4	0.273201	8.007	0.022
5	0.495236	8.082	0.040
6	0.389976	7.043	0.027
7	0.646879	10.580	0.068
8	0.239587	5.961	0.014
9	0.411571	1.480	0.006
10	0.666494	1.442	0.010
11	0.435097	1.439	0.006
12	0.648457	1.768	0.011
13	0.550504	6.180	0.034
14	0.51675	5.878	0.030
Mean	0.422971	5.50	0.022

5.5 Results

5.5.1 Modelling results

Simulation of geomorphologic responses of Old Alresford catchment were carried out from 1889-2009 and data of spin-up time (30 years as described in Chapter 4) has been removed. Figure 5.17 shows the climate and land cover indices as well as the simulated sediment discharge. The overall pattern of sediment discharge in Alresford catchment reveals that high values in the periods of 1891-1897, 1903-1915, 1925-1940, 1951-1960, 1974-1979 and 2001-2003 are synchronous with wetter climate phases, suggesting that climate is a main driving factor of sediment transport in this catchment. Sediment discharge started to gradually decline after the first peak at about 1891 with two small peaks occurring at 1894 and 1897 in response to large storm events. After 1901, sediment discharge increased suddenly to another peak at 1903 and this trend was sustained until 1915, then decreased again and kept steady for a long period. From 1945, sediment discharge started to increase again and reached another high value at 1951, lasting for about 9 years until 1960 before declining again with fluctuating values until the present day. Two other clear peaks in sediment discharge occurred at 1974 and 2001, both of which coincided with the large storm peaks. These peaks therefore demonstrate a rapid catchment response to climatic events, with changes in sediment discharges corresponding with floods and droughts taking place in a single year or over longer periods of time. The 1921 drought event produced extremely low amounts of sediment discharge. In contrast, large floods (e.g., 1891, 1903, 1915, 1951, 1960 and 2001) generated a mass of sediment discharge which made the whole catchment particularly sediment rich. Sediment remaining in the catchment was available to transport for the following years, even with relatively small scale climate changes which produced noticeable large sediment peak exemplified by the years 1906, 1954 and 2003. Further evidence which clearly exhibits the sediment availability and supply is shown in the graph of cumulative sediment discharge (Figure 5.17d), which shows larger jumps in cumulative sediment discharge at the rainfall peaks during the periods of the 1890s, 1903-1915 and 1951-1960. These peaks were of short duration and delivered over 50% of the sediment discharge in less than 30 years. Although Figure 5.17c displays an abrupt swing in sediment discharge, the cumulative total rises more gently excepting

several large erosion jumps, suggesting that the process driving a relatively small change in rate is mainly soil creeps.

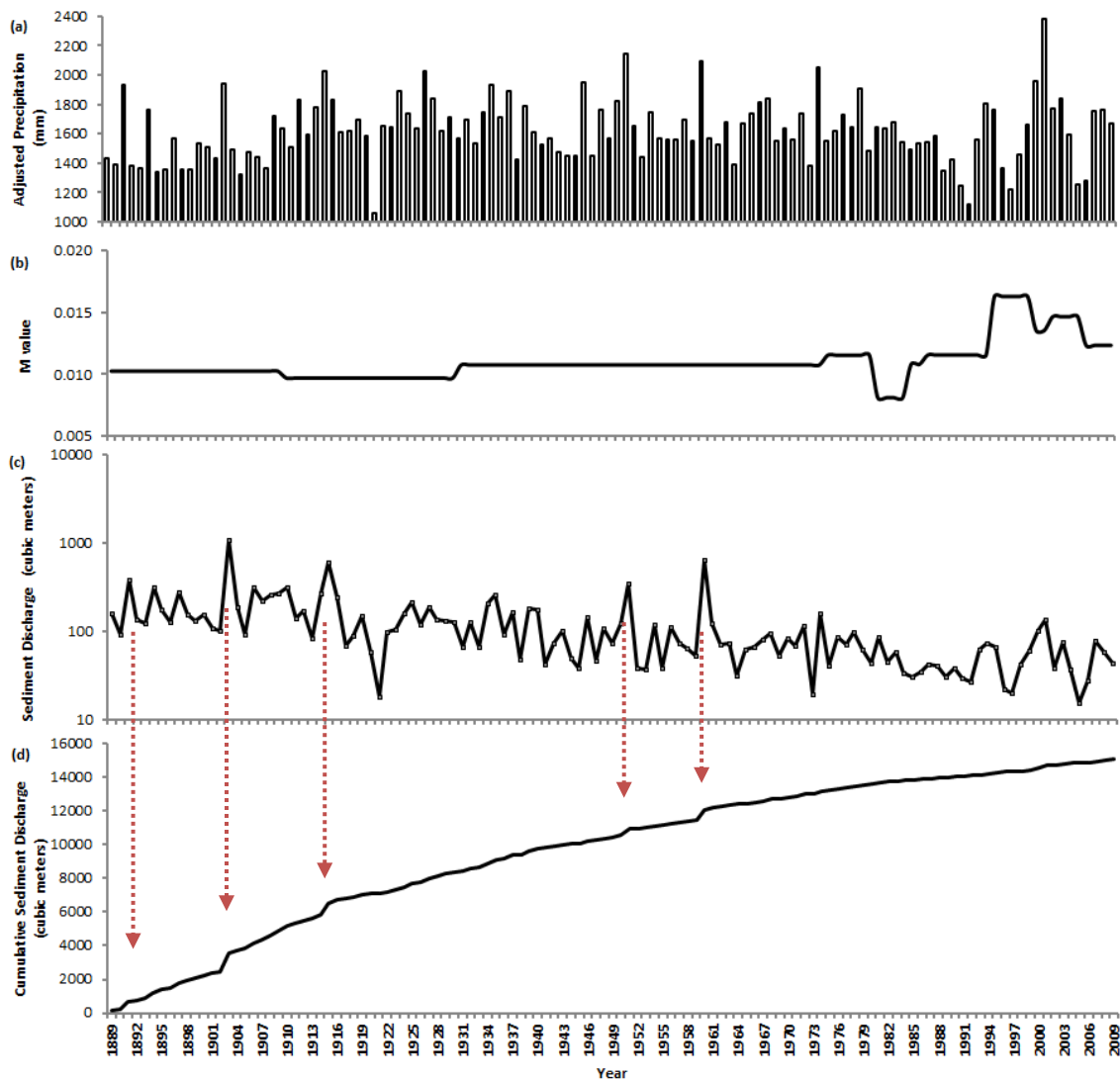


Figure 5.17 (a) Total annual adjusted effective precipitation used to drive catchment simulation; (b) land cover index (*M* value); (c) total annual sediment discharge; (d) total cumulative sediment discharge.

The magnitude of precipitation is not the only factor that can affect sediment supply and erosion. The effect of vegetation cover also plays an important role in changing the geomorphic and hydrological reaction of a catchment. The amount of rainfall in 1996 was the same as that in 1893, but it produced a much lower sediment discharge. Similarly, the 2005 drought event had a stronger impact on sediment discharge decrease than the drier 1921 phase as afforestation decelerated the transmission of

sediment and protected the catchment from soil erosion. The increase in forest cover (represented by M values) after 1934 coincides with minor falls in sediment discharge as well as with a time when peaks of discharge were low. Coulthard *et al.* (2005) suggest that the reduction or increase of tree cover has an impact on catchment response to climate change by amplifying or reducing the amplitude of the sediment peak under the same storm events. This impact is more pronounced when comparing peaks of sediment discharge between 1951 and 2001. The forest cover slowed down sediment conveyance, so the fluvial system produced lower sediment discharge in 2001, which nevertheless has the highest magnitude of precipitation, compared with discharge in 1951, which is characterised by less precipitation and a lower M value.

The response of catchments to climate changes with a series of meteorological events and human-induced land use changes is complex. Their relationship is non-linear as similar wet peaks can generate very different sediment discharges with the same M values. This may be interpreted with reference to sediment supply, remobilisation and storage in the valley floor, or by the non-linear dynamic interactions between topography, flow and sediment transport within the model (Coulthard *et al.*, 2001; Coulthard *et al.*, 2012). For instance, the amount of sediment discharge produced in 1966 was lower than the amount in 1970 despite having wetter weather, suggesting that the large 1960 sediment discharge peak followed by a series of smaller erosive events temporarily exhausted sediment supply. This is similar to the quick drop in sediment discharges in 2004 and 2005, which demonstrates the lowest discharge values in the entire climate sequence.

Figure 5.18 displays the spatial and temporal patterns of channel erosion and localised sediment aggradation in and around the channel. The catchment generated a significant sediment response to a series of large flood events (i.e. 1903, 1915, 1951, 1960 and 2001) shown as corresponding peaks in sediment discharge through the whole period (Figure 5.17c). Soil erosion or soil creep occurs gradually during the simulation process and becomes more noticeable along with the increasing amounts of sediment removal and aggradation across the whole DEM (Figure 5.18a-d). In the first peak of sediment discharge around 1903, the system experienced erosion (<1 m incision) in the main channel and adjacent tributaries, with deposition at the valley

floor (Figure 5.19a). However, Alresford catchment has a broad floodplain which provides great capacity for long term sediment storage resulting in the growth of small alluvial fans, especially at tributary junctions (e.g. Figure 5.19a.1). The erosion process was accelerated after flood peaks during 1911-1920 as the main channel and branch systems were broadened (Figure 5.19b). High sediment discharge in the period of 1951 to 1960 rendered the catchment sediment-rich and river channels and tributary systems continued to be broadened and incised to up to 3 m until 2009 (Figure 5.19c). These large flood events from 1951 to 1960 and in 2001 enabled extended erosion in small tributary valleys (e.g. Figure 5.19c.1) as well. There is evidence of progressive erosion on hillslopes (as shown in Figure 5.18, marked by circles) after the 1960s, when increasing sediment supply from high flows or previously deposited materials exceeded the catchment's capacity for storage, thus remobilising and transporting sediment through the fluvial system. Since chalk catchments are characterised by low and steady flows resulting from the groundwater effect, there is no apparent change of landform morphology over the entire simulation. Erosion and deposition mostly occurred in and along channels and their tributary systems. However, the large depocenters created as a result of this erosion may render the catchment at risk of massive sediment movements toward the lower reaches in the event of further large floods.

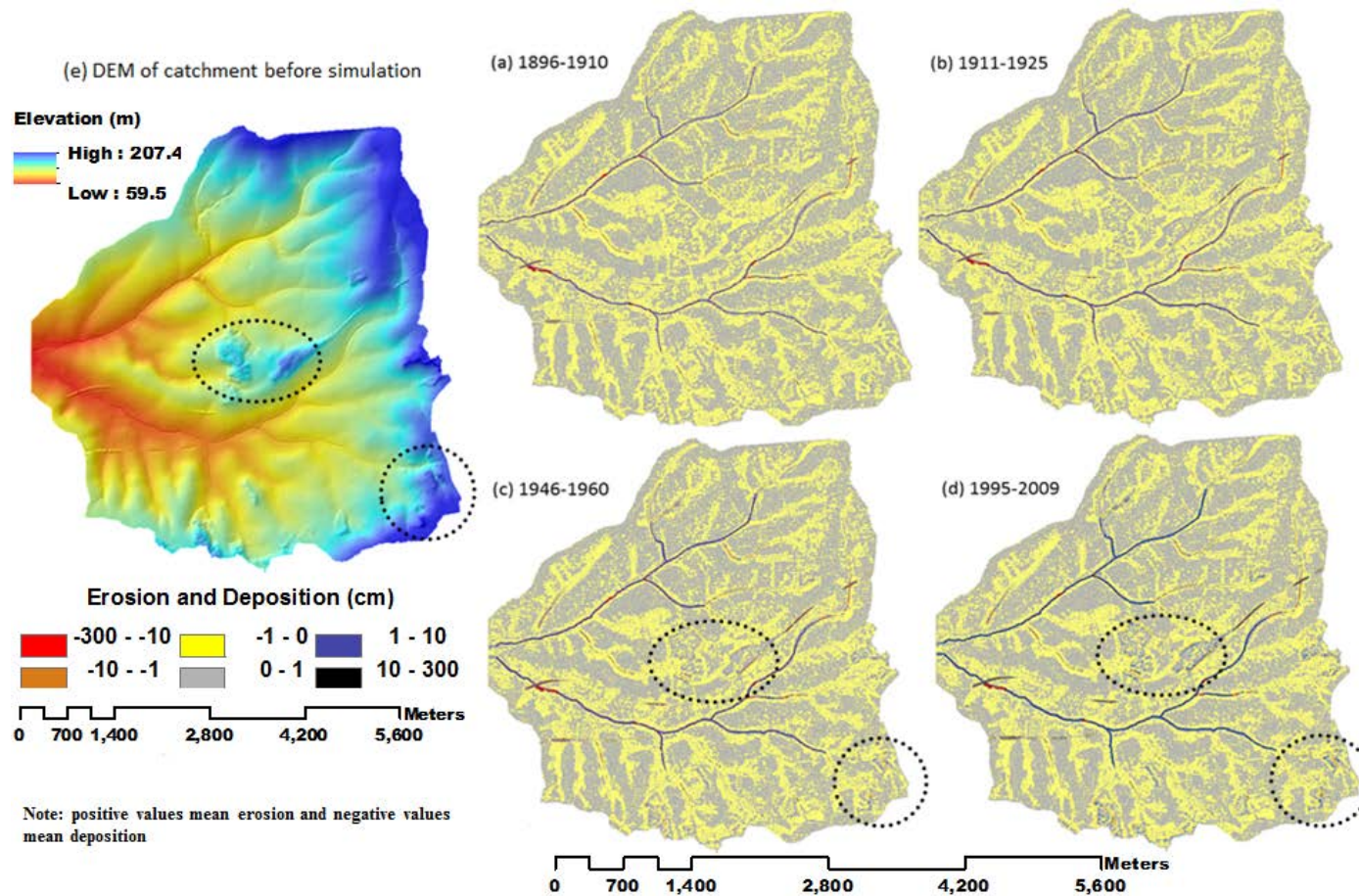


Figure 5.18 Erosion and deposition in Alresford catchment at different time phases (a) 1896-1910, (b) 1911-1925, (c) 1946-1960, (d) 1995-2009 compared with (e) DEM before simulation.

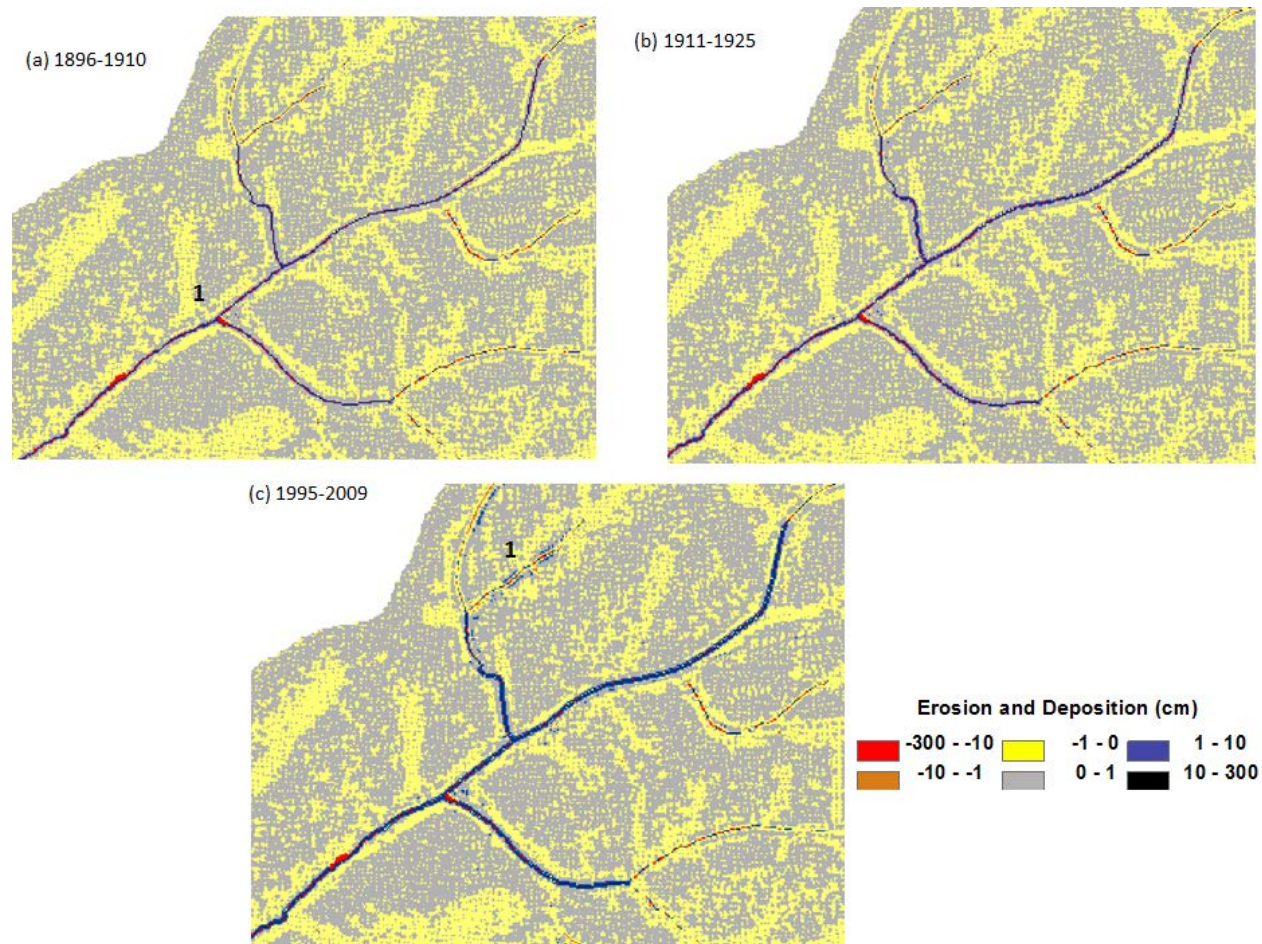


Figure 5.19 Patterns of erosion and deposition at different time phases (a) 1896-1910, (b) 1911-1925 and (c) 1995-2000.

5.5.2 Model validation

The accumulation rate of lake sediment was compared with modelled sediment transport rate on an annual scale (Figure 5.20). The SCP chronology-derived sediment mass accumulation rate (SAR) for Alresford shows a notable correlation with the simulated sediment discharge (QS) over the past 121 years, especially at peak values. Total annual sediment discharge demonstrates an obvious increase from 1901 to the first peak around 1903 before declining and then rising again to a smaller peak around 1915. Similarly, sustained increases of sedimentation accumulation rate are observed between 1905 and 1920 before declining to a minimum around 1922. The period of 1907 to 1921 exhibited low levels of forest cover (Figure 5.17b) and relatively high precipitation (Figure 5.17a) that may have led to flooding, therefore elevating the peaks in sediment discharges and increasing the amount of detrital sediment. The curve of modelled sediment discharge ascends gradually from 1921 to 1935 and descends slightly after that period until 1945, which correlates with sediment accumulation rates. Several large peaks of sediment discharge occur during the period from 1951 to 1960 followed by another decline again up to 2009. These peaks appear to correspond to the SAR records, with delayed peaks between 1954 and 1964. Since the chronology resolution of lake sediment in Alresford is about ± 10 years, model validation should focus on the long term pattern of changes instead of individual transient events in the time series, which may not be sufficiently accurately dated (Welsh *et al.*, 2009). Consequently, modelled sediment discharge data is logically acceptable within error margins (see highlighted areas 1903-1920 and 1950-1964) when comparing with sediment flux data. Meanwhile, after 1965, the lake sediment record indicates lower rates of geomorphologic activity that also match well with the low sediment discharge from the model at the same period. A slight increase in sediment discharge starts after 1970 and tails off until recent years, which is also largely in agreement with the sediment accumulation rate curve. Precipitation was extremely high in 1998 and 2004, while the response of the river and catchment system is diminished as a result of high vegetation cover. Although peaks in sediment discharge were observed owing to the nature of hydrological response to rainfall, the magnitude of these peaks were reduced at that time. This situation is more conspicuous in the curve of sediment accumulation rate with minor fluctuations after 1965. The similarity between QS and SAR records may reflect the

reducing effect of increased forest cover on sediment transport within the fluvial system.

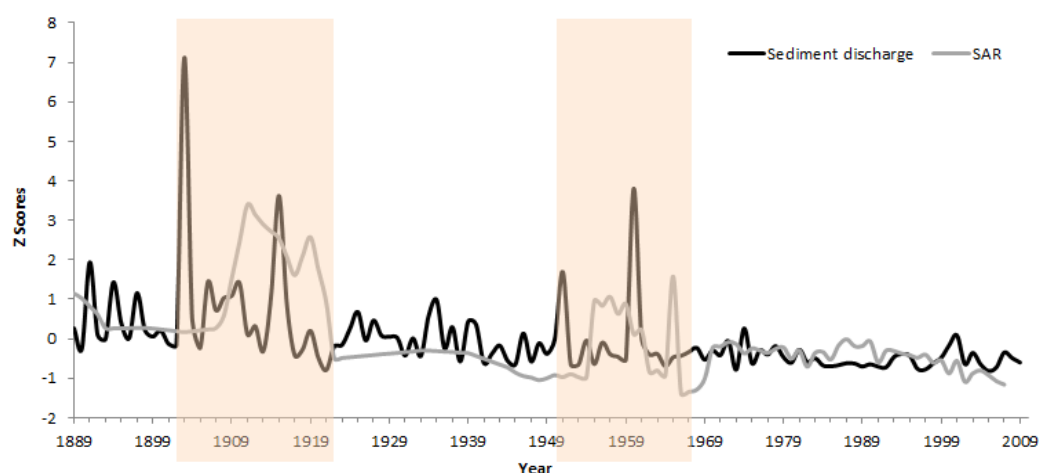


Figure 5.20 Comparison of modelled annual sediment discharge and lake sediment accumulation rate from 1889 to 2009.

5.6 Discussion

5.6.1 Catchment response to environmental changes

In chalky catchments, fluvial system evolution, resulting from sequences of flood events, is usually manifested in changes in sedimentation style or hydrological regime rather than changes in channel patterns or alluvial morphologies (Macklin *et al.*, 2010). Hydrological variability in Alresford catchment demonstrates a regular pattern (Figure 5.21) over the past 121 years. It is noted that the chalky catchment produces most runoff in the winter and spring, with the exception of occasional droughts (e.g. spring of 1921) and summer rainstorms (e.g. July of 2001). Water discharge is strongly controlled by precipitation in wet season when soil is relatively moist. This is a crucial trigger for chalk erosion as less water is needed to saturate the wind-dried surfaces of chalky soils, inducing erosion more quickly (Mutter and Burnham, 1990). The relationship between erosion and precipitation is clear in Figure 5.22. Relatively high precipitation during the periods of 1903-1915, 1925-1935, 1950-1952, 1959-62 and 2001 coincides with peaks in the sediment discharge curve (Figure 5.22d), and this correlation is also reflected by lower sediment discharge and less precipitation in, for instance, 1896 and 1921. When soils have

been saturated by abundant rainfall, erosion may be triggered by subsequent lower magnitude rainfall events (e.g. 1955 and 2003) as a result of antecedent geomorphologic and hydrological conditions and sediment transportation with changes in sediment discharge. When large quantities of sediment were eroded and transported out of the catchment during the two periods of 1950-1952 and 1959-1962, the depth of soil to rocks decreased quickly and this lessened the volume of soils which could be mobilised. Furthermore, the chalk became dry due to soil crusting after heavy rainfall and erosion which reduced infiltration to very low values (Boardman *et al.*, 1983; Boardman, 2003), which led to reduced water and sediment discharge after the 1960s.

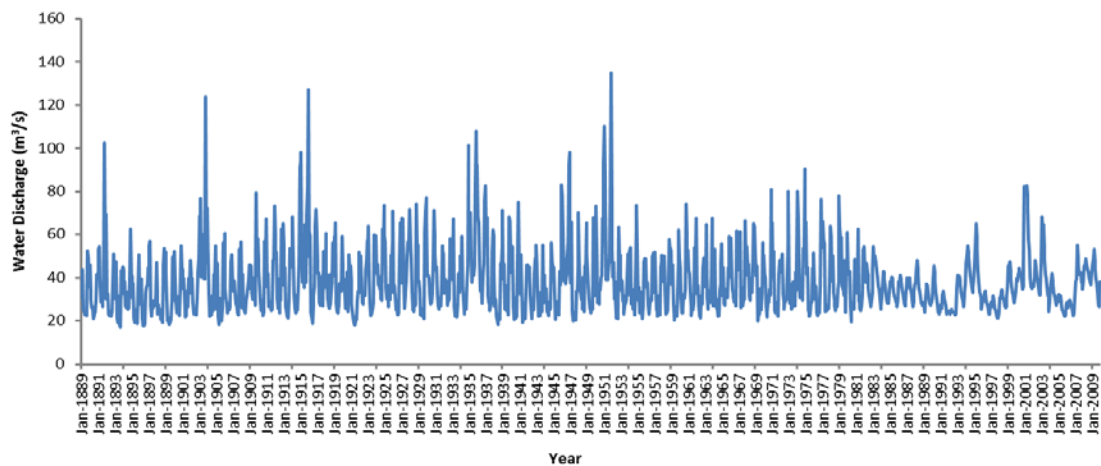


Figure 5.21 Record of modelled monthly water discharge.

Despite climate signals, human activities such as land use change play a vital role in sediment transport and deposition into Alresford basin, especially in the last 50 years. Vegetation cover is represented as M values in CAESAR by alteration of the flood hydrograph (Welsh, 2009). The high correlation between precipitation and sediment discharge gradually decreases after the 1960s. In contrast, the relationship between M values and sediment behaviour becomes closer. This evidence has been demonstrated by Evans (1990) with the perspective that erosion risk is minimal if land is under grass or woodland. Collins and Walling (2007) applied a combination of fingerprinting technique and uncertainty analysis to explore the fine sediment supply in a lowland catchment fed by groundwater in the UK and concluded cultivated surfaces as the dominant source. In both modelling studies and field observation of anthropogenic erosion on South Downs, UK, Boardman (1988) and

Favis-Mortlock *et al.* (1997) found high erosion between winter wheat field and ploughed land and indicated that a change of arable crop type can generate greater influence on erosion rates than did a changes in climate.

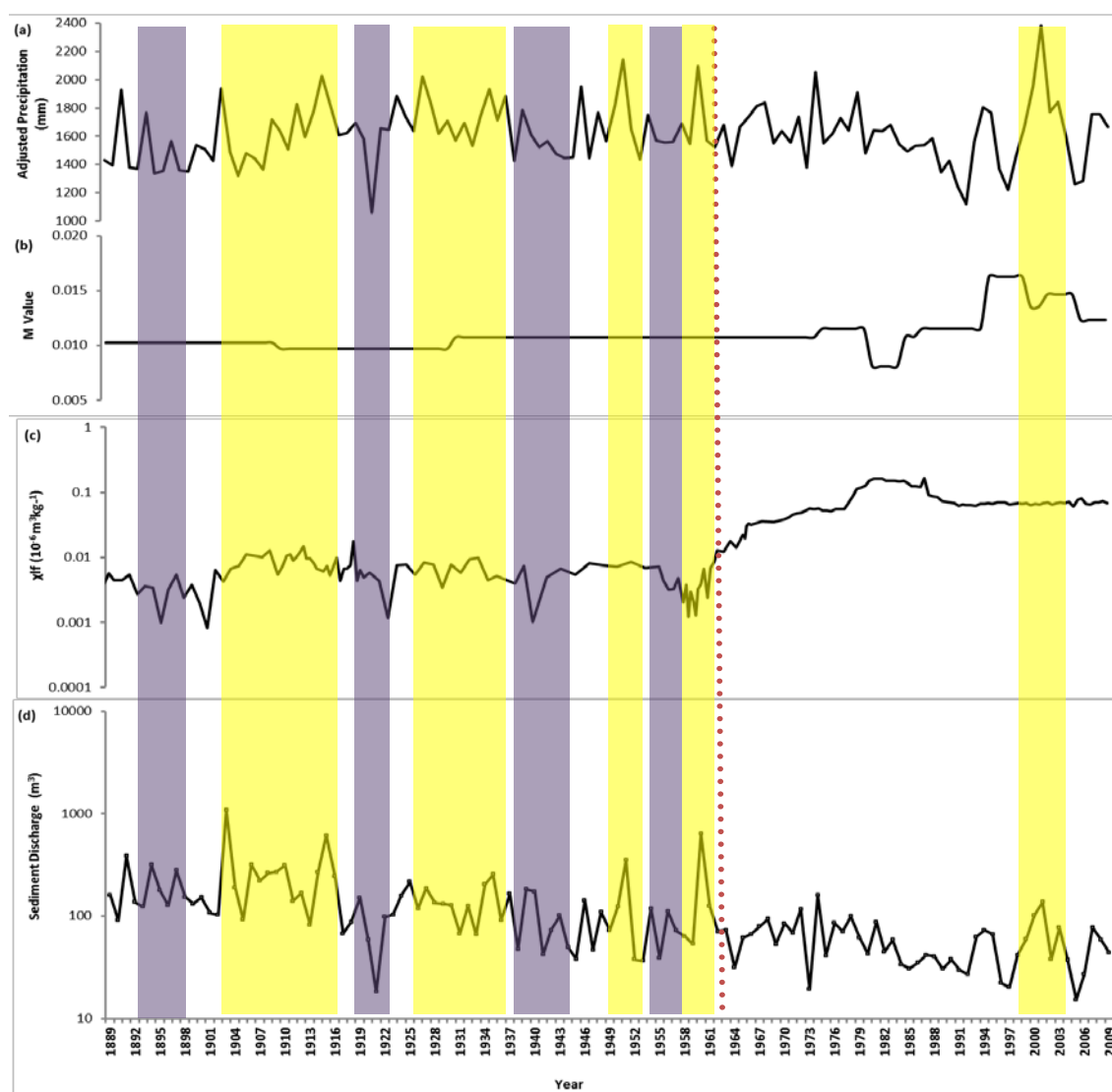


Figure 5.22 (a) Annual precipitation (b) forest cover represented in *M* values (c) logged low frequency susceptibility (d) total annual sediment discharge.

Alresford catchment experienced a conversion from sheep-grazed pasture to wheat farming in the 1890s and 1900s (Stowell, 2000; Monkhouse, 1964) and watercress cultivation in the late 1800s and early 1900s is also recorded. These drove the initial high sediment supply and aggravated the sediment discharge to peaks during 1903 to 1915 (Figure 5.22 d). It is reported that a drought event occurred in the winter of 1979 in most of areas in Britain (Price, 1985), which is also noted by the landowner

of the pond (Environment Agency, 2007). The reduced M value (1980-1983) resulting from increased areas of bare or sparsely covered ground, explains the increase in erosion. Further watercress beds were constructed with modern cultivation methods since 1938 (Wilson, 2000) and it became an important industry in Alresford area, as in many parts of the river valley a green carpet of cress can be seen covering the shallow beds. The watercress beds are usually irrigated by water from springs, boreholes and stream water which passes through the beds before entering the pond. In order to ensure a constant flow for watercress growing, many beds contained in earth banks were replaced by low concrete walls since 1955 (Crisp, 1970; Wilson, 2000). In the early 1990s, silt traps were installed to alleviate the severe silting problem in the Alresford pond (Environment Agency, 2007). These actions, coupled with increased vegetation cover, led to decreased sediment discharge after the 1970s. Compared to the extremely high precipitation in 2001, a relatively moderate amount of sediment was delivered to the pond. A significant reduction in the sediment depth and volume of the pond is also recorded by the Environment Agency (2007) from 1994 to 2006. This sediment survey showed that the average depth of the silt was reduced from 3m in 1994 to less than 1m in 2000 and the total sediment volume was also calculated to be 42.363 m^3 in 2000 when the volume was in excess of $200,000 \text{ m}^3$ in 1994.

The magnetism records of AP 09-01 and 02 are strongly affected by the sediment from watercress beds, especially in recent period, with higher values than those of soils. Sediments from AP 09-03 reflect sediment transport and erosion patterns in the catchment better. The magnetism record of AP 09-03 shows reasonable values that are lower than soil samples (Figure 5.16a), thus they are used for further analysis and comparison with model outputs. The sediment magnetism record (AP 09-03) suggests that, prior to 1963 channel erosion or sediment removal from high altitudes due to storm events was the dominant erosion process in the basin (Figure 5.22c). The curve of low frequency magnetic susceptibility well tracks changes in sediment supply (Figure 5.22d) before 1963 (within chronology errors). Precipitation increase or decrease is reflected in the amount of eroded materials in the chalk catchment, which is described by peaks and troughs in magnetic susceptibility (highlighted in Figure 5.22c before 1963). Therefore, the concentration of magnetic susceptibility may be climatically influenced by high storm energies and consequent channel

erosion, with a resultant increase in transport and deposition of coarser magnetic particles (Thompson and Oldfield, 1986; Verosub and Roberts, 1995; Stage, 2001). However, values of magnetic susceptibility continue to increase after 1961 erosion event, and reach a peak in the period of 1980-1986, instead of slightly decreasing in line with the reduced sediment discharge. The magnetic enhancement since 1963 demonstrates that sediment sources have been shifted to surface soils eroded from the intensively cultivated catchment (Dearing, 1999a). Local land use history suggests that the construction of more watercress beds and the increased farming of cereal and maize between 1939 and 1964 (Monkhouse, 1964), the drought and associated vegetation cover decline in southern England in 1979 (Environment Agency, 2007; Dearing *et al.*, 1996a; Le Borgne, 1955), the rise of fertiliser usage from 1953 to 1961 (Monkhouse, 1964) and the re-opening of nearby railway as the watercress line in 1977 (The Mid-Hants Railway Preservation Society, 1978) may contribute to the peaks in magnetic susceptibility. The presence of both SP and MD or SD domain ferrimagnetic grains in topsoil samples supports the evidence of surface soil erosion in the catchment (Oldfield *et al.*, 1989; Dearing, 1999a). Over 70% soil samples show high values of χ_{LF} and soils in arable lands have higher χ_{LF} values than soils in woodland and around the head-water of the channel. It is suggested that soils which have χ_{LF} values > 0.38 ($10^{-6}\text{m}^3\text{kg}^{-1}$) and $\chi_{FD}\%$ values $< 2\%$ can be defined as anthropogenic polluted topsoils (Hay *et al.*, 1997; Blundell *et al.*, 2009a). Four polluted soil samples are detected in the catchment and they were derived from areas close to watercress farms, the ‘Watercress Line’ railway track and the roadside. Therefore, vehicle emissions, fly ashes and waste products from farming activities may have contributed to the pollution of these surface soils (Oldfield *et al.*, 1985; Maher, 1998; Lu *et al.*, 2007).

5.6.2 Model validation

In order to determine whether a model is adaptable for further application of landscape evolution and projection under climate and land use changes, model validation or corroboration is essential to evaluate model results by comparison with field data. Water depth and inundation areas have been used by Thomas and Nicolas (2002) for model validation, both of which have associated difficulties including limited data sets and time consuming measurement (Coulthard *et al.*, 2007). Aerial

photographs or historical maps may be an alternative for investigating morphological changes of braided channels (e.g. Hooke, 1984) to compare with modelled landscape changes, but are restricted by geomorphic type. Coulthard *et al.* (2005) used a histogram of radiocarbon-dated alluvial units for comparison with sedimentation style and rates resulting from long term simulation of geomorphologic changes in river systems. A combination of ^{137}Cs measurement, RUSLE (Revised Universal Soil Loss Evolution) and SDR (Sediment Delivery Ratio) was used by Hancock (2012) to assess the eroded materials delivered to the water in comparison with sediment discharge from modelling.

Given the evidence that lake sediment sequences are an alternative for model validation, the good correlation between modelled sediment discharge from CAESAR and sedimentation rate from lake sediment profiles is a positive feature. However, the influence of groundwater on the hydrological cycle and sediment delivery in chalk catchment is still unclear. A comparison of flood behaviour between the ‘original rainfall’ (rainfall data directly from stations) and the ‘effective rainfall’ (rainfall data modified by groundwater) is shown in Table 5.4. A prominent difference (Figure 5.23) in the frequency and magnitude of runoff driven by original and effective rainfall is that groundwater cushions the production of peak flows and the variation of flows become more even throughout the year. Under ‘no groundwater’ condition, the highest peak of runoff can reach $22.51 \text{ m}^3/\text{s}$ with almost 200 days exhibiting high magnitude flow events greater than $8 \text{ m}^3/\text{s}$, while there is a great number of low flow events with a magnitude less than $0.5 \text{ m}^3/\text{s}$, and the lowest of which is $0.000194 \text{ m}^3/\text{s}$. The large variation between low and high flow events may be due to the additional runoff from minor summer storms or intense winter precipitation, and the lack of rainfall events. There is no flow of magnitude greater than $10 \text{ m}^3/\text{s}$ under the ‘effective rainfall’ regime. The highest flood peak is reduced to $9.39 \text{ m}^3/\text{s}$ and the runoff magnitude is reduced to $1\text{-}3 \text{ m}^3/\text{s}$. Rainfall tends to infiltrate into chalk and emerges as baseflow. The aquifers of a chalk catchment have a stabilising influence on streams, reducing the possibility of flooding by taking water into storage during heavy rainfall periods and releasing it slowly during dry weather (Price, 1985). The relatively smooth change in daily flow, on account of large contributions of the baseflow to streams, is representative of a typical hydrological regime in the catchment (Gustard, 1996; Sear *et al.*, 1999).

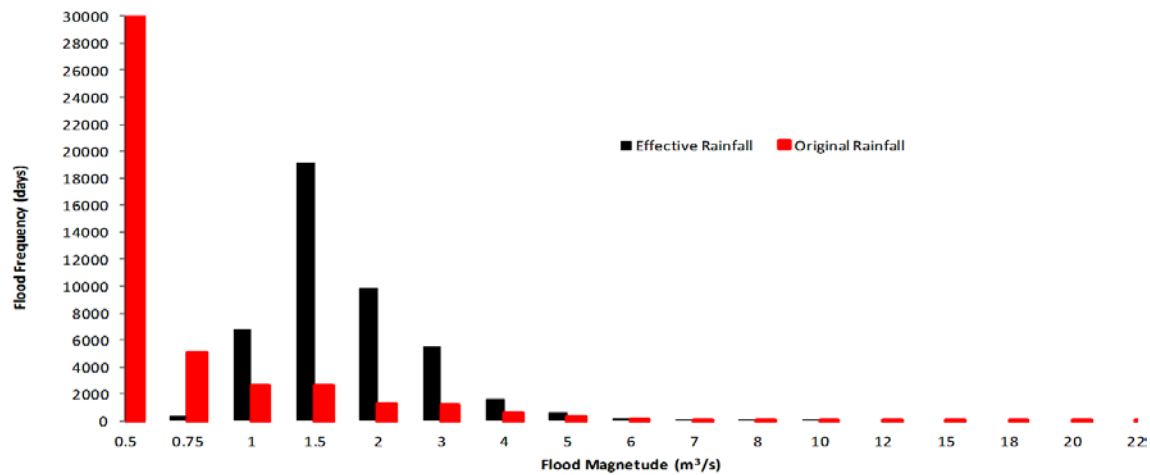


Figure 5.23 Flood frequency distribution of ‘original rainfall’ and ‘effective rainfall’ water discharge.

Table 5.5 Number of flooding days with a magnitude of water discharge greater than 2, 5, 8 and 10 m³/s for original and effective rainfall inputs, maximum and minimum water discharge.

Flooding condition	Original Rainfall (days)	Effective Rainfall (days)	Difference
Number of flood days with water discharge above 2 m ³ /s	8063	2655	3.04
Number of flood days with water discharge above 5 m ³ /s	545	281	1.94
Number of flood days with water discharge above 8 m ³ /s	189	4	47.25
Number of flood days with water discharge above 10 m ³ /s	109	0	--
Maximum Water discharge (m ³ /s)	22.51	9.39	2.40
Minimum Water discharge (m ³ /s)	0.000194	0.61	0.000318

Comparisons of geomorphic pattern and sediment delivery between these two rainfall input conditions are shown in Table 5.5. Similar to the pattern of the hydrological cycle in original and effective rainfall driven simulations, more sediment is delivered under ‘no groundwater’ conditions and there is greater

variability in sediment discharge throughout the whole simulation. Extremely low sediment discharge may result from low flows or after a rapid increase of sediment discharge as a result of large flooding events which exhaust the soils in the catchment. However, there is no obvious difference of landform changes (Figure 5.24) across the catchment between these two rainfall input conditions: erosion and deposition occur primarily in channels and their tributaries. Under ‘no groundwater’ conditions, a large proportion of eroded particles are deposited along the streams or in the alluvium of the inflowing river (Zolitschka, 1998) coupled with the creation of more small tributary streams. In fact, water is prone to percolate through the chalk to main channels rather than developing tributaries at the surface (Berrie, 1992). Under the ‘effective rainfall’ simulation, erosion in this chalk catchment is characterised by low number of small streams, which is better reflected in the landform pattern.

Table 5.6 *Total, maximum and minimum sediment discharges and their differences.*

Rainfall condition	Original Rainfall	Effective Rainfall	Difference
Total sediment discharge (m ³)	33003.4977	15054.8737	2.19
Maximum sediment discharge (m ³)	10138.7981	1083.0232	9.36
Minimum sediment discharge (m ³)	0.0044	15.2891	0.0003

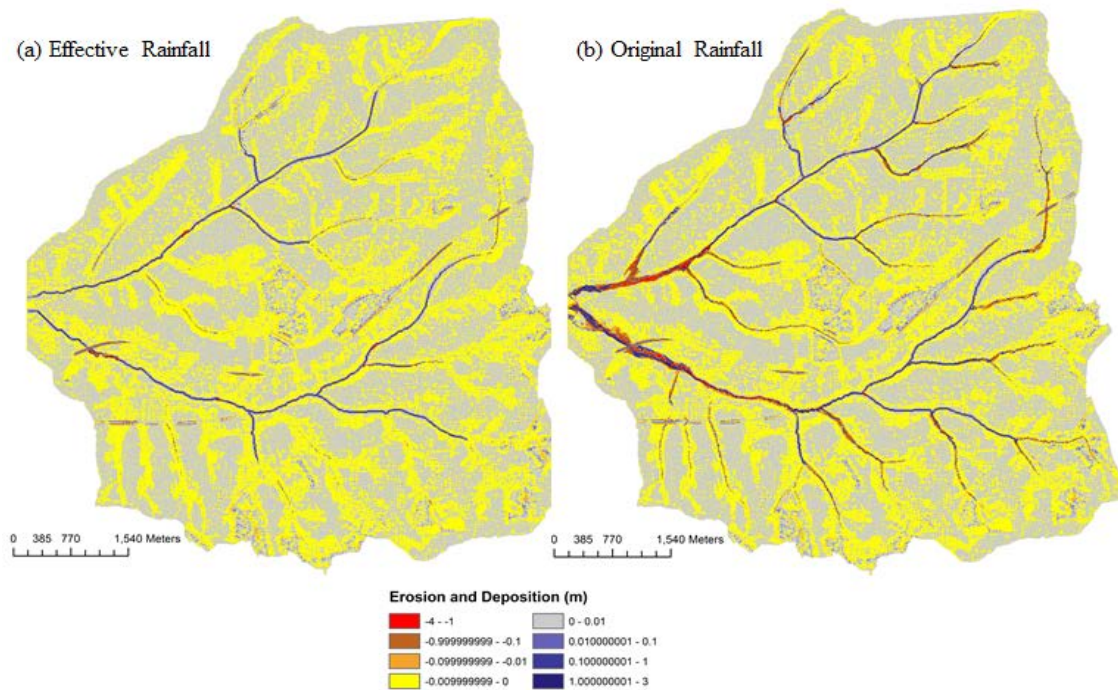


Figure 5.24 Geomorphic patterns after simulation of (a) effective rainfall, (b) original rainfall over 151 years.

Soil erosion monitoring programmes from 1982 to 1991 were carried out by John Boardman (2003) on the eastern South Downs, a chalky upland in southern England with an area of 36 km² of farm land. He found that localized erosion and flooding had occurred on the South Downs in the very wet autumn of 1958, which matches the second crest appearing in Figure 5.20. The annual erosion rates measured on eroded arable field during the 1980s ranged from 0.5 to 5.0 m³ ha⁻¹. The sediment erosion rate under ‘effective rainfall’ conditions is between 0.18 to 0.35 m³ ha⁻¹ with a mean value of 0.22 m³ ha⁻¹ from 1981 to 1991. The erosion rate is 0-0.15 m³ ha⁻¹ with a mean of 0.11 m³ ha⁻¹ during the same period under ‘original rainfall’ condition. Although both of the sediment erosion rates are low, the modelled results under ‘effective rainfall’ conditions are much closer to John Boardman’s data. It is difficult to compare the modelled sediment discharge with the measured soil loss values from South Downs. The monitoring of soil erosion was a field-based measurement of soil loss, while CAESAR calculated the mass of eroded materials during the whole process of erosion and deposition in the catchment. Meanwhile, the hillslope process has a greater effect on soil production in upland catchments than in lowland catchments. Morgan (1980) suggested an acceptable erosion rate of 2 t ha⁻¹ yr⁻¹ as a maximum for chalky soils in southern England. Estimated rates of soil

erosion of the catchment during 1990s by the Revised Universal Soil Loss Equation (RUSLE) is between 0-0.35 t ha⁻¹ yr⁻¹, on average of 0.24 t ha⁻¹ yr⁻¹. Similarly, the modelled sediment discharge under ‘effective rainfall’ conditions is more appropriate with values ranging from 0.04-0.34 t ha⁻¹ yr⁻¹ with a mean of 0.13 t ha⁻¹ yr⁻¹ when compared to the values between 0-0.14 t ha⁻¹ yr⁻¹ in mean of 0.05 t ha⁻¹ yr⁻¹ under ‘original rainfall’ conditions. Thus, the best match was observed between modelled records using effective rainfall and field data. This highlights the potential of using effective rainfall as a simulation input for studying the hydro-geomorphic changes in Alresford fluvial system. The method of effective rainfall is only useful for Alresford simulations after model calibrations. Different simulations with different landscapes, rainfall and M values may require different approaches to the factor of groundwater.

Given the evidence that the CAESAR model can capture the sediment transport pattern over time, in particular simulating the impact of individual large storm events, but not accurately describing the impact of smaller events, model results should be regarded as preliminary. The changing and relative magnitude of the peaks of simulated sediment outputs are of more importance than predicted sediment volumes (Coulthard and Macklin, 2001). The overall match between the modelled and lake sediment proxy implies that the model is functioning correctly and also indicates the potential for using simulated catchment-wide sediment records in comparison with lake sediment proxies (Welsh *et al.*, 2009). The results are difficult to accurately validate. However, the capability of CAESAR to be used as a tool to investigate river dynamics and landscape evolution, which allows us to study the relationship between environmental factors and geomorphic changes rather than values, is promising.

5.7 Summary

The CAESAR simulations in this study have produced the evolution of fluvial system in the form of hydrological and sedimentological behaviour in response to environmental changes. This numerical modelling approach is conducive to understanding the pattern of sediment conveyance within the catchment through outputs of not only the temporal distribution of sediment and water discharge but also the spatial erosion and deposition morphology. The modelled peaks in sediment discharge are consistent with the flood magnitude driven by precipitation and

groundwater before the 1960s. Climate (e.g. rainfall energy and volume) may play a more direct role resulting in increased sediment discharge from soil erosion enhancement. However, plant cover becomes more effective in reducing perturbations in the sediment regime. The reduction in sediment delivered to the pond is less correlated to rainfall than to changes in land use and management since the 1960s. The increased demand for arable agriculture, the construction of concrete walls for more watercress cultivation, the drought event and the silt control activity in the catchment seem to be the most likely influences on erosion patterns in the last 50 years.

The correlation between modelled results and palaeorecords of lake sediment, in particular sediment accumulation rates, suggests the potential of the model to be used as a tool for capturing the sediment transport pattern over time. Model validation between simulations of 'original rainfall' and 'effective rainfall' conditions indicated the effect of groundwater in controlling surface flow and erosion. The magnetic properties of sediment and soil for detrital sediment supply demonstrate the shift in sediment source and the sensitivity of the lake sediment to agricultural expansion and farming activities, climatic fluctuations and soil pollution.

Although the annual amount of sediment discharge is not great, the chalk catchment is vulnerable to water erosion due to its shallow soils. The principle soils in the catchment are classified as Andover I Association which contains silt loams or silty clay loams, rarely thicker than 23 cm and frequently with A horizons of about 16 cm over chalk bedrocks (Favis-Mortlock *et al.*, 1997). Most watercress farms are located along channels and their tributaries, fed by chalk streams. Furthermore, the water depth of the pond is very shallow with an average of 0.25 m recorded in summer and 0.35 m in autumn as assessed by the English Nature (Environment Agency, 2007). Soil erosion investigation and land use management is of importance to maintain soil depths for arable land and erosion control.

Chapter 6

Simulating catchment response to environmental changes over 5000 years

6.1 Introduction

To test the feasibility of the CAESAR model over different spatial and temporal scales, a longer term (5000 years) simulation of catchment response and evolution to climate change and human activities has been attempted. The simulation was undertaken on a river catchment (Holzmaar, Germany) with a long and well documented lake sediment record. Varved lacustrine deposits that contain a variety of sedimentological, botanical and geochemical information have been utilised not only for model validation but also for exploring the linkage between environmental changes, both anthropogenic and climatic, and the fluvial system. In general, lake sediments are the archives that integrate limnological, hydrological and geomorphological processes in lakes and their catchments (Zolitschka *et al.*, 2003), and they can be used as a powerful basis for understanding their ecosystems (Oldfield, 1977). Enhancing our understanding of the relationships between palaeoenvironmental conditions, climate and human activities through a precise chronology, the quantification of sediment delivery and an understanding of the intensity of land use changes are crucial further directions for environmental sustainability research.

Climate controlled environmental changes in Lake Holzmaar during the Late Glacial and early Holocene (Zolitschka *et al.*, 2003). Signs of human influence are observed in records dating to the Neolithic climatic optimum (ca. 8000–6000 calendar year BP). Towards the late Neolithic and early Bronze Age, agricultural expansion and regression (animal husbandry, cultivation) and associated deforestation and reforestation occurred over almost all of central Europe; this is seen in the Holzmaar pollen record as changing forest percentages (Dotterweich, 2012). Changes in the landscape thus reveal increasing human interaction with the environment over a long

period, and this is also indicated by regional hydrological and sedimentological information (Dotterweich, 2012).

In a reconstruction of sediment yield and soil erosion based on an absolutely dated chemical and physical analysis from a 14,000 year annually laminated sediment sequence, Zolitschka (1998) provided the evidence that sediment yields are directly linked to the degree of forest cover. Similar evidence was also found by Dearing and Zolitschka (1999) by focusing on temporal changes in system behaviour instead of individual processes. They analysed the frequency distribution curves of time series to distinguish the dominant behaviour in proxy data from Holzmaar and described a self-organized critical state within the catchment. They also showed the dominant force of human impact, particularly deforestation, on the major shifts in sediment delivery to the lake. As sediment discharge and movement from old Alresford catchment is mainly forced by climatic factors, modelling the catchment response in Holzmaar over a longer time period can help to explore the human impact on the fluvial system, thus testing the feasibility of the CAESAR model for simulating the hydro-geomorphic changes in the future. Furthermore, the small scale of the catchment saves modelling time, and there is sufficient available data to make model validation more robust.

6.2 Site description

6.2.1 West Eifel Volcanic Field

The Holzmaar is one of 6 maars filled with water in the west Eifel region of western Germany (Figure 6.1a). The Quaternary west Eifel volcanic field is a predominantly Pleistocene group of over 240 scoria cones, maars and volcanoes, covering an area of approximately 600 km² (Herbig and Sirocko, 2012). The field extends about 50 km from the border with Belgium on the northwest, to the Moselle River which crosses Luxemburg on the southeast (Figure 6.1b).

A maar is a volcanic eruption crater cut into country rock and consists of a low ring wall of pyroclastic debris, crater sediments and a diatreme, approximately 100 m to 2000 m in width and 10 m to more than 200 m in depth (Lorenz, 1973; Ollier, 1967). Maars form when fissures opened at a certain depth below the surface allowing the

groundwater to come into contact with rising magma. Most of the eruptions occurred during the past ca. 700, 000 to ca. 11, 000 years (last glacial cycle period) (Lorenz, 1973; Herbig and Sirocko, 2012). Volcanic activities may have reached a peak between the past ca. 550, 000 and 450,000 years, with a subsequent lull in activity until about 100,000 years ago. This was then followed by an increase in volcano formation though no volcanic activity has been detected in the past 10, 000 years (Schmincke, 2007). The central part of most west Eifel maar lakes are flat; they may have been formed in the early stages of lake development and. It is also assumed that in deep maar lakes the materials eroded from the littoral zone are deposited on the slope of the lake (Scharf and Menn, 1992).

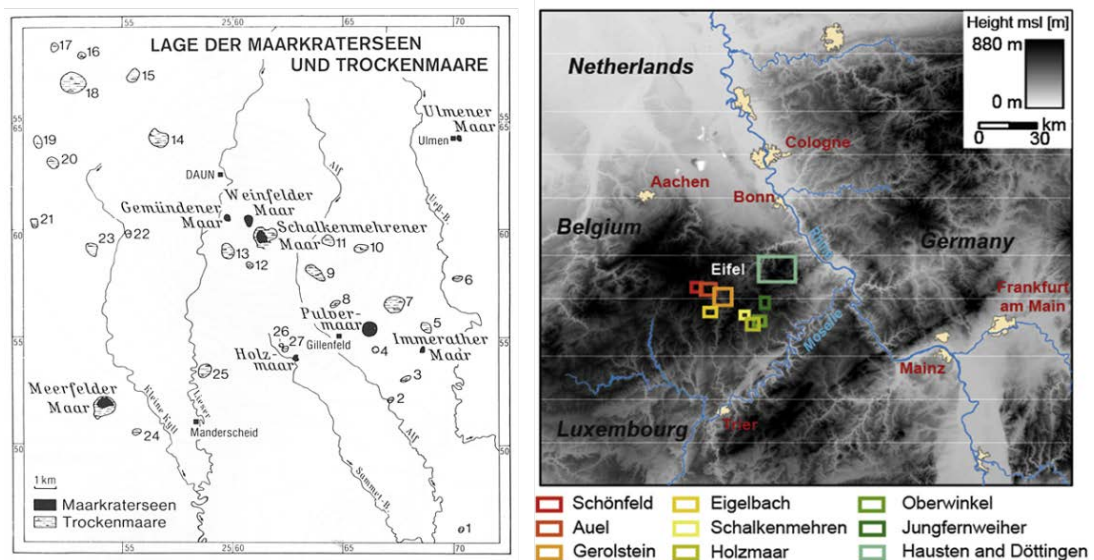


Figure 6.1 (a) Distribution of maar lakes in the west Eifel region (from Scharf and Menn, 1992; Negendank *et al.*, 1990); (b) Location of Eifel volcanic field (from Sirocko *et al.*, 2013).

Deposits in maar lakes, well known for their preservation of high-resolution and relatively undisturbed varved sediments, provide essential information on palaeoclimatic history, volcanic activities, palaeoenvironmental changes and human impact in the west Eifel region. Therefore, the west Eifel volcanic field has been selected as a reference area for varve chronologies and palaeoenvironmental studies by the ELSA project (Eifel Laminated Sediment Archive) (Sirocko *et al.*, 2005). Since 1998, all maar lakes in the Eifel field have been cored systematically to establish consecutive varve chronologies back to ca. 500, 000 years ago using

radionuclide dating, varve counting, historical events, palynostratigraphy, radiocarbon dating, palaeomagnetic analysis, tephrochronology and greyscale tuning (Sirocko *et al.*, 2013).

A series of prominent climatic fluctuations from the decadal to the millennial scale have been recorded not only in ice cores (Dansgaard *et al.*, 1993) but also in maar lake sediments. Palynological analyses of laminated sediments in the Eifel region have provided evidence of three cold periods (i.e. the Older Dryas, the Younger Dryas and the Rammelsbeek phase) during the Late Glacial and Early Holocene (Leroy *et al.*, 2000). Climate change in the Younger Dryas is bipartite with a generally cold winter and mild summer at the beginning of this period, followed by a drier and colder climate, particularly in summer. In addition, a steep rise in temperature has also been detected at the transition from the Late Glacial to the early Holocene. The correlation between variations in varve thickness and composition and climate change from Alpine glacier fluctuations suggests cool/warm cycles that recur approximately every 1000 years during the Holocene (Zolitschka, 1992a). Prasad *et al.* (2006) reconstructed a continuous record of seasonal climate instability and its impact in Western Europe through varve thickness record and the seasonal diatom and clastic sublaminae in the varves. They demonstrated drier winters and drier and cooler summers in Western Europe during the cooling events around 8.2 calendar ka in Greenland. The late Holocene sediments of Eifel maars record three periods of cold events in the Little Ice Age (AD 1300-1900) resulting from reduced solar activity and volcanic eruptions (Kienel *et al.*, 2005).

The first occurrence of trees in the Eifel region is recorded around 14,700 calendar year BP (Sirocko *et al.*, 2013). Parts of the Eifel have been colonized by humans since the Early Neolithic (ca. 7450-6850 calendar year BP; Herbig and Sirocko, 2012). However Holocene environmental changes were mainly driven by climate until the onset of the Iron Age (ca. 2800 calendar year BP). Increased human impact (i.e. settlement, woodland clearing and cultivation) in the Eifel region around the maar lakes became another driver of environmental change, particularly during periods of favourably warm climate conditions (e.g. the Roman and Medieval times; Rein *et al.*, 2007). At this time, instead of cool and humid climatic conditions accelerating sediment accumulation rates, increased runoff and sediment transfer to the lake may

reflect intensification of land use, deforestation and anthropogenically induced soil erosion (Barber *et al.*, 2004; Rein *et al.*, 2007). The Migration Period from about 300 to 900 AD is linked to forest recovery, and the first active re-afforestation took effect from the early 19th century (Zolitschka, 1996).

6.2.2 Why choose Holzmaar?



Figure 6.2 Aerial photograph of Lake Holzmaar (from <http://www.gesundland-vulkaneifel.de/gesundland/vulkanismus/maare-kraterseen/holzmaar.html>).

Lakes are typically hydrologically open systems, and their dynamics are closely connected with temperature, precipitation and surrounding environmental changes. Small simple lake systems are usually favoured over large, complex systems for research on limnology and climate change, as well as human impact (Baiera *et al.*, 2004a). Therefore, Lake Holzmaar (Figure 6.2) was selected in this study not only due to its small size and relative simple water body, with only one inflow and outflow, but also for its quick response to environmental effects owing to its relatively short water residence time (Moschen *et al.*, 2009). Increased sediment accumulation rates, changes in diatoms and other algae and changes in sediment chemistry are the most common indications of human impact on the lake (Saarnisto, 1986). For example, increased nutrient loading often leads to increased productivity. Laminated sediments are valuable archives of such change because of the accurate time series they provide. Holzmaar is also one of the most intensively investigated maars of the Eifel with detailed sedimentary records of human activities (Baier *et al.*, 2004b; Zolitschka, 1992b).

6.2.3 The Holzmaar catchment

Lake Holzmaar (6°53' E, 50° 7' N) is located in the highlands of the Eifel Volcanic Field in the Rhineland-Palatinate region, western Germany, ca. 100 km south of the city of Bonn and ca. 45 km northeast of Trier (Figure 6.3). It is a small circular maar lake with a diameter of 250-325 m and has a water surface area of 0.058 km² (Baier *et al.*, 2004a; Moschen *et al.*, 2009). Lake Holzmaar is formed within a crater of phreatomagmatic volcanism which most likely erupted between 70,000 and 40,000 years BP, prior to the Last Glacial Maximum as estimated by Büchel (1993) and Negendank and Zolitschka (1993). Lake Holzmaar has steep-sided walls and a relatively wide flat bottom at ca. 425 m above sea level (Zolitschka, 1998). The geology of the catchment is composed of Lower Devonian greywackes, clay and siltstones with a thin covering of young Quaternary loess and pyroclastics, amongst which the Laacher See Tephra may be the foremost (Stockhausen and Zolitschka, 1999).

The inflow and outflow of the lake consist of a single stream, the Sammetbach, which passes through the whole basin from an embankment and drains a small catchment area of approximately 2.06 km² before entering the River Alf, a tributary of the River Mosel. This shallow embankment is situated in the southwest corner of the lake and was formed by dam construction during the Late Middle Ages, subsequently raising the original water level by around 1.5 m (Zolitschka, 1998).

Since Holzmaar has a maximum water depth of almost 20 m, the modern lake is dimictic and holomictic and susceptible to monomictic conditions in years with ice cover (Fuhrmann *et al.*, 2004; Baier *et al.*, 2004a). Seasonal anoxic conditions, especially during the summer months, exist from the lake bottom to a depth of about 8 m in the hypolimnion (Scharf and Oehms, 1992; Moschen *et al.*, 2009). The Sammetbach brook has little erosivity due to the relatively low relief (52 m) of the catchment, and there is also evidence of a non-prograding delta (Zolitschka, 1998). However, it carries a large amount of dissolved nutrients when discharging into the lake, which has contributed to a transition since the Late Glacial from the natural mesotrophic state to a eutrophic state (Scharf and Oehms, 1992). A recent study of primary production in Holzmaar gave evidence of increased diatom sedimentation

beginning in late April and developing in June and September (Raubitschek *et al.*, 1999) in relation to altered nutrient concentrations resulting from changes in temperature, precipitation and lake circulation patterns (Baier *et al.*, 2004a; Prasad *et al.*, 2006). Under the present conditions, Lake Holzmaar is recorded as a soft-water lake where low carbonate levels have been observed, with mean total inorganic carbon of 0.45 wt% in the sediments of the past 14, 000 varve years (Lücke *et al.*, 2003). Some geographical, morphometric and chemical characteristics are summarised in Table 6.1.

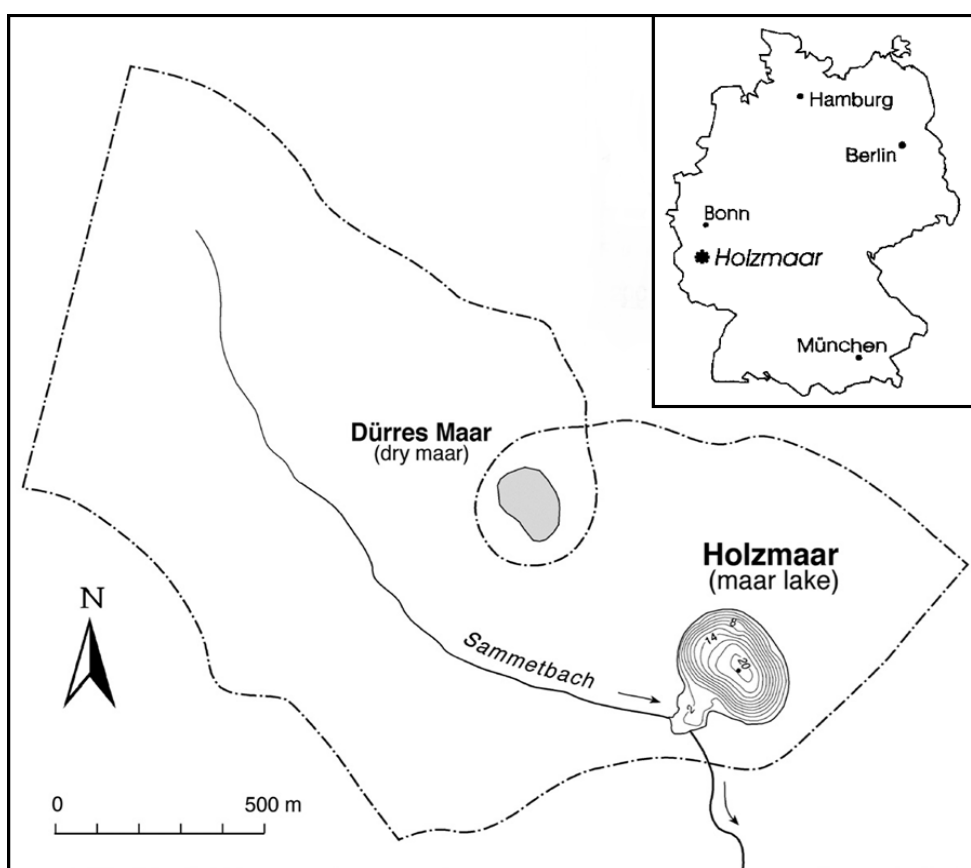


Figure 6.3 Location of Lake Holzmaar and its catchment (from Zolitschka, 1998; Lücke *et al.*, 2003).

Table 6.1 *Geographical, morphometric and chemical characteristics of Lake Holzmaar, Germany (after Scharf, 1987; Scharf and Menn, 1992; Scharf and Oehms, 1992; Lottermoser et al., 1997; Zolitschka, 1998; Lücke et al., 2003; Baier et al., 2004a; Kienel et al., 2005).*

Variable	Value
Catchment area	2.06 km ²
Maximum water depth	20 m
Lake surface area	0.058 km ²
Mean water depth	8.8-11 m
Elevation	418.2-476.3 m
Water volume	0.51-0.64 km ³
Mean total inorganic carbon	0.45 wt%
Theoretical water retention time	0.6 a
Electrical conductivity	197-303 µS cm ⁻¹
Total phosphorus concentrations	18-23 mg l ⁻¹
Epilimnion depth	6-8 m
Average water pH	9

Local climate information is documented from the nearest weather station the Deutscher Wetterdienst (German National Meteorological Service) in the format of long-term (1961-1990) mean values. The air temperature of the warmest month (July) is 16 °C and January is the coldest month with a mean value of -1 °C. Compared to the mean annual (1961-1990) temperature of 7.8 °C, data for the period 2004-2008 show an increased annual average of 8.7 °C. The maximum temperature may reach as high as 31 °C in July. Mean annual precipitation is 908 mm for the period of 1961-1990, and largely derives from Atlantic cyclones driven by the subtropical jet stream (Prasad *et al.*, 2006). As shown in Figure 6.4, the precipitation in the region

is relatively equally distributed, with highest in winter (95 and 96mm in November and December, respectively) and lowest in spring (April, 62mm).

The small catchment of Holzmaar is characterised by extensive land use in the present day. Approximately 60% of the land is farmed and dominated by pastures with a minor composition of cultivated farming (Kienel *et al.*, 2005; Zolitschka, 1998). The remaining land and the crater wall are mainly beech and beech–oak forests (Schwind, 1984), described as mesophytic deciduous broad leaved and mixed coniferous broad leaved forests (Litt *et al.*, 2009).

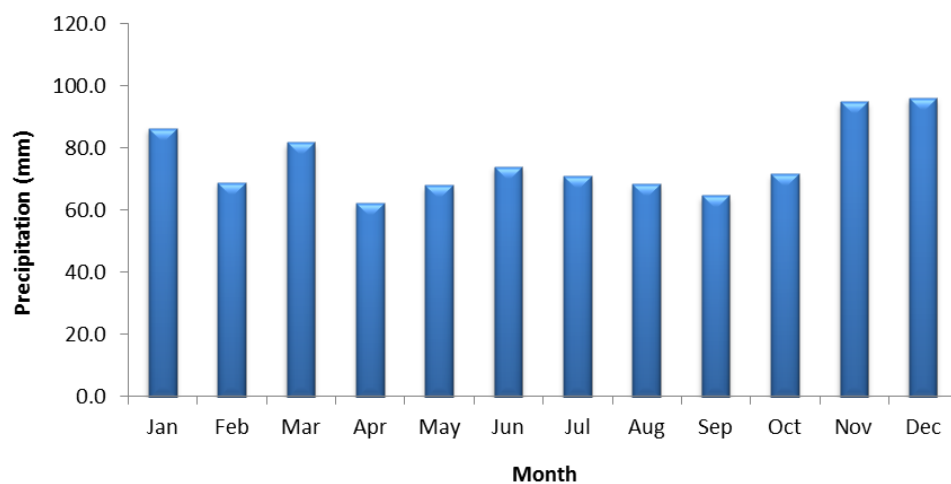


Figure 6.4 Average monthly distribution of precipitation from 1961 to 1990 in the Holzmaar catchment, Germany.

6.3 Model setup

A concise description of the model setup follows, with more details given in Chapter 4.

The Holzmaar catchment is simulated to generate a long term record of sediment delivery to the lake and catchment morphology adjustment in response to environmental changes over a 5000 year periods. An hourly input file of precipitation is derived and modified from high-resolution meteorological records, medium-resolution reconstructed palaeoprecipitation (Casty *et al.*, 2007; Pauling *et al.*, 2006) and low-resolution precipitation reconstructed from pollen data (Litt *et al.*, 2009), all of which cover the area of the catchment. The pollen record, and in

particular the percentages of arboreal pollen, are converted to M values for the same periods at an hourly scale in the catchment (Zolitschka, 1998). Along with rainfall and M value data, a 10m by 10m DEM and associated bedrock data comprise the input files. The initial sediment particle size distribution was setup according to the approach described in Chapter 4. Modelled daily total sediment discharge is recalculated every 50 years and compared to proxies of minerogenic sediment accumulation rates and magnetic susceptibility from the lake sediment record. A spatial pattern of net erosion and deposition is displayed using ArcMap 10 software.

6.4 Results

6.4.1 Catchment sensitivity to land use and climate changes-model simulation

The overall temporal distribution of sediment discharge for the Holzmaar catchment is displayed in Figure 6.5. The catchment behaves differently in response to precipitation and land use changes. It delivered a total amount of approximately 3000 m³ of material out of the catchment over the whole 5000-year period. The relative relief of the catchment above lake level is only 52m and the Sammetbach is the only stream draining the catchment. Annual varve thickness measurement (Zolitschka, 1998) suggests that annual sediment accumulation rates range between 0.4 to 12 mm with no evidence of a prograding delta. Simulated total sediment discharge is lower than the empirically estimated lake sediment volume (estimated as 50,000 – 116,000 m³/year), because modelled water discharge could not be calibrated with real flow record due to data limitation. The setting of M values could be adjusted according to the real flow record to mitigate this problem. However the long-term pattern of changes in sediment discharge represents the landscape evolution history well and this is discussed in the following sections. Furthermore, gaining an understanding of the sensitivity of catchment response to environmental changes is the main focus of this thesis.

During the past 5000 years, the Holzmaar catchment has experienced a long history of land use change, in which there have been six periods of substantial and significant reduction in forest cover, starting from approximately 1600 BC (3550 calendar year BP) and continuing to 1950 AD (Figure 6.5). Prior to 2800 calendar year BP, only three events of short term land use change are detectable.

Simulated sediment discharge shows a temporal synchronicity with these events as sediment delivery increases within every period of reduced forest cover.

Occasionally, the increase in sediment delivery shows a lagged response. For instance, in the 3300-3200 calendar year BP (1350 BC-1250 BC) and 350-250 calendar year BP (1600 AD-1700 AD) period, the appearance of sediment peaks are delayed by around 50 years during the phase of reduced land cover. Between 3550 and 3200 calendar year BP (1600 BC-1250 BC), there were two phases of forest reduction with the same amplitude, but the magnitude of total sediment discharge during these phases was different. This was due to the behaviour of sediment storage and supply cycles of the catchment and channel. The increase in sediment discharge due to the first reduction in forest cover (around 3500 calendar year BP) follows a series of large sediment transport events that coincide with precipitation events that may have flushed out the sediment stored in the channel and slope systems. The insufficient sediment storage and the reduced capacity to transport sediment under the next land cover change may have limited the peak of sediment discharge even though there were larger water discharges around 3300 calendar year BP. Despite the lower and lagged peaks of sediment discharge, the catchment remains sensitive to changes in land use throughout the whole 5000 year timeframe.

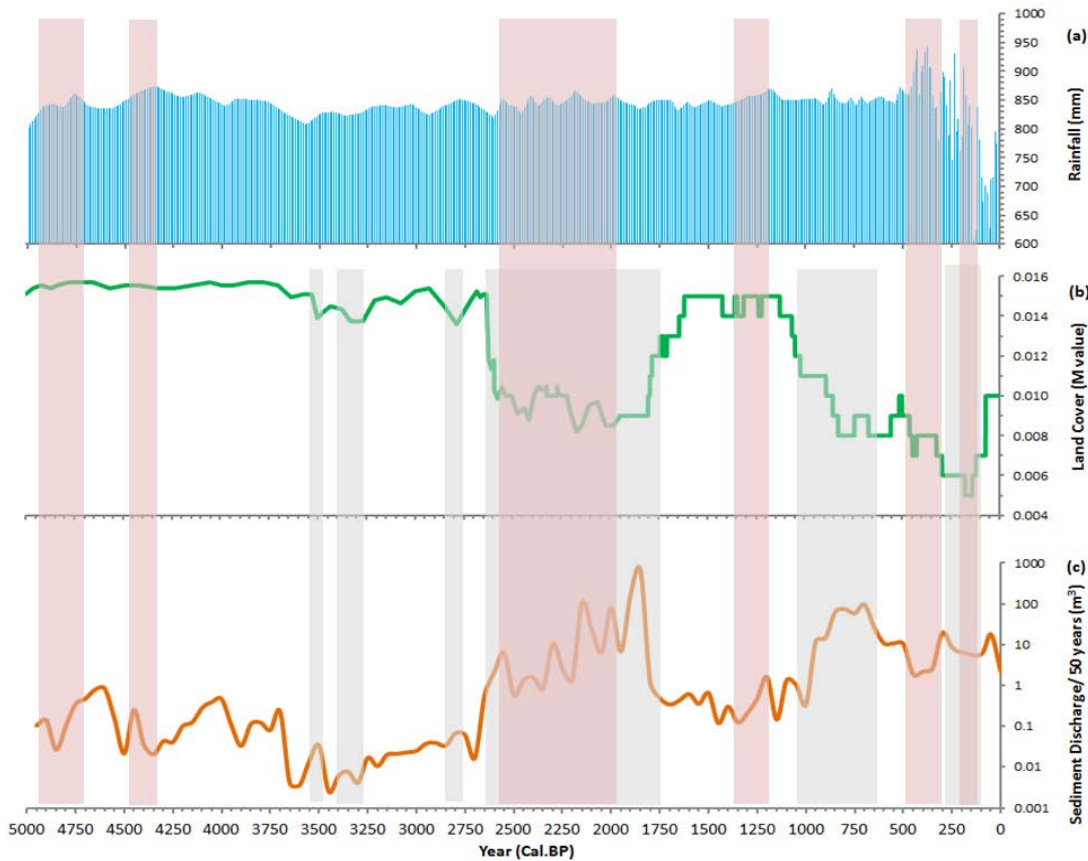


Figure 6.5(a) Decadal precipitation; (b) annual forest-cover in *M* values; (c) total sediment discharge every 50 years; light grey shadows highlight forest cover reduction and pink shadows highlight precipitation peaks.

After approximately 2700 calendar year BP (750 BC), a period of relatively stable land use was disturbed due to the development of an iron smelting industry, a development that accelerated with the subsequent Roman invasion. Intensified human activities resulted in more frequent land use changes, which in turn are reflected by the high magnitude of sediment transport. The longest and most obvious changes in land use occurred from 2800 to 1800 calendar year BP (750 BC-150 AD). Rapid and progressive increases in sediment delivery correspond to these changes. Enormous quantities of sediment were released into the system, which may be a function of increased sediment supply under low forest cover, exceeding the sediment transport capacity threshold of the system. Sediment response to the reduced land cover may have grown over time as the rise in sediment discharge increased gradually over the 1000 year period, peaking at around 1850 calendar year BP, which corresponds with the cessation of forest cover reduction. It is likely that much of the sediment moved during the substantial increase in sediment supply may

have been deposited along the channel and within the system, and it may then have been re-mobilised during long term large erosion events. Between 1100 and 600 calendar year BP (850 AD to 1350 AD), deforestation resulting from rapid population growth was another significant land use change event. A notable increase in sediment delivery corresponds to this deforestation event.

Sediment response is also sensitive to afforestation during the whole 5000-year periods. Reduced sediment delivery, due to a decline in sediment supply as a result of increased land cover between 1750 calendar year BP (200 AD) and the next large erosion event, is also recorded in Figure 6.5. The most recent deforestation event took place between 250 and 150 calendar year BP (1700-1800AD); however, the sediment response was reversed with a slight decrease in sediment delivery. The considerable decline in precipitation, particularly around 130 and 50 calendar year BP (1820 AD and 1900 AD) may have contributed to the slightly decline in sediment discharge between 250 and 50 calendar year BP. Therefore, precipitation also plays an important role in delivering sediment in the fluvial system.

There have been several large precipitation events during the past ca.5000 years. The Holzmaar catchment responds to these annual precipitation maxima with some smaller responses or lagged responses during certain periods. Since the beginning of the period of record, simulated sediment discharge shows a small peak at 4900 calendar year BP (2950 BC) which coincides with high precipitation. This marked peak was sustained and intensified by the subsequent increase in rainfall which lasted for 100 years until ca.4800 calendar year BP. There is a relatively instant response of sediment to the precipitation increase occurring approximately 1350 to 1150 calendar year BP (600 AD-800AD), which indicates that the catchment was sensitive to rainfall extremes when there was no notable land use change during that period. The appearance of high sediment delivery rates before the annual precipitation maximum from 4500 to 4300 calendar year BP (2550 BC-2350BC) suggests that the sediment generated during this phase was either delivered rapidly or deposited in the system and may be released at a later time during subsequent rainfall events. Support for this latter sediment remobilisation seems to be provided by the successive increase in modelled sediment discharge after 4300 calendar year BP, which lasts for approximately 200 years, even there is no large rainfall event during that time phase.

Although it is obvious that the substantial forest cover reduction produced the largest sediment discharges, the effect of rainfall can also be detected from the correspondence of sediment peaks and rainfall extremes. The sensitivity of sediment response to climate change is also reflected in some low precipitation events. For example, in 3625 and 2700 calendar year BP (1675 BC and 750 BC), there were noticeable decreases in sediment discharge that match the low precipitation events. There is another example shows that, in 450-375 calendar year BP (1500 AD -1575 AD) sediment delivery increases only slightly compared to the large amount of precipitation. This may be due to the fact that the previous massive erosion resulting from the rapid reduction of forest cover may have exhausted the sediment in the catchment. Changes in the erosion-deposition cycle and intrinsic system control may have reduced the sediment erodibility, whereas the sustained increase in rainfall coupled with the decline in land cover after 375 calendar year BP accelerated sediment delivery with the lagged small peak of sediment discharge appearing around 300 calendar year BP (1650 AD).

6.4.2 Catchment behaviour in response to environmental changes-spatial simulation

In addition to the temporal response of sediment movement to environmental changes, raster outputs from CAESAR modelling can give an insight into the spatial distribution of erosion and deposition in the Holzmaar. A sequence of simulations have been carried out based on various time periods and Figure 6.6 displays the elevation differences after simulations during the 5000-3000 calendar year BP and 2999-0 calendar year BP periods. The discrepancy between the general patterns of erosion and deposition before and after the Iron Age underlines the significant impact of land use change on sediment movement.

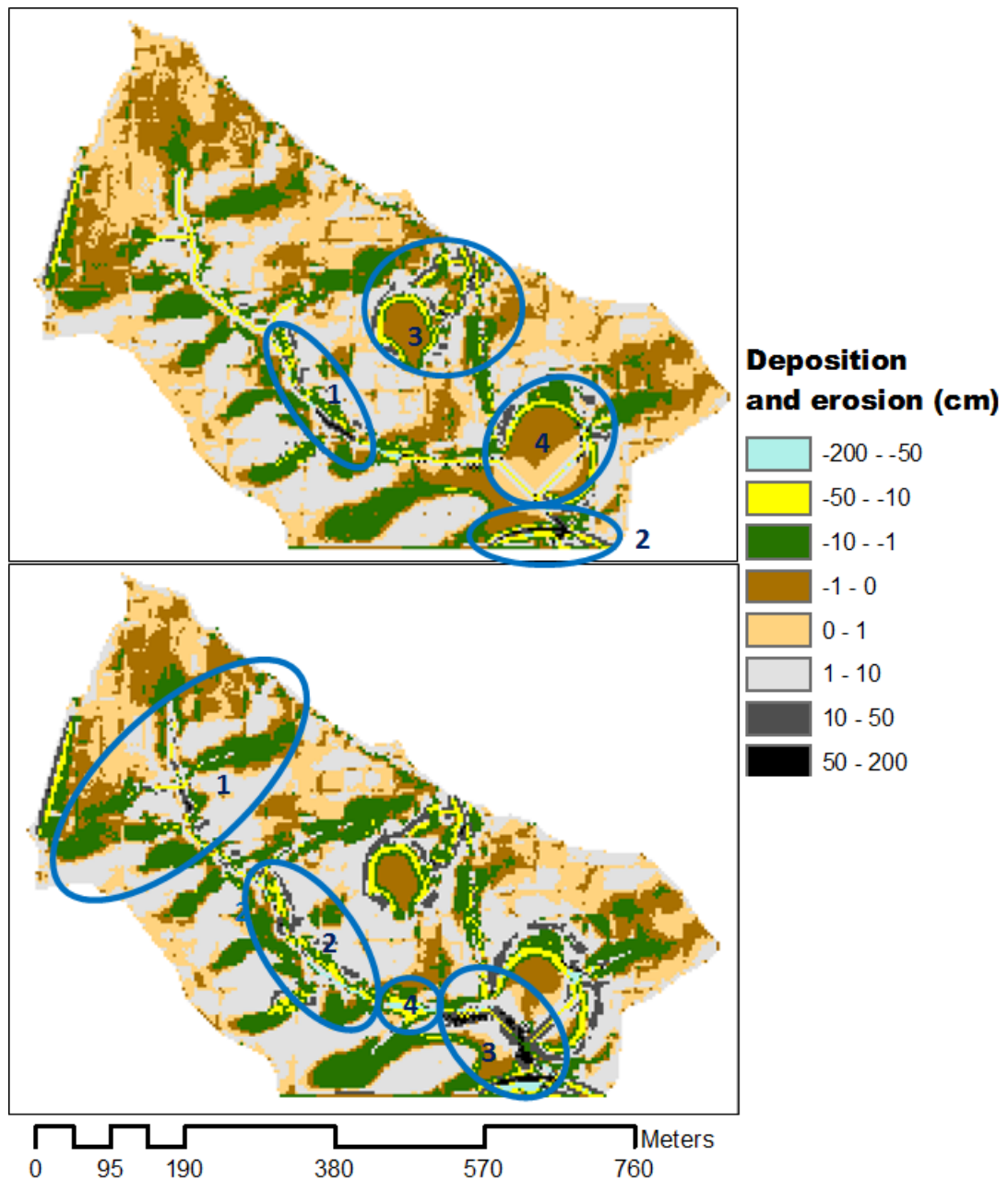


Figure 6.6 Erosion and deposition during (a) 5000-3000 calendar year BP (3050-1000 BC) and (b) 2999-0 calendar year BP (999 BC-1950 AD) in Holzmaar catchment. Positive values indicate erosion and negative values indicate deposition. Blue circles with numbers indicate focus areas that are discussed.

During the first 2000 years, the sediment discharge curve exhibits a relatively gently fluctuation under low levels of land use change throughout the time sequence (Figure 6.5). Similarly, this temporal pattern of the sediment erosion-deposition cycle is reflected in spatial maps (Figure 6.6). It is clear that a large amount of sediment has been eroded from hillslope zones owing to some flooding events resulted in

significant sediment deposition in the main channel and its tributaries. Sediment supplied from slope erosion, coupled with erosion in watershed zones, also generated gullies adjacent to the main channel, providing a route for incessant sediment delivery from the slopes. Despite high rates of accumulation, there is also a visible degree of erosion in the main channel. Part of the channel, especially around the outlet of the lake, has been significantly eroded with channel incision of up to 2m (Areas 1 and 2: Figure 6.6a) which may indicate that the capacity of the channel is greater than the supply of sediment during periods of reduced precipitation magnitude. Two further detectable erosion conditions are shown in areas 3 and 4 in Figure 6.6a, which mainly surround the bank of Holzmarr and another dried maar lake. Sediment has been rapidly delivered from the steepest slope to the less steep slopes to the floodplain resulting in massive deposition due to decelerated sediment delivery rates.

From ca. 3000 calendar year BP (1000 BC), the fluctuation of sediment discharge is stronger due to intensive land use change since the early Iron Age, as shown by peaks and troughs in sediment delivery throughout the time series (Figure 6.5). Rising sediment accumulation in gullies (Areas 1: Figure 6.6b) and intensified hillslope erosion constituted the primary sources of sediment supply during the period of rapid forest cover reduction that lasted for about 1000 years. This massive sediment supply not only accelerated sediment delivery out of the catchment (as shown in Figure 6.5) with substantial peaks of sediment discharge, but also led to high volumes of sediment deposition in the gullies and tributary channels when the sediment supply exceeded the capacity of the channel transporting the sediment.

The catchment experienced approximately 800 years of forest recovery during the migration period (1800- 1000 calendar year BP), when people left due to unfavourable climatic conditions. Time series of sediment delivery patterns display a significant reduction in both total sediment discharge and erosion events, while lower erodibility of the system due to higher forest cover limits the supply of sediment from steep slopes. However, it is suggested that sediments start to remobilise from gullies and the channel where they have previously been stored, with large areas of overbank erosion (Area 2: Figure 6.6b). Meanwhile, part of the downstream section

of the channel is eroding at a faster rate with up to 2 m of incision (Area 3: Figure 6.6b) during this period.

In the last 1000 years, rates of land use change have again increased due to greater levels of anthropogenic impact. There were also several large flood and drought events between 500 and 0 calendar year BP (AD 1450-1950, Modern Times). Consequently, the catchment is characterised by considerable erosion and deposition particularly surrounding the lake margin and another dried maar lake. It is most likely that high sediment delivery rates from eroding slopes either transport a massive amount of sediment out of the area or deposit it to the valley at a lower elevation. There is still some in-channel storage of sediment (Area 4: Figure 6.6b), but this is distributed in a more concentrated manner in some areas and at larger volumes than the first 2000 years of the time series, which have an equivalent distribution of sediment accumulation in the channel.

6.5 Discussion

6.5.1 Overall patterns of model validation

Following the simulation of landscape evolution in the Holzmaar catchment over 5000 years, the distribution of total sediment discharge was calculated by summing the continuous sediment discharge data for each grain size section, recorded at intervals of 50 simulated years. Zolitschka (1998) has previously converted sediment accumulation rates of allochthonous minerogenic deposition to reconstruct Pleistocene / Holocene sediment yield. This study demonstrated not only the reliability of quantitatively reconstructed Holzmaar sediment, but also its strong dependence on anthropogenic activities by comparison with similar data from southern Sweden and published data from other monitoring sites in Europe. Magnetic susceptibility, which is often used as an indicator of environmental change via changes in magnetic material concentration in erosional processes, has been investigated by Stockhausen and Zolitschka (1999). Their study suggested that the variation in magnetic susceptibility is related to climate prior to the existence of human settlements but after settlement it reflects high levels of human activity in the region of Lake Holzmaar. Studies from both a model simulation of forest cover and pollen data sequences in the catchment area emphasized the link between

deforestation and intensive human land use and agriculture during the Holocene (Kleinen *et al.*, 2011). Consequently, palaeoenvironmental data from sediment cores reflect general variations in sediment and soil supply in the catchment. Climate and human-induced land-use changes over thousands of years can be applied to validate the simulated sediment distribution records. Model validation focuses on the broad patterns of changes rather than the synchrony of peaks and troughs in the long time series (Welsh *et al.*, 2009).

The overall pattern of modelled sediment discharge shows a trend similar to that of minerogenic sediment accumulation rates (SAR-min) and magnetic susceptibility from sediment proxies (Figure 6.7) over 5000 years. In these records, two features are significant: minor changes that are nearly synchronous between records before ca. 2800 calendar year BP (The Iron Age) and sharp shifts in records after this date. During the initial 1000 years of the entire 5000-year record, sediment delivery in both the model and the natural system were kept in a steady state then followed by a slight downward trend until ca. 3000 calendar year BP, before the rapid increase in sediment and mineral material occurred. The sediment transport rate slowed down after ca. 1800 calendar year BP, a trend that lasted for approximately 800 years. Once again, sediment delivery in both systems accelerated after ca. 1000 calendar year BP, reaching a second peak that continued to the end of the record. Despite the similar trajectories of change between records, the general behavioural response of sediment to climate (e.g. precipitation) and vegetation (e.g. non-arboreal pollen percentages, NAP %) changes are similar.

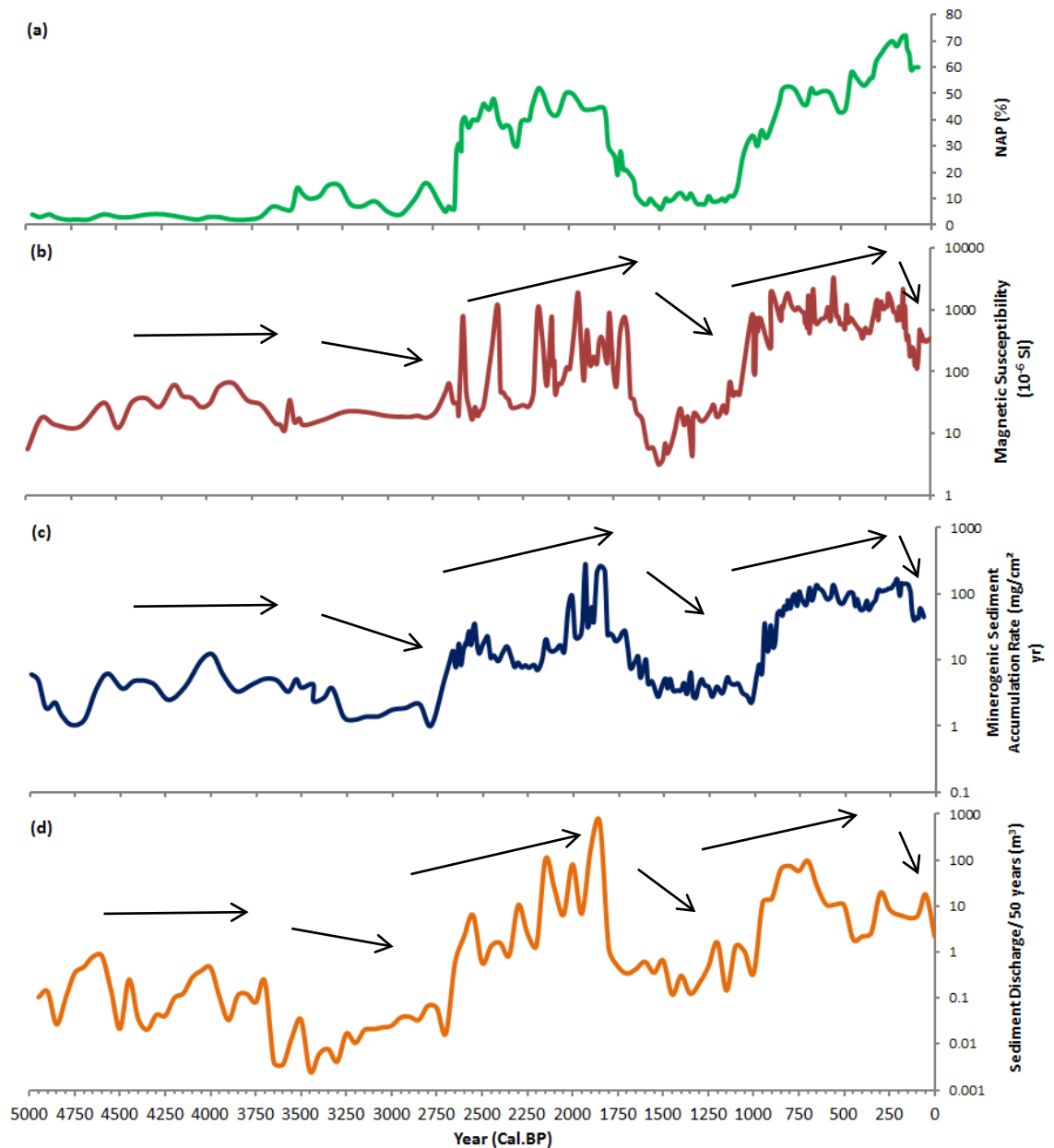


Figure 6.7 Comparison of (a) non-arboreal pollen percentages (NAP %), (b) Magnetic susceptibility, (c) sediment accumulation rate of mineral material from lake sediment records and (d) modelled total sediment discharge from CAESAR in the Holzmaar catchment.

6.5.2 Model validation for the time period of 5000 - 3750 calendar year BP

According to the pollen diagram produced by Litt *et al.* (2009), the first occurrence of anthropogenic signals (i.e. single pollen of cereals and ribwort plantain) proves the presence of middle Neolithic settlement in the Holzmaar catchment (Figure 6.8 and 6.9). However, a low NAP value (Figure 6.7a), which is mainly related to the degree

of open landscape (forest cover), indicates limited forest clearance activities during the late Neolithic and early Bronze Age (ca. 5000 - 3750 calendar year BP). In contrast to the relatively constant NAP values, the sediment discharge recorded in CAESAR associated with SAR-min and magnetic susceptibility records displays fluctuations within a narrow range with some small peaks and troughs during the same period. Between approximately 3750 and 3000 calendar year BP, there is an increase of NAP by 10% due to the development of grassland (Figure 6.7 and Figure 6.8). Nevertheless, clear reductions in modelled sediment flux, SAR-min and magnetic susceptibility suggest a lower erosion rate during the middle Bronze Age. This distribution pattern of mineral sedimentary delivery and rates corresponds with changes in the magnitude of precipitation events (Figure 6.5a), with small peaks occurring around 4600 and 4000 calendar year BP then declining until around 2800-2900 calendar year BP. Moreover, variations in sedimentary records are related to climatic cooling events beginning in the late Holocene (ca. 5000 calendar year BP) as shown by the $\delta^{13}\text{C}$ record in Lücke *et al.* (2003). More convincing evidence for a cold climate between 5000 and 2800 calendar year BP comes from glacier advances in the Austrian and Swiss Alps (Patzelt and Bortenschlager, 1973; Haas *et al.*, 1998; Baier *et al.*, 2004a) and ice rafted debris events in the North Atlantic (Bond *et al.*, 1997), as well as from lake level fluctuations in the French Jura (Magny, 1992) and Scotland (Dubois and Ferguson, 1985). During colder and moister periods (ca. 5000 - 3750 calendar year BP), shifts in temperature and humidity may have caused changes in ice thickness in Greenland and atmospheric circulation (Stockhausen and Zolitschka, 1999), resulting in variations in erosion and minerogenic deposition in Europe. With the relatively low precipitation between ca. 3750 and 2800 calendar year BP, as simulated in CAESAR the minerogenic input slowed and there was a reduction in sediment delivery; this was also recorded in magnetic susceptibility (Zolitschka, 1992a, b).

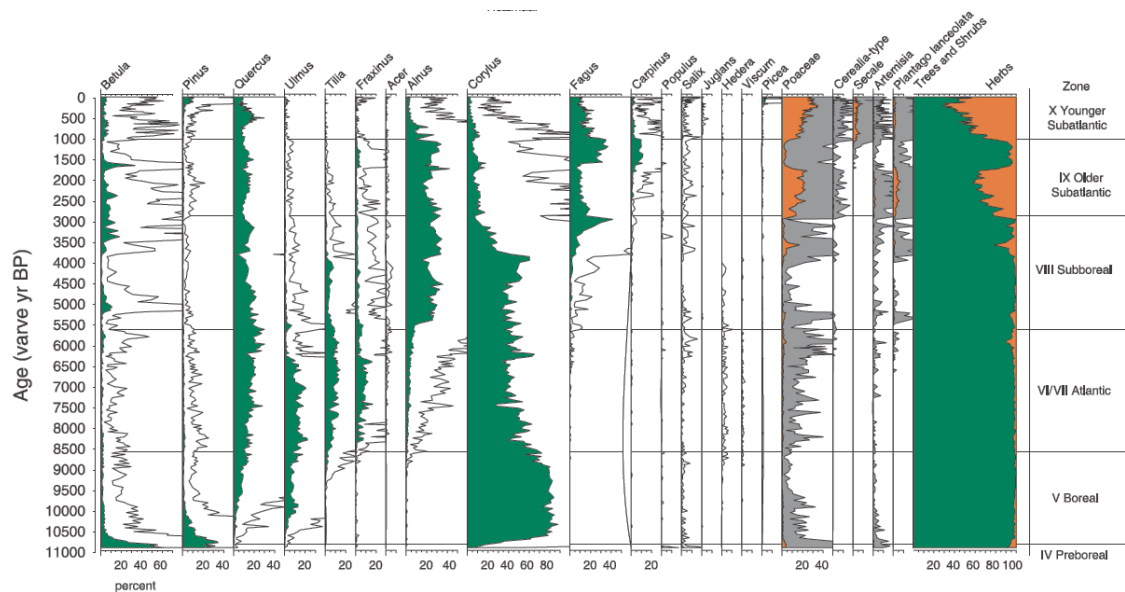


Figure 6.8 Simplified pollen data from Lake Holzmaar for 11, 000 varve years (from Litt et al., 2009).

	Period		Palaeobotanical evidence for agriculture activities
0	Modern Times		Prussian reforestation
500 Cal BP	Late Middle Ages		Hemp cultivation Rye mono-culture
1000 Cal BP	High Middle Ages		
1500 Cal BP	Early Middle Ages		
2000 Cal BP	Roman Times		No significant change between Iron Age and Roman Times
3000 Cal BP	Latène Period		
4000 Cal BP	Hallstatt Culture		
5000 Cal BP	Late Bronze Age		Hulled wheat First flax Opening of landscape Spread of beech
	Middle Bronze Age		
	Early Bronze Age		
5000 Cal BP	Late Neolithic	Latest phase	Beginning cereal cultivation First cereal pollen
		Middle phase	
		Early phase	

Figure 6.9 Chronological table for land use and pollen record (based on Löhr and Nortmann, 2008; Herbig and Sirocko, 2012).

6.5.3 Model validation for the time period of 2750-1750 calendar year BP

From the early Iron Age (2750 calendar year BP), the curve of non-arboreal pollen increases drastically. All simulated and measured sedimentary parameters respond simultaneously to this distinct and rapid forest clearance, presumably indicating the strongest prehistoric human impact in the region. The value of NAP increases to more than 50% (Figure 6.7a) and the amount of minerogenic matter washed into the lake increases correspondingly, reaching a maximum with slight fluctuations, a trend which lasted for approximately 1000 years in conjunction with vegetation changes (Figure 6.7b, c, d). Lottermoser *et al.* (1997) found human-induced disturbances of the natural geochemical cycle from increasing tracer element and heavy metal fluxes in association with increased clastic material inputs in the Holzmaar sediment since the onset of the Iron Age. The pollen diagram shows an increase in herb pollen, including indicators of human activities such as cereals, grasses and mugwort etc., resulting from intensive woodland clearance for agriculture during the pre-Roman Iron Age (Litt *et al.*, 2009). Due to the favourable mild climate (Rein *et al.*, 2007), human settlements and agricultural activities were highly developed during the Roman period. Modelled sediment discharge remained high during this period, broadly tracing the curve of the NAP values, sediment accumulation rate and magnetic susceptibility as shown in Figure 6.7. It is recorded that under Roman occupation, timber was widely used for infrastructure and there was charcoal production for iron smelting (Zolitschka, 1996). Furthermore, intensified crop cultivation and the utilisation of iron tools and ploughs altered the catchment system abruptly with reduced vegetation cover, open landscape, exposed soils and consequently accelerated soil erosion processes (Zolitschka, 1998).

6.5.4 Model validation for the time period of 1750-1000 calendar year BP

At the transition from the Roman period to the Migration Period (around 1750 calendar year BP), the percentage of non-arboreal pollen quickly drops again, reaching about 10% until the early Middle Ages (ca.1000 calendar year BP), indicating forest regeneration. Synchronously, a distinctive decline in sediment

discharge occurs in the model output and this pattern is also paralleled by the SAR-min and magnetic susceptibility curves. Research on the $\delta^{13}\text{C}$ record (Lücke *et al.*, 2003) from Lake Holzmaar points to wetter climatic conditions. Both a reduction in nutrient concentrations and diatom abundance (Baier *et al.*, 2004a) and increased varve thickness record which was dated by tree-ring based global radiocarbon records (Zolitschka, 1996; Stuiver *et al.*, 1998) document the cold climate during the Migration Period. This climatic deterioration forced the migration of people throughout Europe, leading to reduced levels of human activity in the study area. As a consequence, forest cover increased, as revealed by the increase of *Fagus* (beech), *Betula* (birch), *Corylus* (hazel), *Fraxinus* (ash) and *Carpinus* (hornbeam) in pollen records (Figure 6.8; Kubitz, 2000; Bienert, 2008; Litt *et al.*, 2009), as well as decelerated sediment delivery.

6.5.5 Model validation for the time period of 1000-0 calendar year BP

From ca. 1000 calendar year BP (AD 950) onwards, modelled sediment discharge again increases gradually to a small peak around 750 calendar year BP (AD 1200) before declining slightly at about 500 calendar year BP (AD 1450). It then remains stable with minor fluctuations until the present day. These patterns are also mirrored in the SAR-min and magnetic susceptibility curves during the late Middle Ages (700-550 calendar year BP), the 15th and 16th centuries (ca. 300-400 calendar year BP) and the 17th and 18th centuries (ca. 150-200 calendar year BP) as an indication of relatively high sediment delivery rates in the Middle Ages and modern times. The overall pattern of the NAP curve exhibits a continuous increasing trend with the exception of a slight decrease in the percentage of non-arboreal pollen around 500 calendar year BP (AD 1450). After that time, the deforestation process continued until less than 30% of the land in the Holzmaar region was covered by trees and shrubs (the NAP value is over 70% as shown in Figure 6.7a) in the 19th century (ca. 100 calendar year BP). An obvious increase in the percentage of cereal and Poaceae (grasses) pollen has been observed in the late Medieval period (AD 1000-1450), wherein cereal pollen occupies more than 10% of the pollen spectra (Herbig and Sirocko, 2012). Herbig and Sirocko (2012) suggest the development of wet meadows based on the marked decrease in alder woods from more than 40% to less than 10% of land cover due to the growing demand for grazing in the Middle Ages.

Further evidence of human impact from the pollen record is the cultivation of flax in the early 14th century. Climate variability between ca. 1000 and 200 calendar year BP is characterised by the well-known Little Ice Age (LIA, AD 1300-1900), which is described as a cold period in contrast to the warmer climatic conditions in the Middle Ages and modern times. Reduced sunspots and solar activity (Vos *et al.*, 1997; Reid, 2000), increased atmospheric radiocarbon (Crowley, 2000; Stuiver and Polach, 1977) and large volcanic eruptions (Fischer *et al.*, 2007; Briffa *et al.*, 1998) delineate this cold phase. Instead of population migration due to low temperature, the population in close proximity to Lake Holzmaar increased slightly (Rein *et al.*, 2007). Accelerated industrial development and new techniques led to forest clearance to satisfy increased demand for charcoal and agricultural activities. High soil erosion rates can be attributed only to increased human impact. From the early 19th century, anthropogenic afforestation was carried out after the establishment of the Prussian kingdom in Eifel area (Zolitschka, 1998). The Prussians planted substantial areas of fast growing coniferous trees, which are recorded in the pollen diagram as an increased percentage of *Picea* (spruce) and *Pinus sylvestris* (Scots pine) pollen (Herbig and Sirocko, 2012).

6.6 Summary

The important findings obtained from these simulation results is that the CAESAR model has the capability to model sediment discharge and that modelling results are comparable to high resolution lake sediment records. Simulated patterns of sediment delivery are in close correspondence to the general trajectory (e.g. increases and decreases in the sediment flux), magnitude (e.g. major peaks in sediment discharge) and behaviour (e.g. erosion and deposition cycle) of the minerogenic sediment accumulation rate and magnetic susceptibility of laminated sediment in the catchment over the 5000 year period. Time lags of forcing-response processes between model results and the sediment record are inevitable due to errors in the varve chronology which are however within acceptable limits. It is concluded that the CAESAR model can be used as a tool to simulate system sensitivity and behaviour in response to a changing climate and land use at a long time scale (approximately 5000 years).

Holzmaar catchment records provide signals of complex system process-response to Holocene environmental variations, a combination of both climatic and anthropogenic factors. Modelled sediment results demonstrate that the catchment has been most sensitive to changes in precipitation and forest cover during the last 5000 years. With the information provided by pollen records and historical precipitation data, this highly efficient varved lake-catchment system shows clear and significant responses, summarised as minor changes in sediment discharge before the Iron Age and extremely sharp shifts in records in the post-Iron Age period.

At the time of high forest cover, especially before the onset of human settlement and during the Migration periods, the supply of sediment to the catchment was mainly controlled by precipitation and runoff. Warmer and drier climates cause slow erosional processes with decreased minerogenic deposition and low susceptibility. Reduced sediment discharge reflects this condition, and the majority of the eroded sediment is stored within the system. However, wetter climates with high-magnitude precipitation events are characterised by high minerogenic deposition and susceptibility due to increased runoff and erosion and elevated sediment discharge. Precipitation peaks may supply the system with increased sediment derived from the remobilisation of previously deposited sediment and the delivery of fresh materials resulting from hillslope erosion.

The Holzmaar system has experienced two distinct periods of anthropogenic influence (e.g. deforestation and intensified agricultural activities), from the beginning of the Iron Age to the end of the Roman period and from the Middle Ages to the present day. These human impacts have manifested themselves in the simultaneous rise in magnetic materials washed into the lake, non-arboreal pollen values and minerogenic deposition. Rapid sediment movement is also recorded in sediment records, both temporally and spatially, with not only massive sediment discharge but also sediment deposition in the catchment which can be removed under flooding events after the passage of several decades.

In summary, model simulations support inferences that climate and human activities are two key factors responsible for erosional processes in the fluvial system of Holzmaar and they have complex interactions. A cool and humid climate plays a role

in determining precipitation and flood magnitude leading to fluctuations in sediment discharge. However, intensified human activities resulting from a warm climate and improved technology may modify the climate signal and lead to increased sediment delivery and accumulation. Meanwhile, system landform and internal properties, such as channel capacity, soil erodibility and the system's erosion-deposition cycle are equally responsible for sediment supply. It is difficult to differentiate these forcings, particularly during the last 500 years.

Chapter 7

The role of non-linearity and self-organisation in complex river systems

7.1 Introduction

The stationarity of natural fluvial systems is no longer a relevant concept due to substantial human disturbance (e.g. flood risk, channel modification and land-use change), natural climate changes (e.g. global warming) and internal variability (e.g. landform structure, slopes) enhanced by the dynamics of the system itself (Veldkamp and van Dijke, 2000; Vandenberghe, 2003; Barnett *et al.*, 2005; Milly *et al.*, 2008; Bakker, 2012; Chapman *et al.*, 2013). As a consequence, river systems should behave in the form of non-linear complexity, in which the responses of the system are disproportionate to the disturbances over the entire range of possible disturbances (Phillips, 2006). Different types of non-linear dynamics have been recognised, including deterministic chaos, dynamical instability, fractals, multiple equilibrium, strange attractors and self-organization, details of their definitions are summarised in Phillips (2003). They may appear independently or, more usually, linking and interacting with each other. For example, in identifying dominant behaviour in a 10,000- year sediment archive from Holzmaar, Germany, Dearing and Zolitschka (1999) demonstrated that the system was close to either a self-organised critical state or maximized disorder state at different stages of its evolution. They explained how complex internal reorganisation rather than external controls account for system steady state and how the interaction of climate change and human impact contribute to major shifts in system state. Similarly, Allison *et al.* (1994) linked non-linear dynamics to hillslope processes, showing steady state, cyclical and chaotic behaviour in regolith evolution.

Causes of non-linearity in environmental systems have been classified by Phillips (2006) as thresholds, storage effects, self-organisation, saturation and depletion, feedbacks, hysteresis, multiple modes of adjustment and competitive relationships. Among these, self-organisation has been widely discussed since it does not specify

causalities for pattern formation in systems and is driven internally by system dynamics only (Bolliger *et al.*, 2003). The key rules of self-organisation are summarised as the following (Phillips, 1999):

- (1) Self-organisation in landscape evolution is a systematic progression and developmental trajectory toward steady-state equilibrium.
- (2) Self-organisation is formed through mutual adjustment of disturbance and state by a system's internal mechanisms (e.g. channel morphology and flow regimes).
- (3) Self-organisation is formed from chaotic behaviour, that is, minuscule initial variations or minor perturbations may be amplified exponentially in unstable systems producing large results (e.g. landslide).
- (4) The magnitude of response events and their frequency of occurrence follow a power law distribution that suggest a system changing toward self-organisation (small events are more likely occur than large events).
- (5) Self-organised systems are maintained in structure and organisation by energy dissipation, away from thermodynamic equilibrium.
- (6) Systems tend to organise into a critical state or threshold with no intrinsic spatial and temporal scales. This state is known as self-organised criticality (SOC).

The theory of self-organisation or self-organised criticality has been proposed and applied widely to earthquakes, ecosystems, geomorphic systems and other natural systems. Sneppen *et al.* (1995) used a mathematical model to display the intermittency pattern of biological evolution and its possible attribution to self-organised criticality. Sapozhnikov and Foufoula-Georgiou (1997) found that braided rivers exhibit dynamic scaling and behave as self-organized critical systems by monitoring braided river evolution in a laboratory. Lake sediment records in New Zealand (Gomez *et al.*, 2002) revealed evidence that landslides originated from self-organised criticality, with power law distributions in sediment deposition. In riverbank systems, the existence of SOC in bank failure and river width adjustments has been investigated by Fonstad and Marcus (2003) who analysed power law structure in spatial patterns of bank failure.

In recent years, numerical models have been gradually applied to simulate system non-linear dynamics, particularly cellular automata (CA) models in terms of their non-linear outputs and self-organisation tendencies (Coulthard, 1999). Murray and Paola (1997) used a cellular model with a simple expression of water flow and sediment delivery in braided streams and found that lateral sediment transport is important in maintaining a continuing dynamic behaviour in the system. Simulations of gully evolution under three designed scenarios (Sidorchuk, 2004) showed that the dynamic system is at a critical state of self-organisation. Sidorchuk (2004) found some of natural surface landforms can really be at the SOC state, and SOC attributes can really diagnose system activity. Other landforms can only show SOC-like attributes, being stable and far from crisis. Applying the CA model CAESAR to a simple catchment with regular rainfall inputs, Van De Wiel and Coulthard (2010) found non-linear fluctuations in sediment yield which indicated the presence of SOC in a river basin and illustrated the mechanism of internal dynamics instead of external drivers in fluvial systems.

In this study, the CA landscape model CAESAR is used to simulate sediment transport and landscape evolution upon three different types of fluvial system from a simple catchment to real complex systems at different time scales (300 days to 5000 years). The aim is to investigate the non-linear behaviours of different fluvial systems in response to possible drivers under a changing environment.

7.2 Methods

The main approach is to compare sediment erosion dynamics with both external and internal forcing so as to find evidence of non-linear behaviours and self-organised states in the open river systems. A sequence of numerical simulations have been designed and applied to three different types of lake-catchment systems, from a simple and virtual system to complex and real systems with different landscapes and environmental changes. All the simulations were accomplished by using CAESAR (details about this model and its application can be found in chapter 3).

The first simulation was based on a deliberately simplified catchment in the shape of rectangle with a thalweg (Figure 7.1) to minimize topographic effects after Van De Wiel and Coulthard (2010). This simple catchment has an area of 1km×2km and the

elevation ranges from 0 to 249 m. Five runs were designed for this simulation, each with a regular and repeated daily rainfall scenario, of 1 hour of rainfall (25 mm/h) at the beginning of each day and 23 hours of no rainfall (0 mm/h) in the rest of the day. Parameter (e.g. vegetation cover, rainfall, sediment size and duration) setup for different runs is shown in Table 7.1 and Figure 7.2. Model outputs of hourly water discharge (m^3/s) and daily sediment discharge (m^3) were analysed for display and comparison through time.

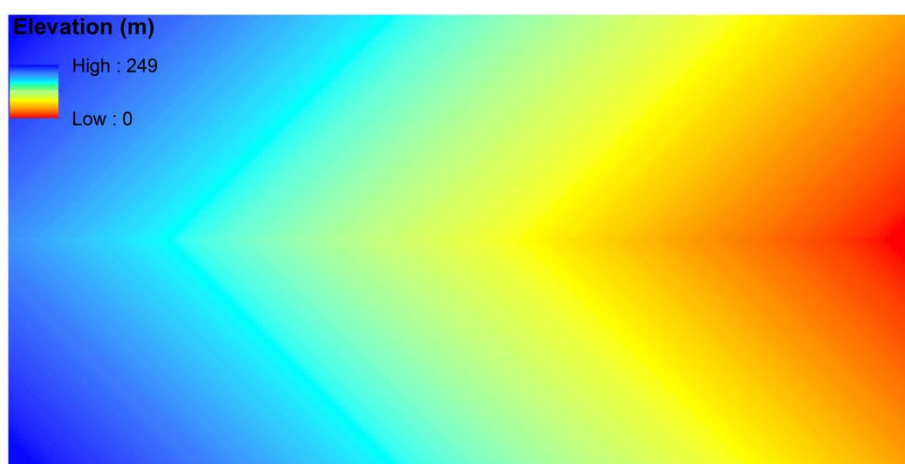


Figure 7.1 DEM of the designed simple catchment.

Table 7.1 Combination of different runs in first simulation.

Run No.	M value (vegetation cover %)	Daily Rainfall	Sediment size	Duration (days)
1	0.01(40-50%)	25mm	Coarse	300
2	0.01(40-50%)	25mm	Coarse	25,000
3	0.005 (0-10%)	25mm	Coarse	25,000
4	0.02 (90-100%)	25mm	Coarse	25,000
5	0.01(40-50%)	25mm	Fine	25,000

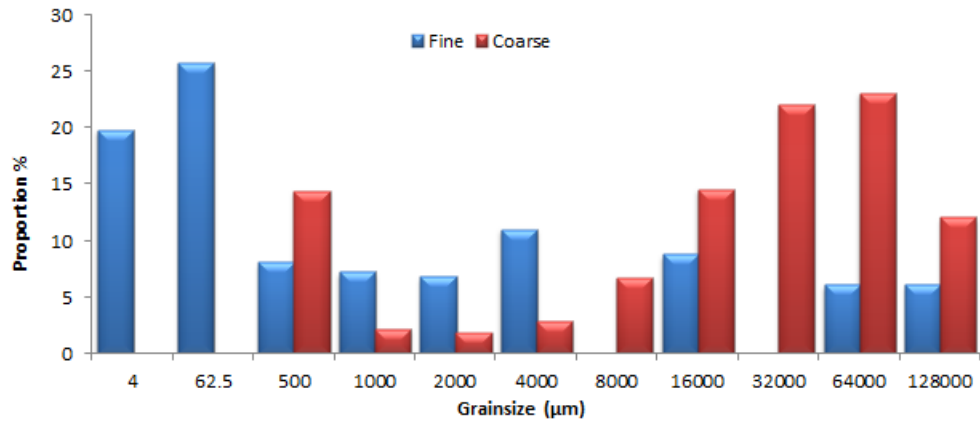


Figure 7.2 Sediment grain size distributions for run 1 to 4 (coarse sediment) and run 5 (fine sediment).

The second and third simulations utilised both modelled sediment yields and large palaeo-environmental data sets available for the Alresford and Holzmaar catchments over a period of 152 years and 5000 years, respectively. The Holzmaar catchment is a small Maar lake with well-preserved varve sediment that facilitates reconstruction of the palaeo-environment (Zolitschka, 1998; Zolitschka *et al.*, 2000). Human induced land use changes played an important role in sediment delivery in the past 5000 years (Litt and Stebich, 1999; Brauer *et al.*, 2001). The Alresford catchment is a groundwater dominated catchment (Sear *et al.*, 1999) with intensive agricultural activities (Monkhouse, 1964; Waller and Hamilton, 2000). Climate change, especially precipitation intensity and duration influence the storage of groundwater, which alters the runoff and sediment delivery in the catchment. Detailed description of these two catchments and the model setup can be found in Chapter 5 and Chapter 6. All the palaeo-environmental data sets were analysed and compared with modelled results in a phase diagram to try to find non-linear characteristics in complex river systems, and power-law distributions were calculated to find evidence for system self-organisation behaviour.

7.3 Results

7.3.1 Simple catchment

The result for the short term (300 days) simulation based on a simple rectangular catchment is displayed in Figure 7.3 with the temporal variation in daily sediment discharge. Daily total sediment discharge is high at the initial stage of landscape evolution, and gradually declines over a period of 50-100 days. The rate of sediment delivery declines after 100 days to the end of the simulation at 300 days. This pattern of sediment discharge with initial peak and tail off is also evidenced by similar numerical simulations of a small and simple basin (Coulthard and Van De Wiel, 2007) and explained as ‘spin up’ by Coulthard *et al.* (1998). From the first several days of simulation, the catchment generated a large amount of sediment in response to the sudden input of rainfall. With the material being eroded from high slope, catchment topography was gradually adjusted until an armour layer was developed on the channel bed. The lowered channel gradient reduced the energy available to transport the coarsening bed material resulting in less erosion and more deposition along the channel and its vicinity. Therefore, during the spin up period there should be no self-organisation because the system has not reached steady state or equilibrium. Outputs during the spin up period need to be removed from investigation of self-organisation in complex systems for all the following simulations. Simulations for 25000 days have been carried out for the simple catchment under the same initial conditions.

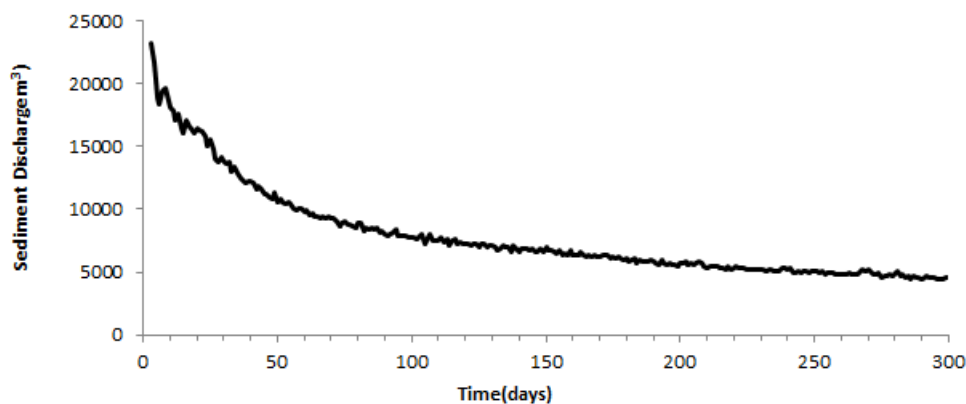


Figure 7.3 Simulated daily sediment discharge for 300 days.

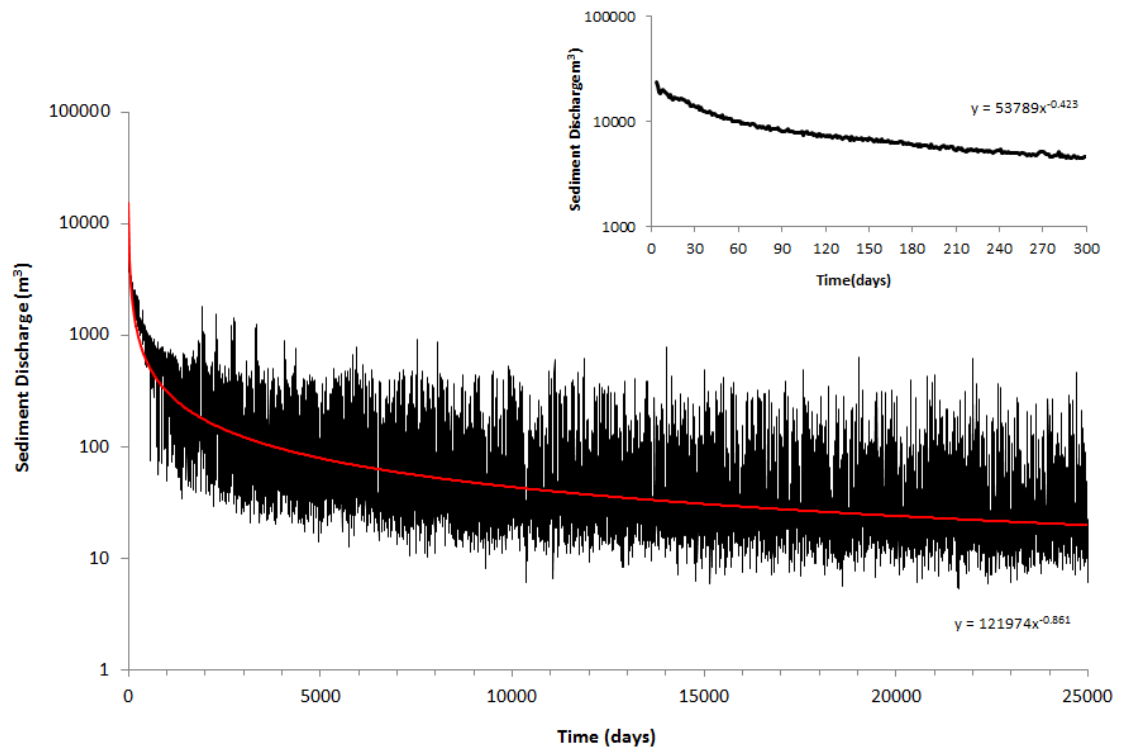


Figure 7.4 Simulated daily sediment discharge for 25,000 days. Insert graph shows the simulation for 300 days under same initial conditions, the vertical scale is recalculated for comparison. Red solid line is the smoothed trend of temporal sediment discharge.

Modelled daily sediment delivery over 25,000 days displays a similar pattern of decline as the shorter 300-day simulation (Figure 7.4, red line). However, the recession of sediment output has much larger variations with three or more orders of magnitude after approximately 800 days which is in contrast to the much smoother curve of sediment discharge over 300 days, even though the daily precipitation is constant. Simulated water discharge indicates regular temporal variation as an instant response to regular precipitation on an hourly scale as expected (Figure 7.5), whereas changes of sediment discharge over time amplify the variability with a high abnormal pattern on a day to day basis. Therefore, this non-linear fluctuation of sediment yields, showing a significant divergence from the homogeneity between rainfall and flow, is possibly a signal of system self-organisation. Consequently, flow increases downstream with a resulting gradual increase in channel width, as well as deposition along the channel from sediments eroded from upslope (Figure

7.6). The erosion and deposition are concentrated in the bottom of the valley and develop irregularly as an indication of non-linear response.

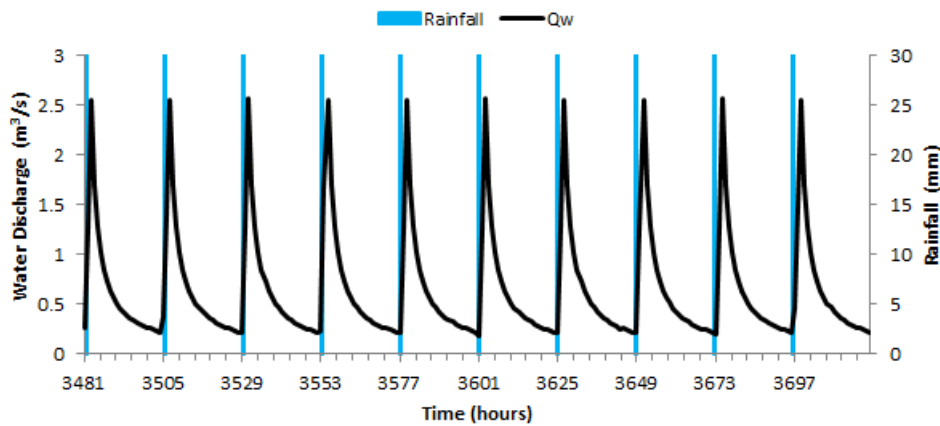


Figure 7.5 Regular hourly rainfall distribution and simulated water discharge.

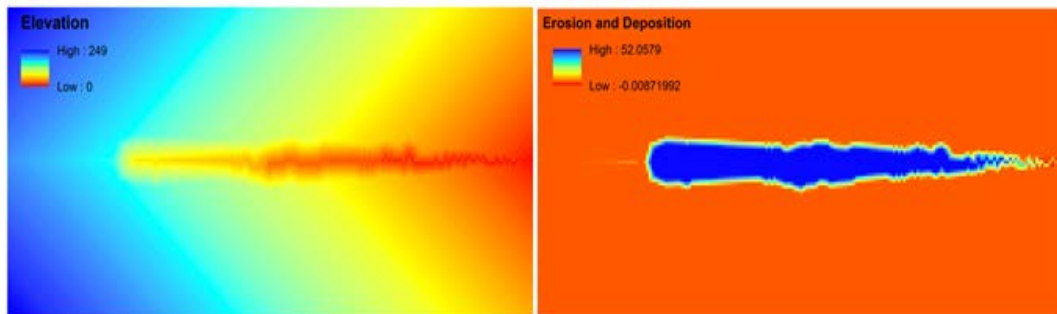


Figure 7.6 Spatial pattern of simulation after 25,000 days. Left: catchment elevation model; right: net erosion (positive value) and deposition (negative value) of catchment.

Different M values ($M=0.005$ and $M=0.02$) have been applied to the simulations to explore the potential impact of land use changes on sediment distribution. Sediment outputs from the three simulations with different M values exhibit a similar pattern of decreasing long term trend, despite different magnitude and variability in sediment outputs (Figure 7.7). Sediment yields vary over a wider range of magnitude with less forest cover ($M=0.005$). Additionally, more large erosion events are characterised for simulations in sparser vegetation cover. In the CAESAR model simulations, vegetation plays an important role, reducing flood size driven mainly by rainfall as well as moderating the rate of eroded materials from slopes. Accordingly, this may indicate that dense forest cover can help to reduce the variability of sediment yields, smoothing the unstable response of the channel bed.

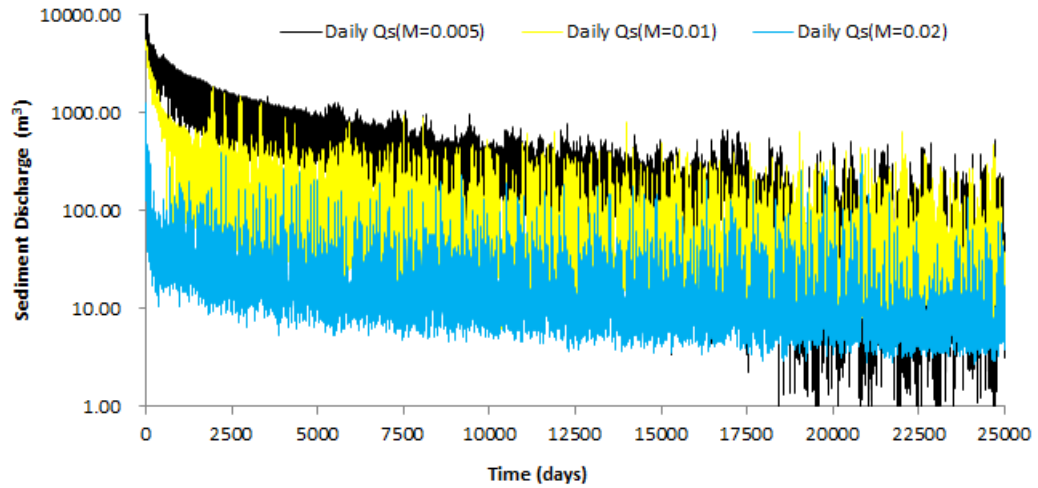


Figure 7.7 Simulated daily sediment discharge (Q_s) from different M values over 25,000 days.

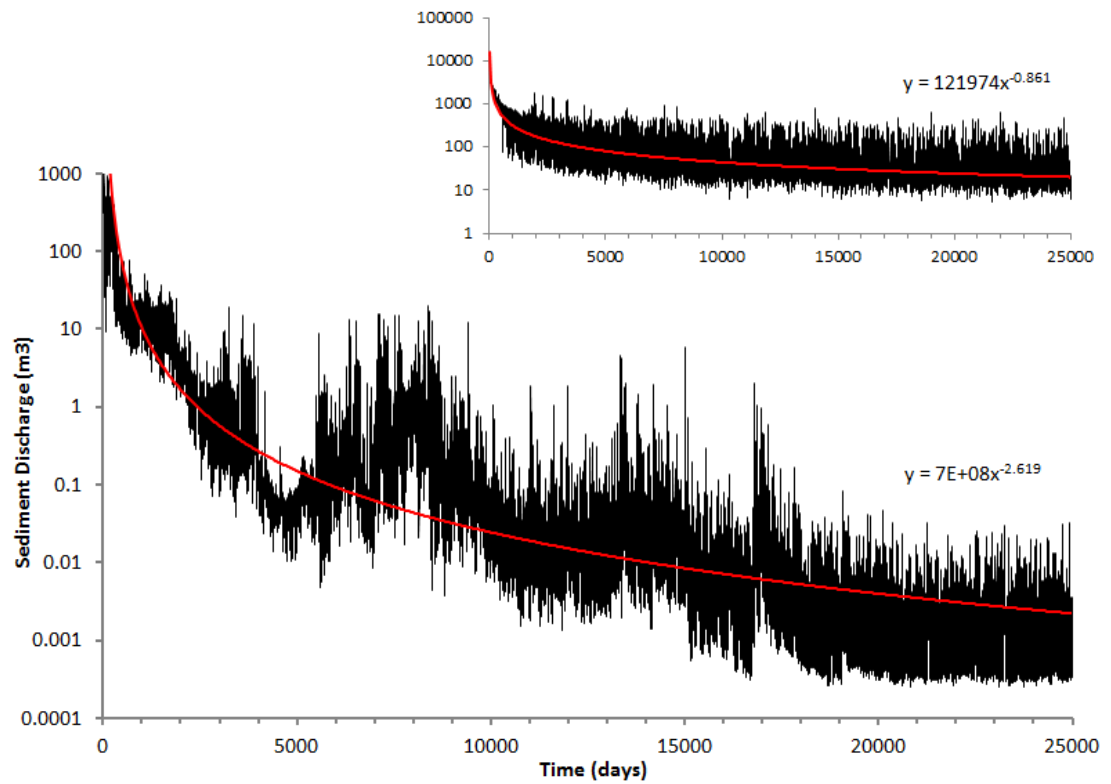


Figure 7.8 Simulated sediment discharges with alternative grain size distribution (finer) over 25,000 days. Inserted graph shows the simulation for original grain size distribution (coarser) under same initial conditions. Red solid lines are the smoothed trend of temporal sediment discharge.

Figure 7.8 suggests a notably different response to simulations with a finer grain size distribution of bedload, despite the same intensity of rainfall. A significant non-linearity occurs in sediment discharge, although a general declining trend of sediment production still exists. Daily total sediment yields are much lower than those revealed in simulations with coarser bedload, however the range of the sediment variability is extended to almost seven orders of the magnitude. In the initial ca.5000 days, the amount of sediment discharge drops quickly as a response to the development of an armour layer which is also observed in other simulations. During the period of approximately 5000 to 8000 days, sediment delivery has experienced a re-working process contributed to the supply of previously deposited sediments along the channel. After this period, sediment delivery decreases dramatically again as a result of sediment exhaustion. From ca.14, 000 days the sediment discharge variability is gradually reduced and the catchment starts to enter a period of relatively steady state. The shift in catchment behaviour from intense geomorphic activities to a stable channel indicates a grain-size driven propensity towards system non-linearity.

7.3.2 Holzmaar catchment

Previous discussion based on palaeoenvironmental records and modelling results from the Holzmaar catchment demonstrates complex and sensitive interactions between human activities in the landscape, climate change and landscape evolution (Figure 7.9). Compared to the relatively higher frequency and longer term changes in forest cover, precipitation change is less active during the Holocene, with the exception of the recent 500 years. The catchment behaves as a non-linear positive feedback system (Favis-Mortlock and Boardman, 1995), with irregular peaks in the sediment discharge which may be related to the movement and remobilisation of small 'slugs' of sediment downstream (Nicholas, 1995). Moreover, sediment discharge is increasing or decreasing in parallel with either successive NAP% increases and decreases when precipitation changes are minor (e.g. 2650-1900 cal. yr BP and 1850-1500 cal. yr BP) or with a combination of these two effects (e.g.450-0 cal. yr BP). However, system behaviour of erosion rate to precipitation and forest cover for individual years may vary notably from the overall pattern (see discussion in chapter 6) in a complex way.

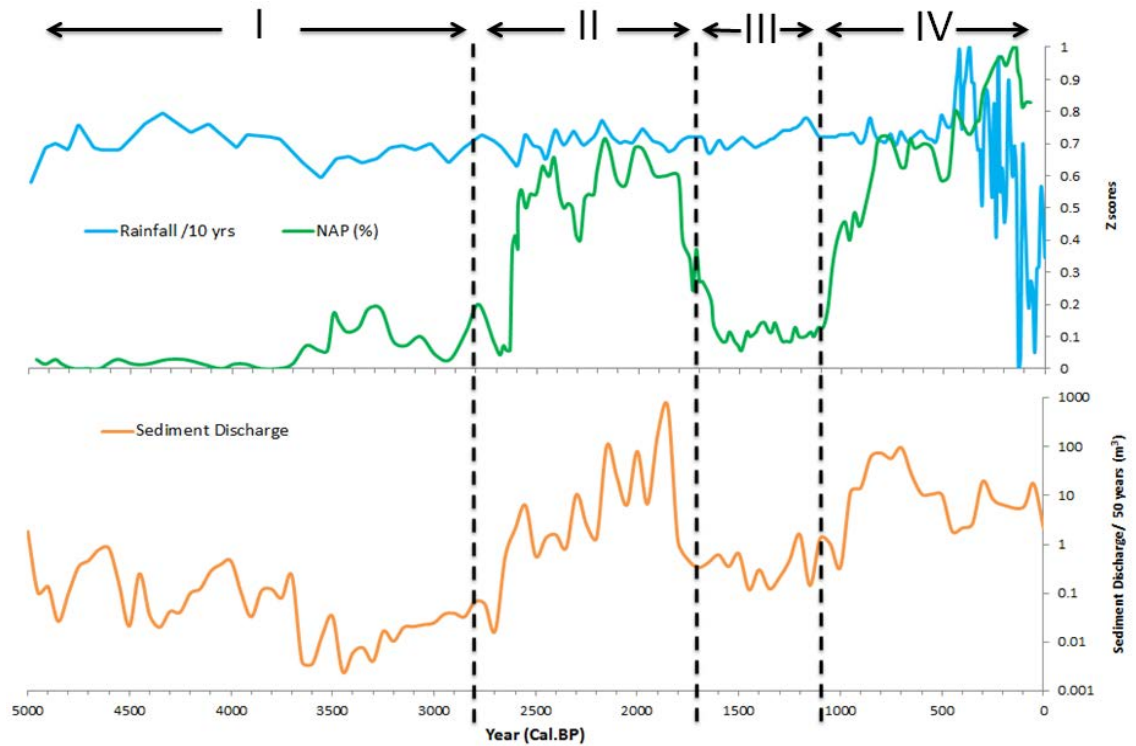


Figure 7.9 Comparison of simulated sediment discharge and rainfall and non-arboreal pollen (NAP %). The entire timescale is divided into four phases representing specific time periods in terms of variability in sediment yield.

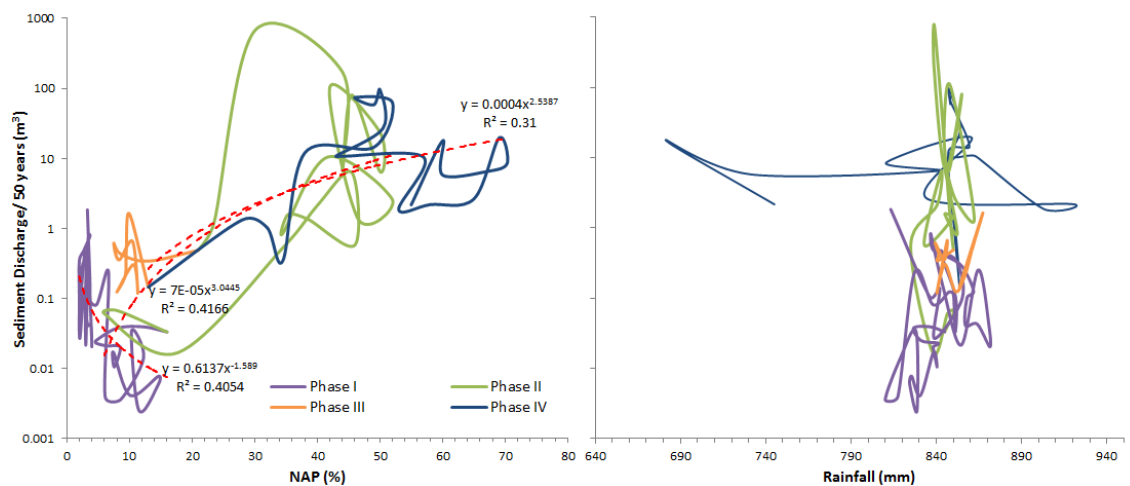


Figure 7.10 Bivariate plots for 4 phases (cal. yr BP). Phase I: ca.5000-2800; Phase II: ca.2800-1700; Phase III: ca.1700-1100 and Phase IV: ca.1100-0. Left: non-forest cover (NAP %) versus sediment discharge (QS); Right: Rainfall versus sediment discharge (QS). Red dotted lines are smoothed trend of sediment discharge for Phase II and IV.

In the interest of exploring the non-linear system behaviours in relation to both external and internal factors and their associations, bivariate log-normal plots have been used that are based on simulated sediment yield and the two main drivers, vegetation cover (expressed as pollen proxy, NAP%) and precipitation data, at 50-year time steps over the total 5000 years of landscape evolution. Distinctions may exist in erosion patterns during different periods according to Figure 7.9, thus modelled and proxy data have been divided into four phases of development. Figure 7.10 demonstrates significant differences in trajectories for sediment yield responses to land use and rainfall disturbances. The phase diagram of precipitation versus sediment discharge (Figure 7.10, right) displays little coherence in all time periods with no explicit trend or no organisation in phase time, which is an indication of strong non-linear dynamics in sediment yield in relation to climate changes (Dearing and Zolitschka, 1999). In contrast, the phase diagram of non-forest cover versus sediment discharge (Figure 7.10, left) displays an apparent trend and organisation within different time periods. The erosion shows strong insensitivities to the percentage of non-forest cover during two phases: Phase I and III, with random trajectories and fluctuations. A trend of weak negative correlation between sediment discharge and forest cover is even observed in the first phase. Furthermore, these two phases are in accordance with low variability in non-forest cover (2-16% of NAP) as shown in Figure 7.9. Therefore, the increase of sediment discharge in the absence of correlations to land use change may imply that low frequency fluctuation of land use change is not the major control of erosion in Holzmaar catchment for the periods of 5000-2800 cal. yr BP and 1700-1100 cal. yr BP (Dearing, 2008). The first significant shift of land use took place after ca.2800 cal. yr BP and lasted for approximately 1100 years until ca.1700 cal. yr BP, with a rapid increase of NAP from 10% to 50%. Accordingly, more sediment was delivered to the lake represented by increases of sediment discharge of up to 5 orders of magnitude. Similar to this positive trend, sediment response after ca.1100 cal. yr BP exhibits an irregular but generally increasing trajectory with the rising of NAP percentage. However, these two phases of marked land use disturbances suggest complex relationships with erosion pattern in terms of weak linear correlation ($r^2 = 0.42$ for phase II and $r^2 = 0.31$ for phase IV, respectively) and a large number of non-linear fluctuations in the bivariate plot. One possible explanation for the complexity in this river system is that land use change plays a direct and primary role in erosional processes. Climate and internal forcing

and the interaction of positive and negative feedback from system may contribute to the system dynamics as well (Dearing and Zolitschka, 1999).

7.3.3 Alresford catchment

Previous discussion about modelled sediment delivery pattern compared with palaeoenvironmental archives has revealed the interaction of climate and land use changes in Alresford catchment in the past 151 years (Chapter 5). More apparent fluctuations and higher values have been observed in simulated sediment discharge before the 1960s with several large peaks. After the 1960s, sediment behaviour displays a relative stable pattern with less variability. Therefore, the whole time scale was divided into two phases (before and after the year 1960) and sediment data were expressed as bivariate plots for exploring non-linear behaviour in erosion pattern.

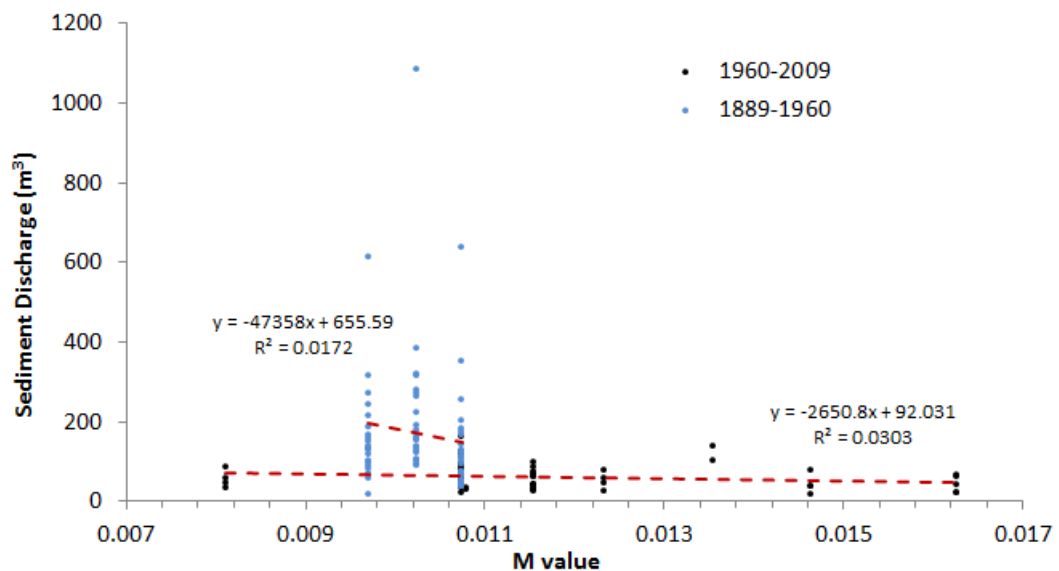


Figure 7.11 Relationship between vegetation cover (*M* value) and sediment discharge, showing in two phases (1889-1960 and 1960-2009). Red dotted lines are regression lines.

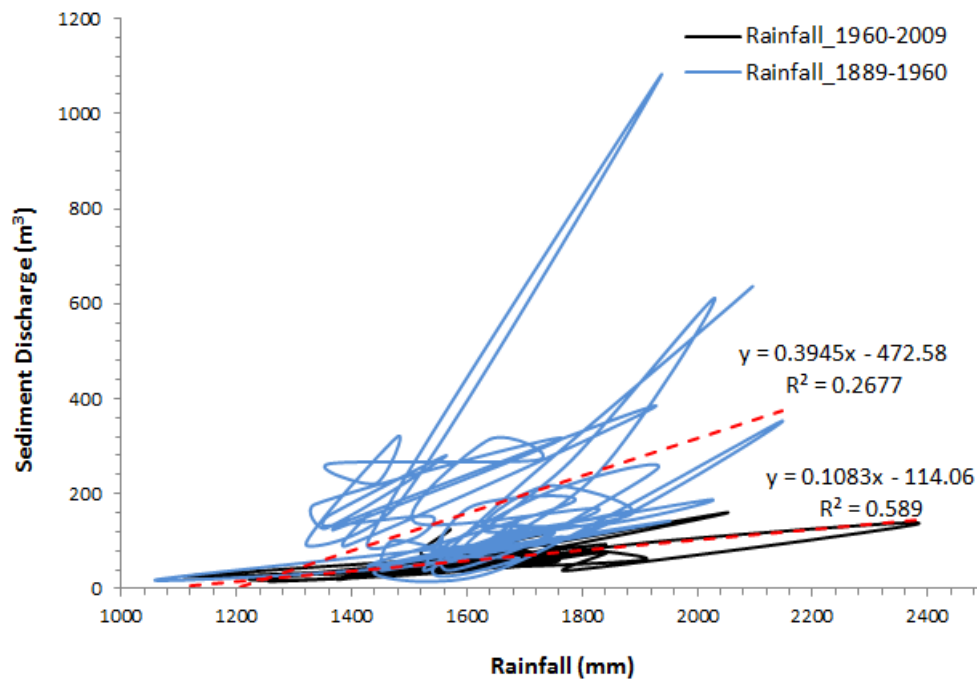


Figure 7.12 Relationship between precipitation and sediment discharge, showing in two phases (1889-1960 and 1960-2009). Red dotted lines are regression lines.

It is clear that there is little correlation between sediment discharge and vegetation cover, showing no positive trend and no organisation (Figure 7.11). For any given M value, sediment discharge can vary irregularly in different values which are indicative of non-linear relationship between sediment discharge and land use change. In the early phase (1889- 1960 AD), annual sediment discharge varies between 20 and 1100 m³ when M values change in a narrow range of 0.009-0.011. However, the variation in sediment discharge is lower and the catchment produced sediment less than 200 m³ every year in the period of 1960 -2009 even when the range of M values is extended from 0.008 to 0.016. The contribution of vegetation cover has less effect on sediment discharge in both phases.

Figure 7.12 exhibits a complex relationship between rainfall and sediment discharge. The early phase is represented by an increasing trend in response to rainfall disturbances. The trajectory starts from low values of sediment discharge and extends to high values rapidly, displaying a weak linear relationship between rainfall and sediment discharge. The correlation coefficient of the regression line is low and the data are scattered dispersive. After 1960, this relationship returns to the earlier low values, with a longer and narrower phase domain than the first phase. The linear

behaviour in sediment discharge is enhanced in the latter phase, its correlation coefficient (r^2) being 0.59, compared with 0.27 during 1889-1960. Although both phases show organisation in sediment behaviour, their positive relationships to rainfall are very weak (low r^2), with strong fluctuations and several irregular high values. Similar to Holzmaar, the system behaves in a complex way to environmental disturbances. But in the Alresford catchment, the contribution of rainfall intensity and amount has a more direct impact on the system dynamics.

7.4 Discussion

The famous sand-pile gravitational mass-movement experiment performed by Bak (1997) has revealed evidence for self-organised criticality (SOC), which is developed from the theory of complexity and non-linearity in natural open systems. Dynamic lake-catchment systems are intuitively good examples of non-linear behaviour (Sidorchuk, 2006), for which different factors and sources may participate qualitatively and quantitatively. Sediment movement, which is mainly triggered by flow movement in rills and gullies and is represented by sediment delivery rate, is a complicated environmental process with comparable features to the sand-pile example. Numerically models can be used to depict this complex process after validations. All the simulations based on three groups of scenarios display clear non-linear behaviour. The transformation between stabilisation and variation in erosion process and catchment evolution pattern give rise to the self-organisation behaviour.

7.4.1 Non-linear behaviour

7.4.1.1 Critical state / threshold

A critical state or threshold (the latter term typically applied in more ecology) can be simply defined as a change point of a system's behaviour in response to changes in different drivers (Phillips, 2003; Andersen *et al.*, 2009). When the force-resistance relationship in the dynamic fluvial system is upset due to, for example, a large rainfall event, sediment is entrained. With growing sediment load, the threshold of sediment transport capacity is exceeded, thus sediment accumulation causes a shift in catchment slope from upstream to downstream as well as in sediment discharge (Van De Wiel and Coulthard, 2010). Similarly, this self-adjustment of a fluvial system

occurs through erosion when the threshold of sediment transport capacity is increased. This critical state is displayed by the irregularities in sediment discharge through time in the three groups of simulations.

Thresholds in non-linear systems may be related to either internal factors (e.g. structure or dynamics of the fluvial system) or external factors (i.e. environmental changes) (Phillips, 2003). In the same daily rainfall scenario, changes in the magnitude of vegetation cover (run 2, run 3 and run 4 of the simple catchment simulations) show some effects on non-linearity of the catchment with changing sediment discharge. Sparse forest cover increases the total volume of sediment discharge with higher peaks. However, it also shows lower values after 18,000 days simulation when compared to the results from dense forest cover for the same time period. Its larger variation in sediment discharge is indicative of system instability in response to deforestation. It seems that systems with less forest cover are prone to evolve to a critical state that leads to a non-linear shift of erosion and deposition when forest cover is the main forcing. However, the impact of vegetation cover on non-linear dynamics may be limited to the catchment landform or rainfall since vegetation cover only alters the magnitude of sediment discharge and it has little effect on non-linear pattern and variability (as shown in Figure 7.7). The bivariate plot of simulated water and sediment discharge (Figure 7.13) demonstrates that sediment yield has little correlation with water discharge arising from regular precipitation. In a study exploring fluvial non-linearity in simple basins evolution, Coulthard and Van De Wiel (2007) simulated system behaviour by controlling possible drivers for non-linearity and SOC. They concluded that the magnitude of regular storm events is not a major control on variability of sediment yields. Inherent dynamics of the fluvial system play an important role in non-linear dynamics. Evidence can be detected from considerably different non-linear variability in sediment discharge when the simulation (run 5 of the simple catchment simulation) was initialised with fine grain size distribution, keeping the same inputs of rainfall, land cover and modelling duration as in run 2. It is clear that coarser material on the bed is more resistant to erosion than fine material, which is reflected in the higher erosional threshold in fluvial system with less sediment discharge to be produced. A system with a fine grain size has a quicker response to both external and internal factors and takes a longer time to reach dynamic equilibrium.

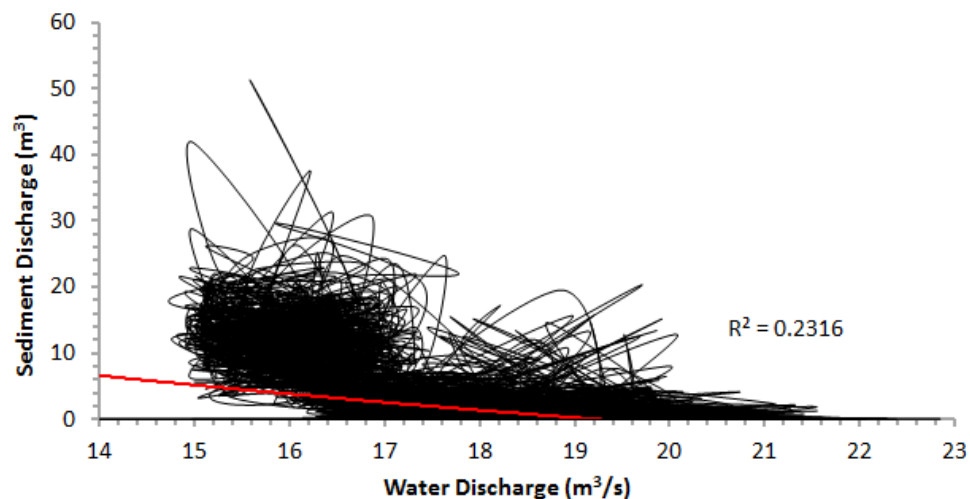


Figure 7.13 Relationship between water and sediment discharge for simple catchment over 25,000 days.

In contrast to the simple catchment, simulation of Holzmaar displays a relatively stronger impact of external drivers on sediment delivery (Figure 7.10). The correlation between sediment discharge and non-forest cover is better than the relationship between sediment discharge and precipitation, particularly in specific time series. This indicates a relatively stronger control of vegetation on soil erosion rather than control by precipitation. This obvious correlation occurs in two phases: 2800-1700 cal. yr BP and 1100-0 cal. yr BP that can be explained as the result of a series of large, rapid and irreversible human induced deforestation events (Leroy *et al.*, 2000; Litt *et al.*, 2009). When external disturbances like human activities exceed internal resistance, it is possible for systems to be forced to make major shifts from one state into another state. Therefore, external thresholds are the main sources of dynamic non-linearity for Holzmaar catchment.

7.4.1.2 Feedback

In natural fluvial systems, feedback can be related to erosion processes, whereby system state may change in response to disturbances. Positive and negative feedbacks are associated with soil erosion and deposition within a catchment, respectively. The interaction of positive and negative feedback is important in the formation of spatial and temporal patterns in landscape evolution (Favis-Mortlock *et al.*, 2004). Taking the simple catchment as an example, the formation of a channel in

the central part of the catchment (Figure 7.6) is a direct result of positive feedback of sediment movement by enhancing elevation difference. Simultaneously, negative feedback in the form of deposition of coarse sediment shapes the channel, thus keeping a non-linear balance in catchment morphology. Since floods and land cover are regular in the simple catchment simulations, the irregular sediment discharge may be attributed to the non-linear feedbacks between sediment movement and deposition.

For real lake-catchment systems, this dynamic equilibrium based on feedbacks is more complicated. For instance, the bivariate relationship between rainfall intensity and sediment discharge in Alresford catchment (Figure 7.12) displays a weak linear relationship, but it involves a large degree of data scatter, with non-linear step changes or thresholds. Figure 7.14, which combines the normalised rainfall and sediment discharge data, also suggests both linear and non-linear behaviour in catchment response. It appears that increases in precipitation would lead to increased sediment delivery, but a large flood event does not always result in large sediment erosion. Meanwhile, disproportionately large amounts of sediment may be generated from low stream power. Sediment discharge reaches high values when experiencing a series of small floods followed by a large storm event. Since small stream power generates minor sediment transport events that may store sediment in the catchment before flowing into lakes. When a large flood occurs, greater supply of sediment is produced from remobilisation and dispersal of sediment from pre-existing deposits. Sediment supply would be reduced after large flooding events, further increases in rainfall have little impact on sediment delivery due to sediment exhaustion from previous erosion and this process may last until sediment storage recovers. Therefore, the effect of slope-channel coupling that either delivers sediment to the lake or form an armour layer on the bed (Emmett and Wolman, 2001), and the temporary build-up of sediment stored in the channel, are vital for catchment responses to external factors (Phillips, 2003). Newson (1980) found different geomorphic effectiveness of two floods with peak discharges of similar return periods. Furthermore, sediment transport and storage in fluvial systems are associated with the nature of landscape system, as an event will alter the landform and the relative persistence of the altered landform under the disturbance of erosional processes (Miller, 1990). As a groundwater driven catchment (Alresford catchment), the balance between

infiltration and runoff generation also depends on the soil moisture, groundwater storage, soil porosity, which is unstable in the system (Phillips, 1992b). Non-linear responses in sediment discharge can be produced by the combination of these processes.

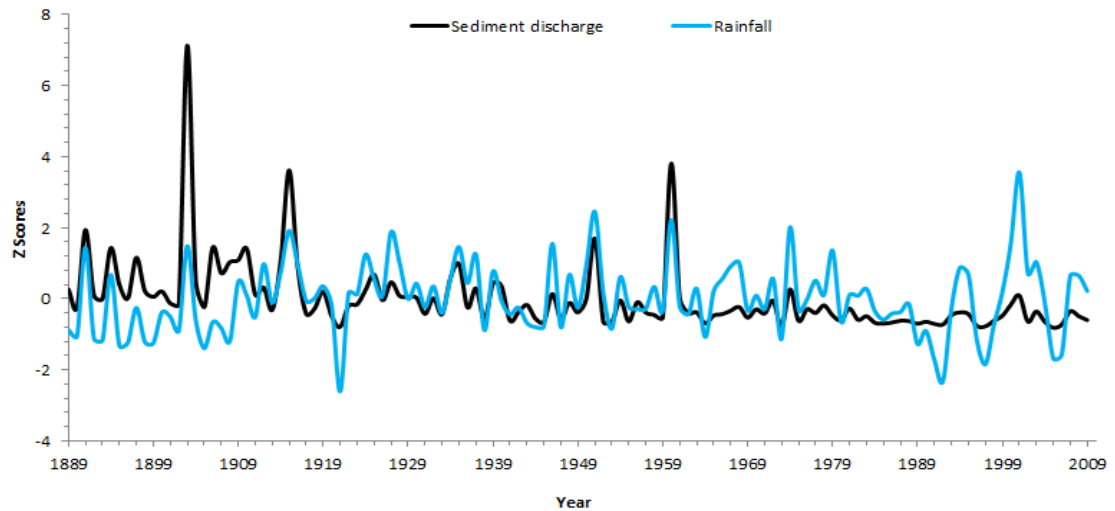


Figure 7.14 Comparison between simulated sediment discharge and rainfall in Alresford catchment.

7.4.2 Self-organisation behaviour

Self-organisation occurs in the evolution of a complex fluvial system due to the formation of patterns that are derived from the gradual aggregation of landscape elements; this is driven mainly by configurations of internal dynamics of the system itself, independently of external controls (Bolliger *et al.*, 2003). Therefore, it is generally regarded as a possible source of non-linearity in natural system (Phillips, 2003). Temporal behaviour of self-organisation to a critical state can be manifested by the presence of power-law relationships between the frequency of a phenomenon and its magnitude (Bak, 1997; Sidorchuk, 2006). The power laws obey the basic rule that specifies a few large events and many small events in the form of log-log size distribution graph (Fonstad and Marcu, 2003), and they normally display a heavy-tailed distribution pattern (Stumpf and Porter, 2012).

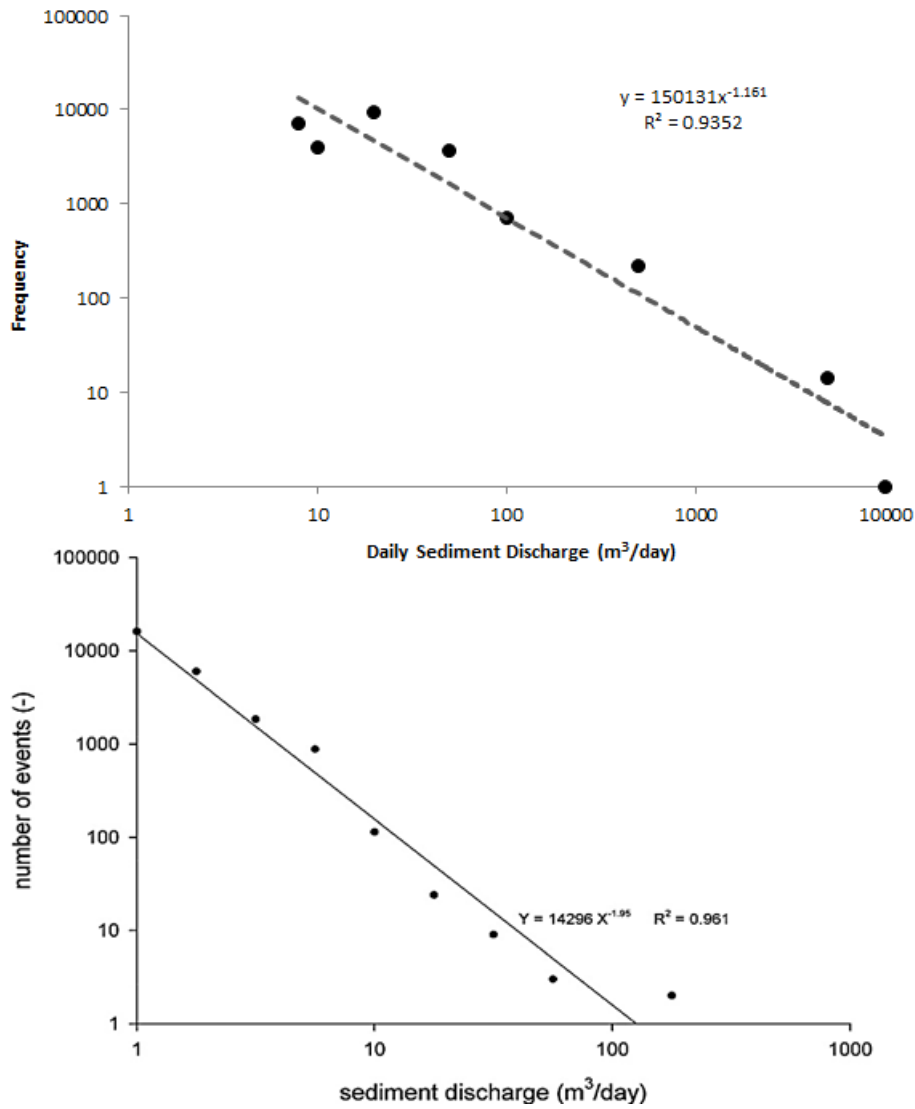


Figure 7.15 Magnitude-frequency distribution of modelled sediment discharge for the simple catchment (upper) and the simulation from Coulthard and Van De Wiel (lower, 2007).

For the simple catchment simulation under regular rainfall, the power-law relationship (Figure 7.15) is very pronounced ($r^2 = 0.94$), which is consistent with the expectation of self-organisation (after spin up period) when the system is separated from the impact of external factors of environmental change. Similar studies from Coulthard and Van De Wiel (2007) and Van De Wiel and Coulthard (2010) also display a power law distribution of sediment discharge though their simulations have a different slope and intercept due to differences in model parameterisation. The simple catchment is a self-organised system with alternate feedbacks of sediment mass movement and storage, and thresholds dominated by internal dynamics (as

discussed above) for the whole evolution process. De Boer (2001) used a cellular model to simulate the evolution of a simple fluvial system by applying rainfall to a square grid with cells of random elevations and at a random location within the grid. Results from the modelling also demonstrate that the sediment dynamics of a simple basin arise from self-organisation and are an emergent property of the system itself. These studies suggest that self-organisation is an important property of fluvial erosion processes. Therefore, do natural catchment systems with different landforms, which experience variable external and internal impacts, exhibit self-organisation?

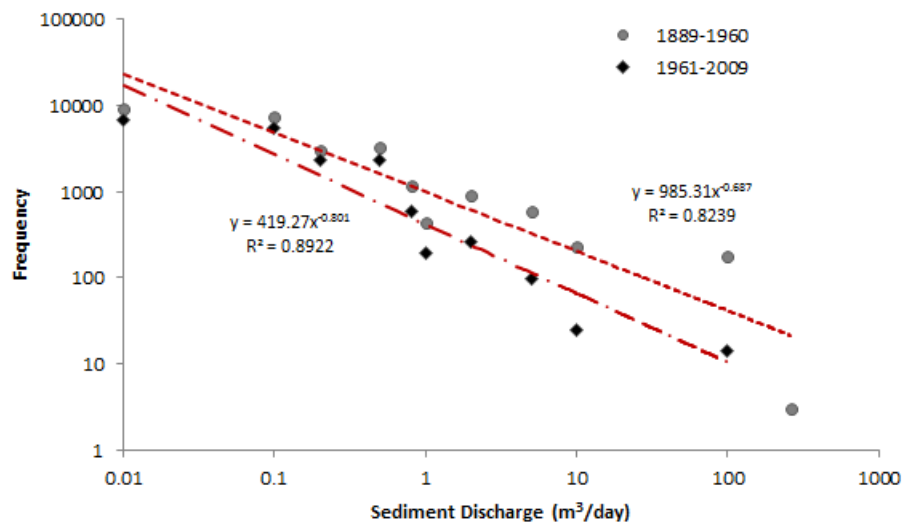


Figure 7.16 Magnitude-frequency distribution of sediment discharge for Alresford catchment in two time phases: 1889-1960 and 1961-2009.

For Alresford catchment, both phases display explicit power law relationships (Figure 7.16), although with varying degrees of scatter (after the spin up period). It appears that attributes of self-organisation exist in the Alresford catchment. As discussed above, sediment transport capacity in Alresford catchment is dominated by the hydrological properties of runoff, which is closely related to the groundwater storage, soil properties and system dynamics, besides the amount and intensity of precipitation. There is a difference in the sediment discharge distribution between these two phases, with a stronger power law relationship being observed in the second phase (1961-2009). It appears that the system organises itself into a relatively stable state with diminished erosion following a period of more active geomorphic processes. This suggests that self-organisation may behave via energy dissipation in

systems contributing to the complex non-linear dynamics (Huggett, 1988; Ibañez *et al.*, 1994).

The power law relationship in the Holzmaar catchment manifests a notable difference in self-organisation attributes for four time slices (after spin up period; Figure 7.17). It is suggested that a power law should display a nearly linear relationship on a log-log plot with exponents lying between 0 and -2 (Bak, 1997) and cover at least two orders of magnitude in both axis (Stumpf and Porter, 2012). Two phases, 5000-2800 cal. yr BP (Phase I) and 1700-1100 cal. yr BP (Phase III), show a dominance of small and medium magnitude events indicating the evidence of self-organisation. In contrast, other two periods 2800-1700 cal. yr BP (Phase II) and 1100-0 cal. yr BP (Phase IV) show a weak or no power law relationship. Obviously, Phase II and Phase IV have more large magnitude events than medium magnitude events, although small size events are still dominant. Moreover, their frequencies of occurrence are within two orders of magnitude.

Bivariate plot analysis (Figure 7.10) has revealed the prevailing influence of land use change on sediment delivery. The occurrence of self-organization behaviours corresponds with periods of relatively low magnitude ($NAP\% < 20\%$) and less variation in forest cover. The earliest phase is prior to the period of intensive human settlement and rapid deforestation, and the phase III is after the period of sharp rise in non- arboreal pollen from approximately 2800 cal. yr BP to 1700 cal. yr BP. It seems that the self-organised system is prone to evolve under a natural steady-state with little interference from major climate change or human activities (Dearing and Zolitschka, 1999). In a self-organised system, fluvial processes are dominated by system inherent dynamics, for example erosion-deposition feedbacks and system reorganisation. Furthermore, the existence of SOC in the Holzmaar system is in accordance with the finding from the similar study of Holzmaar by Dearing and Zolitschka (1999). They made the frequency distribution curve for the period of 3000-10,000 cal. yr BP, prior to major environmental disturbance, and demonstrated the curve showing a positive skewed distribution and inverse power functions as evidence for SOC. However, they did not discuss the existence of SOC in time series of 1700-1100 cal. yr BP (phase III). In the current study, phase III has a strong power law relationship with an exponent of -0.4. This demonstrates that the catchment was

evolved to an energy dissipative dynamic system through self-organisation processes (Gomez *et al.*, 2002; Coulthard and Van De Wiel, 2007). Inherent soil exhaustion from previous major erosion in combination with afforestation and inactive climate change produced a sudden shift of the system state with self-organisation behaviour.

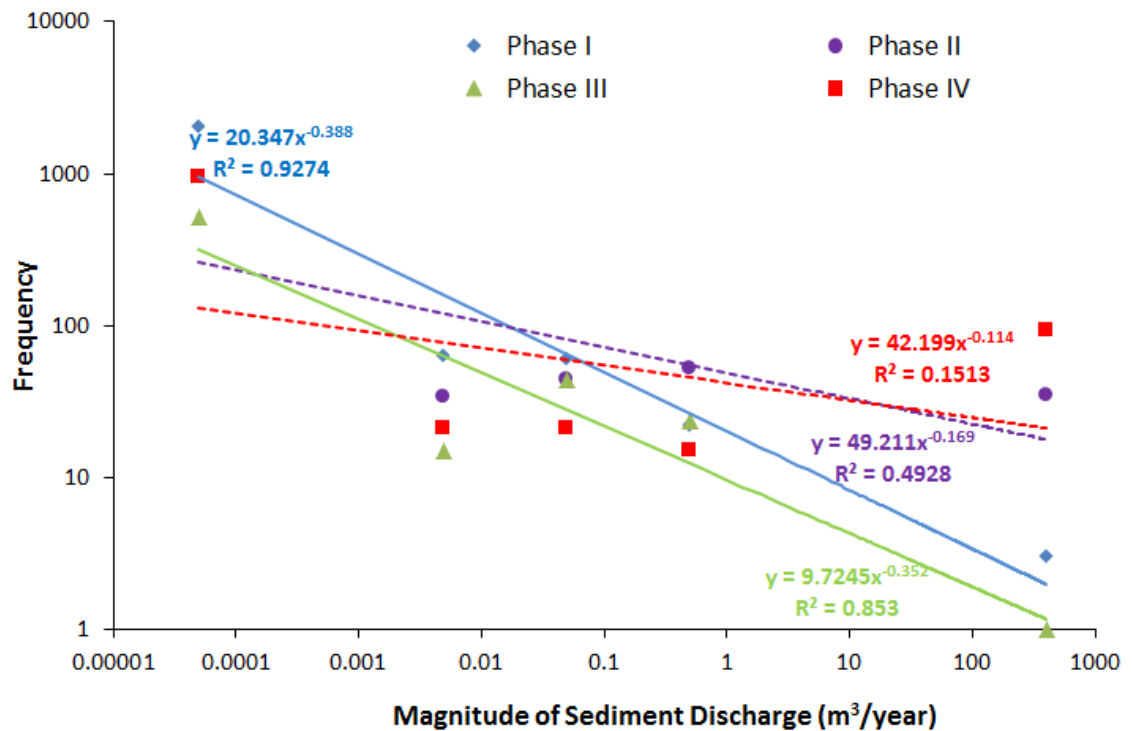


Figure 7.17 Magnitude-frequency distribution of modelled sediment discharge for Holzmaar catchment in four time phases: Phase I: ca.5000-2800 cal. yr BP; Phase II: ca.2800-1700 cal. yr BP; Phase III: ca.1700-1100 and Phase IV: ca.1100-0 cal. yr BP.

In general, self-organisation behaviour is most significant and sustained in the whole evolution of a simple catchment when the catchment is governed by intrinsic factors with little or no external forcing. Compared with the simple system, the Alresford catchment is under the control of rainfall, but it also shows the characteristics of self-organisation in both phases. It is possible that chalk properties of groundwater storage and supply for runoff, soil properties and energy dissipation, have stronger effects on changes in sediment discharge and consequent alterations in system state. In contrast, variations in sediment discharge in Holzmaar are closely related to forest cover changes. Overall, the evidence of self-organisation can be found in two

conditions, that is, when climate and land use changes are show less variability or when the system is out of erosional energy after large erosion events.

7.5 Summary

- (1) All the simulations discussed show characteristics of both linearity and non-linearity and their interrelationships, as seen by analysing system behaviour through bivariate phase diagrams. Evidence lies in the existence of thresholds with considerably irregular fluctuations in sediment discharge and is seen from a simple catchment to real landscapes and from 300 days to 5000 years of evolution.
- (2) The variability in sediment discharge may result from external change (e.g. climate changes and human impact) that is internally processed in highly complex fluvial systems. For simple catchments, changes of rainfall and land use have an effect on the magnitude of sediment discharge. However they have little influence on non-linear performances, which indicates the important role of inherent dynamics in systems. When external forces are large enough (e.g. Holzmaar simulation), systems may experience major shifts from one state to another state.
- (3) In the erosion process, the interaction of positive and negative feedbacks (e.g. sediment mass storage and delivery, time lags of system response to environmental forces and system landforms) are crucial in the formation of river drainage network and catchment dynamic evolution.
- (4) Analysing power law relationships between magnitude and frequency indicates that self-organisation exists in all simulations but is manifested differently. Self-organisation behaviour is significant and sustained in the whole evolution of the simple catchment and in the first phase of Holzmaar simulation in the absence of climate change and human impact. Self-organisation also appears at different landscape evolution stages and phases depending on a combination of erosion intensity, cascading mechanism, environmental disturbances (e.g. Alresford simulation and phase III in Holzmaar simulation) in complex system.
- (5) The three types of simulation show different patterns of sediment delivery and system states in a land-use forced system (Holzmaar), a climate forced system (Alresford) and a simple system with few little external disturbances. System

landforms, slopes, drainage networks, external environmental drivers, time scales etc. are all of importance in landscape evolution. The fluvial system responds to these initial conditions and their interactions in a complex and non-linear way.

- (6) The identification of non-linear responses has considerable implications for our understanding of the nature of fluvial systems. However, self-organisation and non-linear processes make it difficult to predict system behaviour in response to external conditions. However, studying the fluvial dynamics in the light of non-linearity theory offers the potential of understanding critical states in a system. Knowing a system is evolving towards a threshold and is unstable to environmental disturbance in the future can enable us to be aware of risks and make proper management.

Chapter 8

Testing a modelling approach to simulate hydro-geomorphological processes based on future climate scenarios

8.1 Introduction

Over the past decades, a perception has arisen that Europe is in a period of increasing hazard of flooding and drought. In the UK, widespread recorded events include several droughts, especially summer droughts, resulting from hydrological seasonality in the 1990s and in 2003 (Marsh and Monkhouse, 1993; Fowler *et al.*, 2004; Beniston, 2004), the wettest autumn and winter of 2000/2001 on record back to 1766 in England and Wales (Alexander and Jones, 2001) and flash flooding in the spring of 2004 and in the summer of 2007 (Wilby *et al.*, 2008). These hydrological events are generally described as due to precipitation extremes that are increasing under global warming (Pall *et al.*, 2011). The pursuit of energy and economic prosperity has changed the concentration of carbon dioxide (greenhouse gas) in the lower atmosphere after the industrial revolution. Global mean surface-air temperature is now 0.74°C (0.56-0.92 °C) warmer than the beginning of the century, with a warming trend of $0.13 \pm 0.03^\circ\text{C}$ in the last 50 years (IPCC, 2007). There is also a shift toward increasing global averaged precipitation resulting from the intensification of hydrological cycle with anthropogenic global warming (Osborn and Hulme, 2002). Many studies of observed and instrumental data for the UK suggest stronger hydrological seasonality, resulting in warmer and wetter winters with increased total winter precipitation, more wet days in western UK and increased frequency of rainfall extremes (Harris *et al.*, 2012; Osborn and Hulme, 2002). These studies also reported hotter and drier summers with declined total summer precipitation between 10% and 40%, in combination with fewer wet days.

In turn, climate change is likely to exert pressures on the global water cycle such as rising magnitude and frequency of flood events and associated damage to, for

example, agriculture and ecosystems. Similarly, hydrological changes would influence both surface water and groundwater resources for domestic and industrial demands. There is evidence of a substantial increase in the frequency of great floods in the last 50 years (Milly *et al.*, 2002) which may cause fluvial drainage defences, road surfaces and dam spillways to fail (Jones and Reid, 2001). In the UK, southern areas where groundwater is the main source to streams and rivers, especially in regression periods (e.g. spring and summer), are susceptible to the reduction in groundwater levels and surface flows due to prolonged dry records and high temperatures. As a consequence, land use and agricultural activities, such as irrigation, that require groundwater from aquifers could be affected significantly by climate change in these areas (Brouyère *et al.*, 2004).

Along with climate change, land use change due to human activities can alter groundwater storage as well as the volume and path of surface runoff, thus playing an important role in environmental sustainability. Some studies indicate average decreases of the agricultural area by about 13% over the past 50 years in the whole Europe (FAO, 2003; Rounsevell *et al.*, 2003). Reynard *et al.* (2001) estimated a 47% increase in the 50-year peak daily flow when a tripling of the urban area was applied in simulations of the Thames catchment. Although there is little evidence that local land cover can amplify or dampen climate driven changes to downstream flooding directly (Hiscock *et al.*, 2001; Lane, 2002; Wilby *et al.*, 2008), the lower precipitation and warmer surface in summer may cause the land surface to become drier. Thus changes in vegetated area and plant type can alter the soil erodibility (Loáiciga, 2003). Furthermore, flood events that are triggered by both climate variability and land use/cover change will affect soil stability within river basins by intensification of soil erosion. Their impacts on fluvial systems have been summarised by Coulthard *et al.* (2012) as channel incision and aggradation which may lead to dynamic changes of channel pattern, structural damage, increased concentration of fine sediment and contaminants in downstream areas and associated habitat changes. Therefore, predicting the possible occurrence of flood events under climate and land use change scenarios is essential for understanding and investigating the spatial and temporal patterns of soil erosion and deposition as well as their further changes and distributions over the next 50-100 years.

Many studies have used numerical models running under different environmental conditions to investigate climate changes with and without anthropogenic drivers (Pall *et al.*, 2011). Meanwhile, models are confirmed as useful tools to quantify the impacts of climate change on river flows, water resources and flood risks. Soil erosion models (e.g. the landscape evolution model CAESAR) that utilise scenarios of different climate projections in association with land use controls have become increasingly important in the assessment of geomorphic responses to potential future environmental changes. Two kinds of model, global climate models (GCMs) and downscaled regional climate models (RCMs) are widely used for studies of future climate change. In contrast to the coarse horizontal resolution of GCMs, RCMs that are driven by initial and boundary conditions provided by GCMs have an improved resolution of 50 km, making possible representation of sub-grid variability (e.g. small-scale topography and land use) and improved simulation of local-scale atmospheric processes (Madsen *et al.*, 2012; Roosmalen *et al.*, 2011). Jones and Reid (2001) analysed the results from a regional climate model for a future scenario of enhanced greenhouse emission by both quantile (Karl and Knight, 1998; Osborn *et al.*, 2000) and return periods (Fowler and Hennessy, 1995) analysis to explore changes in precipitation extremes in Britain. They showed an increase in heavy rainfall events with a higher likelihood of the heaviest events to emerge during the winter season in southern England. Wilby *et al.* (2006) used an integrated modelling approach to predict future water resource and quality under climate change impact and indicated a potential flood risk with increases in winter flow by approximately 10% for the 2050s and 2080s and reductions in summer and autumn flows in the 2080s by approximately 20% and 50%, respectively. Jackson *et al.* (2011) simulated the groundwater resource of a chalk catchment in southern England for the 2080s by applying climate change factors derived from an ensemble of GCMs under a medium-high emission scenario. Their projections suggest a reduction in annual potential groundwater recharge over the whole area and a greater seasonal variation with higher recharge rate in winter. In order to meet the requirement for climate models and scenarios with higher spatial resolution for hydro-climatological assessment, researchers have used different approaches to downscale both GCMs and RCMs information (Kilsby *et al.*, 2007; Semenov, 2007; Schmidli *et al.*, 2007; Maraun *et al.*, 2010). The latest UK Climate Projections 2009 (UKCP09) produce probabilistic projections of future climate based on an ensemble of the Met Office

HadCM3 climate model by running a perturbed physics experiment, with a spatial resolution of 25 km and a daily time solution (Jones *et al.*, 2011; Harris *et al.*, 2012; Murphy *et al.*, 2009). They indicate that both mean daily maximum and minimum temperature will rise everywhere in the UK over the year by the 2080s. This is coupled with a wet winter and dry summer in the south of England and decreases in precipitation in parts of the Scottish Highlands. Assessment of water resources based on UKCP09 climate scenarios demonstrated a reduction in mean annual flow over most of the UK with a more significant decline in summer flows (Christierson *et al.*, 2011).

There are fewer studies on future land use change in comparison with climate change projections and most have focused on the changes of agricultural land use under climate changes scenarios. Forest recovery policy has been encouraged worldwide. However, expansion of forest may not be reflected immediately due to the slow growth rate of trees (Rounsevell *et al.*, 2006). Therefore, changes in forest lands of today may continue into the future until the 2080s. Assessment of future agricultural land use is more complicated as it depends on different drivers, such as population and economic pressure and associated food demand; technology development and farming intensity; rural development policy; environment policy and the soil property itself (Ewert *et al.*, 2005; Rounsevell *et al.*, 2006; Haygarth and Ritz, 2009). Land abandonment was suggested by Verburg *et al.* (2006) as a potential land use change in Europe. However, according to a MAFF (2000) report, arable production may increase by 20-30% in the 2080s and crops may be produced at higher altitudes in the UK in association with a greater possibility of soil erosion. Other researchers suggest an increase in agricultural demand by 25–180% by the 2050s (Henriques *et al.*, 2008; Johnson *et al.*, 2009).

These these environmental changes may influence the frequency and magnitude of soil erosion through a variety of ways, such as the combination of erosive power of rainfall and increased soil erodibility (Mullan *et al.*, 2012). The current study aims to evaluate the impact of future climate variability and land use change of the Alresford catchment, UK, using an integrated modelling approach. Probabilistic precipitation data (up to 2099 under three future CO₂ emission scenarios from UKCP09) were used to drive the landscape evolution model CAESAR and to simulate hydrological

and geomorphic response in fluvial systems to projected changes. Modelling results were analysed and compared with current discharge of flow and sediment in the Alresford catchment during the baseline time series (1961-1990) to assess future potential flood and soil erosion risks.

8.2 Model setup

Probabilistic projections of soil erosion in Alresford pond catchment based on future climate and land use change were implemented by using the CAESAR model. The major input files used in these simulations were 90 year (2010-2099) precipitation series derived from UKCP09 climatic scenarios. Nine groups of monthly mean precipitation data in terms of three emission scenarios and three probability levels were converted into hourly rainfall input files based on baseline (1961-1990) series as described in the Methodology chapter.

The other input file is the future land use data in the form of constant hourly M value, which was generated for three scenarios. The first scenario is on the assumption of no change of land use in the future. M values are identical to the value of 2009, which has been used in Chapter 5, named 'original'. The second scenario was referred to as 'clear' when M values were reduced by ~20% during the entire period of 2010-2099, indicating more intensive agricultural activities in the area. The third 'forest' scenario was generated by increasing M values of ~20% for forest recovery throughout the whole future period. These three land use scenarios were combined with 9 precipitation scenarios, consisting of 27 simulations in CAESAR for the purpose of quantifying the effect of forest cover and climate change on sediment delivery in the following 90 years.

Previous outputs of bedrock and grain size distribution from simulations in Chapter 5 were used as input files for projections as an appropriate landscape setting. All these simulations started from 1961 and lasted 139 years to 2099, and included a 30-year spin-up period. Modelling results of sediment (m^3) and water discharge (m^3/s) for 2010-2099 were extracted from the entire time series for further analysis (Figure 8.1).

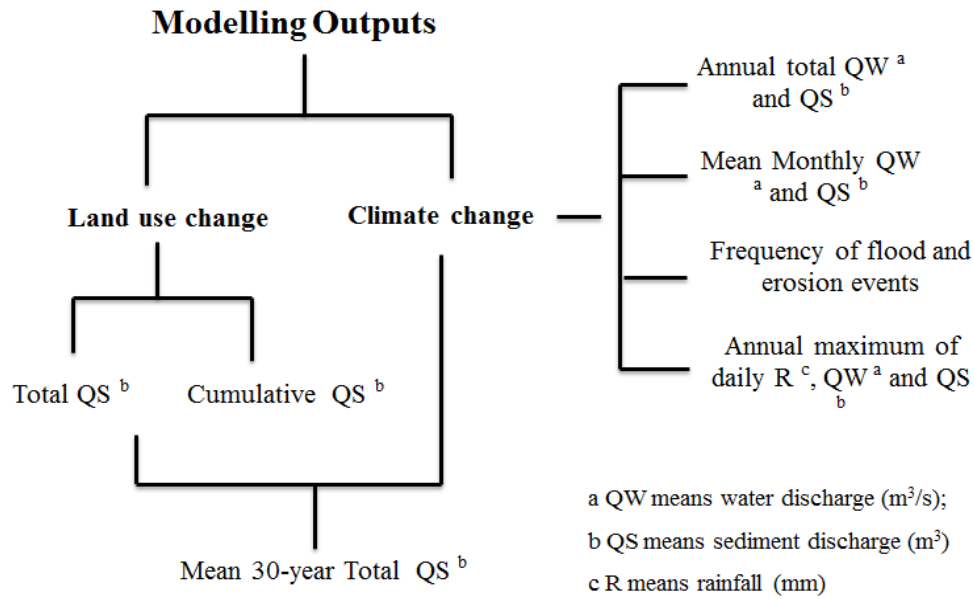


Figure 8.1 Flow chart of modelling results analysis.

8.3 Results and interpretations

8.3.1 Catchment response to future climate change

Estimation of changes in the 30-year mean annual and monthly river flow and sediment delivery by the 2020s, 2050s and 2080s based on the UKCP09 scenarios have been routed through the CAESAR model. Modelling results are regrouped and sorted out in terms of the probability levels, emission scenarios and time series before being compared to observations from the baseline period (1961-1990) time series in the following sections. The three probability levels provide a range of possible climate changes that can make robust estimates of the variability of flow and sediment discharge (Jenkins *et al.*, 2009; Christerson *et al.*, 2012).

8.3.1.1 Annual changes in water and sediment discharge

Box plots (Figure 8.2) illustrate the modelled river flow response to the full range of climate projections for baseline and future time slices under three emission scenarios. Results show a trend of slightly increasing projected future runoff over time at 50% and 90% probability level under each scenario. There is a stronger increasing trend in annual river flow at the 90% probability level with a higher emission scenario and

for the later period. Compared to baseline flow, water discharge could increase by up to 66% for the 2080s (2079-2099) high emission scenario and by at least 30% even under low emissions. At median level (50% probability), the pattern of change is similar but weaker, with 5% to 10% increases in the future. Where differences are suggested between three emission scenarios by median results, for example, the water discharge for the 2020s (2010-2039) the high emission value is lower than that for the low emission at the same periods, the magnitude of changes is small and all the runoffs are slightly higher than baseline values. In contrast, simulated mean annual changes in water discharge at the very unlikely condition (10% probability) range from -20% to -15% when compared to baseline periods. Results also show little difference between the three emission scenarios. The spread of changes is greatest in the 2080s period under high emissions and lowest for the 2020s low emission scenario. Regarding all the future projections, it is very unlikely that simulated mean annual water discharge will be less than about 361m³/s and very likely that it will be less than about 750 m³/s, with central estimates ranging between 472 and 488 m³/s, in comparison with baseline observations of 451 m³/s (Jenkins *et al.*, 2009). In general, river flow results reveal an explicit climate change signal with an upward trend of yearly results reflected in the median and high probability bounds for all future periods and emission scenarios.

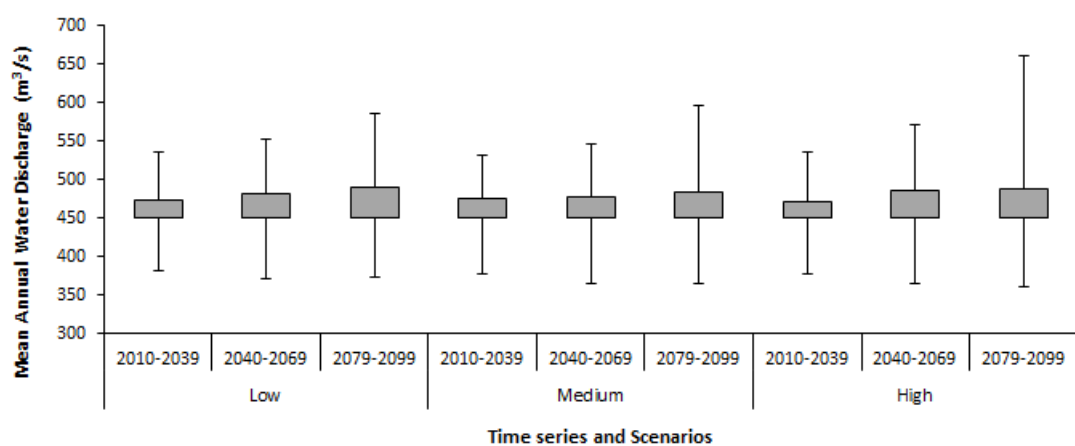


Figure 8.2 The distribution of mean annual water discharge lumped every 30 years for the Low, Medium and High emission scenarios. The lower and upper limits of each box are baseline and 50% probability level, respectively. The down whiskers are 10% probability level and the up whiskers are 90% probability level.

Cumulative sediment outputs for all the simulations and baseline references at different probability levels are displayed in Figure 8.3. The distribution of total sediment discharge over 30-year runs declines over time slices mainly at the 90% probability level. Notable large differences occur in all scenarios with the greatest accumulated sediment discharge exceeding approximately 170% of baseline values. However, the shift of sediment discharge at 50% level differs between emission scenarios. The volume of sediment discharge gradually increases for later time phases within an increasing range from about -12% to 11% in comparison with the baseline for medium and high emissions, rather than slightly descending or declining under a low emission scenario. No distinct change of sediment discharge is indicative at the 10% level. There is significant variability of erosion patterns under different scenarios. For instance, the magnitude of sediment discharge from the low emission scenario for 2010-2039 is greater than that from high emission scenario for the same time period. Nevertheless, the modelling result from the low emission scenario is only 78% of that from high scenario for 2070-2099 at 90% probability. For the 2020s, all the simulations show a downward trend of sediment discharge when emissions are increasing. In contrast, for the 2050s and 2080s, sediment discharge accumulates with the increasing of emissions. There is also some evidence that sudden boosts in sediment discharge appear owing to large flood events, which are shown as sharp jumps in the cumulative curves. In summary, sediment discharge from high climate change scenario and 2020s runs are broadly different from all other projections. Central estimates (50% level) of erosion generate the most complicated sediment response to climate change projections.

Interestingly, there is no clear and identifiable trend of annual changes in water and sediment discharge in the future, where as we might have expected that water and sediment discharges increase with higher emissions in later time series. In contrast, water and sediment patterns are complicated and show distinct nonlinear features. Since the annual changes mainly depend on daily or seasonal values, the large increase in winter rainfall combined with larger summer and autumn reduction in rainfall may account for the decreased total water discharge under medium and high scenarios (Fowler and Kilsby, 2004). Meanwhile, it is also agreed that the seasonal variability may cause a complex erosion-deposition cycle which results in different rates of sediment delivery. Furthermore, soil depth reduction resulting from large

erosion events and the consequent insufficient supply of sediment to the rivers is a potential reason for the reduction of total sediment discharge, especially at 90% probability level.

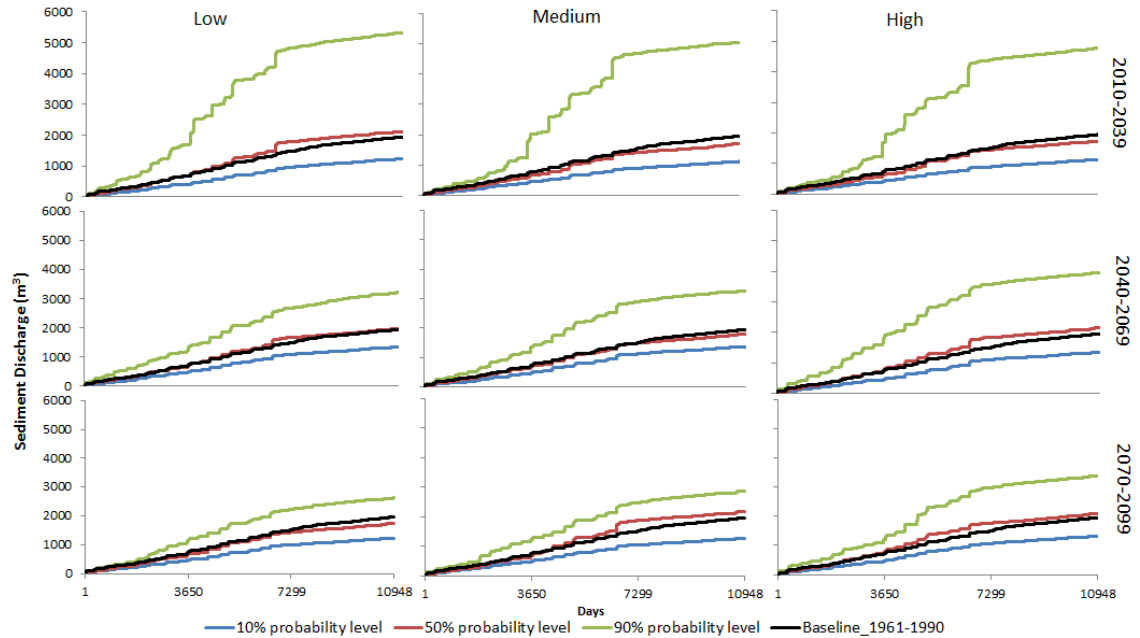


Figure 8.3 Cumulative daily sediment discharges for all probability levels (blue, red and green lines) and baseline (black lines) in the periods of 2020s, 2050s and 2080s (vertically) under the Low, Medium and High emission scenarios (horizontally).

8.3.1.2 Seasonal changes in water and sediment discharge

The effect of changes in the magnitude and timing of water and sediment discharge on monthly mean values based on all climate change scenarios have been calculated and presented in Figure 8.4 and Figure 8.5. A pronounced feature for simulated potential flooding and erosion is their similar seasonal distribution. Almost all projections indicate higher values of both runoff and sediment discharge in winter and autumn seasons (from October to March) than values in spring and summer (from April to September) seasons. Similar evidence was found by Jackson *et al.* (2011) when modelling the impact of future climate change on chalk groundwater resources in Berkshire Downs, southern England. They demonstrated an enhanced seasonal variation in groundwater recharge with less potential recharge generated during April and October. Adams *et al.* (2000) concluded that significant groundwater recharge in the UK only occurs during the winter months with different

periods and quantities. Fluctuations of sediment discharge are more pronounced compared to the low variability of summer runoff. The emissions trajectory plays an important role in changes of potential erosion in the future climate changes, especially for the summer season. Notably, the wetter winter will produce more sediment at almost all probability levels and in all time slices within the three emission scenarios. However, all the results from 10% probability level suggest a decrease when compared with base line values, while the reduction becomes smaller in later time slices. Although sediment discharge shows a remarkable decline due to drier summers in all emission scenarios, simulated outputs at 90% probability level in the 2010 -2039 time slice show an increasing trend to the upper end of the autumn. The most interesting seasonal change of erosion is the distribution patterns projected for the high emission scenario. The impact of high emission scenario on higher temperature and less rainfall is amplified by generating less sediment discharge, particularly for low (10% level) and central (50% level) estimates. However, when the drought is gradually released after August, sediment delivered to the pond increases more quickly and by a greater amount than in the low and medium emission scenarios. It seems that sediment is prone to be eroded after dry summers. The differences of runoff and sediment discharge between months illustrate the great variability and complexity in hydro-geomorphic behaviour due to seasonal climate change scenarios (Coulthard *et al.*, 2012). Clearly, these changes are expected to increase over time, of which the 2080s show more outstanding changes among most of the simulations.

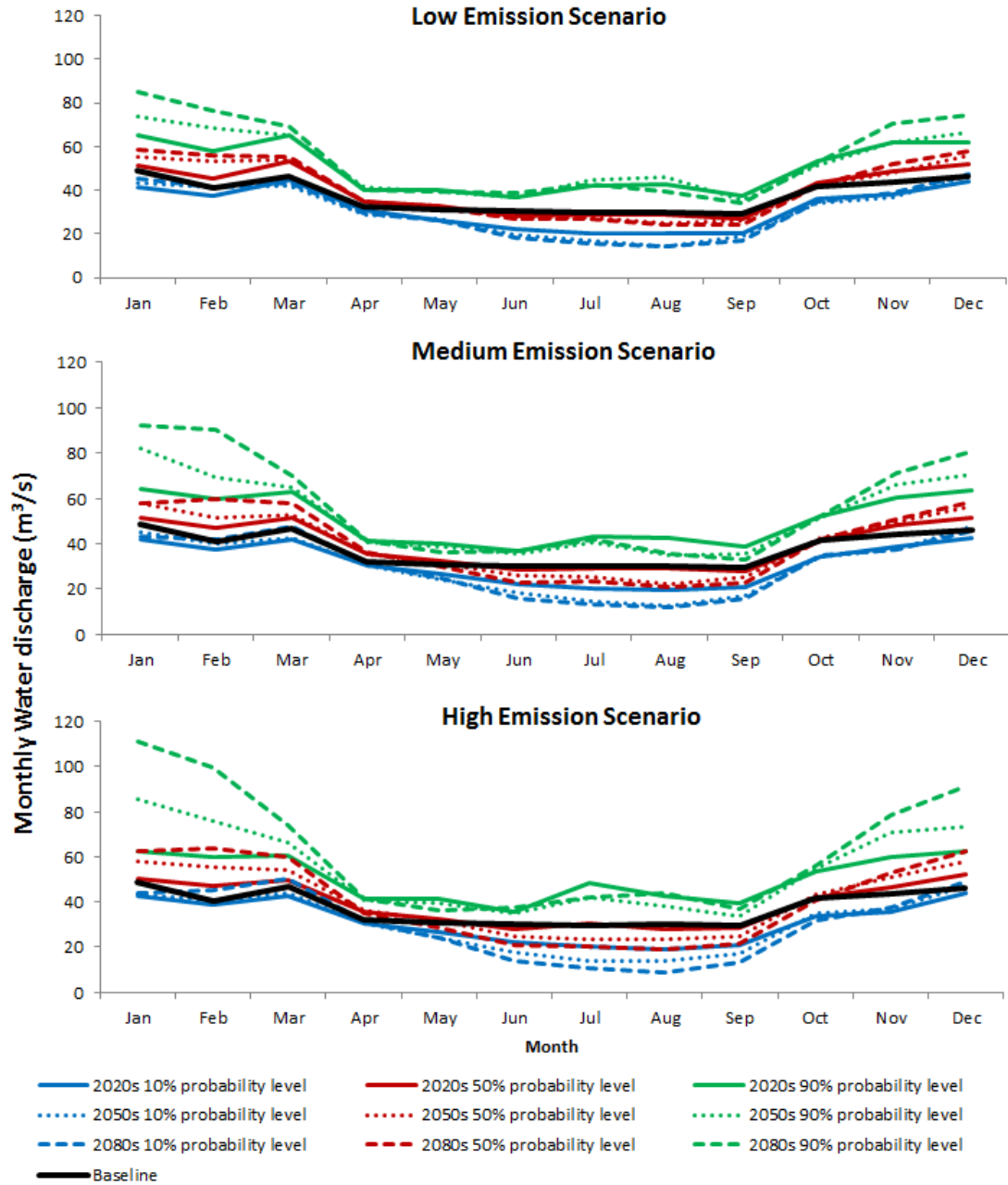


Figure 8.4 Comparison of mean monthly water discharge and baseline results (1961-1990) for all probability projections from 2010-2099 under three different emission scenarios.

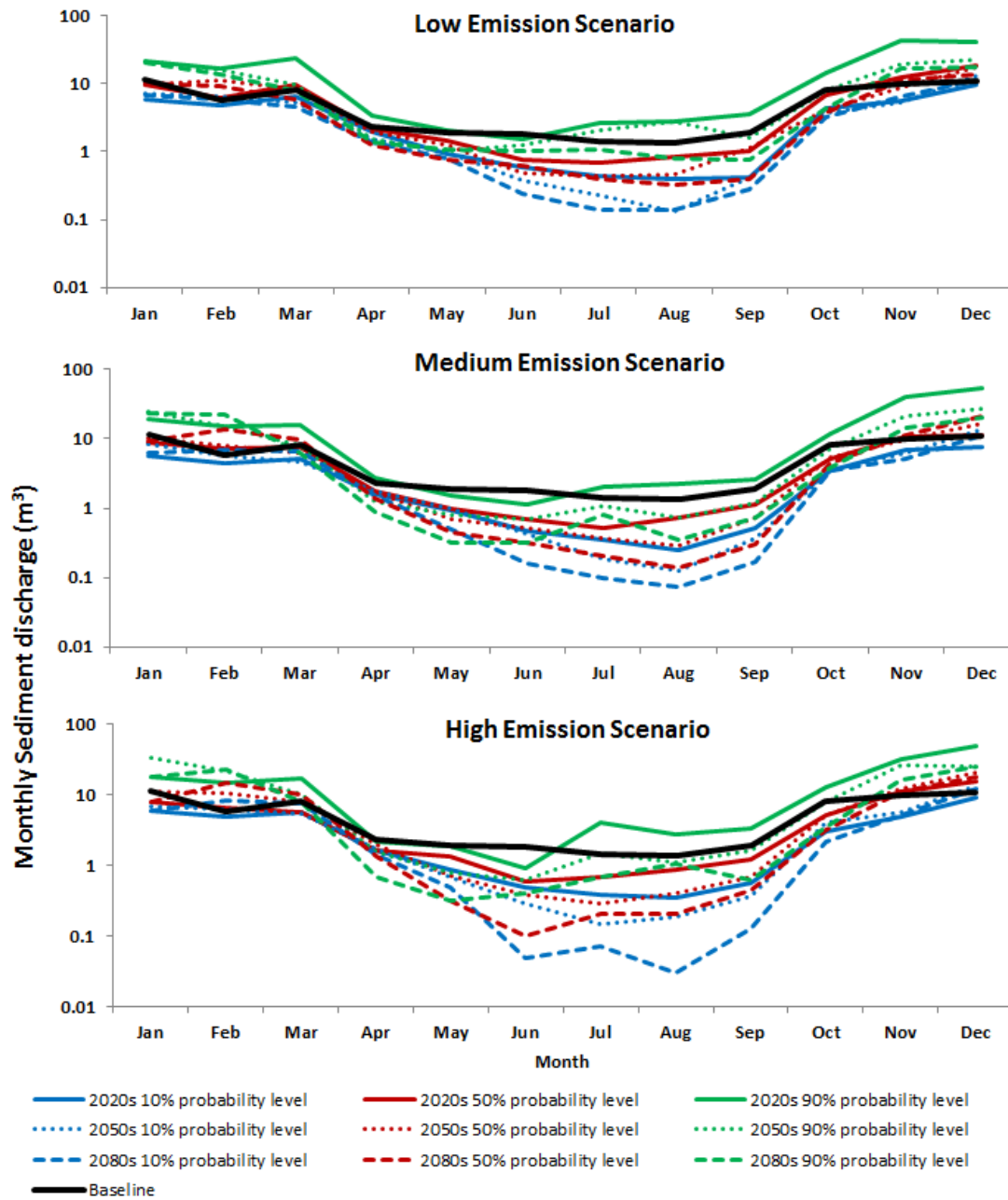


Figure 8.5 Comparison of mean monthly sediment discharge and baseline results (1961-1990) for all probability projections from 2010-2099 under three different emission scenarios.

The range of changes in monthly flow and sediment volumes, which is mainly controlled by catchment geological and climatic conditions, influences changes in annual totals (Arnell, 1992). Figure 8.6 demonstrates how rainfall changes in UKCP09 probability projections may influence catchment flow and sediment delivery in the future time series under the medium emission scenario based on monthly mean percentage changes. Results in terms of central estimates (50% probability level) exhibit an obvious seasonal cycle, with decreasing summer runoff. Given the evidence that winter is the main flood season across England (Bayliss and Jones, 1993; Kay *et al.*, 2006), the associated change of runoff shows a positive percentage up to 70% higher than baseline values between November and April for 50% and 90% probability levels with the exception of 10% probability. There is a conspicuous shift projected in the monthly distribution, with spring and summer water and sediment discharge experiencing greater percentage changes when compared to 1961-1990 baseline in reflection of decreased precipitation for most of the simulations. Mean monthly sediment delivery is complex. It decreases from March at all rainfall probability levels. One explanation is likely to lie in the previous changes in winter, as high winter rainfall flushes out a large amount of sediment and limits the sediment delivery afterwards. The decreased rainfall and higher temperature in spring lead to decreased soil water content and erodibility in the chalk catchment (Favis-Mortlock and Boardman, 1995). Changed soil moisture deficits will be adjusted by the increased autumn and winter rainfall thus accelerating the erosion rate. It is also apparent that water and sediment discharge display a multiplier effect with enhanced differences between observed and projected values in the future (Coulthard *et al.*, 2012). It is possible that the low flow in summer may destroy the water supply-demand balance in the Alresford chalk catchment, which is fed by groundwater. The limited groundwater may influence the irrigation of most watercress beds cultivated along channels (Boardman *et al.*, 1990; Adams *et al.*, 2000; Loáiciga, 2003). Although, the reduced sediment delivery may alleviate the summer erosion, the deposited coarser materials that are mainly assembled in the channels and tributaries could be the potential supply of sediment in the following winter.

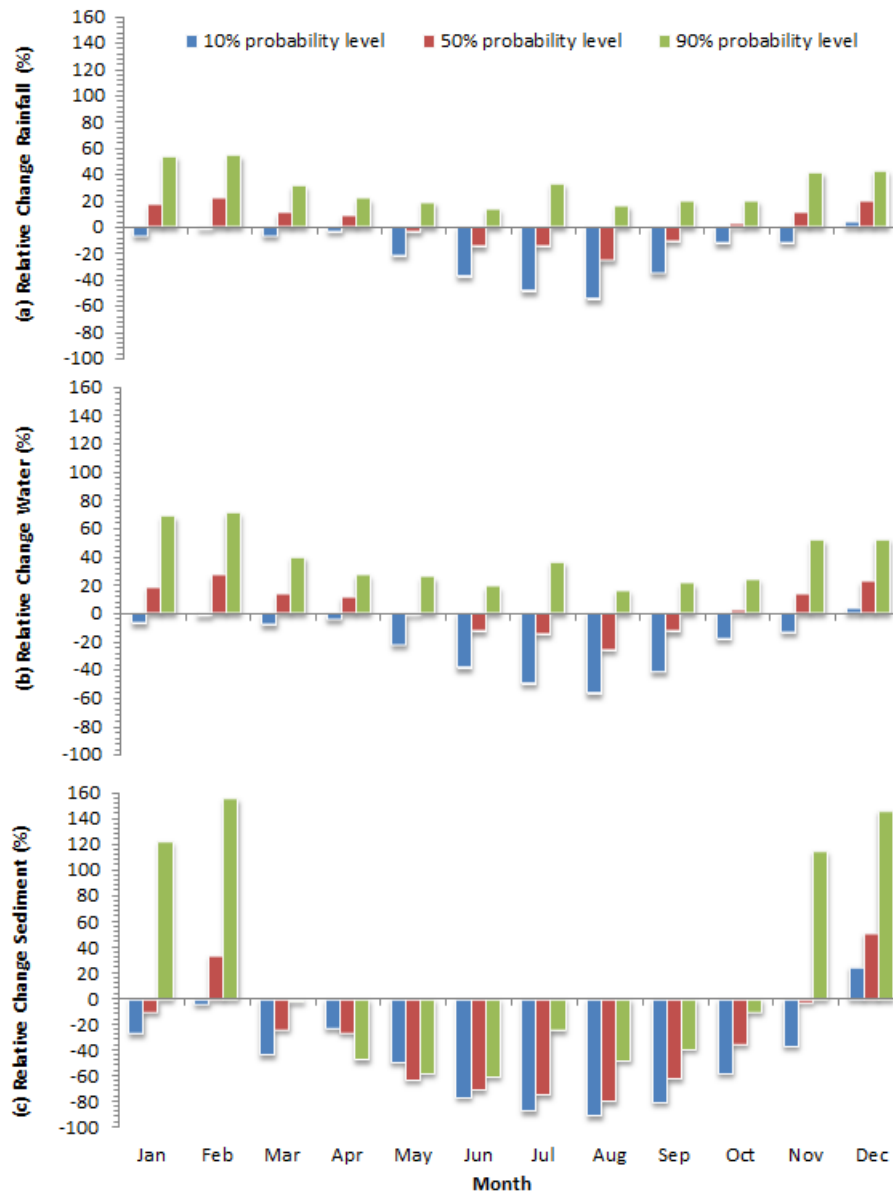


Figure 8.6 Relative changes (%), to the 1961-1990 baseline, in mean monthly (a) precipitation, (b) water and (c) sediment discharge for the future periods at 10%, 50% and 90% probability levels under medium scenario in 2050s.

8.3.1.3 Changes based on different sized events

By calculating the flood and sediment frequency for all nine scenarios and baseline, daily events based on analyses of water and sediment discharge are displayed in Figure 8.7 and Figure 8.8.

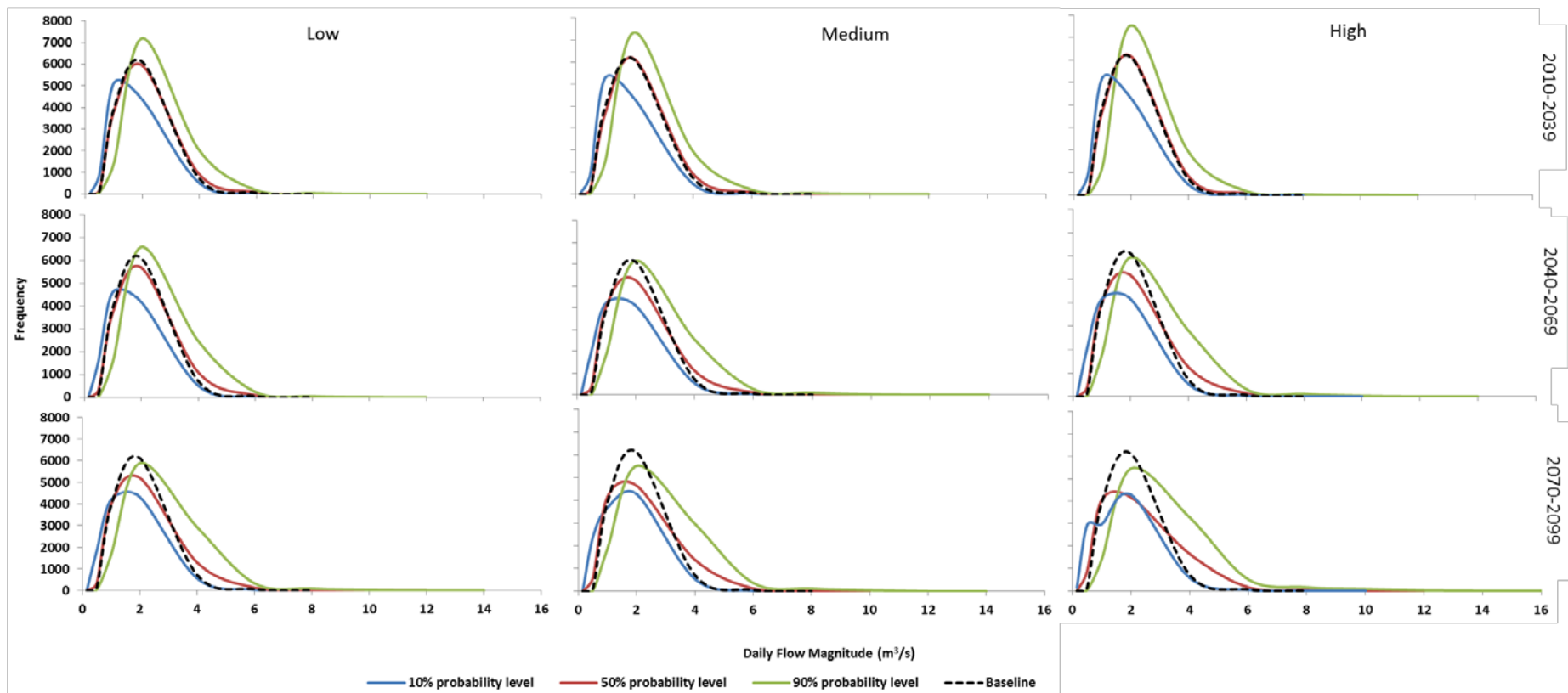


Figure 8.7 Frequency distribution plots of daily flow for all future climate change scenarios (straight lines) compared with 1961-1990 baseline results (black dashed line).

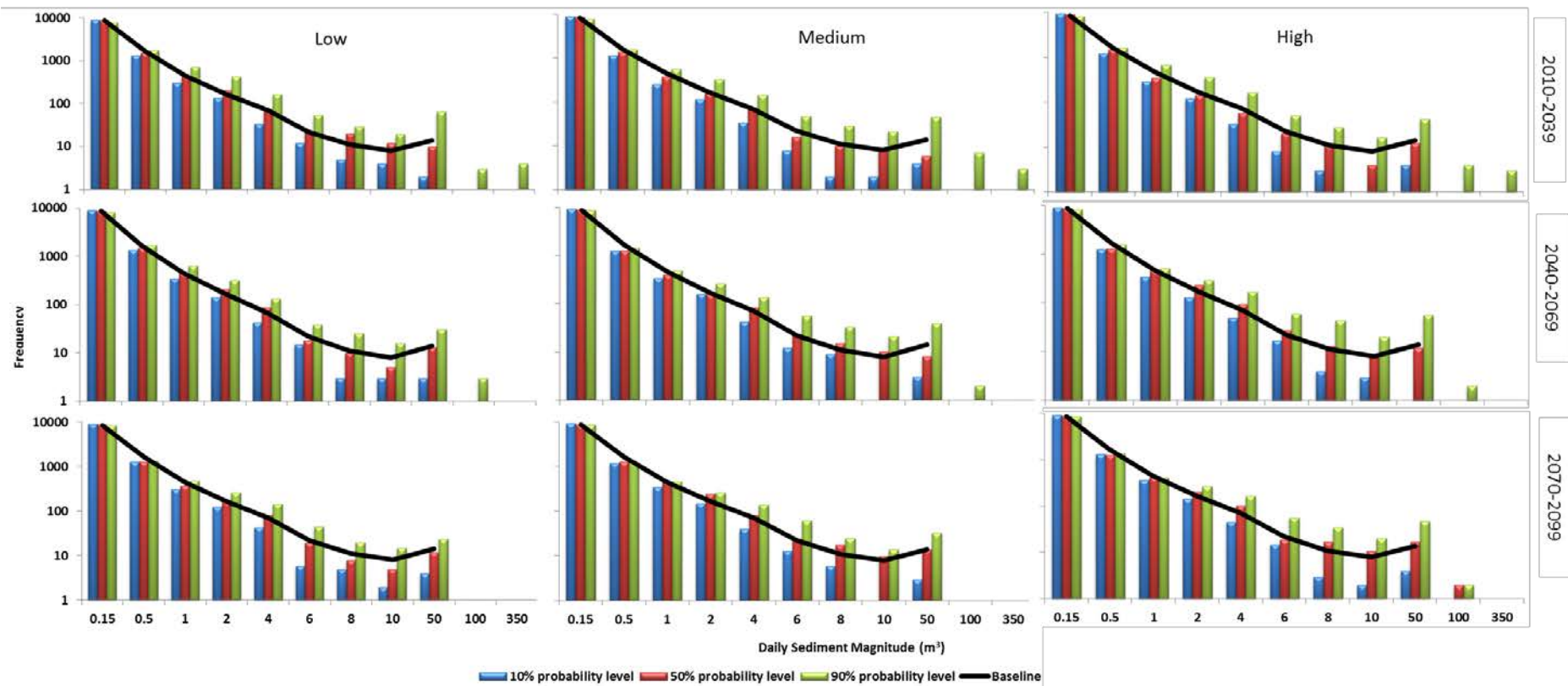


Figure 8.8 Frequency distribution plots of daily Sediment discharge for all future climate change scenarios (column charts) compared with 1961-1990 baseline results (black line).

For river flows, there is a considerable increase in the frequency of medium to large sized events with time and with higher emission scenarios. From the 2020s to the 2080s, frequency peaks of low flow events (daily water discharge $< 2 \text{ m}^3/\text{s}$) gradually decline in comparison to baseline results at all probability levels under three emission scenarios. Even at the 10% probability level, frequency peaks are moving toward larger flow events, especially for the high emission scenario. There is little change in the number of smaller runoff events between scenarios for the first 30 years in the future. Significant increments in the frequency of medium sized runoff events ($3 \text{ to } 8 \text{ m}^3/\text{s}$) are suggested where gaps between projected and observed results are widened in the curve at median and high probability levels. This effect also follows the upwards trend over the year and with higher emission scenarios. Another notable change is the occurrence of flood events with large or even huge size in future simulations. Simulated daily water discharge at median and high estimates will exceed $8 \text{ m}^3/\text{s}$ in the future, which is the maximum under the baseline scenario. The largest magnitude of runoff can rise to as high as $16 \text{ m}^3/\text{s}$ in 2070-2099 under a high emission scenario at 90% probability level, which is twice the observed mean value for 1961 -1990. Moreover, large sized flood events exist at low climate change levels after the 2020s.

Projected responses of sediment distribution to rainfall changes for all scenarios manifest a similar behaviour. As displayed in Figure 8.8, there is little difference of erosion events of small size (daily sediment discharge $< 2 \text{ m}^3$) between different emission scenarios and probability levels. One notable trend is the reduced frequency of smaller events over time. Frequency estimates at the 50% probability level show fluctuations in narrow ranges with most of the outputs close to baseline values except the appearance of two very large sediment events that exceed 100 m^3 of daily yields in 2080s under the high emission scenario. There is a clear growing trend in the frequency of medium sized erosion events in central estimates (50% level) with higher emission scenarios and later time slices. The largest size of daily sediment discharge is 50 m^3 from baseline scenarios. However, larger sediment accumulation events have been produced at 90% probability level with event size reaching 350 m^3 , which is seven times the magnitude of the largest events generated from baseline simulations. Although it is projected that there will be no significant increase in total sediment discharge for 2020s, 2050s and 2080s (Table 8.1), risks of larger sized

erosion events are becoming more apparent under future climate change and emission scenarios.

Table 8.1 Total every 30-year sediment discharge (m^3) for all climate change scenarios at three probability levels.

Emission scenario		Low			Medium			High		
Year	Probability level	10%	50%	90%	10%	50%	90%	10%	50%	90%
2010-2039		1237	2123	5330	1121	1700	5047	1130	1727	4768
2040-2069		1350	1981	3207	1372	1797	3273	1336	2134	3945
2070-2099		1231	1731	2617	1261	2157	2851	1325	2090	3365
Total		3817	5835	11154	3754	5654	11171	3791	5951	12079

For the most severe events, Table 8.2 demonstrates a comparison of the maximum daily rainfall, river flow and sediment discharge during every 30 year period (from 1961 to 1990 and 2010 to 2099) for observed and projected data under nine future climate change scenarios. Obviously, there is a positive change between the baseline and future maximum values at both 50% and 90% probability levels for all emission scenarios and time phases. Maximum rainfall intensity is projected to increase with a changing ratio by up to 1.96 by 2099 and increments are larger in the high emission scenario and later time slices than in low and medium future scenarios and earlier periods. This trajectory is paralleled by maximum daily flows with the most extreme flooding doubled under a high emission scenario within the 2080s period, possibly due to the effect of large increases in winter rainfall. Sediment discharge is also changed; however, the largest increase occurred at the 90% probability in the first 30 years of the future high emission scenario. The development and distribution of erosion is complicated in the future. Catchment response to climate change may be

illustrated by the special contribution of groundwater storage and deficit. One apparent feature can be detected from Table 8.2 is the amplification effect from rainfall to flooding to erosion. For instance, compared to the doubled growth of both rainfall and flow, the largest amount of sediment delivered to the pond shows more than a 10-fold increase over to the baseline values. This amplification effect is even exaggerated in future high emission scenarios.

Table 8.2 Comparisons of annual maximum of (a) rainfall, (b) water discharge and (c) sediment discharge between baseline and projected data for climate change scenarios.

(a) Annual Maximum of daily Rainfall (mm)		10%	50%	90%
Baseline (1961-1990)			16.205	
Low	2010-2039 (2020s)	14.651	17.409	20.811
	2040-2069 (2050s)	15.780	19.134	23.601
	2070-2099 (2080s)	15.667	19.755	25.577
Medium	2010-2039 (2020s)	14.523	17.481	21.086
	2040-2069 (2050s)	15.693	18.196	21.685
	2070-2099 (2080s)	16.078	21.497	29.616
High	2010-2039 (2020s)	15.062	17.828	21.223
	2040-2069 (2050s)	15.594	19.932	25.980
	2070-2099 (2080s)	16.893	22.593	31.777
(b) Annual Maximum of daily QW (m ³ /s)		10%	50%	90%
Baseline (1961-1990)			7.737	
Low	2010-2039 (2020s)	7.113	8.669	10.837
	2040-2069 (2050s)	8.354	9.294	11.742
	2070-2099 (2080s)	8.109	10.141	13.059
Medium	2010-2039 (2020s)	7.220	8.764	11.103
	2040-2069 (2050s)	8.135	9.598	12.391
	2070-2099 (2080s)	7.908	9.827	13.782
High	2010-2039 (2020s)	7.427	8.440	10.869
	2040-2069 (2050s)	8.074	9.745	12.812
	2070-2099 (2080s)	8.423	10.384	15.540
(c) Annual Maximum of daily QS(m ³)		10%	50%	90%
Baseline (1961-1990)			40.204	
Low	2010-2039 (2020s)	34.624	163.959	349.126

Medium	2040-2069 (2050s)	61.153	132.299	98.567
	2070-2099 (2080s)	35.316	70.504	82.735
	2010-2039 (2020s)	33.676	57.077	472.822
	2040-2069 (2050s)	83.278	85.767	164.594
	2070-2099 (2080s)	43.049	130.692	96.073
	2010-2039 (2020s)	33.353	76.363	520.689
High	2040-2069 (2050s)	69.097	144.280	101.377
	2070-2099 (2080s)	48.952	65.506	81.899

Results demonstrate that monthly changes in precipitation suggested by the UKCP09 projection would translate into a robustly detectable severity and frequency of flood and erosion events compared to the currently observed baseline (Prudhomme *et al.*, 2003). Meanwhile, flood and erosion events with medium to large sizes are likely to occur more frequently. The magnitude of sediment extremes is expected to be proportionately greater than the magnitude in observed extremes, though there are no significant changes in total sediment discharge during three 30 year periods.

8.3.2 Catchment response to future land use change

To discuss how the projected land use changes may affect the distribution of sediment delivery, results, analysis and interpretation that are based on the medium emission scenario are used as an example.

For each probability level, there is a clear trend of total sediment reduction with the gradual clearance of forest cover (Figure 8.9). Although forest cover changes equally for each land use scenario, with a 20% increase from ‘original’ to ‘forest’ and a 20% reduction from ‘original’ to ‘clear’, the ranges of sediment discharge change are not equivalent. The increase in forest cover reduced sediment production more than the increase in sediment production from the ‘original’ to ‘clear’ scenario, which is most significant at the 50% probability level. In terms of their values, Table 8.3 calculated the amount and difference of sediment discharge between different land use scenarios. For the most severe scenario (‘clear’) in the future, it is very unlikely that total sediment discharge would be less than approximately 3900 m³ and it is very likely that soils would be eroded without exceeding 11433 m³. ‘Original’

simulations lead to a 3.3%, 7.9% and 2.4% decrease in sediment discharge for 10%, 50% and 90% probability bounds. However, for the ‘forest’ scenario, there would be approximately 4.7%, 17.45% and 2.4% reductions in sediment compared with the ‘original’ condition in the catchment over 100 years. The larger variance of sediment discharge between ‘original’ and ‘forest’ simulations reflects the afforestation effect on soil erosion reduction. More forest cover may alter the sediment carrying capacity and increase the threshold of sediment storage in the fluvial system, and that diminishes the sediment delivery within the catchment. This effect can be amplified to a 27% reduction of sediment discharge with a 40% increase in forest cover from ‘clear’ to ‘forest’ in the 50% probability estimates until the 2090s, thus indicating that afforestation can mitigate the risk of potential soil erosion.

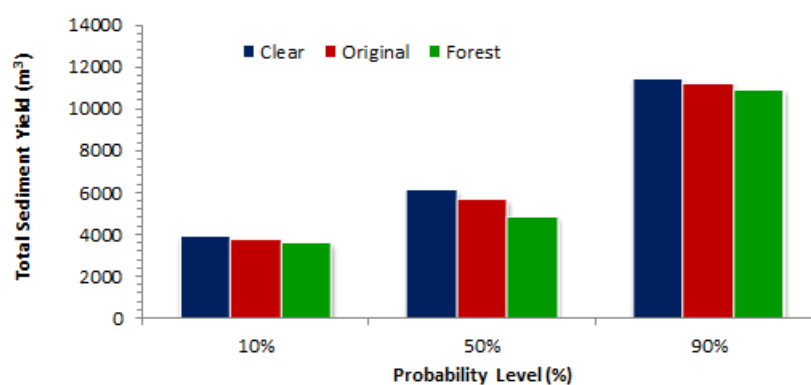


Figure 8.9 Total sediment yields for different land use scenarios within three climate change bounds in the future 100 years (from 2010 to 2090).

Table 8.3 Total amount of projected sediment discharge for every land use and climate change scenarios in the future.

Land use change scenario	Sediment discharge (m ³) and variance (%) at different probability levels		
	10%	50%	90%
Clear (M=0.008)	3879.35	6100.53	11433.60
Original (M=0.01)	3753.98 (3.34)	5654.39 (7.89)	11171.07 (2.35)
Forest (M=0.013)	3577.68 (4.70)	4812.70 (17.49)	10910.69 (2.39)

Sediment accumulates gradually in the future 100 years in response to climate and land use changes in different simulations (Figure 8.10). Projected outputs are clustered into three groups according to rainfall changes at three probability levels, where faster sediment erosion follows larger rainfall varieties. This emphasizes the climate effect on sediment delivery regardless of land use changes. However, land use change may play an important role in accelerating or decelerating sediment movement under the same climate scenarios (Reynard *et al.*, 2001; Wilby *et al.*, 2008). There is little disparity between three land use scenarios at the 10% probability level of rainfall change throughout the entire future time series. Increased sediment transport is detectable in 'clear' simulation at 50% probability level of rainfall change, particularly after the 2060s. Sediment accumulates steadily with a similar pattern in 'original' and 'forest' simulations until a greater difference appears after 2080, and 'forest' scenario produced the least sediment over the whole 100 years simulation. The sediment response to land use changes is amplified in the 90% probability level simulations. A rapid increase of sediment discharge starts from 2020 in the 'clear', 'original' and 'forest' scenarios. Again, the 'clear' scenario shows the fastest sediment delivery over the whole future period. The difference of cumulative sediment discharge between 'clear' scenario and 'forest' scenario is less significant after 2070, which may contribute to the insufficient storage of sediment after large erosion events.

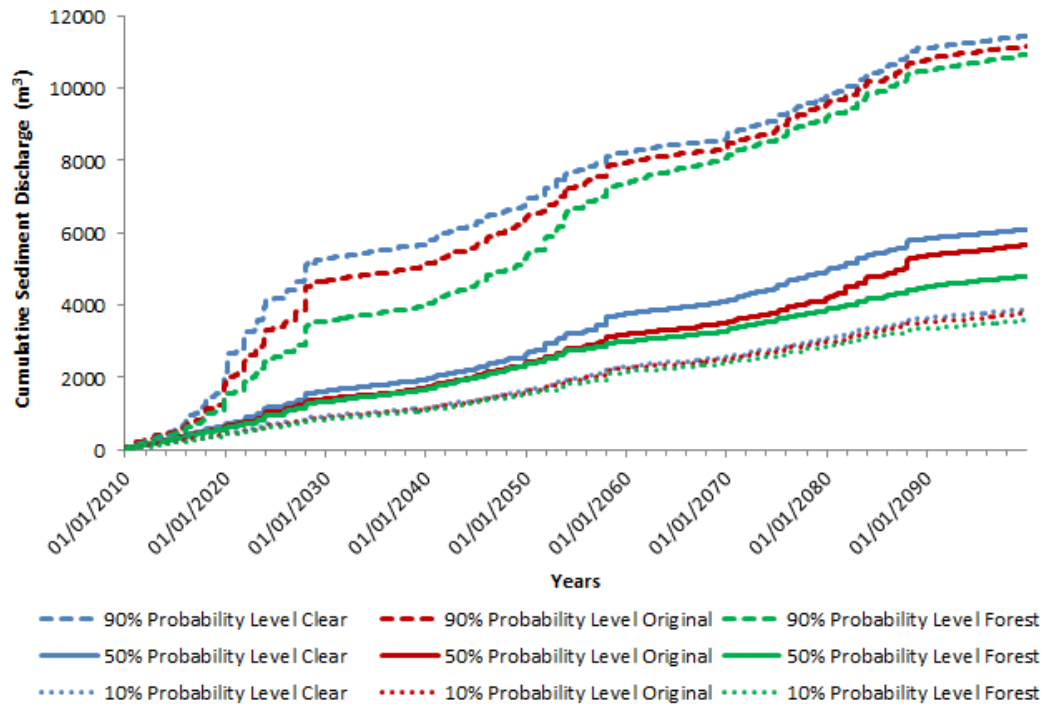


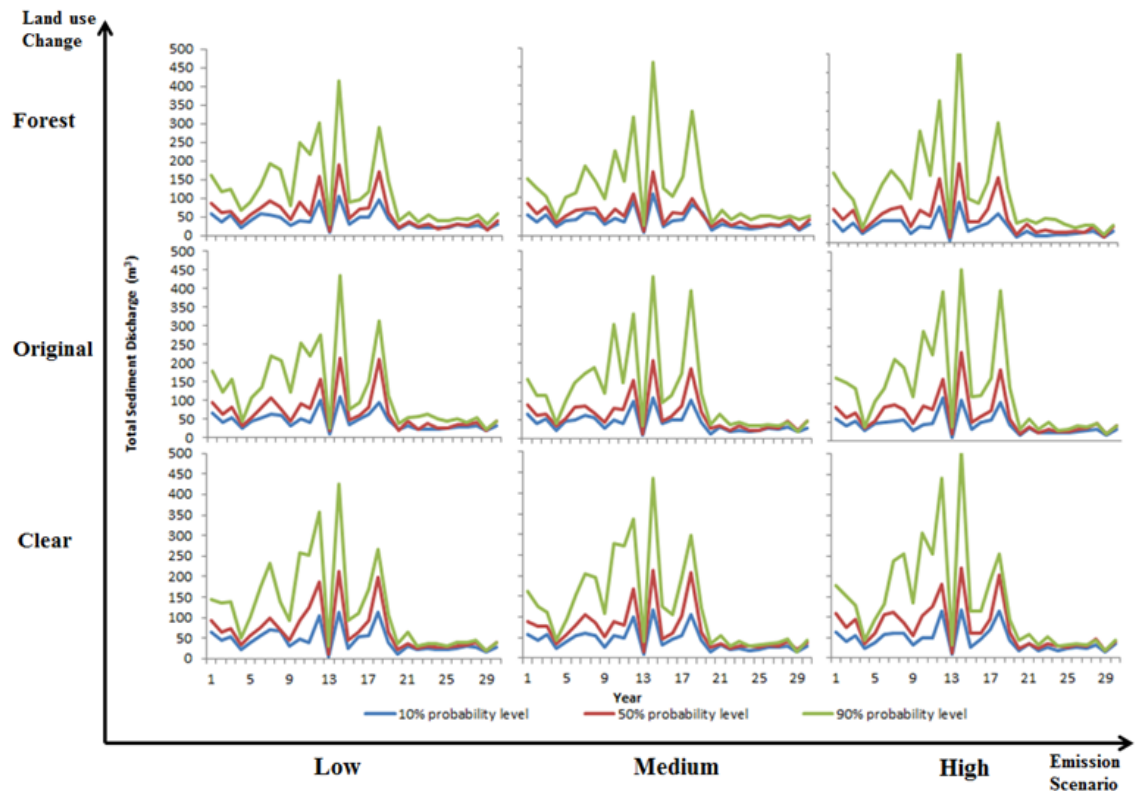
Figure 8.10 Cumulative sediment discharge for each scenario (blue =clear, red=original, green=forest; dotted line = 10% probability level, straight line =50% probability level, dashed line=90% probability level).

All the results suggest a complex non-linear erosion-deposition process, of which the catchment records a different sediment response to different land use and climate changes. The climate change scenario at the 10% probability level tends not to display any response to the land use change as the low flow results in low sediment delivery across the catchment and channels. There are much greater differences in the amount of sediment between the three land use scenarios with increased rainfall at the 90% probability level. It is likely that sediment deposited in the catchment and channels will be remobilised and delivered rapidly during large flood events with a large amount of sediment flushed out of the catchment, particularly during the decrease in forest cover. However, with the increasing timing and magnitude of sediment delivery, the system reaches a threshold where no fresh supply of sediment is available due to supply limitation after a large erosion event. Medium magnitude runoff (50% probability level) may carry less sediment than high floods that causes more sediment deposition which becomes future additional erosion sources. The lowest forest cover reacts to this alteration first with increased sediment accumulation after 2060, followed by 'original' simulation after 2080 with enlarged

gaps between three land use changes scenarios. Generally, the erosion-deposition cycles as well as catchment carrying efficiency are subject to alteration in land use and climate (Welsh *et al.*, 2009). The discrepancies of sediment delivery are also sensitive to different climate and land use change scenarios.

8.3.3 The impact of future climate and deforestation

The occurrence of erosion is controlled by a number of factors interacting in a complex way, of which climate change, particularly the intensity and frequency of rainfall, along with land use change can theoretically affect the sediment generation and conveyance (Wilby *et al.*, 2008; Kay *et al.*, 2006). The UKCP09 (Jenkins *et al.*, 2009) climate projection suggests wetter winters and drier and warmer summers. Moreover, some research suggests an increasing demand for agricultural land by 25–180% until the 2050s, depending on the socio-economic scenario (Weatherhead and Knox, 2000; Henriques *et al.*, 2008; Johnson *et al.*, 2009). To investigate the potential impact of these projections, we simulate the system response to future environmental changes for the Alresford catchment as displayed in Figure 8.11. Results indicate a detectable increase in both mean and total sediment discharge with a decrease in forest cover, especially the appearance of higher peaks at 50% and 90% probability levels. The fluctuation of sediment discharge over time is a reflection of system dynamic equilibrium, as the supplement of sediment discharge produced from erosion may decline and stabilize until greater runoff occurs above a certain rainfall threshold (Coulthard *et al.*, 2000).



Land Use Change	Emission scenario								
	Low			Medium			High		
	10%	50%	90%	10%	50%	90%	10%	50%	90%
Forest	3631	5424	10785	3578	4813	10911	3593	5863	12096
Original	3817	5835	11154	3754	5654	11171	3791	5951	12079
Clear	3972	6141	11134	3879	6101	11434	3996	6562	12244

Figure 8.11 Sediment response to land use changes under different emission scenarios; upper: distribution of mean 30 year total sediment discharge; Lower: calculated total sediment discharge (m^3).

Almost all simulations from central estimates (50% probability level) exceed the values from baseline observation. However, the magnitude of sediment delivery is not simply that higher emission scenario will result in higher sediment delivery. Central estimates under medium emission scenarios generate less sediment than both low and high scenarios and the effect is amplified with increased forest cover. The discrepancy between sediment reduction in summer and winter flooding events may contribute to the decrease of totals from medium scenarios. Land cover intervention is also important in triggering changes of soil erodibility by amplifying or dampening

climate driven changes (Lane, 2002; Lane *et al.*, 2003; Wilby *et al.*, 2008).

Furthermore, the groundwater effect of chalk catchment can play an important role in controlling flooding and erosion. Most rainfall is stored in the chalk aquifer before generating runoff (Berrie, 1992; Smith *et al.*, 2003). When precipitation increases, particularly under high emission scenarios, the aquifer storage threshold is exceeded, and the additional runoff produced may carry more sediment into the river.

8.4 Summary

Climate change and its potential impact on the fluvial system is a hot topic worldwide with numerous climate projections based on different models (Jones and Reid, 2001; Arnell, 2004; Ekström *et al.*, 2005; Cloke *et al.*, 2010). As mentioned by Johnson *et al.* (2009) '*no climate change model can provide a certain picture of the future*'. This study is seeking to estimate the behaviour of flow and sediment in response to climatic and anthropogenic change in the future through the implications of climate changes in the UKCP09 scenarios. Based on the projected climate scenarios and the hypothesised vegetation cover in the future, the key findings of all the simulations in the chalk catchment are summarised below:

(1) For total water and sediment discharge over a 30-year period, most of changes at the 50% probability level and all the changes at the 90% probability level show an increasing trend compared to baseline values.

(2) The seasonal pattern of flow and sediment delivery is significant, with lower flow values and increases in sediment variability in spring and summer in all time slices and emission scenarios. Results also suggest an increase of water and sediment discharge in wetter winters and autumns. Most simulations generate less sediment than baseline values in drier and warmer summer seasons, except simulations at the 90% probability level. Winter seasons produce more sediment than baseline time series at 50% and 90% probability levels.

(3) For individual events, notable increases are projected in medium and large flow and erosion events in all precipitation probability distributions. Heavy flooding and extreme sediment erosion events, which do not occur in the baseline condition, also exist in the projections. Furthermore, comparing maximal daily values between

precipitation, water and sediment discharges reveals an amplification effect of extreme events on catchment erosion.

(4) Taking account of land use change in projections suggests a large variation of results. A 20% increase in vegetation cover across the catchment demonstrates a reduction in total sediment discharge at all probability levels, reaching to 17.5% at the 50% probability level. This finding is in accordance with many studies that afforestation may help mitigate local flooding by decreasing erodibility (Favis-Mortlock and Boardman, 1995). In contrast, a catchment with reduced vegetation cover is sensitive to erosive precipitation (Boardman, 1993). In this study, modelling results show elevated sediment discharge when vegetation cover is reduced by 20%, especially at 90% probability level with higher erosion rate and more sediment delivered out of the catchment.

All the simulations generate complex and non-linear sediment feedbacks that arise in connection with land use change associated with climate projection scenarios. Changes in landscape behaviour are not evenly distributed across all years or not simply show increasing flooding and erosion following larger emission scenarios and later time series. Sediment discharge is very likely to increase disproportionately in wetter seasons at 50% and 90% probability levels between three emission scenarios and to decrease in drier seasons at all levels. Forest clearance or arable land expansion has considerable impact on sediment delivery. However, the total amount of sediment eroded in medium emission scenarios are less than values in low and high scenarios. These non-linear changes can be a function of alterations in rainfall scenarios, sediment storage and delivery balance, and changes in geomorphology. Furthermore, a complex interplay of changes in soil depth, soil properties and particle size re-distribution during erosional process is of considerable importance.

Keeping the current land use conditions (the 'original' scenario), Alresford catchment is very likely to generate 30-year total sediment discharge more than 3754 m³ and less than 12079 m³ in the 2020s, 2050s and 2080s with central estimates in a range of 5654-5951 m³, compared to the period of 1961-1990 (5843 m³). It seems that erosion is not likely to be a severe and urgent problem in the future. Although Alresford catchment is a typical groundwater fed catchment with relatively resilient

base flow (Monkhouse, 1964), the direct impact of precipitation to surface flow and groundwater resource for irrigation practices of arable land (Brouyère *et al.*, 2004), particularly in hotter and drier summer is not negligible. Land use management and aquifer exploitation should be adapted to climate variability (Loáiciga, 2003) to meet the balance between human demand and environmental sustainability in a warming planet. Although precipitation increases in winter and autumn can help store groundwater, the consequent appearance of flooding results in large / extreme erosion events. On chalk landscapes, soil is always delivered to storage sites in the valley bottom and valley sides (Adams *et al.*, 2000) which is a potential sediment supply for further erosion. Furthermore, the Alresford catchment has very thin soils rarely thicker than 23 cm (Favis-Mortlock *et al.*, 1997) which makes it vulnerable to soil depletion. In a complex chalk system, it is difficult to summarise the potential hydrological and geomorphic responses of the catchment to climate and land use change due to not only the intrinsic uncertainties that exist in climate projections (Hannaford and Marsh, 2006), but also the complex relationships between temperature, rainfall, soil properties, hydrological and geological features (Prudhomme *et al.*, 2003). Further modelling studies are necessary in order to reduce the uncertainty of responses to climate scenarios in association with land management choices.

Chapter 9

Synthesis and further research

The research presented in this thesis covered the dynamic behaviour of geomorphic systems, past and present interactions among landscape elements and environmental controls, and potential future impact, by modelling approaches in complex lake-catchment systems. With respect to the research aims and objectives, this thesis provides the following achievements.

(1) A holistic view of soil erosion and landscape evolution as complex earth surface processes. This thesis reviewed the system sensitivity to climate and human forcings in hydrological and geomorphic processes, the natural of system complexity and the application of models in modelling dynamics and complexity of river-catchment systems.

(2) The application of a CA model to the natural sciences. This study developed and applied the dynamic model CAESAR to simulate the landscape evolution of different catchments (simple catchment, Old Alresford Pond, UK and Holzmaar, Germany) over different timescales (approximately 25,000 days, 150 years and 5000 years).

(3) Interpretations of the interconnections between systems and environmental factors, and attendant system responses to disturbances and initial conditions. This thesis interpreted the contribution of climate and land use to temporal and spatial patterns of erosion and deposition through the results from both long-term and short-term simulations.

(4) A multidisciplinary perspective that incorporates palaeo-environmental studies, modelling approaches and landscape evolution theory into complex system theory. This study compared modelled water and sediment discharge results with lake sediment records (e.g. sediment accumulation rate and magnetic data) for both natural catchments for model validation.

(5) The recognition of non-linearity (e.g. thresholds and feedbacks) and self-organisation in fluvial systems. This study explored the role of non-linearity and self-organisation and their behaviour in complex river-catchment systems through a series of experiments (from designed simple catchment to real dynamic systems)

(6) The evidence of qualitative changes of state in the system, in response to environmental factors at different time scales. This studied analysed the relationship between sediment response and possible drivers through bivariate plots and power-law distribution approaches and found a system's state may change in different time periods during the entire simulation.

(7) A prediction of possible erosion risks under future natural and human pressures. This study simulated the nature of hydro-geomorphological processes based on a series of possible scenarios built for land use and climate changes in the coming 100 years.

In general, the findings have major implications for future investigations of system complexity (e.g. hydro-geomorphic processes and system controls), and the challenge of modelling complex natural systems. The next sections explore those implications and review the study limitations that need to be overcome in subsequent work.

9.1 System complexity

The Earth system behaves as a complex dynamic system (Johnson *et al.*, 1997), consisting of integrated disciplines of physical basis (e.g. geology, chemistry, oceanography, atmospheric physics, geomorphology, ecology and biology) and societal dimensions (e.g. population change and human actions). Complex systems have emergent properties that should be viewed and understood holistically. The study of complex systems seeks to explore major processes and non-linearities in their dynamics, and to reveal complex patterns and structures of the system and, linkages and feedbacks between components of the system (Lawton, 2001). As a part of the Earth system, the fluvial system is also a complex system that consists of not only the drainage basin but also the river channel and the floodplain associated with their subsystems (Schumm, 2005). Each section is an open system (Michaelides and

Wainwright, 2004), with interactions between flows, hydrological cycles, sediment transport, and energy or material storage and release (Phillips, 1992a). This process-response complexity can be represented and observed through the evolutionary development of the catchment's response of erosion and deposition over time (Figure 9.1).

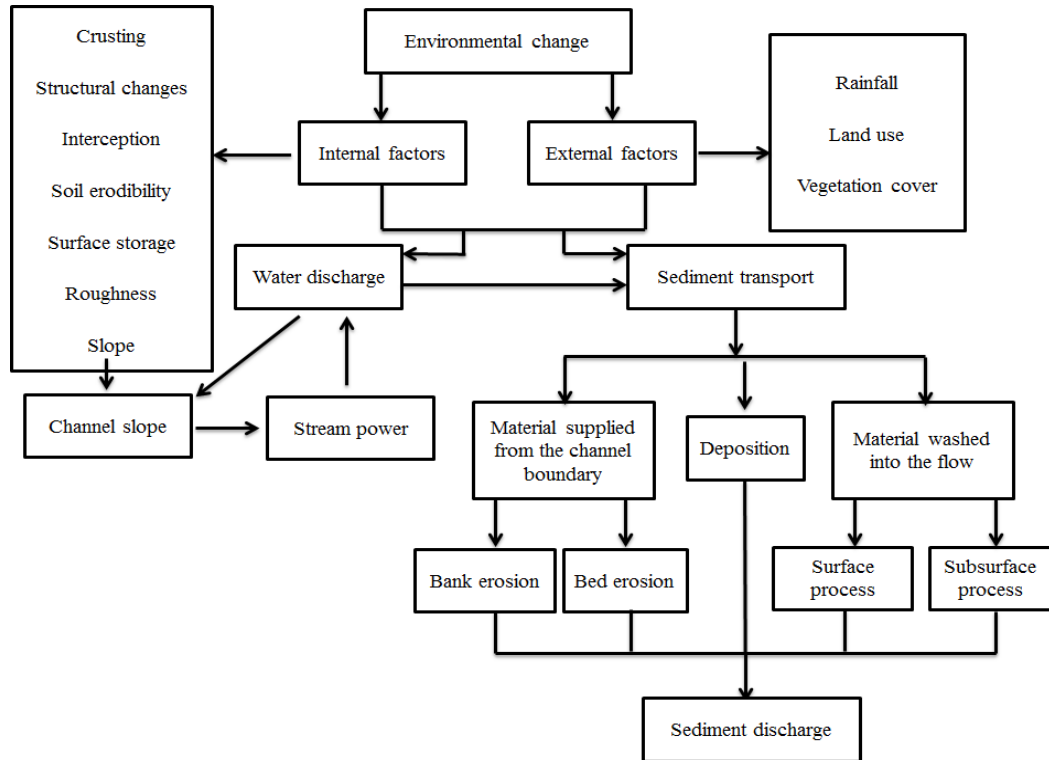


Figure 9.1 Complexity of the erosion process in fluvial systems (modified from Knighton, 1998; Michaelides and Wainwright, 2004; Quinton, 2004; Brazier, 2012).

Reconstructions of trajectories of natural environmental evolution through palaeo-environmental sciences can provide a series of parallel histories (Dearing, 2007) that improve our learning of process controls, such as external drivers (e.g. global and regional climatic variability, human-induced forest clearance) and system internal organisation, and the sensitivity of system to these perturbations, allowing measurement of current and potential landscape behaviours and adaptive capacity in different social-geographic and cultural frameworks (Reid *et al.*, 2010). Furthermore, understanding the nonlinear dynamics in Earth systems in the target of effective landscape management needs development and application of modelling approaches that provide a powerful tool combining natural science with complexity theories.

9.1.1 The complexity of system responses to environmental controls

Earth systems, for example fluvial environments at the catchment scale (Alresford catchment and Holzmaar catchment), are affected by multiple controls and forcings, including the external forcings of climate and land use changes and internal properties of the system. These forcings play a role in the natural environment as a set of multidirectional impact-response interactions. Human activities are treated as stressors on landscapes (Dearing, 2000) and climatic systems, which in turn, have effects on human society (Chin *et al.*, 2013). One of the key aims of this study has been the quantification of the impact of environmental changes on landscape evolution. In order to make these quantifications, a series of simulations have been applied to two catchments under different environmental controls and processes at both short and long scales. Modelling results from simulations demonstrate complex system responses to these controls and forcings in various degrees. Water discharge varies mainly with rainfall, but also vegetation cover, gradients, flow power etc., and in turn affects the pattern and threshold of sediment movement, together with other factors such as topographic changes and soil erodibility.

The results produced from the Alresford catchment simulations suggest notable system complexity to rainfall events at varying magnitudes, before the 1960s. Surface soil erosion and channel incision may dominate the catchment behaviour under strong precipitation controls with soil erosion enhancement caused by a rapid increase in sediment discharge. The effect of a large event may last for a long time and may take several to hundreds of years for the system to recover, which can affect subsequent events. Mass movement processes may also be activated after large storm events when rainfall is transformed to groundwater storage, generating reduced amount of sediment discharge. Since the 1960s, natural and anthropogenically induced changes in vegetation cover have become more important than rainfall in terms of perturbations on the sediment regime and the reduction in sediment delivered to the pond through changes in land use and management. During this period, the system is controlled by mass movement processes with stable sediment discharge and few peaks. The increased demand for arable agriculture, the construction of concrete walls for more watercress cultivation, drought events and the silt control activity in the catchment seem to be the predominant influences on

erosion in the last 50 years. The degree of system complexity depends on the variability of environmental controls and also on the evolutionary processes. Large amounts of sediment eroded during flooding events may be deposited on the system floor as debris flow deposits (Betts *et al.*, 2003) and gradually released during small rainfall events.

Simulations of the Holzmaar catchment give an insight into the complex effects of land use change, especially in the case of changes in forest cover during environmental evolution in the Holocene. The most widespread examples of land use change are deforestation and land use intensification related to agriculture and grazing activities, which directly transform vegetation cover in the system (Lambin, 2004). Vegetation acts as a protective layer or buffer on the soil surface (Morgan, 1995), which has complex implications in terms of stream energy dissipation and the extent to which other disturbances will be preserved in the system (Phillips *et al.*, 1999). Quantified modelling outputs show minor changes in sediment discharge before the Iron Age and extremely sharp shifts in records afterward. Human impacts of rapid deforestation and intensified agricultural activities have caused notable landscape discontinuities and abrupt rises in sediment discharge in the erosional processes of the drainage system from the beginning of the Iron Age to the end of the Roman Period and from the Middle Ages to the present time. Obviously, forest cover changes in Holzmaar catchment are not constant and continuous. The evolution of landscape over thousands of years may develop both progressively and by leaps from one dynamic state to a new state. When forest cover recovered to a high level and remained constant, the system generated a reduced amount of sediment discharge, but with variable values as a result of geomorphic adjustment of the system itself. Land use change may have modified the climate signal and led to variations in sediment supply, especially during the last 500 years. Therefore, it is the existence of external controls interacting with the complex responses of the fluvial system that allows large variation in forest cover to play an important role in landscape evolution.

9.1.2 The application of complexity theory

With so many impacts arising from these environmental drivers and more importantly their interactions within the system, it is evident that the Earth system's

complexity can result in dynamic nonlinear behaviours in response to external drivers and internal organisation. As stated by Dearing (2007), non-linear is likely to be the rule rather than the exception. Non-linearities are explicitly exhibited in different fluvial systems. The very dynamics between periods of abrupt and gentle changes, the capacity to transform and persist (Folke *et al.*, 2010) and the alternative system state of stability and instability, are the focus of the non-linear research of earth systems. It is the non-linear properties of feedbacks, thresholds and self-organisation that determine their complex and dynamics.

Nonlinearities exist whenever some small changes in initial conditions can become disproportionately larger and eventually disturb the state of the system in fractal patterns (Manson, 2009) due to the presence and prevalence of thresholds. This is clearly the case in Alresford and Holzmaar catchments; for example, the behaviours of sediment discharge are considerably irregular through time, depending on various rainfall intensity and amount, forest cover changes, soil moisture storage, system erosivity and force-resistance relationship. The dynamic sediment transport and the non-linear system behaviour displayed in simulations provide a better understanding of the application of complex system theory to dynamic landscape evolution.

The simple catchment simulations demonstrate that spatial and temporal complexity in sediment delivery may be intrinsic in dynamic systems, independent of external drivers. When stream power and land cover remain constant, changes in the system itself render the system unstable with progressive erosion or significant landscape modifications. Following these complex events for a long period of time until the system has evolved to a critical state through self-adjustment, the system may reach a relatively stable state. External factors are vital in controlling the frequency and magnitude of sediment discharge. However, the intrinsic factors which are related to geomorphic properties of landform, particle size distribution, sediment supply-capacity balance and slope- channel coupling have a contribution to nonlinear performances.

In natural landscapes, dynamic systems are rarely static due to the feedback loop (Chin *et al.*, 2013) which is associated with soil erosion and deposition. Positive feedbacks are crucial in the formation of river drainage networks by enhancing

surface elevation differences (Favis-Mortlock *et al.*, 2004). Meanwhile, negative feedbacks provide system stability through sediment deposition in or along the channel. The slope-channel coupling processes that either deliver sediment to the lake or forming armour layers (Emmett and Wolman, 2001) on the bed, and the sediment storage-release cycle in the system are good examples of this complex system adjustment mechanism. In Alresford catchment, it appears that increases in precipitation would lead to increased sediment delivery, but negative feedbacks can dampen the erosive effect of a large flood event. Meanwhile, low stream power persists or grows over time can generate disproportionately large amounts of sediment and increase system complexity. This feedback loop also has the capacity to change system state. Soil erosion, for example, is not static and may experience changes in soil delivery rates (Phillips, 1998), displaying different system states between erosion, acceleration, remobilisation, transformation, dissipation and stable state. Simulations of Holzmaar catchment suggest that when external forces such as deforestation are large enough, systems may generate abrupt shifts from stability to high fluctuations.

Self-organisation, which is mainly driven by the internal dynamics of the system itself, (Bolliger *et al.*, 2003) is a part of complexity theory. When controlling the external factors in simple catchment simulations, this self-organisation behaviour is significant and sustained in the whole evolutionary process following the power-law rule. Similarly, the Holzmaar simulation also exhibits self-organisation as the catchment was not disturbed by strong climate change and human impact before the Iron Age. Self-organisation also appears at different landscape evolution stages and phases depending on a combination of erosion intensity, cascading mechanism and environmental disturbances in complex systems, such as phase III (1700-1100 cal. yr BP) in Holzmaar simulation. The fluvial system is considered dissipative (Huggett, 1988; Baas, 2002). For example, the erosional energy generated from large storm events is dissipated as the system reorganises itself to accommodate the instability. Energy dissipation is a characteristic of self-organisational behaviour which can be shown from the power-law relationship in Alresford catchment simulation, although it is also a rainfall-controlled system.

9.2 The complexity of modelling

Adoption of numerical models in the study of complex hydro-geomorphological processes is widespread (Smith, 1991; Favis-Mortlock ,1996; Favis-Mortlock *et al.*, 2000; Sidorchuk, 2004; Coulthard *et al.*, 2007; Van De Wiel and Coulthard, 2010; Heung *et al.*, 2013). Modelling technologies designed to deal with complex systems demonstrate the nature of change through thresholds, feedback loops and self-organisation (De Vries, 2007). CA-based landscape evolution models are particularly useful for understanding of system complexity owing to their capability of capturing emergent behaviour (Dearing, 2007) and simplifying system complexity (Mulligan and Wainwright, 2009). The serviceability of models is always judged by whether they can produce reasonable and testable outputs when comparing with palaeo-environmental records. No matter how complicated the models are and how accurately and powerfully they perform, there remain gaps and uncertainties between modelled dynamics and complex nature of Earth-environmental systems. As this study has shown, it is important to test models through numerous calibrations and validations over a variety of spatial and temporal scales.

9.2.1 Model performance

9.2.1.1 The complexity of system prediction

The Alresford study has demonstrated the challenge of simulating future states of complex systems. Under the pressure of warmer and wetter winters and hotter and drier summers in the UK, future predictions of the frequency and magnitude of potential flood and soil erosion in complex systems are important. The existence of dynamic nonlinearity means that deterministic prediction is difficult or even impossible. However, short-term probabilistic prediction of the complicated catchment behaviour, taking the form of model-based scenarios constructed from trajectories of past and present environmental evolution and processes, is possible. Scenario-based simulations demonstrate the individual and combined roles of external environmental drivers in generating threshold-dependent changes and suggest possible timescales and actions under control to be selected appropriately,

which can help to inform environmental management and sustainability (Dearing, 2007).

Based on the projected climate scenarios (UPCP09) and the hypothesised vegetation cover in the future, modelling efforts suggest complex landscape behaviour in the future. Sediment discharge is very likely to increase disproportionately in wetter seasons at 50% and 90% probability levels between three emission scenarios and to decrease in drier seasons at all levels. More medium and large flow and erosion events will be produced in all precipitation probability distributions. There will also be the occurrence of heavy flooding and extreme sediment erosion events. A 20% increase in forest cover across the catchment demonstrates a reduction in total sediment discharge at all probability levels. In contrast, all the results show elevated sediment discharge when vegetation cover is reduced by 20%. There would be more variations in sediment delivery due to the disruption of sediment supply-storage balance in the system as well as landform alterations. These findings demonstrate increasing variations in sediment discharge in response to intensified environmental forcings at temporal scales. However, there is no significant spatial manifestation of sediment variation in landscape evolution. Questions concerns which locations will be most affected and how the morphology of the system will be modified in the future are unanswerable in this study. The chalk catchment is sensitive to the direct influence of precipitation to runoff and groundwater resource. The availability of groundwater is important for human demand and agriculture activities. The chalk catchment is also vulnerable to soil depletion due to its thin soils. Furthermore, the complexity system theory of feedbacks and their interactions may result in uncertainties regarding which feedback will dominate the system behaviour under different scenarios. Although it is impossible to neglect the challenge of complexity in landscape evolution, these modelling efforts represent a step toward explaining hydro-geomorphic processes and forcing-response relationships in the future. Simulation modelling is a valuable approach in complex Earth system studies and strategic decision making for sustainable system management.

9.2.1.2 Modelling calibration

As a chalk catchment, the effect of groundwater storage and supply for surface runoff is very important for modelling. However, the CAESAR model is not designed for this kind of system; the calibration between modelled water discharge and instrumental flow data from national river flow achieves (NRFA) showed little correlation. Modelled water discharge was underestimated on low flows and overestimated on flood discharge events. The effect of rainfall was not buffered by groundwater, thus exaggerated runoff to rise to large crests when extreme storms happened, and gave excessively low values in drought periods. In order to resolve this limitation, the groundwater component in the discharge was considered by converting the precipitation series into a groundwater-adjusted effective precipitation series. The groundwater-adjusted precipitation was created by a trial and error adjustment approach in terms of the seasonal characteristics of groundwater and vegetation cover. Simulated water discharge driven by groundwater-adjusted effective rainfall matched well with recorded flow and this approach was applied to the whole time series for sediment discharge simulation. It is difficult to calibrate water discharge in the absence of available hydrological data in Holzmaar catchment. However, surface runoff in Holzmaar catchment is generated directly from rainfall with no groundwater disturbance. Previous research from Coulthard et al. (2000, 2002) and Welsh et al. (2009) have successfully applied CAESAR to model landscape evolution in similar catchments.

9.2.1.3 Modelling validation

The term validation refers to the testing of the model output to address how exactly a model reproduces observed system dynamics (Fishman and Kiviat, 1968; Perry, 2009). Validation is important but difficult to operate. In this research, the method of validation employed was the comparison of palaeo-environmental records from lake sediments with modelling outputs and, sensitivity analyses.

Palaeo-environmental achieves can help establish the trajectories of forcing and response of the past that led to the present conditions (Dearing and Jones, 2003) and the likelihood thresholds (for example, sensitivity or resilience to particular climate

and human impacts) in the future (Dearing, 2006c). Model-data comparison in Alresford Pond shows a good match between modelled sediment discharge (driven by effective rainfall) and sediment accumulation rate in 121 years of simulation, especially for peak values. Furthermore, the comparison was extended to longer terms by using 5000 years of records of minerogenic sediment accumulation rate and magnetic susceptibility from high resolution varved sediment in Holzmaar (Germany, Zolitschka, 1998) to compare with modelled sediment data. The simulated pattern of sediment delivery displays close correlation with the general trajectory (e.g. ups and downs in sediment flux), magnitude (e.g. major peaks in sediment discharge) and behaviour (e.g. erosion and deposition cycle) to palaeo-records in Holzmaar catchment over 5000 years. Model validation should focus on the long-time pattern of changes instead of accurate replication of crests and troughs in the time series (Welsh *et al.*, 2009). Generally, the modelling results from two catchments are logically acceptable within error margins and CAESAR can be used as a tool to simulate system sensitivity and behaviour with respect to changing climate and land use.

Sensitivity analysis is required to identify reasonable changes in modelling results produced from changes in parameter values (Mulligan and Wainwright, 2012a). In order to investigate the influence of groundwater on the hydrological cycle and sediment delivery in chalk catchment, a comparison of flood behaviour between the ‘original rainfall’ (rainfall data directly from stations) and the ‘effective rainfall’ (rainfall data modified by groundwater) was taken into account. Modelled results from ‘effective rainfall’ conditions are much closer to published data in South Downs, UK (Boardman, 2003) and estimated soil erosion rate by the empirical model (RUSLE). Comparisons of geomorphic patterns indicate no obvious difference in landform across the catchment between these two rainfall input conditions, and erosion and deposition occurred primarily in channels and their tributaries. The ‘effective rainfall’ simulation generated fewer small tributary streams, which is in accordance with the established erosion feature of few and short streams in chalk catchments (Berrie, 1992).

It is noted by Kirkby *et al.* (1993) that models will never be more than analogues of the real world. The results are difficult to accurately validate. The model developers

(Coulthard *et al.*, 2007) have argued that the CAESAR model cannot and should not be used in a strictly quantitative way of exact prediction, but more to produce qualitative answers such as how rivers behave and what causes them to change. In this study, the CAESAR model was able to capture sediment transport pattern over time, especially in the case of the impact of individual large storm events. This allows us to study the complex relationships between environmental factors and geomorphic changes.

9.2.2 Modelling constraints

Undoubtedly, models can support the exploration of system behaviours, processes and their interactions, thereby providing a better understanding of system complexity. However, no model is perfect, and complexity and uncertainty may be the two challenges of bottom-up modelling (Bankes, 2002; Grimm *et al.*, 2005; Grimm and Railsback, 2005). There are several limitations in the CAESAR modelling, the three most important of which are discussed below.

First of all is the availability of hourly rainfall data. CAESAR requires high-resolution hourly data to drive the modelling. However, records of hourly rainfall monitored by gauging stations are always short term (5-50 years) and not available for catchments in remote areas (Tucker and Hancock, 2010). Therefore, the accurate construction of hourly rainfall data from daily or even low resolution data, such as reconstructed palaeo-precipitation data based on pollen records in Holzmaar catchment, is one of the biggest limitations in this study. Available hourly precipitation was repeated for 121 years (Alresford catchment) and 5000 years (Holzmaar catchment) respectively, and scaled against related daily or annual data. This approach reflects only rainfall magnitude changes, but previous research from Coulthard *et al.* (2000, 2002) argued that frequency changes have less effect on sediment discharge than magnitude. Furthermore, CAESAR is not able to simulate sediment and water dynamics for chalk catchments due to the groundwater effect on surface runoff, whose function is not considered in the model. Coulthard (personal communication, 2012) suggested adjusting the rainfall data in terms of observed flow record and M values. It seems that this is the only effective way to match the modelled water discharge to flow data. However, this method requires sufficient

observed flow data for calibration and takes a long time for repetitive running of testing and adjusting.

Secondly, despite spatially distributed DEM data used in CAESAR, changes in vegetation cover and particle size distribution are uniform across the catchment. Hancock *et al.* (2011) demonstrate the point-specific nature of the soil particle size data, and it varies considerably on the hillslope and catchment scale which may affect sediment transport rates. Vegetation cover varies in different parts of the system, and is also of importance for landscape evolution.

The third limitation refers to the uncertainties of climate change scenarios in the future and their potential impact on sediment production in the modelling process. Due to the study time and computational capacity, predictions of the potential impact of future climate and land use changes on Alresford catchment are based on selected probabilistic precipitation data from UKCP09. In fact, UKCP09 can generate a large ensemble of 10,000 samples for each time slice and the selected precipitation data at 10%, 50% and 90% probability level give a general view of climate change scenarios. Uncertainties in future climate change should be considered in sediment dynamic simulations to improve the quality of predictions.

9.3 Future perspectives and further work

In studying Earth system science for sustainable environmental management, we are facing a series of challenges, of which two aspects are key future perspectives. Firstly, to meet the goals of environmental management, enhanced understanding of complex system response to global and regional environmental changes by linking the functioning of the system and its thresholds in various social, economic and environmental issues (Reid *et al.*, 2010), is necessary. A full explanation of past environmental processes and dynamic interactions of forcing and response, in a theoretical framework of complexity, could contribute to sustainable environmental development. Secondly, addressing foresight into future global change and Earth-environmental states require step changes from fundamental environmental observations to continued development of dynamic modelling approach, ensuring functionally and dynamically realistic (Dearing, 2007; Oldfield, 2007). More

modelling work is necessary in this research not only for future predictions of landscape evolution, but also for further model development.

Questions about environmental change, especially the effects of climate change, are endless. Scientific research into their impacts is likely to continue for the foreseeable future. Improved climate change scenarios with reduced uncertainties will be applied in simulations of hydro-geomorphic changes in complex fluvial systems. These scenarios need to be logically structured in consideration of the nature of the real world and the biophysical process operating in it (Pitman, 2005), and calibrated and validated with baseline data for uncertainty analysis. Furthermore, multiple sensitivity tests of hypothetical scenarios of land use change, based on landscape management policies, and designed extreme climatic events, are taken into account in further simulations. These can be operated by setting rainfall and spatially-distributed M values at different magnitudes, so as to find the threshold values for potential soil erosion.

The next step for the CA model development would be to incorporate groundwater parameters in erosional processes by considering more factors such as soil water balance, evapotranspiration, temperature, infiltration and soil moisture deficits and their interactions. Other parameters for vegetation cover and particle size distribution would be developed by allowing different parts of the catchment to be assigned different initial values. This is useful to improve our knowledge of potential changes in complex systems with different land use types and soil properties. With the development of computer science and stronger computer processing power, it is possible to simulate catchment landscape evolution by using finer resolution topographic data. Detailed geomorphic changes in catchments would be detectable for better spatial validation via GIS technology. It is especially important for Alresford catchment to predict the geomorphic response to future climate change and human activities at spatial scale. Furthermore, it is challenging but valuable to incorporate landscape management policies in modelling processes and to define sustainable boundaries in their results analysis.

Bibliography

- Acornley, R. M. and Sear, D. A. (1999). Sediment transport and siltation of brown trout (*Salmo trutta* L.) spawning gravels in chalk streams. *Hydrological Processes* 13(3), 447-458.
- Adams, B., Gale, I., Younger, P., Lerner, D. and Chilton, J. (2000). Groundwater. In: Acreman, M. and British Hydrological Society (Ed.) *The hydrology of the UK-a study of change*, London and New York, pp. 150-175.
- ADAS. (1994). Old Alresford Pond Analysis of Silt. Report to Hampshire County Council.
- Alexander, L.V. and Jones, P.D. (2001). Updated precipitation series for the UK and discussion of recent extremes. *Atmospheric Science Letters* 1, 142–150.
- Allison, R.J. (1994). Slopes and slope processes. *Progress in Physical Geography* 18, 425–35.
- Anderson, N. J., Bugmann, H., Dearing, J. A., and Gaillard, M. J. (2006). Linking palaeoenvironmental data and models to understand the past and to predict the future. *Trends in Ecology & Evolution* 21(12), 696-704.
- Andersen, T., Carstensen, J., Hernandez-Garcia, E., and Duarte, C. M. (2009). Ecological thresholds and regime shifts: approaches to identification. *Trends in Ecology & Evolution* 24(1), 49-57.
- Anderson R.Y. and Dean W. E. (1988). Lacustrine varve formation through time. *Palaeogeography, Palaeoclimatology, Palaeoecology* 62, 215–235.
- Anderson, N. J., Korsman, T. and Renberg, I. (1994). Spatial heterogeneity of diatom stratigraphy in varved and non-varved sediments of a small, boreal-forest lake. *Aquatic Sciences* 56(1), 40-58.
- Anhert, F. (1976). Brief description of a comprehensive three-dimensional process-response model of landform development. *Zeitschrift für Geomorphologie* 25: 29–49.

Angima, S. D., Stott, D. E., O'Neill, M. K., Ong, C. K. and Weesies, G. A. (2003). Soil erosion prediction using RUSLE for central Kenyan highland conditions. *Agriculture, Ecosystems & Environment* 97 (1–3), 295–308.

Alresford Chamber of Commerce (2011). *About Alresford: Old Alresford Pond*. [online], available: http://www.alresford.org/info_pages/pond.php [accessed 1/10/2011].

Appleby, P. G. (2001). Chronostratigraphic techniques in recent sediment. In Last, W. M. and Smol, J. P (Ed.) *Tracking Environmental Change Using Lake Sediments. Volume 1: Basin Analysis, Coring, and Chronological Techniques*. Dordrecht: Kluwer Academic Publishers, pp. 171-203.

Appleby, P. G. (2008). Three decades of dating recent sediments by fallout radionuclides: a review. *The Holocene* 18 (1), 83-93.

Appleby, P. G., Dearing, J. A. and Oldfield, F. (1985). Magnetic studies of erosion in a Scottish lake catchment. 1. Core chronology and correlation. *Limnology and Oceanography* 30(6), 1144-1153.

Appleby, P.G. and Oldfield, F. (1978). The calculation of ^{210}Pb dates assuming a constant rate of supply of unsupported ^{210}Pb to the sediment. *Catena* 5, 1–8.

Appleby, P. G., Oldfield, F., Thompson, R., Huttunen, P. and Tolonen, K. (1979). ^{210}Pb dating of annually laminated lake sediments from Finland. *Nature* 280, 53 - 55.

Appleby, P. G., Richardson, N. and Nolan, P. J. (1991). ^{241}Am dating of lake sediments. *Hydrobiologia* 214, 35-42.

Arnell, N.W. (1992). Factors controlling the effects of climate change on river flow regimes in a humid temperate environment. *Journal of Hydrology* 132, 321-342.

Arnell, N. W. (2004). Climate-change impacts on river flows in Britain: the UKCIP02 Scenarios. *Water and Environment Journal* 18 (2), 112–117.

- Aslan, A. (2007). Fluvial systems: sediments. In: Elias, S. and Mock, C. (Ed.) *Encyclopedia of Quaternary science*. [Online], Access via Elsevier.
- Asselman, N. E. and Middelkoop, H. (1995). Floodplain sedimentation: quantities, patterns and processes. *Earth Surface Processes and Landforms* 20(6), 481-499.
- Auyang, S. Y. (1998). *Foundations of Complex System Theories in Economics, Evolutionary Biology, and Statistical Physics*. New York: Cambridge University Press.
- Baas, A. C. (2002). Chaos, fractals and self-organization in coastal geomorphology: simulating dune landscapes in vegetated environments. *Geomorphology* 48(1), 309-328.
- Baier, J., Lücke, A., Negendank, J. F., Schleser, G. H. and Zolitschka, B. (2004a). Diatom and geochemical evidence of mid-to late Holocene climatic changes at Lake Holzmaar, West-Eifel (Germany). *Quaternary international* 113(1), 81-96.
- Baier J., Negendank, J. F. and Zolitschka, B. (2004b). Mid- to Late Holocene lake ecosystem response to catchment and climatic changes - a detailed varve analysis of Lake Holzmaar (Germany). In: Miller, H., Negendank, J.F., Flöser, G., vonStorch, H., Fischer, H., Lohmann, G. and Kumke, T. (Ed.) *The Climate in Historical Times – Towards a Synthesis of Holocene Proxy Data and Climate Models*. Berlin: Springer-Verlag, pp. 195–208.
- Bak, P. (1997). *How Nature Works: The Science of Self-organized Criticality*. Oxford: Oxford University Press.
- Bakker, K. (2012). Water security: research challenges and opportunities. *Science* 337(6097), 914-915.
- Bankes, S. C. (2002). Agent-based modeling: A revolution?. *Proceedings of the National Academy of Sciences of the United States of America* 99(3), 7199-7200.
- Bar-Yam, Y. (1997). *Dynamics of Complex Systems*. Reading: Perseus Books.

Barber, K., Zolitschka, B., Tarasov, P. and Lotter, A.F. (2004) Atlantic to Urals: the Holocene climatic record of Mid-Latitude Europe. In, Battarbee, R.W., Gasse, F. and Stickley, C.E. (Ed.) *Past climate variability through Europe and Africa*. Dordrecht: Kluwer Academic, pp. 417-442.

Barnett, T. P., Adam, J. C. and Lettenmaier, D. P. (2005). Potential impacts of a warming climate on water availability in snow-dominated regions. *Nature* 438(7066), 303-309.

Battarbee, R. W., Appleby, P. G., Odell, K. and Flower, R. J. (1985). ^{210}Pb dating of Scottish lake sediments, afforestation and accelerated soil erosion. *Earth Surface Processes and Landforms* 10(2), 137-142.

Bayliss, A.C. and Jones, R.C. (1993). *Peaks-over-threshold flood database: Summary statistics and seasonality*. Wallingford: Natural Environment Research Council. (Institute of Hydrology Report No. 121).

Beniston, M. (2004). The 2003 heat wave in Europe: a shape of things to come? An analysis based on Swiss climatological data and model simulations. *Geophysical Research Letters* 31 (2), 1-4.

Bennett, J. P. (1974). Concepts of mathematical modeling of sediment yield. *Water Resources Research* 10: 485-492.

Berrie, A.D. (1992). The chalk stream environment. *Hrdrobiologia* 248, 3-9.

Betts, H. D., Trustrum, N. A. and Rose, R. C. D. (2003). Geomorphic changes in a complex gully system measured from sequential digital elevation models, and implications for management. *Earth Surface Processes and Landforms* 28(10), 1043-1058.

Beven, K. (1985). Distributed models. In: Anderson, M.G. and T.P. Burt (Ed.) *Hydrological Forecasting*. London: John Wiley & Sons Ltd.

Beven, K. (1997). TOPMODEL: A critique. *Hydrological Processes* 11: 1069-1085.

- Beven, K.J. and M.J. Kirkby. (1979). A physically based variable contributing-area model of catchment hydrology. *Hydrological Science Bulletin* 24(1): 43–69.
- Bienert, B. (2008). Merowingerzeitliche Besiedlung-Archäologische Befunde in den südlichen Rheinlanden. In: Irsigler, F. (Ed.) *Geschichtlicher Atlas der Rheinlande IV.13. Habelt, Bonn*.
- Birks, H.J.B. (1998). Numerical tools in palaeolimnology - progress, potentialities, and problems. *Journal of Paleolimnology* 20: 307–332.
- Birky, A. K. (2001). NDVI and a simple model of deciduous forest seasonal dynamics. *Ecological Modelling* 143(1), 43-58.
- Björck, S., Sandgren, P. and Holmquist, B. (1987). A magnetostratigraphic comparison between ^{14}C years and varve years during the Late Weichselian, indicating significant differences between the time-scales. *Journal of Quaternary Science* 2(2), 133-140.
- Black, S. (2007). *An investigation into the response of chironomidae (Insecta: Diptera), in a shallow calcareous pond in southern England, to environmental changes over the last 300 years*. Undergraduate dissertation, University of Southampton.
- Blundell, A., Hannam, J. A., Dearing, J. A. and Boyle, J. F. (2009a). Detecting atmospheric pollution in surface soils using magnetic measurements: A reappraisal using an England and Wales database. *Environmental Pollution* 157(10), 2878-2890.
- Blundell, A., Dearing, J. A., Boyle, J. F. and Hannam, J. A. (2009b). Controlling factors for the spatial variability of soil magnetic susceptibility across England and Wales. *Earth-Science Reviews* 95(3), 158-188.
- Boardman, J. (1988). Severe erosion on agricultural land in East Sussex, UK, October 1987. *Soil Technology* 1, 333-48.

Boardman, J. (1993). The sensitivity of Downland arable land to erosion by water. In: Thomas, D.S.G. and Allison, R.J. (Ed.) *Landscape Sensitivity*. Chichester: Wiley, pp. 211-228.

Boardman, J. (2003). Soil erosion and flooding on the eastern South Downs, southern England, 1976-2001. *Transactions of the Institute of British Geographers* 28(2), 176-196.

Boardman, J. (2010). A short history of muddy floods. *Land Degradation & Development* 21(4), 303-309.

Boardman, J., Evans, R., Favis-Mortlock, D. T. and Harris, T. M. (1990). Climate change and soil erosion on agricultural land in England and Wales. *Land Degradation & Development* 2(2), 95-106.

Boardman, J. and Robinson, D. A. (1985). Soil erosion, climatic vagary and agricultural change on the Downs around Lewes and Brighton, Autumn 1982. *Applied Geography* 5 (3), 243–258.

Boardman, J., Stammers, R. and Chestney, D. (1983). *High-down- Lewes Flooding Report*. Lewes District Council.

De Boer, D.H. (2001). Self-organization in fluvial landscapes: sediment dynamics as an emergent property. *Computers and Geosciences* 27 (8), 995–1003.

Bolliger, J., Sprott, J. C. and Mladenoff, D. J. (2003). Self-organization and complexity in historical landscape patterns. *Oikos* 100(3), 541-553.

Bond, G., Showers, W., Cheseby, M., Lotti, R., Almasi, P., deMenocal, P., Priore, P., Cullen, H., Hajdas, I. and Bonani, G. (1997). A pervasive millennial-scale cycle in North Atlantic Holocene and glacial climates. *Science* 278, 1257–1266.

Le Borgne, E. (1955). Susceptibilité magnétique anormale du sol superficiel, *Annales de Geophysique* 11, 399-419.

Boyle, J. F., Plater, A. J., Mayers, C., Turner, S. D., Stroud, R. W. and Weber, J. E.

- (2011). Land use, soil erosion, and sediment yield at Pinto Lake, California: comparison of a simplified USLE model with the lake sediment record. *Journal of Paleolimnology* 45(2), 199-212.
- Bradford, R.B. (2002). Controls on the discharge of Chalk streams of the Berkshire Downs, UK. *The Science of the Total Environment* 282-283, 65-80.
- Bragg, O. M. and Tallis, J. H. (2001). *The sensitivity of peat-covered upland landscapes*. *Catena* 42 (2–4), 345-360.
- Brasington, J. and Richards, K. (2007). Reduced-complexity, physically-based geomorphological modelling for catchment and river management. *Geomorphology* 90, 171–177
- Brauer, A., Endres, C. and Negendank, J. F. (1999). Lateglacial calendar year chronology based on annually laminated sediments from Lake Meerfelder Maar, Germany. *Quaternary International* 61(1), 17-25.
- Brauer, A., Litt, T., Negendank, J.F.W. and Zolitschka, B. (2001). Lateglacial varve chronology and biostratigraphy of lakes Holzmaar and Meerfelder Maar, Germany. *Boreas* 30, 83–88.
- Brazier, R.E. (2012). Erosion and sediment transport: finding simplicity in a complicated erosion model. In: Wainwright, J. and Mulligan, M. (Ed.) *Environmental Modelling: Finding Simplicity in Complexity*. London: John Wiley & Sons, pp. 253-243.
- Briffa, K.R., Jones, P.D., Schweingruber F.H. and Osborn T.J. (1998). Influence of volcanic eruptions on Northern Hemisphere summer temperature over the past 600 years. *Nature* 393: 450–455.
- Bristow, C. R., Mortimore, R. N. and Wood, C. J. (1997). Lithostratigraphy for mapping the Chalk of southern England. *Proceedings of the Geologists' Association* 108: 293-315.

Bronstert, A. (2003). Floods and Climate Change: Interactions and Impacts. *Risk Analysis* 23: 545-557.

Brouyère, S., Carabin, G. and Dassargues, A. (2004). Climate change impacts on groundwater resources: modelled deficits in a chalky aquifer, Geer basin, Belgium. *Hydrogeology Journal* 12(2), 123-134.

Brown, J. D. and Damery, S. L. (2002). Managing flood risk in the UK: towards an integration of social and technical perspectives. *Transactions of the Institute of British Geographers* 27: 412-426.

Brown, T.N. and Kulasiri, D. (1996). Validating models of complex, stochastic, biological systems. *Ecological Modelling* 86, 129–134.

Brüchmann, C., & Negendank, J. F. (2004). Indication of climatically induced natural eutrophication during the early Holocene period, based on annually laminated sediment from Lake Holzmaar, Germany. *Quaternary International* 123, 117-134.

Brune, G.M. (1953). Trap efficiency of reservoirs. *Transactions of the American Geophysical Union* 34, 407–18.

Büchel, G. (1993). Maars of the Westeifel. In Negendank, J. F. W. and Zolitschka, B. (Ed.): *Paleolimnology of Eifel maar Lakes*. Lecture Notes in Earth Sciences 49, 1–13. Berlin and Heidelberg: Springer-Verlag.

Burningham, K., Fielding, J. and Thrush, D. (2008), 'It'll never happen to me': understanding public awareness of local flood risk. *Disasters* 32: 216-238.

Busacca, A. J., Cook, C. A. and Mulla, D. J. (1993). Comparing landscape-scale estimation of soil erosion in the Palouse using Cs-137 and RUSLE. *Journal of Soil and Water Conservation* 48(4), 361-367.

Carlson, J. M. and Doyle, J. (1999). Highly optimized tolerance: A mechanism for power laws in designed systems. *Physical Review E* 60(2), 14-12.

Carlson, T. N., Perry, E. M. and Schmugge, T. J. (1990). Remote estimation of soil moisture availability and fractional vegetation cover for agricultural fields.

Agricultural and Forest Meteorology 52(1), 45-69.

Casey, H. (1981). Discharge and chemical changes in a chalk stream headwater affected by the outflow of a commercial watercress-bed. *Environmental Pollution Series B, Chemical and Physical* 2 (5), 373–385.

Casey, H. and Smith, S.M. (1994). The effects of watercress growing on chalk headwater streams in Dorset and Hampshire. *Environmental Pollution* 85 (2), 217–228.

Casti, J.L. (1994). *Complexification: Explaining a Paradoxical World through the Science of Surprise*. London: Abacus.

Casty, C., Raible, C. C., Stocker, T. F., Wanner, H. and Luterbacher, J. (2007). A European pattern climatology 1766–2000. *Climate Dynamics* 29(7-8), 791-805.

Charman, D. J., Brown, A. D., Hendon, D. and Karofeld, E. (2004). Testing the relationship between Holocene peatland palaeoclimate reconstructions and instrumental data at two European sites. *Quaternary Science Reviews* 23(1), 137-143.

Charman, D. J., Hohl, V., Blundell, A., Mitchell, F., Newberry, J. and Oksanen, P. (2012). A 1000-year reconstruction of summer precipitation from Ireland: Calibration of a peat-based palaeoclimate record. *Quaternary International* 268, 87-97.

Chapman, S. C., Stainforth, D. A., & Watkins, N. W. (2013). On estimating local long-term climate trends. *Philosophical Transactions of the Royal Society A: Mathematical, Physical and Engineering Sciences* 371(1991), 1-15.

Christierson, B. V., Vidal, J. P. and Wade, S. D. (2012). Using UKCP09 probabilistic climate information for UK water resource planning. *Journal of Hydrology* 424, 48-67.

- Herbig, C. and Sirocko, F. (2013). Palaeobotanical evidence for agricultural activities in the Eifel region during the Holocene: plant macro-remain and pollen analyses from sediments of three maar lakes in the Quaternary Westeifel Volcanic Field (Germany, Rheinland-Pfalz). *Vegetation History and Archaeobotany* 1-16.
- Jackson, C. R., Meister, R. and Prudhomme, C. (2011). Modelling the effects of climate change and its uncertainty on UK Chalk groundwater resources from an ensemble of global climate model projections. *Journal of Hydrology* 399(1), 12-28.
- Chin, A., Florsheim, J. L., Wohl, E. and Collins, B. D. (2013). Feedbacks in human landscape systems. *Environmental management* 1-14.
- Church, M. (2010). The trajectory of geomorphology. *Progress in Physical Geography* 34(3), 265–286.
- Cloke, H. L., Jeffers, C., Wetterhall, F., Byrne, T., Lowe, J. and Pappenberger, F. (2010). Climate impacts on river flow: projections for the Medway catchment, UK, with UKCP09 and CATCHMOD. *Hydrological Processes* 24(24), 3476-3489.
- Collins, A.L. and Walling, D.E. (2007). Sources of fine sediment recovered from the channel bed of lowland groundwater-fed catchments in the UK. *Geomorphology* 88, 120–138
- O'Connell, E., Ewen, J., O'Donnell, G. and Quinn, P. (2007). Is there a link between agricultural land-use management and flooding? *Hydrology and Earth System Sciences* 11, 96-107.
- Cooper, M. C., O'Sullivan, P. E. and Shine, A. J. (2000). Climate and solar variability recorded in Holocene laminated sediments-a preliminary assessment. *Quaternary International* 68, 363-371.
- Costa, J. E., Miller, A. J., Potter, K. W. and Wilcock, P. R. (1995). *Natural and anthropogenic influences in fluvial geomorphology*, 89. Washington, DC: American Geophysical Union, pp. 1-239.

- Costanza, R. (1987). Simulation modeling on the Macintosh using STELLA. *BioScience* 37, 129–132.
- Costanza, R., Duplisea, D. and Kautsky U. (1998). Modelling ecological and economic systems with STELLA. *Ecological Modelling* 10, 1–4.
- Costanza, R. and Ruth, M. (1998). Using dynamic modelling to scope environmental problems and build consensus. *Environmental management* 22(2), 183-195.
- Coulthard, T. J. (1999). *Modelling Upland Catchment Response to Holocene Environmental Change*. Unpublished Ph.D. Thesis. University of Leeds, U.K, pp. 181.
- Coulthard, T. J. (2001). Landscape evolution models: a software Review. *Hydrological Process* 15, 165–173.
- Coulthard, T. J., Hancock, G.R. and Lowry, J.B.C. (2012). Modelling soil erosion with a downscaled landscape evolution model. *Earth Surface Processes and Landforms* 37, 1046–1055.
- Coulthard, T. J., Hicks, D. M. and Van De Wiel, M. J. (2007). Cellular modelling of river catchments and reaches: advantages, limitations and prospects. *Geomorphology* 90, 192-207.
- Coulthard, T. J., Kirkby, M. J. and Macklin, M. G. (1999). Non-linearity and spatial resolution in a cellular automaton model of a small upland basin. *Hydrology and Earth System Sciences* 2(2/3), 257-264.
- Coulthard, T.J., Kirkby, M.J. and Macklin, M.G. (2000). Modelling geomorphic response to environmental change in an upland catchment. *Hydrological Processes* 14, 2031–2045.
- Coulthard, T.J., Lewin, J. and Macklin, M.G. (2005). Modelling differential catchment response to environmental change. *Geomorphology* 69, 222–241.
- Coulthard, T.J. and Macklin, M. G. (2001). How sensitive are river systems to

climate and land-use changes? A model-based evaluation. *Journal of Quaternary Science* 16 (4) 347–351.

Coulthard, T.J., Macklin, M.G. and Kirkby, M.J. (2002). A cellular model of Holocene upland river basin and alluvial fan evolution. *Earth Surface Processes and Landforms* 27, 269–288.

Coulthard, T. J., Ramirez, J., Fowler, H. J. and Glenis, V. (2012). Using the UKCP09 probabilistic scenarios to model the amplified impact of climate change on drainage basin sediment yield. *Hydrology and Earth System Sciences* 16(11), 4401–4416.

Coulthard, T.J. and Van De Wiel, M.J. (2007). Quantifying fluvial non linearity and finding self-organized criticality? Insights from simulations of river basin evolution. *Geomorphology* 91, 216–235.

Coulthard, T. J. and Van De Wiel, M. J. (2012). Modelling river history and evolution. *Philosophical Transactions of the Royal Society A* 370 (1966), 2123–2142.

Crisp, D. T. (1970). Input and Output of Minerals for a Small Watercress Bed Fed by Chalk Water. *Journal of Applied Ecology* 7(1), 117–140.

Cross, M. and Moscardini, A.O. (1985). *Learning the Art of Mathematical Modelling*. Chichester: John Wiley & Sons, pp.22.

Crowley, T.J. (2000). Causes of climate change over the past 1000 years. *Science* 289, 270–277.

Dai, X., Dearing, J. A., Yu, L., Zhang, W., Shi, Y., Zhang, F., Gu, C., Boyle, J. F., Coulthard, T. J. and Foster, G. C. (2009). The recent history of hydro-geomorphological processes in the upper Hangbu river system, Anhui Province, China. *Geomorphology* 106(3), 363–375.

Dansgaard, W., Johnsen, S. J., Clausen, H. B., Dahl-Jensen, D., Gundestrup, N. S., Hammer, C. U., Hvidberg, C. S. and Bond, G. (1993). Evidence for general

instability of past climate from a 250-kyr ice-core record. *Nature* 364(6434), 218-220.

Darby, S.E. and Van de Wiel, M.J. (2003). Models in fluvial geomorphology. In: Kondolf, G.M. and Piégay, H (Ed.) *Tools in Fluvial Geomorphology*. Chichester: John Wiley and Sons, 503–537.

Davis, J.J. (1963). Cesium and its relationship to potassium in ecology. In: Schultz, V. and Klement, A. W. (Ed.) *Radioecology*. New York: Reinhold, pp. 539-556.

Davison, P. S., Withers, P. J., Lord, E. I., Betson, M. J. and Strömqvist, J. (2008). PSYCHIC-A process-based model of phosphorus and sediment mobilisation and delivery within agricultural catchments. Part 1: Model description and parameterisation. *Journal of Hydrology* 350(3), 290-302.

Dean, J. M., Kemp, A. E., Bull, D., Pike, J., Patterson, G. and Zolitschka, B. (1999). Taking varves to bits: Scanning electron microscopy in the study of laminated sediments and varves. *Journal of Paleolimnology* 22(2), 121-136.

Dearing, J.A. (1986). Core correlation and total sediment influx. In: Berglund, B.E. (Ed.) *Handbook of Holocene Palaeoecology and Palaeohydrology*. Chichester: Wiley, pp. 247-270.

Dearing, J.A. (1991). Lake sediment records of erosional processes. *Hydrobiologia* 214, 99–106.

Dearing, J.A. (1999a). Holocene environmental change from magnetic proxies in lake sediments. In: Maher, B.A. and Thompson, R. (Ed.) *Quaternary Climates, Environments and Magnetism*. Cambridge: Cambridge University Press, pp. 231–278.

Dearing, J.A. (1999b). Magnetic Susceptibility. In: Walden J., Oldfield, F. and Smith, J. (Ed.) *Environmental Magnetism: a Practical Guide (Technical Guide No. 6)*. London: Quaternary research Association, pp. 35-62.

Dearing J. A. (2000). Human-environment interactions: learning from the past. In: Cohen, J. and Stewart, I. (Ed.) *The Collapse of Chaos: Simple Laws in a Complex World*. London: Viking, pp. 20-36.

Dearing J. A. (2006). Climate-human-environment interactions: resolving our past. *Climate of the Past Discussions* 2, 187–203.

Dearing, J.A. (2007). Integration of world and earth systems: heritage and foresight. In: Hornborg, A. and Crumley, C. L. (Ed.) *The World System and The Earth System: Global Socioenvironmental Change and Sustainability since the Neolithic*. Left Coast Press, pp. 38-57.

Dearing, J.A. (2008). Landscape change and resilience theory: a palaeoenvironmental assessment from Yunnan, SW China. *The Holocene* 18, 117.

Dearing, J.A., Battarbee, R.W., R., Dikau, I., Larocque, I. and Oldfield, F. (2006a). Human-environment interactions: learning from the past. *Regional Environment Change* 6, 1-16.

Dearing, J.A., Battarbee, R.W., R., Dikau, I., Larocque, I. and Oldfield, F. (2006b). Human-environment interactions: towards synthesis and simulation. *Regional Environment Change* 6, 115-123.

Dearing, J. A., Braimoh, A. K., Reenberg, A., Turner, B. L. and van der Leeuw, S. (2010). Complex land systems: the need for long time perspectives to assess their future. *Ecology and Society* 15(4), 21.

Dearing, J.A., Dann, R.J.L., Hay, K., Lees, J.A., Loveland, P.J., Maher, B.A., O'Grady, K. (1996b). Frequency-dependent susceptibility measurements of environmental samples. *Geophysical Journal International* 124, 228–240.

Dearing, J.A. and Flower, R. (1982). The magnetic susceptibility of sedimenting material trapped in Lough Neagh, Northern Ireland and its erosional significance. *Limnology and Oceanography* 17 (5), 969–975.

Dearing, J. A. and Foster, D.L. (1986). Lake sediments and palaeohydrological

studies. In: Berglund, B.E. (Ed.) *Handbook of Holocene Palaeoecology and Palaeohydrology*. Chichester: Wiley, pp. 67-87.

Dearing, J. A., Hay, K. L., Baban, S. M. J., Huddleston, A. S., Wellington, E. M. H. and Loveland, P. J. (1996a). Magnetic susceptibility of soil: an evaluation of conflicting theories using a national data set. *Geophysical Journal International* 127(3), 728-734.

Dearing, J.A. and Jones, R.T. (2003). Coupling temporal and spatial dimensions of global sediment flux through lake and marine sediment records. *Global and Planetary Change* 39, 147–168.

Dearing, J. A., Jones, R. T., Shen, J., Yang, X., Boyle, J. F., Foster, G. C., Crook, D. S. and Elvin, M. J. D. (2008). Using multiple archives to understand past and present climate–human–environment interactions: the lake Erhai catchment, Yunnan Province, China. *Journal of Paleolimnology* 40(1), 3-31.

Dearing, J.A. and Zolitschka, B. (1999). System dynamics and environmental change: an exploratory study of Holocene lake sediments at Holzmaar, Germany. *The Holocene* 9, 531-540.

Dotterweich, M. (2012). Past Soil Erosion in Central Europe: Human Impact and Long Term Effects. *Journal for ancient study* 3, pp. 39-45. In: Bebermeier, W., Hebenstreit, R., Kaiser, E. and Krause, J. (Ed.) *Landscape Archaeology: Proceedings of the International Conference*, Berlin, 6th - 8th June 2012.

Jerolmack, D.J. and Paola, C. (2007). Complexity in a cellular model of river avulsion. *Geomorphology* 91, 259–270.

Downing, R.A. (1998). *Groundwater- our hidden asset*. Nottingham: British Geological Survey, UK.

Dubois, A.D. and Ferguson, D.K. (1985). The climatic history of pine in the Cairngorms based on radiocarbon dates and stable isotope analysis, with an account of the events leading up to its colonization. *Review of Palaeobotany and Palynology* 46, 55–80.

Einstein, H.A. (1950). *The bed-load function for sediment transport on open channel flows (Technical Bulletin 1026)*. US Department of Agriculture: Soil Conservation Service, pp. 71.

Ekström, M., Fowler, H. J., Kilsby, C. G. and Jones, P. D. (2005). New estimates of future changes in extreme rainfall across the UK using regional climate model integrations. 2. Future estimates and use in impact studies. *Journal of Hydrology* 300(1), 234-251.

Emmett, W. W. and Wolman, M. G. (2001). Effective discharge and gravel-bed rivers. *Earth Surface Processes and Landforms* 26(13), 1369-1380.

Environment Agency. (2006). *Survey Results for Old Alresford Pond Sediment Survey*. Environment Agency Science Group – Technology. Unpublished Report.

Environment Agency. (2007). *Alresford Pond SSSI Water Level Management Plan*.

Epstein, J. and Axtell, R. (1996). *Growing Artificial Societies: Social Science from the Bottom Up*. Washington, DC: Brookings Institution/ MIT Press.

European Environment Agency. (2012). *Climate change, impacts and vulnerability in Europe 2012: An indicator-based report*. Denmark.

Evans, R. (1977). Overgrazing and soil erosion on hill pastures with particular reference to the Peak District. *Journal of the British Grassland Society* 32(1), 65-76.

Evans, R. (1990). Soils at risk of accelerated erosion in England and Wales. *Soil Use and Management* 6(3), 125–131.

Ewert, F., Rounsevell, M. D. A., Reginster, I., Metzger, M. J. and Leemans, R. (2005). Future scenarios of European agricultural land use: I. Estimating changes in crop productivity. *Agriculture, Ecosystems & Environment* 107(2), 101-116.

FAO. (2003). *The agricultural statistics of the Food and Agriculture Organisation of the United Nations*. [Online]. (URL www.FAO.org). (Accessed 12 February 2013).

Farrant, A.R. (2002). *Geology of the Alresford district-a brief explanation of the geological map. Sheet explanation of the British Geological Survey, 1:50 000 Sheet 300 Alresford (England and Wales)*. Nottingham: British Geological Survey, UK.

Favis-Mortlock, D.T. (1996). An evolutionary approach to the simulation of rill initiation and development. In: Abrahart, R.J. (Ed.) *Proceedings of the First International Conference on GeoComputation (Volume 1)*. School of Geography, University of Leeds, UK, pp. 248-281.

Favis-Mortlock, D. (2004). Self-organization and cellular automata models. In: Wainwright, J. and Mulligan, M. (Ed.) *Environmental modelling-finding simplicity in complexity*. London: John Wiley & Sons, pp. 349-369.

Favis-Mortlock, D.T. (2012). Non-linear dynamics, self-organization and cellular automata models. In: Wainwright, J. and Mulligan, M. (Ed.) *Environmental Modelling: Finding Simplicity in Complexity*. London: John Wiley & Sons, pp. 45-63.

Favis-Mortlock, D.T. and Boardman, J. (1995). Nonlinear responses of soil erosion to climate change: a modelling study on the UK South Downs. *Catena* 25, 365-387.

Favis-Mortlock, D.T., Boardman, J. and Bell, M. (1997). Modelling long-term anthropogenic erosion of a loess cover: South Downs, UK. *The Holocene* 7, 79-89.

Favis-Mortlock, D. T., Boardman, J., Parsons, A. J. and Lascelles, B. (2000). Emergence and erosion: a model for rill initiation and development. *Hydrological Processes* 4, 2173-2205.

Fischer, E. M., Luterbacher, J., Zorita, E., Tett, S. F. B., Casty, C. and Wanner, H. (2007). European climate response to tropical volcanic eruptions over the last half millennium. *Geophysical Research Letters* 34(5), 1-6.

Fishman, G.S. and Kiviat, P.J. (1968). The statistics of discrete event simulation. *Simulation* 10, 185-191.

Folke, C., Carpenter, S. R., Walker, B., Scheffer, M., Chapin, T. and Rockström, J. (2010). Resilience thinking: integrating resilience, adaptability and transformability. *Ecology and Society* 15(4), 20.

Fonstad, M. A. (2006). Cellular automata as analysis and synthesis engines at the geomorphology-ecology interface. *Geomorphology* 77(3), 217-234.

Fonstad, M. and Marcus, W.A. (2003). Self-organized Criticality in Riverbank Systems. *Annals of the Association of American Geographers* 93 (2), 281-296.

Foster, G. R. (1988). Modeling soil erosion and sediment yield. In: *Soil Erosion Research Methods*. Ankeny: Soil and Water Conservation Society, pp. 97-117.

Foster, I. D., Collins, A. L., Naden, P. S., Sear, D. A., Jones, J. I. and Zhang, Y. (2011). The potential for paleolimnology to determine historic sediment delivery to rivers. *Journal of Paleolimnology* 45(2), 287-306.

Foster, G. C., Dearing, J. A., Jones, R. T., Crook, D. S., Siddle, D. J., Harvey, A. M., James, P. A., Appleby, P. G., Thompson, R., Nicholson, J. and Loizeau, J. L. (2003). Meteorological and land use controls on past and present hydro-geomorphic processes in the pre-alpine environment: an integrated lake-catchment study at the Petit Lac d'Annecy, France. *Hydrological Processes* (16), 3287-3305.

Foster, I. D. L. and Walling, D. E. (1994). Using reservoir deposits to reconstruct changing sediment yields and sources in the catchment of the Old Mill Reservoir, South Devon, over the past 50 years. *Hydrological Sciences Journal* 39, 347–368.

Foulds, S.A., Macklin, M.G. and Brewer, P.A. (2013). Agro-industrial alluvium in the Swale catchment, northern England, as an event marker for the Anthropocene. *The Holocene* 23(4), 587-602.

Fowler, A. M. and Hennessy, K. J. (1995). Potential impacts of global warming on the frequency and magnitude of heavy precipitation. *Natural Hazards* 11, 283–303.

Fowler, H. J., Kilsby, C. G., Webb, B., Arnell, N., Onof, C., MacIntyre, N., Gurney, R. and Kirby, C. (2004). Future increase in UK water resource drought projected by

a regional climate model. In: British Hydrological Society (Ed.) *Hydrology: science and practice for the 21st century. Proceedings of the British Hydrological Society International Conference*. London: Imperial College, pp. 15-21.

Fuhrmann, A., Fischer, T., Lücke, A., Brauer, A., Zolitschka, B., Horsfield, B., Negendank, J. F. W., Schleser, G. H. and Wilkes, H. (2004). Late Quaternary environmental and climatic changes in central Europe as inferred from the composition of organic matter in annually laminated maar lake sediments. *Geochemistry, Geophysics, Geosystems (G3)* 5 (11), 1-20.

Fullen, M. A. (1985). Erosion of arable soils in Britain. *International Journal of Environmental Studies* 25, 55–69.

De Geer, G. (1912). A Geochronology of the Last 12,000 Years. In: *11th International Geological Congress, 1910*. Stockholm, Sweden, pp. 241-253.

Ghaffari, G., Keesstra, S., Ghodousi, J. and Ahmadi, H. (2009). SWAT- simulated hydrological impact of land-use change in the Zanjanrood basin, Northwest Iran. *Hydrological processes* 24(7), 892-903.

Goldberg, E.D. (1985). *Black carbon in the environment: Properties and Distribution*. New York: Wiley Interscience Publication, pp.198.

Gomez, B., Page, M., Bak, P. and Trustrum, N. (2002). Self-organized criticality in layered, lacustrine sediments formed by landsliding. *Geology* 30(6), 519-522.

Goslar, T., Arnold, M., Bard, E., Kuc, T., Pazdur, M. F., Ralska-Jasiewiczowa, M., Rozanski, K., Tisnerat, N., Walanus, A., Wicik, B. and Wieckowski, K. (1995). High concentration of atmospheric ^{14}C during the Younger Dryas cold episode. *Nature* 377(6548), 414-417.

Goslar, T., Kuc, T., Ralska-Jasiewiczowa, M., Różanski, K., Arnold, M., Bard, E., Van Geel, B., Pazdur, M. F., Szeroczyńska, K., Wicik, B., Wieckowski, K. and Walanus, A. (1993). High-resolution lacustrine record of the Late Glacial/Holocene transition in Central Europe. *Quaternary Science Reviews* 12(5), 287-294.

Gregory, K. J. and Walling, D. E. (1973). *Drainage basin form and process: a geomorphological approach*. London: Arnold.

Grimm, V. and Railsback, S. F. (2005). *Individual-based modeling and ecology*. Princeton: Princeton university press.

Grönlund, E. (1991). Sediment characteristics in relation to cultivation history in two varved lake sediments from East Finland. *Hydrobiologia*, 214, 137-142.

Grimm, V., Berger, U., Bastiansen, F., Eliassen, S., Ginot, V., Giske, J., Goss-Custard, J., Grandf, T., Heinz, S.M., Huse, G., Huth, A., Jepsen, J. U., Jørgensen, C., Mooij, W. M., Müller, B., Pe'er, G., Piou, C., Railsback, S. F., Robbins, A. M., Robbins, M. M., Rossmanith, E., Rüger, N., Strand, E., Souissi, S., Stillman, R. A., Vabø, R., Visser, U. and DeAngelis, D. L. (2006). A standard protocol for describing individual-based and agent-based models. *Ecological modelling* 198(1), 115-126.

Grimm, V., Revilla, E., Berger, U., Jeltsch, F., Mooij, W. M., Railsback, S. F., Thulke, H. H., Weiner, J., Wiegand, T. and DeAngelis, D. L. (2005). Pattern-oriented modeling of agent-based complex systems: lessons from ecology. *Science* 310 (5750), 987-991.

Gustard, A. (1996). River flow regimes. In: Petts, G. E. and Calow, P. (Ed.) *River Flows & Channel Forms*. Oxford: Blackwell Scientific, pp.37-58.

Haas, J.N., Richoz, I., Tinner, W., Wick, L. (1998). Synchronous Holocene climatic oscillations recorded on the Swiss Plateau and at timberline in the Alps. *The Holocene* 8, 301–309.

Hajdas, I., Bonani, G. and Zolitschka, B. (2000). Radiocarbon dating of varve chronologies; Soppensee and Holzmaar lakes after ten years. *Radiocarbon* 42(3), 349-353.

Hancock, G.R. (2006). The impact of different gridding methods on catchment geomorphology and soil erosion over long timescales using a landscape evolution model. *Earth Surface Processes and Landforms* 31, 1035–1050.

Hancock, G. R. (2012). Modelling stream sediment concentration: An assessment of enhanced rainfall and storm frequency. *Journal of Hydrology* 430-431, 1-12.

Hancock, G. R., Coulthard, T. J., Martinez, C. and Kalma, J. D. (2011). An evaluation of landscape evolution models to simulate decadal and centennial scale soil erosion in grassland catchments. *Journal of Hydrology* 398(3), 171-183.

Harris, C. N. P., Quinn, A. D. and Bridgeman, J. (2012). The use of probabilistic weather generator information for climate change adaptation in the UK water sector. [Online]. (URL <http://onlinelibrary.wiley.com/doi/10.1002/met.1335/full>). *Meteorological Applications*. (Accessed 12 February 2013).

Hay, K. L., Dearing, J. A., Baban, S. M. J. and Loveland, P. (1997). A preliminary attempt to identify atmospherically-derived pollution particles in English topsoils from magnetic susceptibility measurements. *Physics and Chemistry of the Earth* 22(1), 207-210.

Haygarth, P. M. and Ritz, K. (2009). The future of soils and land use in the UK: Soil systems for the provision of land-based ecosystem services. *Land Use Policy* 26, 187-197.

He, Q., Walling, D.E. and Owens, P.N. (1996). Interpreting the ^{137}Cs profiles observed in several small lakes and reservoirs in southern England. *Chemical Geology* 129, 115-131.

Headworth, H. G. (1978). Hydrogeological characteristics of artesian boreholes in the Chalk of Hampshire. *Quarterly Journal of Engineering Geology and Hydrogeology* 11, 139-144.

Henriques, C., Holman, I. P., Audsley, E. and Pearn, K. (2008). An interactive multi-scale integrated assessment of future regional water availability for agricultural irrigation in East Anglia and North West England. *Climatic Change* 90, 89-111.

Herbig, C. and Sirocko, F. (2013). Palaeobotanical evidence for agricultural activities in the Eifel region during the Holocene: plant macro-remain and pollen

analyses from sediments of three maar lakes in the Quaternary Westeifel Volcanic Field (Germany, Rheinland-Pfalz). *Vegetation History and Archaeobotany*, 1-16.

Hernandez, M., Miller, S. N., Goodrich, D. C., Goff, B. F., Kepner, W. G., Edmonds, C. M. and Jones, K. B. (2000). Modelling runoff response to land cover and rainfall spatial variability in semi-arid watersheds. In: *Monitoring Ecological Condition in the Western United States*. Netherlands: Springer, pp. 285-298.

Heung, B., Bakker, L., Schmidt, M. G. and Dragičević, S. (2013). Modelling the dynamics of soil redistribution induced by sheet erosion using the Universal Soil Loss Equation and cellular automata. *Geoderma* 202, 112-125

Hicks, S., Miller, U. and Saarnisto, M. (1994). Laminated sediments. *Journal of the European Study Group on Physical, Chemical, Biological and Mathematical Techniques Applied to Archaeology* 41, 148.

Hoey, T. and Ferguson, R. (1994). Numerical simulation of downstream fining by selective transport in gravel bed rivers: Model development and illustration. *Water Resources Research* 30(7), 2251–2260.

Hooke, J.M. (1984). Changes in river meanders: a review of techniques and results of analysis. *Progress in Physical Geography* 8, 473–508.

Huggett, R. J. (1988). Dissipative systems: implications for geomorphology. *Earth Surface Processes and Landforms* 13(1), 45-49.

Hunt, J.C.R. (2002). Floods in a changing climate: a review. *Philosophical Transactions of the Royal Society of London* 360, 1531–1543.

Huntington, T. G. (2006). Evidence for intensification of the global water cycle: Review and synthesis. *Journal of Hydrology* 319 (1-4), 83-95.

Ibañez, J.J., Pérez-González, A., Jiménez- Ballesta, R., Saldaña, A. and Gallardo-Díaz, J. (1994). Evolution of fluvial dissection landscapes in mediterranean environments. Quantitative estimates and geomorphological, pedological, and phytocenotic repercussions. *Zeitschrift für Geomorphologie* 38, 105–109.

IPCC. (2007). *Climate Change 2007: The physical science basis*. Cambridge, United Kingdom: Contribution of Working Group I to the Fourth Assessment Report of the Intergovernmental Panel on Climate Change.

Isee Systems. (2006). *Technical document for the iThink and STELLA software*. [Online]. (URL <http://www.iseesystems.com>). (Accessed 10 September 2010).

James, L.A. & Marcus, W.A. (2006). The human role in changing fluvial systems: Retrospect, inventory and prospect. *Geomorphology* 79, 152-171.

Jenkins, G. J., Murphy, J. M., Sexton, D. M. H., Lowe, J. A., Jones, P. and Kilsby, C. G. (2009). *UK Climate Projections: Briefing report*. Exeter, UK: Met Office Hadley Centre.

Jones, P. D., Harpham, C., Goodess, C. M. and Kilsby, C. G. (2011). Perturbing a Weather Generator using change factors derived from Regional Climate Model simulations. *Nonlinear Processes in Geophysics* 18(4), 503-511.

Jones, P. D. and Reid, P. A. (2001). Assessing future changes in extreme precipitation over Britain using regional climate model integrations. *International Journal of Climatology* 21(11), 1337-1356.

Johnson, A. C., Acreman, M. C., Dunbar, M. J., Feist, S. W., Giacomello, A. M., Gozlan, R. E., Hinsley, S.A., Ibbotson, A.T., Jarvie, H.P., Jones, J.I., Longshaw, M., Maberly, S.C., Marsh, T.J., C. Neal, J.R. Newman, M.A. Nunn, R.W. Pickup, N.S. Reynard, C.A. Sullivan, J.P. Sumpter and Williams, R. J. (2009). The British river of the future: how climate change and human activity might affect two contrasting river ecosystems in England. *Science of the Total Environment* 407(17), 4787-4798.

Johnson, D. R., Ruzek, M. and Kalb, M. (1997). What is Earth system science?. In: Geoscience and Remote Sensing (IGARSS'97). *Remote Sensing-A Scientific Vision for Sustainable Development* 2, 688-691.

Karl, T. R. and Knight, R.W. (1998). Secular trends of precipitation amount, frequency, and intensity in the United States. *Bulletin of the American Meteorological Society* 79, 231-241.

Kapička, A., Jordanova, N., Petrovský, E. and Ustjak, S. (2000). Magnetic stability of power-plant fly ash in different soil solutions. *Physics and Chemistry of the Earth, Part A: Solid Earth and Geodesy* 25(5), 431-436.

Kay, A. L., Jones, R. G. and Reynard, N. S. (2006). RCM rainfall for UK flood frequency estimation. II. Climate change results. *Journal of Hydrology* 318(1), 163-172.

Kienel, U., Schwab, M. J. and Schettler, G. (2005). Distinguishing climatic from direct anthropogenic influences during the past 400 years in varved sediments from Lake Holzmaar (Eifel, Germany). *Journal of Paleolimnology* 33(3), 327-347.

Kirkby, M. J., Abrahart, R., McMahon, M. D., Shao, J. and Thornes, J. B. (1998). MEDALUS soil erosion models for global change. *Geomorphology* 24(1), 35-49.

Kilsby, C. G., Jones, P. D., Burton, A., Ford, A. C., Fowler, H. J., Harpham, C., James, P., Smith, A. and Wilby, R. L. (2007). A daily weather generator for use in climate change studies. *Environmental Modelling & Software* 22(12), 1705-1719.

Klaminder, J., Appleby, P., Crook, P. and Renberg, I. (2012). Post-deposition diffusion of ^{137}Cs in lake sediment: Implications for radiocaesium dating. *Sedimentology* 59(7), 2259-2267.

Kleinen, T., Tarasov, P., Brovkin, V., Andreev, A. and Stebich, M. (2011). Comparison of modeled and reconstructed changes in forest cover through the past 8000 years Eurasian perspective. *The Holocene* 21(5), 723-734.

Knighton, D. (1998). *Fluvial Forms and Processes: A New Perspective*. London: Arnold.

Knox, J. C. (2000). Sensitivity of modern and Holocene floods to climate change. *Quaternary Science Reviews* 19, 439-457.

Kosmas, C., Danalatos, N., Cammeraat, L. H., Chabart, M., Diamantopoulos, J., Farand, R., Gutierrez, L., Jacob, A., Marques, H., Martinez-Fernandez, J., Mizara, A., Moustakas, N., Nicolau, J.M., Oliveros, C., Pinna, G., Puddu, R., Puigdefabregas,

- J., Roxo, M., Simao, A., Stamou, G., Tomasi, N., Usaian, D. and Vacca, A. (1997). The effect of land use on runoff and soil erosion rates under Mediterranean conditions. *Catena* 29(1), 45-59.
- Kubitz, S. (2000). Die holozäne Vegetations- und Siedlungsgeschichte in der Westeifel am Beispiel eines hochauflösenden Pollendiagramms aus dem Meerfelder Maar. *Diss Bot* 339, Cramer, Stuttgart Berlin.
- Kühl, N., Moschen, R., Wagner, S., Brewer, S. and Peyron, O. (2010). A multiproxy record of late Holocene natural and anthropogenic environmental change from the Sphagnum peat bog Dürres Maar, Germany: implications for quantitative climate reconstructions based on pollen. *Journal of Quaternary Science* 25 (5), 675–688.
- Lambin, E.F. (2004). Modelling land-use change. In: Wainwright, J. and Mulligan, M. (Ed.) *Environmental Modelling: Finding Simplicity in Complexity*. London: John Wiley & Sons, pp. 245-253.
- Lamoureux, S. (2001). Varve chronology techniques. In: Last, W.M. and Smol, J.P. (Ed.) *Tracking Environmental Change Using Lake Sediments: Basin Analysis, Coring, and Chronological Techniques (vol. 1)*. Dordrecht: Kluwer Academic Publishers, pp. 247-260.
- Landmann, G., Reimer, A., Lemcke, G. & Kempe, S. (1996). Dating Late Glacial abrupt climate changes in the 14,570 yr long continuous varve record of Lake Van, Turkey. *Palaeogeography, Palaeoclimatology, Palaeoecology* 122(1), 107-118.
- Lane, S. N., Tayefi, V., Reid, S. C., Yu, D. and Hardy, R. J. (2007). Interactions between sediment delivery, channel change, climate change and flood risk in a temperate upland environment. *Earth Surface Processes and Landforms* 32(3), 429-446.
- Lang, A. and Zolitschka, B. (2001). Optical dating of annually laminated lake sediments A test case from Holzmaar/Germany. *Quaternary Science Reviews* 20(5), 737-742.
- Lawton, J. (2001). Earth system science. *Science* 292(5524), 1965-1965.

- Leopold, L.B., Wolman, M.G. and Miller, J.P. (1964). *Fluvial Processes in Geomorphology*. San Francisco: Freeman and Company.
- Leroy, S. A. G., Zolitschka, B., Negendank, J. F. W. and Seret, G. (2000). Palynological analyses in the laminated sediment of Lake Holzmaar (Eifel, Germany): duration of Lateglacial and Preboreal biozones. *Boreas* 29, 52-71.
- Lewin, J., Macklin, M. G. and Johnstone, E. (2005). Interpreting alluvial archives: sedimentological factors in the British Holocene fluvial record. *Quaternary Science Reviews* 24(16), 1873-1889.
- Li, W. (1992). Phenomenology of nonlocal cellular automata. *Journal of Statistical Physics* 68(5-6), 829-882.
- Licciardello, F., Govers, G., Cerdan, O., Kirkby, M. J., Vacca, A. and Kwaad, F. J. P. M. (2009). Evaluation of the PESERA model in two contrasting environments. *Earth surface processes and landforms* 34(5), 629-640.
- Limbrick, K.J. (2002). Estimating daily recharge to the Chalk aquifer of southern England – a simple methodology. *Hydrology and Earth System Sciences* 6(3), 485-495.
- Litt, T., Brauer, A., Goslar, T., Merkt, J., Balaga, K., Müller, H., Ralska-Jasiewiczowa, M., Stebich, M. & Negendank, J. F. (2001). Correlation and synchronisation of Lateglacial continental sequences in northern central Europe based on annually laminated lacustrine sediments. *Quaternary Science Reviews* 20(11), 1233-1249.
- Litt, T. and Stebich, M. (1999). Bio- and chronostratigraphy of the Lateglacial in the Eifel region, Germany. *Quaternary International* 61, 5-16.
- Litt, T., Schölzel, C., Kühl, N. and Brauer, A. (2009). Vegetation and climate history in the Westeifel Volcanic Field (Germany) during the past 11 000 years based on annually laminated lacustrine maar sediments. *Boreas* 38, 679-690.

- Loáiciga, H. A. (2003). Climate Change and Ground Water. *Annals of the Association of American Geographers* 93 (1), pp. 30-41.
- Loch, R. J. (2000). Effects of vegetation cover on runoff and erosion under simulated rain and overland flow on a rehabilitated site on the Meandu Mine, Tarong, Queensland. *Soil Research* 38(2), 299-312.
- Löhr, H. and Nortmann, H. (2008). Sichtbares und Unsichtbares. In: Trier, R.L. (Ed.) *Führer zu Archäologischen Denkmälern des Trierer Landes*. Dillingen/Saar, pp. 11–33.
- Longmore, M.E. (1982). The caesium-137 dating technique and associated applications in Australia-a review. In: Ambrose, W. and Duerden, P. (Ed.) *Archaeometry: An Australasian perspective*. Canberra, Australia: Australian National University Press, pp. 310-321.
- Lorenz, V. (1973). On the formation of maars. *Bulletin Volcanologique* 37(2), pp. 183-204.
- Lotter, A.F. (1991). Absolute dating of the late-glacial period in Switzerland using annually laminated sediments. *Quaternary Research* 35, 321-330.
- Lotter, A. F. and Birks, H. J. B. (1997). The separation of the influence of nutrients and climate on the varve time-series of Baldeggersee (Switzerland). *Aquatic Sciences* 59, 362-373.
- Lottermoser, B. G., Schütz, U., Boenecke, J., Oberhänsli, R., Zolitschka, B. and Negendank, J. F. W. (1997). Natural and anthropogenic influences on the geochemistry of Quaternary lake sediments from Holzmaar, Germany. *Environmental Geology* 31(3-4), 236-247.
- Lu, S. G., Bai, S. Q. and Xue, Q. F. (2007). Magnetic properties as indicators of heavy metals pollution in urban topsoils: a case study from the city of Luoyang, China. *Geophysical Journal International* 171(2), 568-580.

- Lücke, A., Schleser, G. H., Zolitschka, B. and Negendank, J. F. (2003). A Lateglacial and Holocene organic carbon isotope record of lacustrine palaeoproductivity and climatic change derived from varved lake sediments of Lake Holzmaar, Germany. *Quaternary Science Reviews* 22(5), 569-580.
- Lüder, B., Kirchner, G., Lücke, A. and Zolitschka, B. (2006). Palaeoenvironmental reconstructions based on geochemical parameters from annually laminated sediments of Sacrower See (northeastern Germany) since the 17th century. *Journal of Paleolimnology* 35(4), 897-912.
- Ma, T. (2009). Modelling of Hillslope Runoff and Soil Erosion at Rainfall Events Using Cellular automata Approach. *Pedosphere* 19 (6), 711-718.
- Sloth Madsen, M., Maule, C. F., MacKellar, N., Olesen, J. E. and Christensen, J. H. (2012). Selection of climate change scenario data for impact modelling. *Food Additives & Contaminants: Part A* 29(10), 1502-1513.
- MAFF. (2000). *Climate change and agriculture in the Kingdom*. Ministry of Agriculture, Fisheries and Food (United Kingdom).
- Magny, M. (1992). Holocene lake-level fluctuations in Jura and the northern subalpine ranges, France: regional pattern and climatic implications. *Boreas* 21, 319-334.
- Macklin, M. G., Jones, A. F. and Lewin, J. (2010). River response to rapid Holocene environmental change: evidence and explanation in British catchments. *Quaternary Science Reviews* 29(13), 1555-1576.
- Macklin, M. G., Benito, G., Gregory, K. J., Johnstone, E., Lewin, J., Michczyńska, D. J., Soja, R., Starkel, V.R. and Thorndycraft, V. R. (2006). Past hydrological events reflected in the Holocene fluvial record of Europe. *Catena* 66(1), 145-154.
- Macklin, M. G. and Lewin, J. (2008). Alluvial responses to the changing Earth system. *Earth Surface Processes and Landforms* 33, 1374-1395.

Macklin, M. G., Lewin, J. and Woodward, J. C. (2012). The fluvial record of climate change. *Philosophical Transactions of the Royal Society A: Mathematical, Physical and Engineering Sciences* 370 (1966), 2143-2172.

Macklin, M. G. and Rumsby, B. T. (2007). Changing climate and extreme floods in the British uplands. *Transactions of the Institute of British Geographers* 32, 168-186.

Maher, B. A. (1998). Magnetic properties of modern soils and Quaternary loessic paleosols: paleoclimatic implications. *Palaeogeography, Palaeoclimatology, Palaeoecology* 137(1), 25-54.

Malanson, G.P. (1999). Considering complexity. *Annals of the Association of American Geographers* 89(4), 746-753

Manson, S.M. (2001). Simplifying complexity: a review of complexity theory. *Geoforum* 32(3), 405-414.

Manson, S.M. (2009). Complexity, Chaos and Emergence. In: Castree, N., Demeritt, D., Liverman, D. and Rhoads, B. (Ed.) *A Companion to Environmental Geography*. Oxford: Wiley-Blackwell.

Maraun, D., Wetterhall, F., Ireson, A. M., Chandler, R. E., Kendon, E. J., Widmann, M., Brienen, S., Rust, H. W., Sauter, T., Themeßl, M., Venema, V. K. C., Chun, K. P., Goodess, C. M., Jones, R. G., Onof, C., Vrac, M. and Thiele-Eich, I. (2010). Precipitation downscaling under climate change: Recent developments to bridge the gap between dynamical models and the end user. *Reviews of Geophysics* 48(3), 1-34.

Marsh, T. J. and Monkhouse, R. A. (1993). Drought in the United Kingdom, 1988 - 92. *Weather*, 48(1): 15-22.

Marshall, M. R., O. J. Francis, Z. L. Frogbrook, B. M. Jackson, N. McIntyre, B. Reynolds, I. Solloway, H. S. Wheeler & J. Chell (2009) The impact of upland land management on flooding: results from an improved pasture hillslope. *Hydrological Processes*, 23: 464-475.

- Marshall, M. R., Francis, O. J., Frogbrook, Z. L., Jackson, B. M., McIntyre, N., Reynolds, B., Solloway, I., Wheater, H. S. and Chell, J. (2009). The impact of upland land management on flooding: results from an improved pasture hillslope. *Hydrological Processes* 23(3), 464-475.
- Martins, C. C., Bicego, M. C., Rose, N. L., Taniguchi, S., Lourenço, R. A., Figueira, R. C.L., Mahiques, M. M. and Montone, R.C. (2010). Historical record of polycyclic aromatic hydrocarbons (PAHs) and spheroidal carbonaceous particles (SCPs) in marine sediment cores from Admiralty Bay, King George Island, Antarctica. *Environmental Pollution* (2010), 192–200.
- McHenry, J.R. and Bubenzer, G.B. (1985). Field erosion estimated from ^{137}Cs activity measurements. *Transactions of the American Society of Agricultural Engineers* 28, 480-483.
- Melville, R.V. and Freshney, R.C. (1982). *The Hampshire Basin and adjoining areas*. London: Geological Sciences Institute.
- Merkt, J. and Müller, H. (1999). Varve chronology and palynology of the Lateglacial in Northwest Germany from lacustrine sediments of Hämelsee in Lower Saxony - a widespread isochronous late Quaternary tephra layer in central and northern Europe. *Quaternary International* 61, 41-59.
- Michaelides, K. and Wainwright, J. (2004). Modelling Fluvial Processes and Interactions. In: Wainwright, J. and Mulligan, M. (Ed.) *Environmental Modelling: Finding Simplicity in Complexity*. London: John Wiley & Sons, pp. 123-138.
- Middelkoop, H., Daamen, K., Gellens, D., Grabs, W., Kwadijk, J. C. J., Lang, H., Parmet, B. W. A. H., Schädler, B., Schulla, J. and Wilke, K. (2001). Impact of climate change on hydrological regimes and water resources management in the Rhine basin. *Climatic Change* 49, 105-128.
- Miller, A. J. (1990). Flood hydrology and geomorphic effectiveness in the central Appalachians. *Earth Surface Processes and Landforms* 15(2), 119-134.

Milly, P. C. D., Julio, B., Malin, F., Robert, M. H., Zbigniew, W. K., Dennis, P. L. and Ronald, J. S. (2008). Stationarity Is Dead: Whither Water Management?. *Science* 319, 573-574.

Milly, P.C.D, Wetherald, R.T., Dunne, K.A. and Delworth, T.L. (2000). Increasing risk of great floods in a changing climate. *Nature* 415, 514–517.

Monkhouse, F.J. (1964). *A Survey of Southampton and its region*. Southampton: British Association for the Advancement of Science.

De Moor, J. J. W. and Verstraeten, G. (2008). Alluvial and colluvial sediment storage in the Geul River catchment (The Netherlands)—combining field and modelling data to construct a Late Holocene sediment budget. *Geomorphology* 95(3), 487-503.

Morgan, R. P. C. (1980). Soil erosion and conservation in Britain. *Progress in Physical Geography* 4 (1), 24-47.

Morgan, R.P.C., (1995). *Soil Erosion and Conservation*. London: Longman, pp.37.

Moschen, R., Lucke, A., Parplies, J. and Schleser, G. H. (2009). Controls on the seasonal and interannual dynamics of organic matter stable carbon isotopes in mesotrophic Lake Holzmaar, Germany. *Limnology and Oceanography* 54(1), 194-209.

Mullan, D., Favis-Mortlock, D. and Fealy, R. (2012). Addressing key limitations associated with modelling soil erosion under the impacts of future climate change. *Agricultural and Forest Meteorology* 156, 18-30.

Mulligan, M. and Wainwright, J. (2012a). Modelling and Model Building. In: Wainwright, J. and Mulligan, M. (Ed.) *Environmental Modelling: Finding Simplicity in Complexity*. London: John Wiley & Sons, pp.11.

Mulligan, M. and Wainwright, J. (2012b). Modelling catchment and fluvial processes and their interactions. In: Wainwright, J. and Mulligan, M. (Ed.)

Environmental Modelling: Finding Simplicity in Complexity. London: John Wiley & Sons, pp. 183-201.

Mullins, C.E. (1977). Magnetic susceptibility of the soil and its significance in soil science: a review. *Journal of Soil Science* 28, 223-246.

Murphy, J.M., Sexton, D.M.H., Jenkins, G.J., Booth, B.B.B., Brown, C.C., Clark, R.T., Collins, M., Harris, G.R., Kendon, E.J., Betts, R.A., Brown, S.J., Humphrey, K.A., McCarthy, M.P., McDonald, R.E., Stephens, A., Wallace, C., Warren, R., Wilby, R. and Wood, R.A. (2009). *Climate change projections (UK Climate Projections Science Report)*. Exeter: Met Office Hadley Centre.

Murray, A. B. (2007). Reducing model complexity for explanation and prediction. *Geomorphology* 90, 178–191.

Murray, A. B. and Paola, C. (1994). A cellular model of braided rivers. *Nature* 371(1), 54–57.

Murray, A. B. and Paola, C. (1997). Properties of a cellular braided-stream model. *Earth Surface Processes and Landforms* 22 (11), 1001–1025.

Murray, A. B., Lazarus, E., Ashton, A., Baas, A., Coco, G., Coulthard, T., Fonstad, M., Haff, P., McNamara, D., Paola, C., Pelletier, J. and Reinhardt, L. (2009). Geomorphology, complexity, and the emerging science of the Earth's surface. *Geomorphology* 103(3), 496-505.

Mutter, G.M. and Burnham, C.P. (1990). Plot studies comparing water erosion on chalky and Non-calcareous soils. In: Bordman, J., Foster, I. D. L. and Dearing, J.A. (Ed.) *Soil Erosion on Agriculture Land*. Chichester: John Wiley & Sons Ltd, pp. 15-23.

Nakićenović, N., Alcamo, J., Davis, G., de Vries, B., Fenhann, J., Gaffin, S., Gregory, K., Grübler, A., Jung, T.Y., Kram, T., La Rovere, E.L., Michaelis, L., Mori, S., Morita, T., Pepper, W., Pitcher, H., Price, L., Riahi, K., Roehrl, A., Rogner, H.H., Sankovski, A., Schlesinger, M., Shukla, P., Smith, S., Swart, R., van Rooijen, S.,

Victor, N. and Dadi, Z. (2000). *IPCC Special Report on Emissions Scenarios*. Cambridge University Press.

Nature England. (2009). *Condition of SSSI units for Alresford Pond*. [Online] (URL http://www.sssi.naturalengland.org.uk/Special/sssi/sssi_details.cfm?sssi_id=1003457). (Accessed 5 December 2012).

Nearing, M. A., Jetten, V., Baffaut, C., Cerdan, O., Couturier, A., Hernandez, M., Le Bissonnais, L., Nichols, M.H., Nunes, J.P., Renschler, C.S., Souchère, V. and Van Oost, K. (2005). Modeling response of soil erosion and runoff to changes in precipitation and cover. *Catena* 61(2), 131-154.

Nearing, M. A., Lane, L. J. and Lopes, V. L. (1994). Modeling soil erosion. In: Lai, R. (Ed.) *Soil Erosion Research Methods*. Soil and Water Conservation Society and St. Lucie Press, pp. 127-156.

NECSI research project. (2012). Visualizing Complex Systems Science (CSS): Characteristics of Complex Systems. [Online]. (URL <http://necsi.edu/projects/mclemens/viscss.html>). (Accessed 10 June 2013).

Negendank, J.EW., Brauer, A. and Zolitschka, B. (1990). Die Eifelmaare als erdgeschichtliche Fallen und Quellen zur Rekonstruktion des Palaeoenvironments. *Mainzer Geowissenschaftliche Mitteilungen* 19, 235-262.

Negendank, J. and Zolitschka, B. (1993) Maars and maar lakes of the Westeifel Volcanic Field. In: Negendank, F. and Zolitschka, B. (Ed.) *Paleolimnology of European Maar Lakes. Lecture Notes in Earth Sciences* 49, 61–80. Berlin and Heidelberg: Springer-Verlag.

Neugebauer, I., Brauer, A., Dräger, N., Dulski, P., Wulf, S., Plessen, B., Mingram, J., Herzsuh, U. and Brande, A. (2012). A Younger Dryas varve chronology from the Rehwise palaeolake record in NE-Germany. *Quaternary Science Reviews* 36, 91-102.

Newson, M. (1980). The geomorphological effectiveness of floods-a contribution stimulated by two recent events in mid-wales. *Earth Surface Processes* 5(1), 1-16.

Newson, M. (1994). *Hydrology and the River Environment*. New York: Oxford University Press.

Nicholas, A.P. (2005). Cellular modelling in fluvial geomorphology. *Earth Surface Processes and Landforms* 30, 645–649.

Nowaczyk, N. R. (2001). Logging of magnetic susceptibility. In: Last, W. M. and Smol, J. P. (Ed.) *Tracking Environmental Change Using Lake Sediments. Volume 1: Basin Analysis, Coring, and Chronological Techniques*. Dordrecht: Kluwer Academic Publishers, pp. 155-170.

Odgaard, B. V. (1993). The sedimentary record of spheroidal carbonaceous fly-ash particles in shallow Danish lakes. *Journal of Paleolimnology* 8(3), 171-187.

Ojala, A. E. (2005). Application of X-ray radiography and densitometry in varve analysis. In: *Image Analysis, Sediments and Paleoenvironments*. Netherlands: Springer, pp. 187-202.

Ojala, A. E., Alenius, T., Seppä, H. and Giesecke, T. (2008). Integrated varve and pollen-based temperature reconstruction from Finland: evidence for Holocene seasonal temperature patterns at high latitudes. *The Holocene* 18(4), 529-538.

Ojala, A. E. and Francus, P. (2002). Comparing X-ray densitometry and BSE-image analysis of thin section in varved sediments. *Boreas* 31(1), 57-64.

Ojala, A. E. K., Francus, P., Zolitschka, B., Besonen, M. and Lamoureux, S. F. (2012). Characteristics of sedimentary varve chronologies-A review. *Quaternary Science Reviews* 43, 45-60.

Ojala, A. E. and Tiljander, M. (2003). Testing the fidelity of sediment chronology: comparison of varve and paleomagnetic results from Holocene lake sediments from central Finland. *Quaternary Science Reviews* 22(15), 1787-1803.

Oldfield, F. (1977). Lakes and their drainage basins as units of sediment based ecological study. *Progress in Physical Geography* 1, 460–504.

Oldfield, F. (2007). Toward developing synergistic linkages between the Biophysical and the culture: a paleoenvironmental perspective. In: Hornborg, A. and Crumley, C. L. (Ed.) *The World System and The Earth System: Global Socioenvironmental Change and Sustainability since the Neolithic*. Left Coast Press, pp. 29-37.

Oldfield, F. and Appleby, P. G. (1984). A combined radiometric and mineral magnetic approach to recent geochronology in lakes affected by catchment disturbance and sediment redistribution. *Chemical geology* 44(1), 67-83.

Oldfield, F., Crooks, P. R., Harkness, D. D. and Petterson, G. (1997). AMS radiocarbon dating of organic fractions from varved lake sediments: an empirical test of reliability. *Journal of Paleolimnology* 18(1), 87-91.

Oldfield, F. and Dearing, J.A. (2003). The role of human activities in past environmental change. In: Alverson, K., Bradley, R.S. and Petterson, T.F. (Ed.) *Paleoclimate, global change and the future*. Springer, 143-62.

Oldfield, F., Hunt, A., Jones, M.D.H., Chester, R., Dearing, J.A., Olsson, L. and Prospero, J.M. (1985). *Magnetic differentiation of atmospheric dusts*, Nature 317, 516-518.

Oldfield, F., Maher, B.A. and Appleby, P.G. (1989) Sediment source variations and ^{210}Pb inventories in recent Potomac Estuary sediment cores. *Journal of Quaternary Science* 4, 189–200.

Ollier, C. D. (1967). Maars their characteristics, varieties and definition. Bulletin Volcanologique, 31 (1), pp. 45-73.

Olsson, I.U. (1986). Radiometric dating. In: Berglund, B.E. (Ed.) *Handbook of Holocene palaeoecology and palaeohydrology*. Chichester: John Wiley and Sons Ltd, pp. 273-306.

Osborn, T. J. and Hulme, M. (2002). Evidence for trends in heavy rainfall events over the UK. *Philosophical Transactions of the Royal Society of London. Series A: Mathematical, Physical and Engineering Sciences* 360(1796), 1313-1325.

- Osborn, T.J., Hulme, M., Jones, P. D and Basnett, T.A. (2000). Observed trends in the daily intensity of United Kingdom precipitation. *International Journal of Climatology* 20, 347–364.
- Paczuski, M. and Bak, P. (1999). *Self-organisation of complex systems*. [Online]. (URL <http://xxx.lanl.gov/list/cond-mat/9906>). (Accessed 20 April 2013).
- Pagels, H.R. (1988). *The Dreams of Reason*. New York: Bantam, pp.36.
- Pall, P., Aina, T., Stone, D. A., Stott, P. A., Nozawa, T., Hilberts, A. G., Lohmann, D. and Allen, M. R. (2011). Anthropogenic greenhouse gas contribution to flood risk in England and Wales in autumn 2000. *Nature* 470(7334), 382-385.
- Pandey, A., Chowdary, V. M., Mal, B. C. and Billib, M. (2009). Application of the WEPP model for prioritization and evaluation of best management practices in an Indian watershed. *Hydrological Processes* 23, 2997–3005.
- Paola, C. (2000). Quantitative models of sedimentary basin filling. *Sedimentology* 47 (1), 121–178.
- Parker, G. (1990). Surface based bedload transport relation for gravel rivers. *Journal of Hydraulic Research* 4, 417–436.
- Patzelt, G. and Bortenschlager, S. (1973). Die postglazialen Gletscher-und Klimaschwankungen in der Venedigergruppe (Hohe Tauern, Ostalpen). *Zeitschrift fur Geomorphologie Neue Folge* 16 (Supplement), 25-72.
- Pauling, A., Luterbacher, J., Casty, C. and Wanner, H. (2006). Five hundred years of gridded high-resolution precipitation reconstructions over Europe and the connection to large-scale circulation. *Climate Dynamics* 26(4), 387-405.
- Perry, G.L.W. (2009). Modeling and simulation. In: Castree, N., Demeritt, D., Liverman, D. and Rhoads, B. (Ed.) *A Companion to Environmental Geography*. Oxford: Wiley-Blackwell.

- Perry, G.L.W. and Bond, N.R. (2012). Spatial Population Models for Animals. In: Wainwright, J. and Mulligan, M. (Ed.) *Environmental Modelling: Finding Simplicity in Complexity*. London: John Wiley & Sons, pp. 158-167.
- Petterson, G. (1996). Varved sediments in Sweden: a brief review. In: Kemp, A.E.S. (Ed.) *Palaeoclimatology and palaeoceanography from laminated sediments (Geological Society Special Publication)* 116, 73–77.
- Petterson, G., Odgaard, B.V. and Renberg, I. (1999). Image analysis as a method to quantify sediment components. *Journal of Paleolimnology* 22, 443–455.
- Pettorelli, N., Vik, J. O., Mysterud, A., Gaillard, J. M., Tucker, C. J. and Stenseth, N. C. (2005). Using the satellite-derived NDVI to assess ecological responses to environmental change. *Trends in Ecology & Evolution* 20(9), 503-510.
- Phillips, J. D. (1992a). The end of equilibrium?. *Geomorphology* 5(3), 195-201.
- Phillips, J. D. (1992b). Nonlinear dynamical systems in geomorphology: revolution or evolution?. *Geomorphology*, 5, 219-229.
- Phillips, J. D. (1992c). Deterministic chaos in surface runoff. In: Parsons, A.J. and Abrahams, A.D. (Ed.) *Overland flow: hydraulics and erosion mechanics*. London: UCL Press, pp.177–97.
- Phillips, J. D. (1995) Self-organization and landscape evolution. *Progress in Physical Geography* 19 (3), 309-321.
- Phillips, J. D. (1998). On the relations between complex systems and the factorial model of soil formation (with discussion). *Geoderma* 86(1), 1-21.
- Phillips, J. D. (1999). Divergence, Convergence, and Self-Organization in Landscapes. *Annals of the Association of American Geographers* 89 (3), 466-488.
- Phillips, J. D. (2003). Sources of nonlinearity and complexity in geomorphic systems. *Progress in Physical Geography* 27(1), pp. 1–23.

- Phillips, J. D. (2006). Evolutionary geomorphology: thresholds and nonlinearity in landform response to environmental change. *Hydrology and Earth System Sciences Discussions* 3, 365–394.
- Phillips, J. D. (2007). Perfection and complexity in the lower Brazos River. *Geomorphology* 91, 364-377.
- Phillips, J. D. (2009). Changes, perturbations, and responses in geomorphic systems. *Progress in Physical Geography* 33, 17-30.
- Phillips, J. D., Gares, P. A. and Slattery, M. C. (1999). Agricultural soil redistribution and landscape complexity. *Landscape Ecology* 14(2), 197-211.
- Piégay, H. and Schumm, S. A. (2003). System approaches in fluvial geomorphology. In: Kondolf, G.M. and Piégay, H. (Ed.) *Tools in Fluvial Geomorphology*. Chichester: John Wiley and Sons, pp.103-134.
- Pitkänen, A. and Huttunen, P. (1999). A 1300-year forest-fire history at a site in eastern Finland based on charcoal and pollen records in laminated lake sediment. *The Holocene* 9(3), 311-320.
- Pitman, A. J. (2005). On the role of geography in earth system science. *Geoforum* 36(2), 137-148.
- du Plessis, W. P. (1999). Linear regression relationships between NDVI, vegetation and rainfall in Etosha National Park, Namibia. *Journal of Arid Environments* 42, 235-260.
- Prasad, S., Brauer, A., Rein, B. and Negendank, J. F. (2006). Rapid climate change during the early Holocene in western Europe and Greenland. *The Holocene* 16(2), 153-158.
- Price, M. (1985). *Introducing groundwater*. London: George Allen & Unwin, pp.101.

Prosser, I.P. (1996). Thresholds of channel initiation in historical and Holocene times, south-eastern Australia. In: Anderson, M.G. and S.M. Brooks (Ed.) *Advances in Hillslope Processes, Volume 2*. Chichester: John Wiley and Sons, pp. 687-708.

Prudhomme, C., Jakob, D. and Svensson, C. (2003). Uncertainty and climate change impact on the flood regime of small UK catchments. *Journal of Hydrology* 277(1), 1-23.

Portela, R. and Rademacher, I. (2001). A dynamic model of patterns of deforestation and their effect on the ability of the Brazilian Amazonia to provide ecosystem services. *Ecological Modelling* 143(1), 115-146.

Van der Post, K. D., Oldfield, F., Haworth, E. Y., Crooks, P. R. J. and Appleby, P. G. (1997). A record of accelerated erosion in the recent sediments of Blelham Tarn in the English Lake District. *Journal of Paleolimnology* 18(2), 103-120.

Purevdorj, T. S., Tateishi, R., Ishiyama, T. and Honda, Y. (1998). Relationships between percent vegetation cover and vegetation indices. *International Journal of Remote Sensing* 19(18), 3519-3535.

Quine, T.A. and Walling, D.E. (1993). Use of caesium-137 measurements to investigate relationships between erosion rates and topography. In: Thomas, D.S.G and Allison, R.J. (Ed.) *Landscape sensitivity*. Chichester: John Wiley and Sons Ltd.

Quinton, J.N. (2004). Erosion and Sediment Transport. In: Wainwright, J. and Mulligan, M. (Ed.) *Environmental Modelling: Finding Simplicity in Complexity*. London: John Wiley & Sons, pp. 187-195.

Raubitschek, S., Lücke, A. and Schleser, G.H. (1999). Sedimentation patterns of diatoms in Lake Holzmaar, Germany - on the transfer of climate signals to biogenic silica oxygen isotope proxies. *Journal of Paleolimnology* 21(4), 437-448.

Raven, P. J., Holmes, N. T. H., Dawson, F. H., Fox, P. J. A., Everard, M., Fozzard, I. and Rouen, K. J. (1998). *River Habitat Quality: the Physical Character of Rivers and Streams in the UK and the Isle of Man*. Environment Agency, Bristol.

Reid, G.C. (2000). Solar Variability and the Earth's Climate: Introduction and Overview. *Space Science Reviews*, 94(1-2), pp. 1-11.

Reid, W. V., Chen, D., Goldfarb, L., Hackmann, H., Lee, Y. T., Mokhele, K., Ostrom, E., Raivio, K., Rockström, J., Schellnhuber, H. J. and Whyte, A. (2010). Earth system science for global sustainability: grand challenges. *Science (Washington)* 330(6006), 916-917.

Rein, B., Jäger, K., Kocot, Y., Grimm, K. and Sirocko, F. (2007). 10. Holocene and Eemian varve types of Eifel maar lake sediments. *Developments in Quaternary Sciences* 7, 141-156.

Reinikainen, P., Meriläinen, J. J., Virtanen, A., Veijola, H. and Äystö, J. (1997). Accuracy of ^{210}Pb dating in two annually laminated lake sediments with high Cs background. *Applied radiation and isotopes* 48(7), 1009-1019.

Renard, K. G., Foster, G. R., Weesies, G. A. and Porter, J. P. (1991). RUSLE: Revised universal soil loss equation. *Journal of soil and Water Conservation* 46(1), 30-33.

Renberg, I. (1981). Improved methods for sampling, photographing and varve-counting of varved lake sediments. *Boreas* 10(3), 255-258.

Renberg, I. and Segerström U. (1980). The initial points on a shoreline displacement curve for southern Västerbotten, dated by varve counts. *Striae* 14, 174-176.

Renberg, I., & Wik, M. (1984). Soot particle counting in recent lake sediments an indirect dating method. *Ecological Bulletins* 53-57.

Renberg, I. and Wik, M. (1985) Carbonaceous particles in lake sediments-Pollutants from fossil fuel combustion. *Ambio* 14 (3), 161-163.

Reynard, N.S., Prudhomme, C. and Crooks, S.M. (2001). The flood characteristics of large UK rivers: potential effects of changing climate and land use. *Climatic Change* 48, 343–359.

- Ritchie, J. C. and McHenry, J. R. (1990). Application of radioactive fallout cesium-137 for measuring soil erosion and sediment accumulation rates and patterns: a review. *Journal of environmental quality* 19(2), 215-233.
- Ritchie, J. C., McHenry, J. R. and Gill, A. C. (1974). Fallout ¹³⁷Cs in the soils and sediments of three small watersheds. *Ecology* 55, 887-890.
- Robinson, D.A. (1999). Agricultural practice, climate change and the soil erosion hazard in parts of southeast England. *Applied Geography* 19, 13–27.
- Robbins, J.A. (1978). Geochemical and geophysical applications of radioactive lead. In: Nriagu, J.O. (Ed.) *Biogeochemistry of lead in the environment*. Elsevier Scientific, 285–393.
- De Roo, A. P. J., Hazelhoff, L. and Burrough, P. A. (1989). Soil erosion modelling using ‘answers’ and geographical information systems. *Earth Surface Processes and Landforms* 14(6), 517-532.
- van Roosmalen, L., Sonnenborg, T. O., Jensen, K. H. and Christensen, J. H. (2011). Comparison of hydrological simulations of climate change using perturbation of observations and distribution-based scaling. *Vadose Zone Journal* 10(1), 136-150.
- Rose, N.L. (1990). A method for the extraction of carbonaceous particles from lake sediments. *Journal of Paleolimnology* 3, 45–53.
- Rose, N.L. (1994). A note on further refinements to a procedure for the extraction of carbonaceous fly-ash particles from lake sediments. *Journal of Paleolimnology* 11, 201–204.
- Rose, N.L. (2001). Fly-ash particles. In: Last, W.M. and Smol, J.P. (Ed.) *Tracking Environmental Change Using Lake Sediments. Volume 2: Physical and Geochemical Methods*. Dordrecht: Kluwer Academic Publishers, pp. 319–349.
- Rose, N.L. (2008). Quality control in the analysis of lake sediments for spheroidal carbonaceous particles. *Limnology and Oceanography: Methods* 6, 172–179.

- Rose, N.L. and Appleby, P.G. (2005). Regional applications of lake sediment dating by spheroidal carbonaceous particle analysis I: United Kingdom. *Journey of Paleolimnology* 34, 349–361
- Rose, N. L., Flower, R. J. and Appleby, P. G. (2003). Spheroidal carbonaceous particles (SCPs) as indicators of atmospherically deposited pollutants in North African wetlands of conservation importance. *Atmospheric Environment* 37(12), 1655-1663.
- Rose, N. L., Harlock, S. and Appleby, P. G. (1999a). Within-basin profile variability and cross-correlation of lake sediment cores using the spheroidal carbonaceous particle record. *Journal of Paleolimnology* 21(1), 85-96.
- Rose, N. L., Harlock, S. and Appleby, P. G. (1999b). The spatial and temporal distributions of spheroidal carbonaceous fly-ash particles (SCP) in the sediment records of European mountain lakes. *Water, Air, and Soil Pollution* 113(1-4), 1-32.
- Rose, N. L., Harlock, S., Appleby, P. G. and Battarbee, R. W. (1995). Dating of recent lake sediments in the United Kingdom and Ireland using spheroidal carbonaceous particle (SCP) concentration profiles. *The Holocene* 5(3): 328–335.
- Rose, N. L., Jones, V. J., Noon, P. E., Hodgson, D. A., Flower, R. J. and Appleby, P. G. (2012). Long-range transport of pollutants to the Falkland Islands and Antarctica: evidence from lake sediment fly ash particle records. *Environmental Science & Technology* 46(18), 9881-9889.
- Rose, N. L., Morley, D., Appleby, P. G., Battarbee, R. W., Alliksaar, T., Guilizzoni, P., Jeppesen, E., Korhola, A. and Punning, J. M. (2011). Sediment accumulation rates in European lakes since AD 1850: trends, reference conditions and exceedence. *Journal of Paleolimnology* 45(4), 447-468.
- Rose, N.L., Rose, C.L., Boyle, J.F. and Appleby, P.G. (2004). Lake-sediment evidence for local and remote sources of atmospherically deposited pollutants on Svalbard. *Journal of Paleolimnology* 31, 499–513.
- Rose, N. L., Shilland, E., Yang, H., Berg, T., Camarero, L., Harriman, R., Koinig, K.,

Lien, L., Nickus, U., Stuchlík, E., Thies, H. and Ventura, M. (2002). Deposition and storage of spheroidal carbonaceous fly-ash particles in European mountain lake sediments and catchment soils. *Water, Air and Soil Pollution: Focus* 2(2), 251-260.

Rose, N. L. and Turner, S. (2007). Report on the spheroidal carbonaceous particle (SCP) dating of sediment core ALRE 1 from Old Alresford Pond, England. In: Environment Agency (Ed.) *Alresford Pond Water Level Management Plan*. London: Environmental Change Research Centre and University College London.

Rounsevell, M.D.A., Annetts, J.E., Audsley, E., Mayr, T. and Reginster, I. (2003). Modelling the spatial distribution of agricultural land use at the regional scale. *Agriculture, Ecosystems & Environment* 95(2), 465-479.

Rounsevell, M. D. A., Reginster, I., Araújo, M. B., Carter, T. R., Dendoncker, N., Ewert, F., House, J.I., Kankaanpää, S., Leemans, R., Metzger, M.J., Schmit, C., Smith, P. and Tuck, G. (2006). A coherent set of future land use change scenarios for Europe. *Agriculture, Ecosystems & Environment* 114(1), 57-68.

Rouse, J. w., Haas, R. H., ScheU, J. A. and Deering, D. W. (1973). *Monitoring vegetation systems in the great plains with ERTS, Third ERTS Symposium*. NASA SP-351 I, 309-317.

Saarinen, T. (1998). High-resolution palaeosecular variation in northern Europe during the last 3200 years. *Physics of the Earth and Planetary Interiors* 106, 299–309.

Saarinen, T. and Petterson, G. (2001). Image analysis techniques. In: Last, W.M. and Smol, J.P. (Ed.) *Tracking Environmental Change Using Lake Sediments: Volume 2: Physical and Geochemical Methods*. Dordrecht: Kluwer Academic Publishers, pp.23-39.

Saarnisto, M. (1986). Annually laminated lake sediments. In: Berglund, B.E. (Ed.) *Handbook of Holocene Palaeoecology and Palaeohydrology*. Chichester: Wiley, pp. 343–370.

Sandgren, P. and Snowball, I. (2001). Application of mineral magnetic techniques to

paleolimnology. In: Last, W.M. and Smol, J.P. (Ed.) *Tracking Environmental Change Using Lake Sediments. Volume 2: Physical and Geochemical Methods*. Dordrecht: Kluwer Academic Publishers, pp. 217-237.

Saldin, D. K. and Wei, C. M. (1996). Rapid climate changes in the tropical Atlantic region during the last deglaciation. *Nature* 380, 7.

Sapozhnikov, V. B. and Foufoula-Georgiou, E. (1997). Experimental evidence of dynamic scaling and indications of self-organized criticality in braided rivers. *Water Resources Research* 33(8), 1983-1991.

Sayer, C., Turner, S. and Rose, N. L. (2007). Report on results of paleolimnological analysis of a core from Old Alresford Pond, England. In: Environment Agency (Ed.) *Alresford Pond Water Level Management Plan*. London: Environmental Change Research Centre and University College London.

Scharf, B.W. and Menn, U. (1992). Hydrology and morphometry. In: Scharf, B.W. and Björk, S. (Ed.) *Limnology of Eifel Maar Lakes*. *Ergebnisse der Limnologie* 38, 43–62.

Scharf, B. W. and Oehms, M. (1992). Physical and chemical characteristics. In: Scharf, B.W. and Björk, S. (Ed.) *Limnology of Eifel Maar Lakes, Advances in Limnology* 38, 63–83. Germany: Schweizerbart.

Scharf, B.W. (1987). *Limnologische Beschreibung, Nutzung and Unterhaltung von Eifelmaaren*. Mainz: Ministry for the Environment and Health, Rhineland-Pfalz, pp. 117.

Scheffer, M., Bascompte, J., Brock, W.A., Brovkin, V., Carpenter, S.R., Dakos, V., Held, H., van Nes, E.H., Rietkerk, M. and Sugihara, G. (2009). Early-warning signals for critical transitions. *Nature* 461, 53–59.

Scheffer, M., Carpenter, S. R., Lenton, T. M., Bascompte, J., Brock, W., Dakos, V., van de Koppel, J., van de Leemput, I. A., Levin, S. A., van Nes, E. H., Pascual, M. and Vandermeer, J. (2012). Anticipating critical transitions. *Science* 338(6105), 344-348.

- Schlüter, M., Müller, B. and Frank, K. (2012). *MORE - Modeling for Resilience Thinking and Ecosystem Stewardship (Working Paper, April 2012)*. Social Science Research Network.
- Schmidli, J., Goodess, C. M., Frei, C., Haylock, M. R., Hurrell, J. W., Ribalaygua, J. and Schmith, T. (2007). Statistical and dynamical downscaling of precipitation: An evaluation and comparison of scenarios for the European Alps. *Journal of Geophysical Research: Atmospheres* (1984–2012), 112 (D4).
- Schumm, S. A. (1965). Quaternary palaeohydrology. In: *The Quaternary of the United States*. Princeton: Princeton University Press, pp.783-794.
- Schumm, S. A. (2005). *River variability and complexity*. Cambridge: Cambridge University Press.
- Schwind, W. (1984). *Der Eifelwald im Wandel der Jahrhunderte, ausgehend von Untersuchungen in der Vulkaneifel*. Duren: Eifelverein, pp. 340.
- Schmincke, H. U. (2007). The Quaternary volcanic fields of the east and west Eifel (Germany). In: Ritter, J. R.R. and Christensen, U.R. (Ed.) *Mantle plumes-a multidisciplinary approach*. Berlin, Heidelberg: Springer- Verlag, pp. 252-253.
- Sear, D. A., Armitage, P. D. and Dawson, F. H. (1999). Groundwater dominated rivers. *Hydrological Processes* 13(3), 255-276.
- Sidorchuk, A. (2006). Stages in gully evolution and self-organized criticality. *Earth Surface Processes and Landforms* 31, 1329–1344.
- Semenov, M. A. (2007). Development of high-resolution UKCIP02-based climate change scenarios in the UK. *Agricultural and Forest Meteorology* 144, 127–138.
- Senarath, D. C. H. (1990). Two case studies in estimation of groundwater recharge. *Groundwater Monitoring and Management: proceedings of the Dresden symposium*, March 1987, 45.
- Shamseldin, A. Y. (1997). Application of a neural network technique to rainfall-

runoff modelling. *Journal of Hydrology* 199, 272-294.

Simola, H. L. K., Coard, M. A. and O'Sullivan, P. E. (1981). Annual laminations in the sediments of Loe Pool, Cornwall. *Nature* 290, 238-241.

Sirocko, F., Dietrich, S., Veres, D., Grootes, P. M., Schaber-Mohr, K., Seelos, K., Nadeau, M. J., Kromer, B., Rothacker, L., Röhner, M., Krbetschek, M., Appleby, P.G., Hambach, U., Rolf, C., Sudo, M. and Grim, S. (2013). Multi-proxy dating of Holocene maar lakes and Pleistocene dry maar sediments in the Eifel, Germany. *Quaternary Science Reviews* 62, 56-76.

Sirocko, F., Seelos, K., Schaber, K., Rein, B., Dreher, F., Diehl, M., Lèhne, R., Jäger, K., Krbetschek, M. and Degering, D. (2005). A Late Eemian aridity pulse in central Europe during the last glacial inception. *Nature* 436, 833-836.

Smith, R. (1991). The application of cellular automata to the erosion of landforms. *Earth Surface Processes and Landforms* 16 (3), 273–281.

Smith, S.V., Bradley, R.S. and Abbott, M.B. (2004). A 300 year record of environmental change from Lake Tuborg, Ellesmere Island, Nunavut, Canada. *Journal of Paleolimnology* 32 (2), 137–148.

Smith, P. A., Dosser, J., Tero, C. and Kite, N. (2003). A methods to identify chalk rivers and assess their nature-conservation values. *Water and Environment Journal*, 17 (3), 140-144.

Smol, J.P. (2002). *Pollution of Lakes and Rivers: A Paleoenvironmental Perspective*. New York: Oxford University Press, pp. 41.

Sneppen, K., Bak, P., Flyvbjerg, H. and Jensen, M. H. (1995). Evolution as a self-organized critical phenomenon. *Proceedings of the National Academy of Sciences* 92(11), 5209-5213.

Snowball, I.F. and Sandgren, P. (2002). Geomagnetic field variations in northern Sweden during the Holocene quantified from varved lake sediments and their implications for cosmogenic nuclide production rates. *The Holocene* 12, 517–530.

- Snowball, I., Sandgren, P. and Petterson, G. (1999). The mineral magnetic properties of an annually laminated Holocene lake-sediment sequence in northern Sweden. *The Holocene* 9, 353–362.
- Stage, M. (2001). Magnetic susceptibility as carrier of a climatic signal in chalk. *Earth and Planetary Science Letters* 188(1), 17-27.
- Stockhausen, H. and Zolitschka, B. (1999). Environmental changes since 13,000 cal. BP reflected in magnetic and sedimentological properties of sediments from Lake Holzmaar (Germany). *Quaternary Science Reviews* 18(7), 913-925.
- Stowell, A. (2000). *The story of Alresford-Its changes and continuity*. Hampshire: Alresford Historical and Literary Society.
- Stuiver, M. and Polach, H.A. (1977). Discussion: reporting of ^{14}C data. *Radiocarbon* 19: 355–363.
- Stuiver, M., Reimer, P. J., Bard, E., Beck, J. W., Burr, G. S., Hughen, K. A., Kromer, B., McCormac, G., van der Plicht, J. and Spurk, M. (1998). INTCAL98 radiocarbon age calibration, 24, 000-0 cal BP. *Radiocarbon* 40, 1041-1083.
- Stumpf, M. P. and Porter, M. A. (2012). Critical truths about power laws. *Science* 335(6069), 665-666.
- O’Sullivan, P.E. (1983). Annually laminated lake sediments and the study of Quaternary environmental changes-a review. *Quaternary Science Reviews* 1, 245–313.
- Svorin, J. (2003). A test of three soil erosion models incorporated into a geographical information system. *Hydrological Processes* 17, 967–977.
- Swindles, G. T. (2010). Dating recent peat profiles using spheroidal carbonaceous particles (SCPs). *Mires and Peat* 7(03), 1-5.

Terranova, O., Antronico, L., Coscarelli, R. and Iaquina, P. (2009). Soil erosion risk scenarios in the Mediterranean environment using RUSLE and GIS: an application model for Calabria (southern Italy). *Geomorphology* 112(3), 228-245.

The Mid-Hants Railway Preservation Society (1978). *The Mid-Hants 'Watercress' Line-A brief history*. Hampshire: Brown & Son (Ringwood) Ltd.

Thompson, R. (1986) Palaeomagnetic dating. In: Berglund, B.E. (Ed.) *Handbook of Holocene palaeoecology and palaeohydrology*. Chichester: John Wiley and Sons Ltd, pp. 313-325.

Thompson, R., Battarbee, R. W., O'sullivan, P. E. and Oldfield, F. (1975). Magnetic susceptibility of lake sediments. *Limnology and Oceanography* 20(5), 687-698.

Thomas, R. and Nicholas, A.P. (2002). Simulation of braided river flow using a new cellular routing scheme. *Geomorphology* 43, 179–195.

Thompson, R. and Morton, D. J. (1979). Magnetic susceptibility and particle-size distribution in recent sediments of the Loch Lomond drainage basin, Scotland. *Journal of Sedimentary Research* 49(3), 801-811.

Thomas, R., Nicholas, A.P. and Quine, T.A. (2007). Cellular modelling as a tool for interpreting historic braided river evolution. *Geomorphology* 90, 302–317.

Thompson, R. and Oldfield, F. (1986). *Environmental Magnetism*. London: George Allen & Unwin, pp.109.

Thouveny, N., de Beaulieu, J. L., Bonifay, E., Creer, K. M., Guiot, J., Icole, M., Johnsen, S., Jouzel, J., Reille, M., Williams, T. and Williamson, D. (1994). Climate variations in Europe over the past 140 kyr deduced from rock magnetism. *Nature* 371, 503-506.

Toro-Escobar, C.M., Parker, G. and Paola, C. (1996). Transfer function for the deposition of poorly sorted gravel in response to streambed aggradation. *Journal of Hydraulic Research* 34, 35-51.

- Trimble, S. W. (2012). Historical sources and watershed evolution. *Philosophical Transactions of the Royal Society A* 370, 2075-2092.
- Tucker, C.J. (1979). Red and Photographic Infrared linear Combinations for Monitoring Vegetation. *Remote sensing of environment* 8, 127-150.
- Tucker, G.E. and Bras, R. L. (1998). Hillslope processes, drainage density, and landscape morphology. *Water Resources Research* 34, 2751-2764.
- Tucker, G. E. and Hancock, G. R. (2010). Modelling landscape evolution. *Earth Surface Processes and Landforms* 35(1), 28-50.
- Tylmann, W., Enters, D., Kinder, M., Moska, P., Ohlendorf, C., Poręba, G. and Zolitschka, B. (2013). Multiple dating of varved sediments from Lake qazduny, northern Poland: Toward an improved chronology for the last 150 years. *Quaternary Geochronology* 15, 98-107.
- Vandenberghe, J. (2003). Climate forcing of fluvial system development: an evolution of ideas. *Quaternary Science Reviews* 22(20), 2053-2060.
- Veldkamp, A. and Van Dijke, J. J. (2000). Simulating internal and external controls on fluvial terrace stratigraphy: a qualitative comparison with the Maas record. *Geomorphology* 33(3), 225-236.
- Verburg, P. H., Schulp, C. J. E., Witte, N. and Veldkamp, A. (2006). Downscaling of land use change scenarios to assess the dynamics of European landscapes. *Agriculture, Ecosystems & Environment* 114(1), 39-56.
- Verosub, K. L. and Roberts, A. P. (1995). Environmental magnetism: Past, present, and future. *Journal of Geophysical Research* 100(B2), 2175-2192.
- Verstraeten, G., Oost, K., Rompaey, A., Poesen, J. and Govers, G. (2002). Evaluating an integrated approach to catchment management to reduce soil loss and sediment pollution through modelling. *Soil Use and Management* 18(4), 386-394.

- Verstraeten, G. and Poesen, J. (1999). The nature of small-scale flooding, muddy floods and retention pond sedimentation in central Belgium. *Geomorphology* 29(3), 275-292.
- Verstraeten, G. and Poesen, J. (2000). Estimating trap efficiency of small reservoirs and ponds: methods and implications for the assessment of sediment yield. *Progress in Physical Geography* 24(2), 219-251.
- Veski, S., Seppä, H. and Ojala, A. E. (2004). Cold event at 8200 yr BP recorded in annually laminated lake sediments in eastern Europe. *Geology* 32(8), 681-684.
- Volchok, H.L. and Chieco, N. (1986). *A compendium of the Environmental Measurements Laboratory's research projects related to the Chernobyl nuclear accident (No. EML-460)*. New York: USDOE Environmental Measurements Lab.
- Volker, G. (1999). Ten years of individual-based modelling in ecology: what have we learned and what could we learn in the future?. *Ecological modelling* 115(2), 129-148.
- Vos, H., Sanchez, A., Zolitschka, B., Brauer, A. and Negendank, J. F. W. (1997). Solar activity variations recorded in varved sediments from the crater lake of Holzmaar—a maar lake in the Westeifel volcanic field, Germany. *Surveys in Geophysics* 18(2-3), 163-182.
- De Vries, B. M. (2007). In search of sustainability: what can we learn from the past?. In: Hornborg, A. and Crumley, C. L. (Ed.) *The World System and The Earth System: Global Socioenvironmental Change and Sustainability since the Neolithic*. Left Coast Press, pp. 243-257.
- Wainwright, J. (2009). Earth-System Science. In: Castree, N., Demeritt, D., Liverman, D. and Rhoads, B. (Ed.) *A Companion to Environmental Geography*. Oxford: Wiley-Blackwell.
- Waller, M. P. and Hamilton, S. (2000). Vegetation history of the English chalklands: a mid-Holocene pollen sequence from the Caburn, East Sussex. *Journal of Quaternary Science* 15(3), 253-272.

Walling, D. E. (1997). The response of sediment yields to environmental change. In: Walling, D. E. and Probst, J.B. (Ed.) *Human impact on erosion and sedimentation: Proceedings of the Rabat Symposium S6*, No. 245, April 1997. Wallingford: International Association of Hydrological Sciences, pp. 77-89.

Walling, D. E. and Woodward, J. C. (1992). Use of radiometric fingerprints to derive information on suspended sediment sources. In: Bogen, J., Walling, D. E. and Day, T. (Ed.) *Erosion and Sediment Transport Monitoring Programmes in River Basins: Proceedings of Oslo Workshop*, No. 210, September 1992, pp.143–152.

Ward, P. J., van Balen, R. T., Verstraeten, G., Renssen, H. and Vandenberghe, J. (2009). The impact of land use and climate change on late Holocene and future suspended sediment yield of the Meuse catchment. *Geomorphology* 103(3), 389-400.

Watson, P. V. (1983). *A palynological study of the impact of man on the landscape of central southern England, with special reference to the chalklands*. Ph.D thesis, University of Southampton.

Weatherhead, E. K. and Knox, J. W. (2000). Predicting and mapping the future demand for irrigation water in England and Wales. *Agriculture Water Management* 43, 203-218.

Welsh, K. E. (2009). *Modelling basin-scale sediment dynamics in the Petit lac d'Annecy catchment, France*. Ph.D thesis, University of Liverpool.

Welsh, K. E., Dearing, J. A., Chiverrell, R. C. and Coulthard, T. J. (2009). Testing a cellular modelling approach to simulating late-Holocene sediment and water transfer from catchment to lake in the French Alps since 1826. *The Holocene* 19(5), 785-798.

Werner, B. T. (1999). Complexity in natural landform patterns. *Science* 284(5411), 102-104.

White, C. J. (2007). *The Use of Joint Probability Analysis to Predict Flood Frequency in Estuaries and Tidal Rivers*. Ph.D thesis, University of Southampton.

- Van De Wiel, M. J and Coulthard, T. J. (2010). Self-organized criticality in river basins: Challenging sedimentary records of environmental change. *Geology* 38, 87-90.
- Van De Wiel, M. J., Coulthard, T. J., Macklin, M. G. and Lewin, J. (2007). Embedding reach-scale fluvial dynamics within the CAESAR cellular automaton landscape evolution model. *Geomorphology* 90(3), 283-301.
- Wigley, T. M. L. and Jones, P.D. (1987). England and Wales precipitation: a discussion of recent changes in variability and an update to 1985. *Journal of Climatology* 7(3), 231-246.
- Wilby, R. L., Beven, K. J. and Reynard, N. S. (2008). Climate change and fluvial flood risk in the UK: more of the same?. *Hydrological Processes* 22(14), 2511-2523.
- Wilby, R. L., Whitehead, P. G., Wade, A. J., Butterfield, D., Davis, R. J. and Watts, G. (2006). Integrated modelling of climate change impacts on water resources and quality in a lowland catchment: River Kennet, UK. *Journal of Hydrology* 330(1), 204-220.
- Wilcock, P. R. and Crowe, J.C. (2003). Surface-based transport model for mixed-size sediment. *Journal of Hydraulic Engineering* 129 (2), 120-128.
- Williams, M. (2012). River sediments. *Philosophical Transactions of the Royal Society A* 370, 2093-2122.
- Willgoose, G. (2005). Mathematical modeling of whole landscape evolution. *Annual Review of Earth and Planetary Sciences* 33, 443-459.
- Wilson, S. (2000). *Alresford Pond Water Level Management Plan (draft report to the Environment Agency)*. Environmental Change Research Centre.
- Wischmeier, W. H. and Smith, D. D. (1978). Predicting rainfall erosion losses-A guide to conservation planning. In: *Agriculture Handbook No. 537*. USA: Science and Education Administration, pp. 58.

- Wohlfarth, B., Björk, S. and Possnert, G. (1995). The Swedish Time Scale - a potential calibration tool for the radiocarbon time-scale during the late Weichselian. *Radiocarbon* 37, 347-359.
- Wolfram, S. (1984). Cellular automata as models of complexity. *Nature* 311 (4), 419-424.
- Wolfram, S. (1994). *Cellular Automata and Complexity: Collected Papers*. Reading: Addison-Wesley.
- Wootton, J. T. (2001). Local interactions predict large-scale pattern in empirically derived cellular automata. *Nature*, 413(6858), 841-844.
- Xue, B. and Yao, S. (2011). Recent sedimentation rates in lakes in lower Yangtze River basin. *Quaternary International* 244(2), 248-253.
- Yang, H., Rose, N. L. and Battarbee, R. W. (2001). Dating of recent catchment peats using spheroidal carbonaceous particle (SCP) concentration profiles with particular reference to Lochnagar, Scotland. *The Holocene* 11(5), 593-597.
- Yin, H. and Li, C. (2001). Human impact on floods and flood disasters on the Yangtze River. *Geomorphology* 41, 105-109.
- Zhang, L., O'Neill, A. L. and Lacey, S. (1996). Modelling approaches to the prediction of soil erosion in catchments. *Environmental Software* 11, 123-133.
- Zillén, L. M., Wastegård, S. and Snowball, I. F. (2002). Calendar year ages of three mid-Holocene tephra layers identified in varved lake sediments in west central Sweden. *Quaternary Science Reviews* 21(14), 1583-1591
- Zolitschka, B. (1992a). Climatic change evidence and lacustrine varves from maar lakes, Germany. *Climate Dynamics* 6, 229-232.
- Zolitschka, B. (1992b). Human history recorded in the annually laminated sediments of Lake Holzmaar, Eifel Mountains Germany. *Geological Survey of Finland Special Paper* 14, 17-24.

Zolitschka, B. (1996). High Resolution Lacustrine Sediments and their Potential for Paleoclimatic Reconstruction. In: Jones, P. D., Bradley, R. S. and Jouzel, J. (Ed.) *Climatic Variations and Forcing mechanisms of the last 2000 years*. Springer.

Zolitschka, B. (1998). A 14,000 year sediment yield record from Western Germany based on annually laminated sediments. *Geomorphology* 22, 1-17

Zolitschka, B. (2007). Varved lake sediments. In: Elias, S.A. (Ed.) *Encyclopedia of Quaternary Science*. Amsterdam: Elsevier, pp. 3105-3114.

Zolitschka, B., Behre, K. E. and Schneider, J. (2003). Human and climatic impact on the environment as derived from colluvial, fluvial and lacustrine archives-examples from the Bronze Age to the Migration period, Germany. *Quaternary Science Reviews* 22(1), 81-100.

Zolitschka, B., Brauer, A., Negendank, J. F. W., Stockhausen, H. and Lang, A. (2000). Annually dated Weichselian continental paleoclimate record from the Eifel, Germany. *Geology* 28, 783-786.

Zolitschka, B., Negendank, J. F. W. and Lottermoser, B. G. (1995). Sedimentological proof and dating of the early Holocene volcanic eruption of Ulmener Maar (Vulkaneifel, Germany). *Geologische Rundschau* 84(1), 213-219.